Dark Higgs Studies and Diboson Production at the Large Hadron Collider

---

Dissertation

zur

Erlangung der naturwissenschaftlichen Doktorwürde
(Dr. sc. nat.)

vorgelegt der

Mathematisch-naturwissenschaftlichen Fakultät

der

Universität Zürich

von

Erich Michael Caspar Maria Weihs

aus

Deutschland

Promotionskomitee

Prof. Dr. Thomas Gehrmann *(Vorsitz & Leitung der Dissertation)*
Prof. Dr. Daniel Wyler
Prof. Dr. Charalampos Anastasiou

Zürich, 2013

Abstract

The detection of New Physics at a high-energy particle collider requires a multitude of complementary efforts. In this thesis it is studied how the an extension of the Standard Model electroweak sector can be explored by the early run of the Large Hadron Collider in connection with constraints from previous precision measurements. This model consists of an additional $U(1)$ gauge force. The corresponding boson obtains its mass through a separate Higgs mechanism, whose Higgs particle mixes with the Standard Model one. It is shown that much of the parameter space can be probed but that relevant regions remain unconstrained.

An important class of processes for the direct and indirect detection of New Physics at the Large Hadron Collider is the production of two electroweak gauge bosons. For improved discriminating power precise Standard Model predictions for these processes are desirable. Two contributions towards their full description at third order in perturbation theory of quantum-chromodynamics are given. First, the two-loop virtual helicity amplitudes for the production of a Z boson in connection with a photon or gluon via the fusion of two gluons are calculated. Second, the planar Feynman master integrals necessary for the two-loop amplitude of W and Z boson pair production are computed.

In order to achieve this, new algebraic methods for multiple polylogarithms are used that make the computation of certain transformations possible. The necessary algorithms are described and implemented in a computer algebra code which is documented as well.

Zusammenfassung

Die Entdeckung neuer Physik an Hochenergie-Teilchenbeschleunigern erfordert eine Vielzahl einander sich ergänzender Leistungen. In dieser Dissertation wird untersucht, wie eine Erweiterung des elektroschwachen Sektors des Standardmodells durch die ersten Daten des großen Hadronen-Speicherrings (LHC) in Verbindung mit Präzissionsmessungen früherer Experimente sondiert werden kann. Das Modell besteht aus einer zusätzlichen $U(1)$ Eichkraft. Dessen Boson erhält seine Masse durch einen separaten Higgsmechanismus, dessen Higgsteilchen mit dem des Standardmodells mischt. Es wird gezeigt, dass ein Großteil des Parameterraums erforscht wird, aber relevante Teile davon ohne Einschränkungen bleiben.

Eine wichtige Klasse von Prozessen für die direkte und indirekte Suche neuer Physik am LHC ist die Produktion zweier Eichbosonen. Um besser zwischen bekannter und neuer Physik unterscheiden zu können sind präzise Standardmodellvorhersagen wünschenswert. Es werden zwei Beiträge zur vollständigen Beschreibung dieser Prozesse in dritter Ordnung Störungstheorie in Quantenchromodynamik beschrieben. Erstens werden die virtuellen zwei-Schleifen-Helizitätsamplituden für die Produktion von einem Z-Boson in Verbindung mit einem Photon oder Gluon durch die Verschmelzung von zwei Gluonen ermittelt. Zweitens werden die planaren Feynman Master-Integrale, die zur Berechnung der zwei-Schleifen-Amplitude der Paarproduktion von W- und Z-Bosonen nötig sind, berechnet.

Um dies zu erreichen werden neue algebraische Methoden für multiple Polylogarithmen angewendet, die die Berechnung bestimmter Transformationen erst ermöglichen. Die nötigen Algorithmen werden beschrieben und sind in einem Computeralgebracode implementiert, welcher ebenfalls dokumentiert ist.

Acknowledgements

First and foremost I would like to thank my supervisor Thomas Gehrmann. He gave me the opportunity to join this institute to explore very different topics. I had great liberty in choosing the projects to work on. He always had time for me when I had questions and his answers proved to be very helpful. I appreciated that he was very supportive when I needed it.

Furthermore, I would like to thank my collaborators José Zurita and Lorenzo Tancredi. It was very interesting to explore the realms of Beyond the Standard Model physics with José who taught me the tricks and trades of BSM studies. It was a great experience to work with him. I am indebted to Lorenzo who taught me the art of multi-loop computations, always willing to explain things in great detail and depth. Pursuing the projects with him was and is a pleasure and I am looking forward to doing so in the coming months.

Claude Duhr's help in understanding the symbol and coproduct calculus was invaluable; I would like to thank him very much for it. Discussions with Andreas von Manteuffel and Marc Gillioz were always insightful and clarifying. I am also thankful to my office mates, Andreas Papaefstathiou and Paolo Torrielli who always lent me an ear to listen to my rants and answer my technical questions.

I thank the people at the institute for creating and living its unique atmosphere. I will always remember the happy days and hours spent together both inside the institute or at the countless excursions. You will truly be missed! A heartfelt "thank you" also goes to the persons that keep this institute running in the background, that is, the administrators Esther Meier and Regina Schmid and Doug Potter and Jonathan Coles who were always very quick to help me with IT issues.

Pier-Francesco Monni, Claude, Lorenzo, José and Thomas each read my thesis and helped me improve it with their valuable, constructive remarks.

Last but certainly not least I would like to thank my family. Jolanda and Peter Jochum's support made it possible for me to pursue my studies in Zurich. My grandmother Gabriele Leinfelder always kept me up to date on the whereabouts and activities of her kin for which I am very thankful for. I am also indebted to my parents, who gave me the opportunity to study without financial worries and backed my plans wherever I went. They sparked an interest in many things in me, taught me perseverance and provided me with a home that I always look forward returning to.

Contents

1

Introduction and Preliminaries

Do we live in a "Golden Age" of particle physics? The discovery of the Higgs particle on the 4^{th} of July 2012 crowned the phenomenal success of the Standard Model of particle physics of the 20^{th} century. Based on the framework of quantum field theory, developed in the forties to sixties of the past century, gauge theories could successfully describe the electroweak force and the mechanism that breaks it, giving mass to three of the four associated gauge bosons. Together with the quark model, non-abelian gauge theories were also successful in describing the nature of the strong nuclear force and to classify the "particle zoo" detected at colliders in the sixties. Both theories could be extrapolated to extraordinarily high energies. Theoretical developments allowed for a better understanding of the underlying structure, which, using refined predictions, were probed at very high precision at colliders in the eighties and nineties, collecting already indirect hints at the existence of "something" that is responsible for the breaking of the electroweak gauge symmetry just beyond the reach of the detectors. With the advent of the LHC this particle could finally be discovered, confirming what has become known as the "Standard Model" (SM) spectacularly. This sounds like, and indeed is, a phenomenal success story.

But scientific advancement often raises more questions than it answers. This is certainly true for the Higgs boson which had already been theorized in 1964. While so far most of the properties of the newly found particle agree with the expectations of a Standard Model Higgs, it still has to be determined whether this is truly the case or whether more precise measurements will reveal discrepancies, which then will have to be explained. Taking a step back even more questions prevail. It is unknown why the strong force does not break charge and parity conjugation symmetry, even though the theory would in principle allow for it; or what the mechanism is that generated the imbalance between matter and antimatter during the Big Bang. Furthermore, nonzero masses for the neutrinos have been measured; but how these masses are generated is unknown. We would also like to understand why gravity is so much weaker than the other elementary forces and what stabilizes this hierarchy against quantum corrections. Can everything be described in one common framework also incorporating General Relativity? For example, we know that the universe's expansion rate accelerates. This amounts to an energy density that permeates space and time. We also have collected independent evidence that there has to

be additional matter in the universe responsible for structure formation and explaining the observed rotation curve observed of stars in galaxies. But the nature of these two, so-called "Dark Energy" and "Dark Matter", which make up more than 95 per cent of the universe's energy and matter budget, is unknown.

Most of these questions have been asked a long time ago and many people have attempted to answer them. While it is more than likely that these questions are related, there exists no generally accepted solution that tackles many of these problems at the same time just waiting for experimental confirmation. On the other hand, we have a wealth of experiments at our disposal that provide us with ever-increasing amounts of data, be it from classical high-energy colliders, low-energy high precision experiments, neutrino detectors, cosmic ray and and conventional telescopes and Dark Matter detection experiments which all become more sensitive with each new generation. Only improved theoretical understanding and additional experimental data will tell whether one of the already proposed theories is indeed realized by nature, if there is another theory that can be cast in the known theoretical language or if we need a new understanding of particle physics to solve the open questions. The next years will help tremendously to clear the mist that currently obstructs our view above the energy scale of the Higgs particle and will help tell which theory is more likely to be true. It could also be that something completely unexpected will be discovered. It is very likely that, at least at high-energy colliders, any discovery will not be a sudden one but will start as a small discrepancy from expected results, growing with additional data until finally certainty about disagreement from the Standard Model prediction will be achieved. The true identification of the new phenomenon will take longer, depending on its signature. Theorists will attempt to explain it with their favorite model and spark new developments along the way.

It could also well be that in the next years no new physics is detected directly. Then one will have to resort to indirect and high-precision measurements which are able to probe physics at energies beyond the reach of the accelerator through its quantum corrections to measurable observables.

What can be done by particle phenomenologists right now to improve the current situation? Even though decades have been spent on the question what comes after the Higgs boson and how to detect this physics, there is still a lot to do. One answer is the study of new observables that can distinguish between known and new physics better. Another answer is to improve theory predictions for observables which also help measure Standard Model parameters more precisely. A popular strategy is to devise generic theories with features that can be reproduced by many others and study what existing and future collider data can say about them. The study of effective theories with a higher number of parameters, which than can on one hand be constrained by experiment and on the other hand be predicted by theories beyond the Standard Model, will also play a role. A different route which is currently being pursued is to deepen the understanding of the mathematical structure of the theories themselves, something that could lead the way to a theory beyond the current ones, or, practically, to simplified ways of making predictions for existing theories. At the same time many theorists and experimentalists are improving the understanding of underlying processes that enter every particle physics prediction and measurement.

In this thesis two of these possibilities are worked on: On one hand it was studied, how a small, well-motivated extension to the Standard Model might alter the phenomenology of the Higgs sector at the LHC and in turn, how much the LHC already could and will be able to constrain the parameters of that theory which will be discussed in the following chapter.

A second topic concerns more precise predictions of the production of two electroweak gauge bosons at hadron colliders. Diboson production processes are not only an important benchmark point for the Standard Model and a background process for many other signals but they can also constrain new physics indirectly. Two steps were taken leading towards a complete description of this important class of processes at third order in perturbation theory, explained in detail in chapters 4 and 5. These computations required the use of relatively new algebraic methods which will be introduced beforehand in chapter 3.

In order to better motivate the following computations and studies, the rest of this chapter will be dedicated to the introduction of most the important features of the Standard Model relevant for this discussion. It will explain how the study of diboson production can be used to constrain new physics indirectly and asses the current state of higher order computations for this class of processes. This review claims is by no means completeness. For a more thorough overview we refer to the many excellent textbooks, lecture notes and reviews, for example [1–4].

1.1 A short overview of Electroweak theory and the Higgs Mechanism

One of the two pillars of the Standard Model, the unified description of the weak force and electromagnetism, was discovered by Sheldon L. Glashow in 1961 [5]. In 1962, the now-called Higgs mechanism was proposed by Philip Warren Anderson [6]. However, it was in 1964 that the full relativistic model was developed by three independent collaborations, namely Robert Brout and Francois Englert [7], Peter Higgs [8] and Gerald Guralnik, Carl Richard Hagen and Tom Kibble [9]. It was only Peter Higgs that realized that this mechanism also implies an additional particle.

In 1967 the Higgs-mechanism was incorporated into electroweak theory by Steven Weinberg and Abdus Salam thus giving it its current form [10] which will be described shortly.

The (classical) Lagrangian of the Electroweak Interaction consists of three parts: the Yang-Mills part $\mathcal{L}_{YM}$ contains the kinetic terms of the Gauge sector, the Higgs part $\mathcal{L}_H$ contains the symmetry breaking terms and the fermionic part $\mathcal{L}_F$ contains the terms governing the evolution and interactions of the fermions. To make the theory a quantized one, gauge fixing terms have to be introduced. Furthermore, in order to cancel divergences appearing at higher orders in perturbation theory counterterms have to be added to the Lagrangian. Both of these contributions are ignored for the sake of this discussion.

1.1.1 The electroweak interaction and the Higgs sector

Let us study first how the Higgs field breaks electroweak symmetry and gives the W and Z bosons mass. The Yang-Mills part can be written as

$$\mathcal{L}_{YM} = -\frac{1}{4}\left(\partial_\mu W^a_\nu - \partial_\nu W^a_\mu + g_2 \varepsilon^{abc} W^b_\mu W^c_\nu\right)^2 - \frac{1}{4}\left(\partial_\mu B_\nu - \partial_\nu B_\mu\right)^2 \ . \tag{1.1}$$

ε^{abc} are the totally antisymmetric structure constants of $SU(2)_W$. The covariant derivative is given as

$$D_\mu = \partial_\mu - i g_2 I^a_W W^a_\mu + i g_1 \frac{Y_W}{2} B_\mu. \tag{1.2}$$

where the $W^a = \sigma^a/2$ are the generators of the weak isospin symmetry group $SU(2)_W$ and B_μ is the generator of the weak hypercharge Y gauge symmetry group $U(1)_Y$.

In the Standard Model, the Higgs sector consists of a single complex scalar $SU(2)_W$ doublet field with hypercharge $Y_W = 1$:

$$\Phi(x) = \begin{pmatrix} \phi^+(x) \\ \phi^0(x) \end{pmatrix} . \tag{1.3}$$

Its interactions with other fields are governed by the usual kinetic energy terms, where the partial derivatives have been replaced by the covariant derivative, and the Higgs potential.

$$\mathcal{L}_H = (D_\mu \Phi)^\dagger (D^\mu \Phi) - V(\Phi). \tag{1.4}$$

The Higgs potential is given by

$$V(\Phi) = \frac{\lambda}{4} \left(\Phi^\dagger \Phi\right)^2 - \mu^2 \Phi^\dagger \Phi . \tag{1.5}$$

If the parameters are chosen such that $\mu^2 > 0$ the potential takes the form of a Mexican hat and the expectation value of the Higgs field in the ground state, that is, where the potential takes its minimum value, is different from zero:

$$|\langle \Phi \rangle|^2 = \frac{2\mu^2}{\lambda} = \frac{v^2}{2} \neq 0 . \tag{1.6}$$

This means that the symmetry is spontaneously broken since the ground state of the field now is less symmetric than the potential. Let us study the effects of this breaking. Since the ground state is now different from zero we shift the fields as

$$\Phi(x) = \begin{pmatrix} \phi^+(x) \\ \frac{1}{\sqrt{2}}\big(v + H(x) + i\chi(x)\big) \end{pmatrix}, \tag{1.7}$$

such that ϕ^+, H and χ have zero vacuum expectation values. We also expand around the ground states to determine the new mass terms of the fields. The neutral field, H, obtains a mass

$$m_H = \sqrt{2}\mu . \tag{1.8}$$

This particle is the one that is commonly called the Higgs particle. The other fields do not obtain a mass. This comes to no surprise. Goldstone's theorem tells us that we should expect massless states for each broken generator of the symmetry. However, since this theorem requires Lorentz invariance and a Hilbert space with positive-definite scalar products at the same time, it cannot be applied here (and we also do not observe them in nature).

A partial answer to this is that using a suitable local gauge transformation, the so called *unitarity gauge*, and thereby fixing the gauge, these fields disappear from the Lagrangian.

To understand what happens to these fields, let us turn our attention to the kinetic terms. We are interested in the terms quadratic in the gauge fields and v. Plugging in the shifted fields into above definitions and choosing that the Higgs field possesses the charges $Y_W = 1$ and $I_3 = 1$ we obtain

$$\begin{aligned} &(D_\mu \Phi)^\dagger (D^\mu \Phi) = \\ &\quad = \left(\partial_\mu + i g_2 \frac{\sigma^{a\dagger}}{2} W^a_\mu - i g_1 \frac{1}{2} B_\mu\right) \begin{pmatrix} 0 & v \end{pmatrix} \left(\partial^\mu - i g_2 \frac{\sigma^a}{2} W^{\mu,a} + i g_1 \frac{1}{2} B^\mu\right) \begin{pmatrix} 0 \\ v \end{pmatrix} \\ &\quad \sim \frac{v^2}{8} \left(\begin{pmatrix} B & W^3_\mu \end{pmatrix} \begin{pmatrix} g_1^2 & g_1 g_2 \\ g_1 g_2 & g_2^2 \end{pmatrix} \begin{pmatrix} B \\ W^3_\mu \end{pmatrix} + g_2^2 ((W^1_\mu)^2 + (W^2_\mu)^2) \right) . \end{aligned} \tag{1.9}$$

Due to the nonzero vacuum expectation value, the gauge fields obtain a mass. Diagonalizing the matrix above we find the charged eigenstates

$$W_\mu^\pm = \frac{1}{\sqrt{2}}\left(W_\mu^1 \pm iW_\mu^2\right) \tag{1.10}$$

with mass

$$m_W = g_2\frac{v}{2} \tag{1.11}$$

and two neutral fields

$$\begin{aligned} Z_\mu &= \frac{1}{\sqrt{g_1^2+g_2^2}}\left(g_1B_\mu + g_2W_\mu^3\right) \ , \\ A_\mu &= \frac{1}{\sqrt{g_1^2+g_2^2}}\left(g_1B_\mu - g_2W_\mu^3\right) \ . \end{aligned} \tag{1.12}$$

Of these, only the Z boson obtains a mass

$$m_Z = \sqrt{g_1^2+g_2^2}\frac{v}{2} \ , \tag{1.13}$$

whereas A_μ, the photon, remains massless. We have seen how the vacuum expectation value of the Higgs field gives masses to the W and Z gauge bosons. Contrary to massless vector bosons, which have two polarization states, massive bosons possess three. Where does the additional degree of freedom come from? These are exactly Goldstone modes from the Higgs field, a fact that is dubbed in physics folklore: "The gauge bosons acquire the extra degree of freedom by *eating* the Goldstone bosons".

Let us now study the physical parameters of our theory. It is useful to define a *weak mixing angle* θ_w and to rewrite the mass matrix in terms of it. We have

$$c_w = \cos\theta_w = \frac{g_2}{\sqrt{g_1^2+g_2^2}} \ , \qquad s_w = \sin\theta_w = \frac{g_1}{\sqrt{g_1^2+g_2^2}} \ , \tag{1.14}$$

such that the transformation to the physical fields becomes

$$\begin{pmatrix} A_\mu \\ Z_\mu \end{pmatrix} = \begin{pmatrix} c_w & -s_w \\ s_w & c_w \end{pmatrix}\begin{pmatrix} B_\mu \\ W_\mu^3 \end{pmatrix} \ . \tag{1.15}$$

We can use these eigenstates to rewrite the covariant derivative. It becomes

$$\begin{aligned} D_\mu =& \partial_\mu - i\frac{g_2}{\sqrt{2}}\left(W_\mu^+ I_W^+ + W_\mu^- I_W^-\right) + i\frac{1}{\sqrt{g_1^2+g_2^2}}Z_\mu(g_2^2I_W^3 + g_1^2Y_W) \\ & - i\frac{g_1g_2}{\sqrt{g_1^2+g_2^2}}A_\mu(I_W^3 + \tfrac{1}{2}Y_W) \ , \end{aligned} \tag{1.16}$$

where $I_W^\pm = \frac{1}{2}(\sigma_1 \pm i\sigma_2)$. We can now identify the coupling of the photon A_μ with the usual coupling of the electromagnetic field

$$e = \frac{g_1g_2}{\sqrt{g_1^2+g_2^2}} \ , \tag{1.17}$$

and also the electric charge quantum number Q with a combination of weak hypercharge and isospin which is known as the Gell-Mann Nishijima relation

$$Q = I_W^3 + \frac{Y_W}{2} \ . \tag{1.18}$$

Using this and the fact that

$$g_1 = \frac{e}{c_W} \quad \text{and} \quad g_2 = \frac{e}{s_W} \tag{1.19}$$

we can rewrite the covariant derivative once more:

$$D_\mu = \partial_\mu - \frac{i}{\sqrt{2}}(\frac{e}{s_w}W_\mu^+ I^+ + W_\mu^- I^-) - i\frac{e}{c_w s_w}Z_\mu(T^3 - s_w^2 Q) - ieA_\mu Q \tag{1.20}$$

we have therefore traded the gauge couplings g_1 and g_2 for the electric charge e and s_w which has to be determined experimentally. However, we find

$$m_w = m_z \sin\theta_w \ . \tag{1.21}$$

So, taking the Z boson mass and the couplings as input, the value of the W boson mass has become a prediction of our theory.

1.1.2 Fermionic part

For completeness, let us study how the Higgs field is also responsible for the masses of the fermions. Usual mass terms are forbidden by the gauge symmetry because left- and right-handed fields belong to different representations of $SU(2)_W$ and carry different $U(1)_Y$ charges. They are generated through the fermion field's Yukawa interaction with the Higgs field, as it will be shown below.

The left-handed fermions of each lepton (L) and quark (Q) generation are grouped into $SU(2)_W$ doublets

$$L'^L_j = \omega_- L'_j = \begin{pmatrix} \nu'^L_j \\ l'^L_j \end{pmatrix}, \quad Q'^L_j = \omega_- Q'_j = \begin{pmatrix} lu'^L_j \\ d'^L_j \end{pmatrix} \tag{1.22}$$

and the right-handed fermions into singlets

$$l'^R_j = \omega_+ l'_j, \quad u'^R_j = \omega_+ u'_j, \quad d'^R_j = \omega_+ d'_j, \tag{1.23}$$

where $\omega_\pm = \frac{1\pm\gamma_5}{2}$ is the projector on right- and left-handed fields, respectively, j is the generation index and ν, l, u and d stand for neutrinos, charged leptons, up-type quarks and down-type quarks, respectively. The color index for the strong interaction has been suppressed.

We can now write down the fermionic part of the Lagrangian:

$$\begin{aligned} \mathcal{L}_F = &\sum_i \left(\overline{L'}^L_i i\gamma^\mu D_\mu L'^L_i + \overline{Q'}^L_i i\gamma^\mu D_\mu Q'^L_i\right) \\ &+ \sum_i \left(\overline{l'}^R_i i\gamma^\mu D_\mu l'^R_i + \overline{u'}^R_i i\gamma^\mu D_\mu u'^R_i + \overline{d'}^R_i i\gamma^\mu D_\mu d'^R_i\right) \\ &- \sum_{ij} \left(\overline{L'}^L_i G^l_{ij} l'^R_j \Phi + \overline{Q'}^L_i G^u_{ij} u'^R_j \tilde{\Phi} + \overline{Q'}^L_i G^d_{ij} d'^R_j \Phi + h.c.\right). \end{aligned} \tag{1.24}$$

The first two lines are responsible for the dynamics and the interactions of the fermion fields with the electroweak gauge fields; the last line contains the Yukawa interaction terms which govern the interaction with the (yet unbroken) Higgs field.

In the covariant derivative D_μ, eq. (1.2), acting on right-handed fermions the term involving g_2 is absent, since they are $SU(2)_W$ singlets. The $U(1)_Y$ charges are chosen such that the electric charges are reproduced, using equation (1.18).

The primed fermion fields in equation (1.24) are the eigenstates of the electroweak gauge interaction. In this basis G^l_{ij}, G^u_{ij} and G^d_{ij} are the Yukawa coupling matrices. The charge conjugated Higgs field $\tilde{\Phi}$ is defined as

$$\tilde{\Phi} = \begin{pmatrix} \phi^{0*} \\ -\phi^- \end{pmatrix} \quad \text{with } \phi^- = \left(\phi^+\right)^* . \tag{1.25}$$

There is no Yukawa coupling for the neutrinos since there are no right-handed neutrinos in the Standard Model. Therefore, neutrinos remain massless in this theory. By now, however, it is established that neutrinos possess a very small mass. In principle, right-handed neutrinos could be added without problem but it is still not known whether they are Dirac fermions like the others in the Standard Model or are in fact Majorana fermions, in which case their mass generation mechanism needs to be different from the Higgs mechanism. However, due to the extreme smallness of the mass and their almost vanishing probability of detection, this does not play a role in traditional accelerator experiments.

Turning back our attention to the Yukawa terms we obtain the mass terms when the Higgs field obtains a vacuum expectation value. To find the mass eigenstates, the G^x_{ij} have to be diagonalized. The mass and interaction eigenstates are related by unitary transformations:

$$L'^L_i = U^{ij}_L L^L_j, \quad Q'^L_i = U^{ij}_Q Q^L_j , \quad u'^R_i = U^{ij}_u u^R_j , \quad d'^R_i = U^{ij}_d d^R_j . \tag{1.26}$$

This, on the other hand, introduces a mixing of the mass eigenstates in the interactions of the W boson. With the unitary matrix

$$V^{ij} = U^{ik}_{u,L} U^{kj}_{d,L\dagger} \tag{1.27}$$

the interactions of the W bosons become

$$\begin{aligned} &\frac{e}{\sqrt{2}s_w}\overline{u}^L_i \gamma^\mu V_{ij} d^L_j W^+_\mu + \text{h.c.} \\ +&\frac{e}{\sqrt{2}s_w}\overline{\nu}^L_i \gamma^\mu l^L_j W^+_\mu + \text{h.c.} , \end{aligned} \tag{1.28}$$

where 'h.c.' stands for the hermitian conjugate of the preceding expression. The mixing matrices cancel in the interaction terms of the Z boson and the photon. Since the neutrinos in the leptonic sector remain massless, they are degenerate. Therefore, U^L_ν can be chosen such that there is no mixing in the leptonic sector. The matrix V_{ij} is called CKM-matrix after Nicola Cabbibo, Makoto Kobayashi and Toshihide Maskawa. Nicola Cabbibo introduced the idea of a mixing of states and first wrote this matrix down for two generations and the latter two generalized it to a third generation. It describes the unitary transformation from the primed interaction to the unprimed mass eigenstates.

A consequence of the fact that the masses are generated by the Higgs Yukawa couplings is that the interaction strength between a fermion and the Higgs is proportional to its mass. The top and bottom quarks are therefore the most important fermions in Higgs phenomenology.

1.1.3 Triple gauge couplings

The electroweak $SU_W(2) \times U_Y(1)$ theory together with the Higgs mechanism is a beautiful theory, as it could be seen in the previous subsections (maybe aside from the fact that of the 17 parameters, 13 stem from the fermion mass sector and weak mixing sector). However, as it has been mentioned previously, there are compelling reasons that there is physics beyond the Standard Model that stabilize the electroweak scale.

The problem can be stated as follows: The natural scale at which gravity becomes as strong as the strong and the electroweak forces is the Planck-scale. This scale is about 10^{17} times larger than the natural scale of the electroweak force. So far there is no experimentally confirmed explanation for this difference in hierarchy. Furthermore, the Standard Model Higgs is a scalar particle (which has been tentatively confirmed by the LHC experiments). Scalar particles are very susceptible to quantum corrections and are thus very sensitive to every particle that couples to them. Of the known particles, especially the top quark generates highly divergent contributions which need to be canceled by a counterterm, which has to be fine-tuned to incredible precision in order to stabilize the electroweak scale against the cutoff at the Planck-energy.

A possibility to protect the Higgs mass against these huge corrections and therefore avoid the so-called "fine-tuning problem" is supersymmetry, an additional symmetry in nature which postulates for every existing particle a so-called super-partner particle. Their masses are expected to lie in proximity of the electroweak scale. Other ideas are the introduction of small additional spatial dimensions which predict particle resonances at energies in the TeV range, e.g. only a couple of times larger than the electroweak scale.

Without going into much detail, these two examples underline that there is compelling reason for physics in the TeV range. The LHC has been built to probe these regions and hopes are high that the mechanism stabilizing the electroweak scale will be discovered there. How could this happen? First of all, through direct production and subsequent decay to SM particles which are then in turn detected. But, also in the event that the new physics particle states are too heavy to be produced directly, they can have an indirect influence on Standard Model observables through loop effects. One place where these effects could show up are the so-called *triple gauge couplings* (TGCs), the couplings of three electroweak gauge bosons. While some, such as $W^+ W^- Z$, exist in the Standard Model and could could be modified by BSM physics, others, for example $Z Z \gamma$, are excluded there and could be generated by nonstandard physics [11].

In the SM the relevant parts of the Lagrangian are given by for the fields $V = Z, \gamma$, denoting the Z boson and photon,

$$\mathcal{L}^{\mathrm{SM}}_{WWV} = i g_{WWV} \left[(W^+_{\mu\nu} W^-_{\mu} - W^-_{\mu\nu} W^+_{\mu}) V^{\nu} + W^+_{\mu} W^-_{\nu} V^{\mu\nu} \right] , \tag{1.29}$$

where $W_{\mu\nu} = \partial_\mu W_\nu - \partial_\nu W_\mu$ denotes the W field-strength tensor and analogously $V^{\mu\nu} = \partial_\mu V_\nu - \partial_\nu V_\mu$. The couplings are $g_{WWA} = -e$ and $g_{WWZ} = -e \cot\theta_w$. In the Standard Model the other triple gauge couplings involving only photons and Z bosons vanish, since neither of them self-interact, the Z boson is electrically neutral and the photon does not carry weak charge.

In order to parametrize possible low energy effects of New Physics the effective Lagrangian approach is often used. It has the advantage that on these parameters experimental bounds can be derived independently of the underlying model. A general parametrization is given by

$$\mathcal{L}^{\mathrm{eff}}_{WWV} = i g_{WWV} \Big[g^V_1 (W^+_{\mu\nu} W^-_{\mu} - W^-_{\mu\nu} W^+_{\mu}) V^{\nu} + \kappa_V W^+_{\mu} W^-_{\nu} V^{\mu\nu}$$

$$+ \frac{\lambda_V}{m_W^2} W_\mu^{+\nu} W_\nu^{-\rho} V_\rho^\mu \Big] \ . \tag{1.30}$$

For the choice $\lambda_V = 0$ the anomalous neutral TGCs disappear from the Lagrangian and for $g_1^V = \kappa_V = 1$ the effective Lagrangian reduces to the SM one (1.29). Electromagnetic gauge invariance requires $g_1^\gamma = 1$; the changes to the other couplings from the Standard Model limits are denoted by Δg_1^Z and $\Delta\kappa_V$. Since these contributions break gauge invariance and lead to divergent cross sections at high energies, a cutoff scale Λ has to be introduced that leads to the suppression of these contributions at large $\sqrt{s}$. At this scale the effective description of the New Physics responsible for the anomalous couplings breaks down. The suppression for a generic contribution is defined as

$$\alpha(\hat{s}) = \frac{\alpha_0}{(1 + \frac{\hat{s}}{\Lambda^2})^2} \ , \tag{1.31}$$

where $\hat{s}$ denotes center-of-mass energy of the colliding partons. The bounds on the deviations derived from experiment are in general dependent on Λ. However, as it will be seen shortly in figures 1.3 and 1.4, this dependence is weak.

Further reasonable assumptions can be made that introduce further dependence among the effective parameters. For example, the "LEP scenario" assumes that the anomalous couplings arise from dimension-6 operators and electroweak symmetry is broken by a light SM Higgs boson. This then leads to

$$\Delta\kappa_\gamma = -\frac{c_w^2}{s_w^2}(\Delta\kappa_Z - \Delta g_1^Z) \text{ and } \lambda_\gamma = \lambda_Z \ . \tag{1.32}$$

The free parameters in this situation, Δg_1^Z, $\Delta\kappa_z$ and λ_Z can be further reduced by requiring equal couplings of the $SU(2)$ and $U(1)$ gauge bosons to the Higgs field. This requirement is known as the "HISZ scenario" and introduces the constraint

$$\Delta g_1^Z = \frac{\Delta\kappa_\gamma}{2c_w^2} \ . \tag{1.33}$$

Similarly, the anomalous couplings in the $Z-\gamma$-sector can be parametrized using vertex functions as [12]

$$g_{ZZV}\Gamma_{ZZV}^{\alpha\beta\mu} = e\frac{P^2 - M_V^2}{M_Z^2}\left[if_4^V(P^\alpha g^{\mu\beta} + P^\beta g^{\mu\alpha}) + if_5^V \epsilon^{\mu\alpha\beta\rho}(q_1 - q_2)_\rho\right] \ , \tag{1.34}$$

where P denotes the momentum of the incoming particle $V = Z, \gamma$. Also in this case the couplings f_4^V and f_5^V have to be regulated using the prescription (1.31).

In the next subsection it will be discussed how these couplings can be measured at a hadron collider.

1.1.4 Diboson production

Diboson production, that is, the production of any two electroweak gauge bosons in the final state, i.e. $\gamma\,\gamma$, $\gamma\,Z/W$, Z, Z, $W\,W$ or $W\,Z$ is an important and interesting class of processes. First of all, with both Quantum-chromodynamics and electroweak theory well established, they are an important benchmark process at colliders with, depending on the decay mode, a clear experimental signature. With the high energies and high luminosity at the LHC they are expected to become high-precision observables. It is also an irreducible

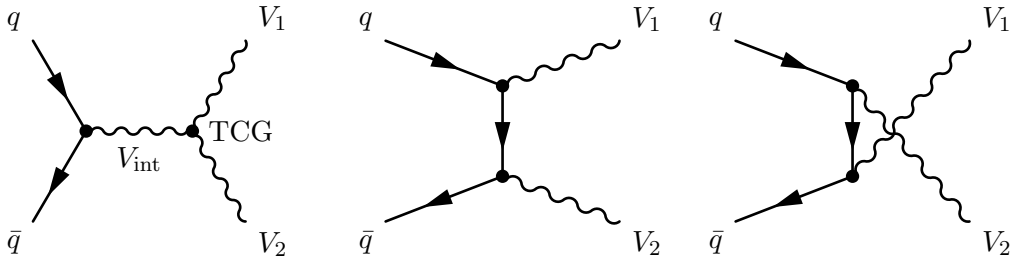

Figure 1.1: The Feynman diagrams contributing to diboson production at hadron colliders at lowest order. In the left diagram the contribution of the triple gauge coupling can be seen. Its value and existence depend on the bosons V_1, V_2, V_{int}.

background for the Higgs decay $H \to W^+W^-$ and $H \to ZZ$ or any new particles that decay to a gauge boson pair. Moreover, new physics effects are expected to show up indirectly in modifications to the triple gauge boson couplings via loops. As it can be seen from the leading order diagrams in figure 1.1, the TGCs already enter at this order, albeit having to compete with the additional diagrams. The power to constrain these couplings does not come from a measurement of total cross sections but rather studying more exclusive quantities such as differential distributions. Often, anomalous TGCs are looked for in the p_T (transversal boson momentum) distributions of diboson events or angular correlations of the decay products because the contribution of anomalous gauge couplings to the total cross section is small. But it is also in the differential cross sections that higher order corrections have been shown to be important and strongly dependent on p_T, both for electroweak and QCD corrections [11, 13].

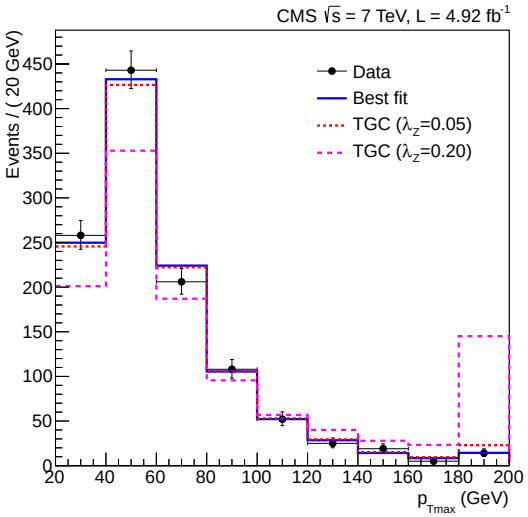

Figure 1.2: Leading lepton p_T distribution data in WW pair production at CMS overlaid with the best-fit of a two-dimensional $\lambda_Z - \Delta g_1^Z$ model and two distributions for different parameter choices [14]. The high-p_T bin also contains the overflow.

As an illustration the leading lepton p_T distribution in WW pair production measured at CMS is shown in figure 1.2. It can be clearly seen how the high p_T bins are affected the most by different choices of λ_Z and Δg_1^Z.

Measurements constraining the TGCs have been performed at LEP and at Tevatron and lately also at the LHC, where the bounds have quickly become competitive to those established previously. In the summary plots in Figure 1.3 current bounds from both LHC experiments [14–17] for the charged triple gauge couplings are given in comparison to older LEP and Tevatron results.

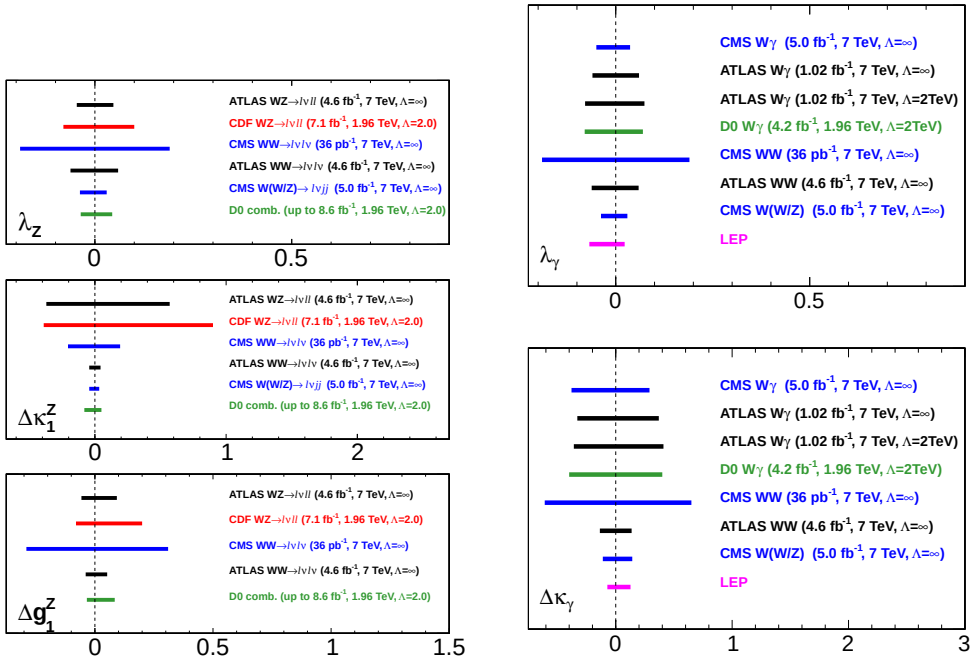

Figure 1.3: Summary plot of the current collider bounds on deviations of the Standard Model gauge boson couplings reproduced from [18]. The left panel contains the limits for anomalous $WW\gamma$ couplings extracted from $W\gamma$ and WW final states. The right panel shows the bounds on anomalous $WW\gamma$ and WWZ TGCs in extracted from the WW, $W\gamma$ and WZ final states.

So far, all results are compatible with the Standard Model hypothesis. It is expected that the experiments will reach a precision at the per mill level at the LHC with 100fb^{-1} for the charged and neutral anomalous couplings, whereas many BSM-models, such as supersymmetry, only induce couplings at the level of 10^{-4} [12].

A more precise Standard Model prediction for these processes helps increase the sensitivity for anomalous and modified triple gauge boson couplings. Before assessing the current state of computations for these processes, let us quickly introduce the second pillar of the Standard Model.

1.2 A short historical introduction to Quantum-chromodynamics

This second pillar of the SM is called *Quantum-chromodynamics* and is a nonabelian gauge theory based on $SU(3)$ describing the strong nuclear force acting among the quarks.

In the fifties and sixties of the past century high energy particle physics experiments were in the lucky state of discovering many new, seemingly elementary particles. The number was so high that this was also dubbed the *particle zoo*. Nevertheless, among these particles many had similar properties which suggested that there had to be a more

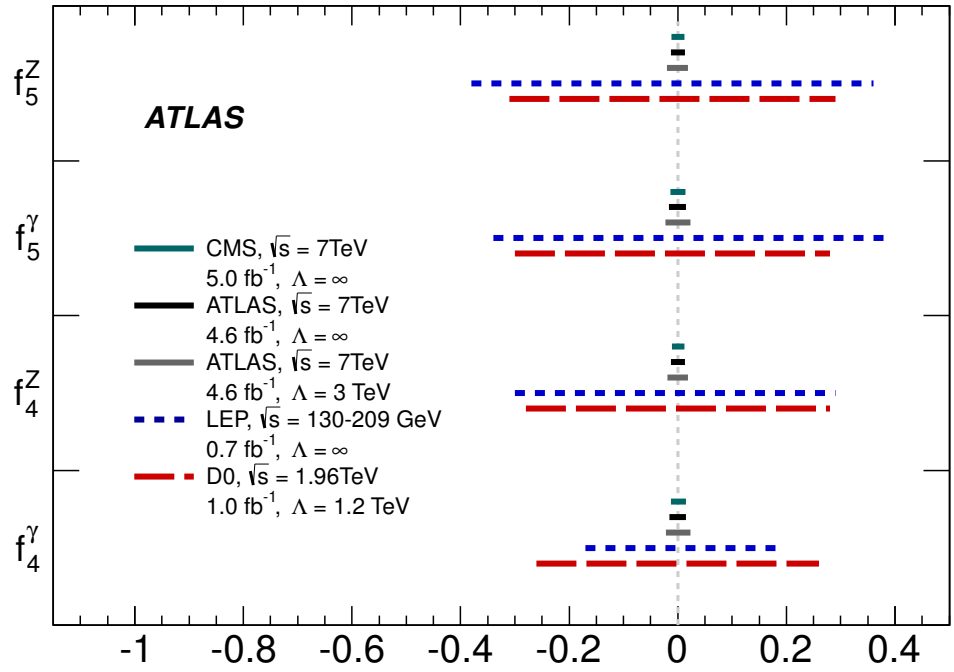

Figure 1.4: Summary plot of the current collider bounds on anomalous neutral gauge boson couplings reproduced from [19], which incorporates results from [20].

elegant way of describing them. In 1964, Murray Gell-Man and George Zweig suggested that all these discovered particles could be classified using three new fermions, the quarks, as constituents [21, 22]. They could group the particles into *hadrons* consisting of three quarks and *mesons* consisting of a quark and antiquark. However, new theoretical problems appeared: According to the quark model, the Δ^{++} would consist of three up-type quarks with parallel spins. Therefore, the spin-part of the wave function had to be totally symmetric under the exchange of any two quarks. Due to the Pauli exclusion principle, which states that the total wave function of a state with identical fermions has to be antisymmetric under the exchange of them, the spacial wave function of this particle had to be antisymmetric. But any potential that would make sense resulted in a spatially symmetric ground state. Not even a year later this problem was circumvented by Oscar W. Greenberg and the collaboration of Moo-Young Han and Yoichiro Nambu by postulating an additional degree of freedom for the quarks: the color charge [23, 24]. But since free quarks were not observed, many theoretical physicists like Gell-Mann at that time believed that the quarks were in fact purely mathematical constructs. On the other hand theorists like Richard Feynman argued that the jets in high-energy experiments showed in fact that quarks were real particles (which he called partons).

In 1973 *asymptotic freedom* was discovered by David Gross, Frank Wilczek and David Politzer [25, 26]. It means that the interaction strength of particles becomes weaker with increased energy or lower distance. With this concept they could describe how on the one hand quarks could act as single particles at high energies, manifesting themselves as jets,

but on the other hand could never be observed directly.

In 1974 and 1977 two more quarks, the charm and bottom, were discovered at detector experiments at the Stanford Linear Accelerator Center (SLAC), the Brookhaven National Laboratory (BNL) and at Fermilab. Together with the evidence for gluons in three-jet-events at the Deutsches Elektronen Syncrotron (DESY) in 1979, the evidence for QCD was firmly established. A spectacular proof that the theory had also been understood at the loop level and that perturbative computations could successfully be performed in QCD was the confirmation of the computed scaling behavior of QCD, which was first observed in deep inelastic scattering experiments at SLAC and Fermilab, to high precision at DESY's H1 and ZEUS detectors.

Before the bottom quark was discovered, it had already been predicted in 1973 by Makoto Kobayashi and Toshihide Maskawa to explain CP-violation in the electroweak sector [27]. The Glashow-Iliopoulos-Maiani (GIM) mechanism then required that it had to have a partner, the top quark. It took 18 years for this prediction to be confirmed at the Tevatron in 1995 but what is interesting is that through high precision computations and measurements its existence in a certain mass range was already known before it could be detected directly. This is the prime example of the power of indirect methods in quantum field theories.

When computing perturbative corrections to diboson production at the LHC Quantum-chromodynamics has to be taken into account for the reasons described in the following.

1.3 Perturbative Corrections to Diboson production

The problems one encounters when attempting to make QCD predictions are manifold. In order to predict quantities in a scattering theory, such as cross-sections or ratios thereof, perturbative expansions have to be performed in the coupling strength of that theory. In electroweak theory, where the coupling constant is very small and only grows too large at very high energies which are irrelevant to experiment, this approach works very well. In QCD one faces two problems.

First of all the coupling constant for this theory is rather large even at high energies, therefore requiring more terms in the expansion for a prediction with a reasonable error. Secondly, due to the consequences of asymptotic freedom the coupling constant becomes infinitely large at low energies, invalidating the perturbative expansion and calling for a different treatment in this regime. This also means that, for a proper description of experiment, we have to take into account that it is not free quarks that collide and are detected in the final state but that the colliding and observed particles are hadrons with all their internal structure.

Luckily, factorization theorems allow to split the problem into parts. They allow to describe separately the high-energy interaction of the partons, how they turn into jets, that is, streams of particles that fly into the same direction, and how the jet constituents then turn into hadrons that are detected in the experiment. While the latter two allow for a general treatment, the former is highly process-dependent. Another problem that both theories face at higher orders in perturbation theory is the appearance of infrared divergences due to the vanishing mass of the force carriers. These only cancel after combining them with the infinities coming from the virtual exchanges of these particles.

A higher order correction needs multiple ingredients: The purely virtual and the real corrections. As it is illustrated in figure 1.5, the virtual corrections contain the same number of initial and final state particles as the process considered but contain both

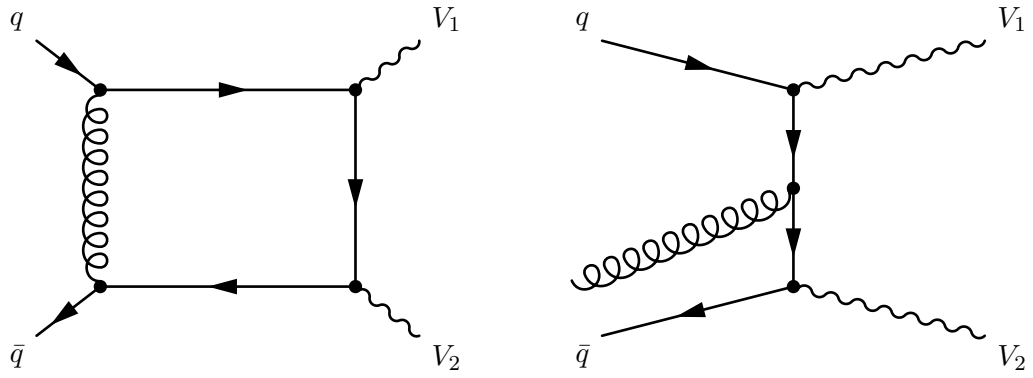

Figure 1.5: Illustrative Feynman diagrams for diboson production at next-to-leading order in QCD. On the left side a typical virtual contribution diagram is shown. On the right: a real radiation contribution diagram.

infrared (IR) and ultraviolet (UV) divergences. Ultraviolet divergences appear because the loop integral diverges for very large energies. They can be renormalized and are well understood. However, they introduce an additional scale, the *renormalization scale*, which can be freely chosen. At all orders in perturbation theory a physical quantity must not depend on this scale but at finite orders its variation around a suitable choice (usually the typical scale of the interaction) is a measurement of theoretical error. The IR divergences have to be treated separately.

The real corrections contain an additional gluon in the initial or final state that is very soft, which means it has a very low energy and/or is collinear to one of the QCD initial or final state particles, such that it cannot be resolved in the detector separately or ends up in one of the hadrons of the final state. Equally, this contribution is infrared divergent, but together with the virtual corrections and a suitable prescription how to group particles into a jet, they form a finite result.

In the processes discussed here, that is the production of two weak bosons at a hadron collider, both electroweak and QCD higher order corrections play a role. The electroweak one-loop corrections for the production of on-shell W^+W^-, ZZ,$ZW^\pm$,$Z\gamma$ and $\gamma\gamma$ production have been computed and discussed in many references, e.g. [28–33], the most recent and complete being [13] where it was shown that the electroweak corrections have an effect on the shapes of the p_T distributions of the decay products, making this an important contribution to the search for anomalous gauge boson couplings.

The next-to-leading order QCD corrections to this process have been computed and implemented in Monte Carlo generators [34–41]. Due to the size of the strong coupling constant, they are important.

At the LHC, where hadrons collide, another effect has to be taken into account at higher orders. Protons do not only consist of three quarks but also of a 'sea' of virtual gluons and quark-antiquark pairs that are exchanged between the quarks. When two protons collide, there exists also a probability that two of these virtual gluons interact and have enough energy to produce a diboson final state through a quark loop. For this reason the cross section is a convolution of the partonic cross section with the probability of finding gluons of these energies inside the colliding protons. These *parton distribution functions* are nonperturbative quantities and have to be measured by experiment and therefore carry an inherent uncertainty. Furthermore, the theoretical treatment introduces an additional scale, the so-called *factorization scale*, which introduces additional freedom. This depen-

dence can be seen as a measure of theoretical error. At the LHC, where the collision energy will reach previously unattained levels, this process will gain in importance when compared to the production via quarks in the initial state, even though it is formally of higher order. Computations of the so-called "gluon fusion" amplitudes have become available [42–46] at the one-loop level. For example, this contribution to the WW background for the decay $H \to WW$ amounts to 35% in the relevant kinematical region [45]. Similarly, there is also a small content of virtual photons contained inside a quark, which can scatter as well. This has been shown to have an effect on diboson production at hadron colliders [28].

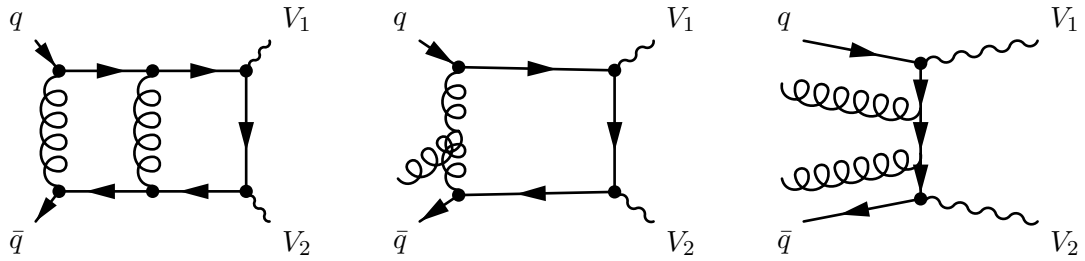

Figure 1.6: Illustrative Feynman diagrams for diboson production at next-next-to-leading order in QCD. From left to right: a typical virtual contribution, real-virtual and double-real diagram.

The fact that the dependence on the renormalization and factorization scales is large and decreases with higher orders in perturbation theory on one hand and the size of the strong coupling constant create a need for higher order computations in QCD.

For a prediction at the next-to-next-to leading order (NNLO) multiple ingredients are needed in order to properly account for the infrared structure of the theory, which are illustrated in figure 1.6. First of all, the two-loop matrix elements $p_1p_2 \to V_1V_2$ for the process under consideration, where p_1 and p_2 are generic partons, that is, gluons or quarks. Secondly, the so-called "real-virtual" contributions of the form $p_1p_2 \to V_1V_2 + p_3$, which is formally of one-loop order and the "double real radiation" contributions $p_1p_2 \to V_1V_2 + p_3p_3$ which have to be taken into account at the tree level. Again, each of these contributions is infrared divergent, but in the sum all infinities cancel, producing a finite result.

The real-virtual contributions are themselves NLO corrections to the production of a vector boson pair with an additional jet. They have been computed in the past for all relevant processes, i.e. for $\gamma\gamma + \text{jet}$ [47], $\gamma W + \text{jet}$ [48, 49], $WW + \text{jet}$ [50, 51], $ZZ + \text{jet}$ [52] and $WZ + \text{jet}$ [53] production. The double virtual contributions have also been computed a long time ago [54]. This makes the two-loop virtual contributions the last missing ingredient.

In the past, these contributions have been computed for diphoton production [55, 56], which were combined with the other contributions into a Monte-Carlo program in [57]. In [58] the two-loop amplitudes for $q\bar{q} \to V\gamma$ were computed, using results from [59, 60].

Two additional building blocks will be presented in this work. Firstly, the contributions gluon fusion contribution amplitudes $gg \to Z\gamma$ were computed at the two-loop level [61], which will be discussed in chapter 4. Secondly, the planar master integrals for the production of equal-mass gauge bosons in massless QCD were computed [62] as described in chapter 5. These integrals present an important step towards the computation of the two-loop virtual amplitude of $W\,W$ and $Z\,Z$ production.

The additional massive particle in the final state complicates the computations insofar,

as it makes the handling the functions that the result is expressed in more complicated. These functions are called "Multiple Polylogarithms" (MPLs) or "Generalized Harmonic Polylogarithms" (GHPLs) in the literature. In the past years much effort has been put into understanding MPLs better [63, 64], making use of developments in number theory and algebra [65, 66]. The multiple polylogarithms form an algebra and can be equipped with additional structures, such that the often cumbersome and tedious manipulations on them become trivial algebraic relations in a certain tensor space, to which the expression has been translated. This expression can then be translated back into the function space. This is commonly called the *symbol formalism*, which has been generalized to the *coproduct* [67, 68]. These two ideas have produced spectacular results, such as the shortening of a particular expression of an amplitude 17 pages long to a two-liner [64] or making the computation of certain three-loop integrals possible [69]. There have also been attempts to bypass the integration of Feynman integrals by writing down the symbol of an amplitude using physical and consistency considerations [70].

In this work, these algorithms are used to write results in a shortened form (for the $gg \to Z\gamma, g$ amplitudes computed in chapter 4) and to perform various transformations in order to compute the planar two-loop integrals for the production of two massive gauge bosons discussed in chapter 5. More precisely, the derivation of various boundary conditions during the solution of the differential equations, analytical continuations to the physical region of the final results and the transformation of a particular differential equation was made possible using these techniques. The mathematical concepts and the algorithms are described in chapter 3, which were implemented in `mathematica` packages. Their usage is described in various examples, also illustrating the workings of the algorithms, in chapter D. The documentation of all packages and their relationship can be found in appendix C.

But before starting this discussion, let us study the prospects of detecting a small, well-motivated extension to the Standard Model gauge sector at the early LHC. As it will be discussed in the following this model can address some of the questions raised in the beginning of this chapter.

2

Dark Higgs Models at the 7 TeV LHC

The original work for this chapter was done in collaboration with José Zurita and appeared in [71] at a time where the Higgs boson was not yet discovered. Even though this is by now the case, most of the discussion is still valid. The conclusions have been amended to reflect the newest developments.

2.1 Introduction

In the beginning of the previous chapter it was stated that there is evidence for additional, "dark" matter in the universe. This matter cannot be baryonic, e.g. made of protons and neutrons, but is needed to explain phenomena as diverse as the observed rotation curves of galaxies, the evolution of structure from the tiny density fluctuations at the time the cosmic microwave background (CMB) was formed to the present day with stars, galaxies and galaxy clusters. It could already be observed through gravitational lensing of the light from remote galaxies by Dark Matter distributions closer to us.

Naturally, there is the possibility of explaining this matter as an particle which does not interact electromagnetically. This particle has yet to be discovered. From the observed large scale distribution of galaxies we can deduce that this matter is necessarily cold, that means non-relativistic. Otherwise the fluctuations in the CMB would have been washed out and no galaxies could have been formed by now. This is why the neutrinos, the only stable Standard Model particles that are neutral, cannot account for Dark Matter.

During the Big Bang, this additional particle is in thermal equilibrium, i.e. annihilations and creation of Dark Matter (DM) particles happen at the same rate. Due to the expansion of the universe and subsequent cooling the density drops so much that the annihilation rate drops below the production rate and the average energy of SM particles is not large enough any more to produce new Dark Matter. "Freeze-out" has occurred. The cross section required to produce the correct observed Dark Matter density which is of order 10^{-40} cm^2 is of order of magnitude of those of the weak interaction. For this coincidence it is a popular idea that the Dark Matter particle is a *weakly interacting massive particle* (WIMP).

There is the possibility of incorporating a Dark Matter particle into many theories, for

example in supersymmetry with R-parity the lightest supersymmetic particle is stable and provides for a natural candidate. Also axions, the particles postulated by Peccei-Quinn symmetry to solve the strong CP-problem, could be such a Dark Matter particle.

In recent years, models which extend the Standard Model by one or more additional gauged singlet symmetries have come under renewed interest. Many theories often encompass one or more beside the Standard Model $U(1)_Y$ hypercharge. Compelling motivation for these extensions arises from grand unified theories (GUT) and from string theory. Their phenomenology of new abelian gauge groups has been widely studied in the literature [72–82].

But the renewed interest stems from the observation that these extensions can incorporate models for Dark Matter easily. The extra gauge symmetry may be hidden from the SM particles, which are singlets under the new force: they constitute the *visible* sector. The particles charged under the new $U(1)_D$ and singlets under the SM gauge groups are often referred to as the *dark* (or hidden, or secluded) sector.

The connection between the *dark* and *visible* sectors is established through mixing operators. One candidate term is kinetic mixing of $U(1)_Y$ with $U(1)_D$ [83, 84]. Since cosmological considerations (like Big Bang Nucleosynthesis) severely constrain a massless gauge boson, the extra $U(1)$ symmetry has to be broken. Its breakdown can be achieved through the introduction of a new Higgs boson, h_D, which can naturally mix with the SM Higgs [85–89], thus providing an extra *portal* between the two worlds. These extensions of the SM have also been studied in the context of electroweak phase transition (EWPT) [90–92] and Dark Matter (DM) since the dark sector provides natural DM candidates [93–113]. In [114, 115] the observation was made that an extra $U(1)_D$ GeV gauge boson would be able to naturally explain the anomalies observed in indirect Dark Matter detection experiments, like the reported PAMELA result on the positron fraction [116]. However, current studies also incorporating recent data from AMS-02 have found it difficult to explain this excess without having to limit the annihilation to leptons exclusively in order to avoid the constraints from gamma ray experiments [117].

While the extra $U(1)$ models are very constrained from current experimental data [118–122], the non-observation of a Higgs boson at the time of this study yields very mild bounds on the Higgs portal parameters. In this chapter we explore the constraints and detectability prospects of the Higgs sector at colliders. Recent work [123] was focused in the potential signatures at the LHC for large luminosities ($\mathcal{O}(30)$ fb^{-1}, see also Refs. [124–131] for older studies). Our interest resides in the reach of the early LHC data ($\sqrt{s} = 7$ TeV, with a total integrated luminosity less or equal than 15 fb^{-1}). Similar work was already done in the context of the MSSM in ref [132].

Due to the mixing with hypercharge, the dark gauge boson can be in conflict with electroweak precision data, such as the Z mass or the effective weak mixing angle. Thus the most natural options, already considered in the literature, is to have either a very heavy (TeV scale) Z' [133–135] or very light (GeV) boson [136–139]. The latter scenario is well-motivated when looking to find a unified explanation of recent results of DM, as suggested in ref [114]. In this work we take an agnostic attitude and consider the Z' mass a free parameter.

This chapter is organized as follows: in section 2.2 we review the model under consideration. In section 2.3 we explain in detail the scan of the parameter space, all the constraints under consideration and the LHC expected reach for different scenarios. Section 2.4 contains the numerical results of our analysis. Finally, we discuss the implications of the Higgs discovery and current LHC results and conclude in section 2.5.

2.2 Model Review

Generic dark sector models were discussed in detail in the literature (e.g. [87]). In this section we briefly review the model used in this study. The relevant parts of the Lagrangian can be written as follows,

$$\mathcal{L} = \mathcal{L}_{SM} + \mathcal{L}_{Dark} + \mathcal{L}_{mix}\,, \tag{2.1}$$

where we have split the contribution into the SM-piece, which corresponds to the Lagrangian in section 1.1, the dark sector and the mixing between the two sectors. For the dark sector, we would like to add the minimum field content. Thus, we include a new dark gauge boson X and a dark Higgs field H_D. The dark sector might contain fermions, which are SM singlets and charged under $U(1)_D$. These fermions are, however, irrelevant in the present context. The dark Higgs field will give mass to the X boson after spontaneous breakdown of the gauge symmetry. We pick a $U(1)$ gauge group for simplicity; that is not to say that the dark sector has to be that simple, but that we choose to parametrize it in a simple way. It is clear that many other, richer possibilities (from a phenomenological point of view) can also be considered [1]. Under these assumptions, the dark Lagrangian reads

$$\mathcal{L}_{Dark} = (D_\mu H_D)^\dagger (D_\mu H_D) + \mu_D H_D^\dagger H_D - \lambda_D (H_D H_D^\dagger)^2 - \frac{1}{4} X_{\mu\nu} X^{\mu\nu} + \dots \tag{2.2}$$

where $D_\mu = \partial_\mu + ig' Y B_\mu + igT^a W_\mu^a + ig_D Q_D X_\mu$ is the covariant derivative, g_D the dark $U(1)_D$ gauge coupling, $X_{\mu\nu}$ its gauge strength tensor and Q_D is the charge under the dark force. The last term is the kinetic term for the dark gauge field, while the remaining terms correspond to the kinetic term for the complex scalar Higgs and the dark Higgs potential. The ellipsis stands for other terms not relevant for this study. The *mixed* Lagrangian will depend upon how X and H_D couple to the SM. In our setup, it is natural to consider kinetic mixing between X_μ and B_μ and a mixing term in the Higgs potential [85,86], since these two are the only renormalizable operators relating X and H_D to the SM. [2] With these assumptions we have

$$\mathcal{L}_{mix} = \frac{\epsilon_A}{2} B_{\mu\nu} X^{\mu\nu} + \epsilon_H (H H^\dagger)(H_D H_D^\dagger), \tag{2.3}$$

where $B_{\mu\nu}$ is the $U(1)_Y$ hypercharge field strength tensor and H is the SM Higgs doublet. It is well known that ϵ_A has to be small in order to be compatible with current experimental limits (see [121] and references therein). The constraints on ϵ_H are less stringent, given our current knowledge of the Higgs sector.

For the sake of completeness, we write down the SM Lagrangian,

$$\begin{aligned}\mathcal{L}_{SM} \;=\; & (D_\mu H)^\dagger (D_\mu H) + \mu H H^\dagger - \lambda (H H^\dagger)^2 \\ & + \sum_f y_f (\bar{f}_L H f_R + \text{ h.c}) - \frac{1}{4}(B_{\mu\nu} B^{\mu\nu} + W_a^\mu W_\mu^a) + \dots,\end{aligned} \tag{2.4}$$

where y_f is the Yukawa coupling for the SM fermion f and the ellipsis indicates the presence of other terms not relevant for our study.

1. One could argue that the details of the dark sector at energies above LEP and SLC could be absorbed into the low energy GeV scale parameters by integrating out the heavy sector. Another option is to work with a different dark gauge group. We will stick, for the sake of simplicity, to this minimum extra added field content.

2. As noted in ref [130], there are other such operators if the dark fermions are also taken into account.

2.2.1 Gauge sector

In order to derive the interactions in the mass eigenstate basis, we have to proceed in several steps. First, one has to diagonalize the kinetic terms for the gauge bosons. This can be achieved by performing a field redefinition of B_μ and X_μ. After this, one finds that the covariant derivative has changed in such a way that now the dark sector interacts directly with the B_μ. Since we want the $U(1)_D$ gauge group to be broken, the vacuum expectation value of H_D will contribute to the masses of the Z and the Z', while the photon will remain massless.

The Lagrangian involving both $U(1)$ strength tensors is given by

$$\mathcal{L} = -\frac{1}{4}\big(B_{\mu\nu}B^{\mu\nu} + X_{\mu\nu}X^{\mu\nu} - 2\epsilon_A B^{\mu\nu}X_{\mu\nu}\big). \tag{2.5}$$

In order to diagonalize the kinetic term, we perform the following redefinition of the fields [82] first:

$$B_\mu \to B_\mu + \frac{\epsilon_A}{\sqrt{1-\epsilon_A^2}}X_\mu\,, \qquad X_\mu \to \frac{1}{\sqrt{1-\epsilon_A^2}}X_\mu\,. \tag{2.6}$$

Then the covariant derivative reads [3]

$$D_\mu = \partial_\mu + ig'YB_\mu + igT^3W_\mu^3 + i\left(g_D\frac{Q_D}{\sqrt{1-\epsilon_A^2}} + g'\frac{\epsilon_A Y}{\sqrt{1-\epsilon_A^2}}\right)X_\mu\,, \tag{2.7}$$

and the mass matrix of the neutral gauge bosons becomes

$$m_{Z_0}^2\begin{pmatrix} s_W^2 & -c_W s_W & a s_W^2 \\ -c_W s_W & c_W^2 & -a c_W s_W \\ a s_W^2 & -a c_W s_W & a^2 s_W^2 + \Delta \end{pmatrix}, \tag{2.8}$$

where s_W, c_W are the sine and cosine of the usual SM electroweak mixing angle and

$$m_{Z_0}^2 = (g^2+g'^2)\frac{v^2}{4}, \qquad m_{X_0}^2 = g_D^2\frac{v_D^2}{4(1-\epsilon_A^2)}, \qquad \Delta = \frac{m_{X_0}^2}{m_{Z_0}^2}, \qquad a = \frac{\epsilon_A}{\sqrt{1-\epsilon_A^2}}\,. \tag{2.9}$$

One of the mass eigenvalues is zero, corresponding to the photon eigenstate, and the two others are given by

$$M^2 = \frac{m_{Z_0}^2}{2}\left[(1+s_W^2a^2+\Delta) \pm \sqrt{(1+s_W^2a^2+\Delta)^2 - 4\Delta}\right]. \tag{2.10}$$

Due to the smallness of ϵ_A it is well justified to take the gauge boson masses at their tree level values, namely, to assume $m_Z = m_{Z_0}$ and $m_{Z'} = m_{X_0}$. We have numerically checked that this approximation has an error below 0.02 %. The relation between mass and interaction eigenstates is given by

$$\begin{pmatrix} B_\mu \\ W_\mu^3 \\ X_\mu \end{pmatrix} = \begin{pmatrix} c_W & -s_W c_\chi & s_W s_\chi \\ s_W & c_W c_\chi & -c_W s_\chi \\ 0 & s_\chi & c_\chi \end{pmatrix}\begin{pmatrix} A_\mu \\ Z_\mu \\ Z'_\mu \end{pmatrix}, \tag{2.11}$$

and the new gauge boson mixing angle by

$$\tan 2\chi = \frac{-2s_W a}{1-s_W^2a^2-\Delta}\,. \tag{2.12}$$

3. In our convention, the SM Higgs doublet has a Y=+1/2, and the dark Higgs doublet also has $Q_D = +1/2$.

2.2.2 Higgs sector

In the unitary gauge, one has

$$H = \frac{1}{\sqrt{2}} \begin{pmatrix} 0 \\ v + h \end{pmatrix}, \qquad H_D = \frac{1}{\sqrt{2}}(v_D + h_D), \tag{2.13}$$

and the minimization of the Higgs potential yields

$$\mu = \lambda v^2 - \epsilon_H \frac{v_D^2}{2}, \qquad \mu_D = \lambda_D v_D^2 - \epsilon_H \frac{v^2}{2}. \tag{2.14}$$

The squared mass matrix of the Higgs sector reads

$$\mathcal{M}^2 = \begin{pmatrix} 2\lambda v^2 & -\epsilon_H v v_D \\ -\epsilon_H v v_D & 2\lambda_D v_D^2 \end{pmatrix}, \tag{2.15}$$

with its eigenvalues given by

$$m_{1,2}^2 = \lambda v^2 + \lambda_D v_D^2 \mp \sqrt{(\lambda v^2 - \lambda_D v_D^2)^2 + \epsilon_H^2 v^2 v_D^2}, \tag{2.16}$$

where $m_2 > m_1$. The mass eigenstates read

$$h_2 = C_A h - s_\alpha h_D, \qquad h_1 = s_\alpha h + C_A h_D, \tag{2.17}$$

and the mixing angle is given by

$$s_{2\alpha} = \frac{\epsilon_H v_D v}{\sqrt{(\lambda v^2 - \lambda_D v_D^2)^2 + \epsilon_H^2 v^2 v_D^2}}, \qquad c_{2\alpha} = \frac{\lambda v^2 - \lambda_D v_D^2}{\sqrt{(\lambda v^2 - \lambda_D v_D^2)^2 + \epsilon_H^2 v^2 v_D^2}}. \tag{2.18}$$

We define the effective Higgs coupling as the coupling in our model normalized to the SM case. Using eq. (2.17) in eqs. (2.4) and (2.2), one has

$$g_{h_1 WW} = g_{h_1 f\bar{f}} = s_\alpha, \qquad g_{h_2 WW} = g_{h_2 f\bar{f}} = C_A. \tag{2.19}$$

The couplings to $Z - Z'$ read

$$g_{h_2 Z_1 Z_2} = C_A g_{h Z_1 Z_2} - s_\alpha g_{h_D Z_1 Z_2} \Delta \frac{v}{v_D}, \qquad g_{h_1 Z_1 Z_2} = s_\alpha g_{h Z_1 Z_2} + C_A g_{h_D Z_1 Z_2} \Delta \frac{v}{v_D}, \tag{2.20}$$

where $Z_{1,2} = Z, Z'$, the $g_{H Z_1 Z_2}$ factors are given in table 2.1. Due to the smallness of the kinetic mixing one finds that $g_{hZZ} \approx g_{h_D Z' Z'} \approx 1$, while all the other are at least suppressed by a power of $\epsilon_A < 0.03$. Therefore, one has that the coupling of h_1 (h_2) to the SM particles is suppressed by a factor of C_A (s_α) with respect to the values of the SM Higgs.

H	ZZ	$Z'Z'$	ZZ'
h	$(-c_\chi + a s_\chi s_W)^2$	$(s_\chi + a c_\chi s_W)^2$	$(-c_\chi + a s_\chi s_W)(s_\chi + a c_\chi s_W)$
h_d	s_χ^2	c_χ^2	$s_\chi c_\chi$

Table 2.1: $g_{H Z_1 Z_2}$ couplings.

There are also interactions involving three and four Higgs fields, as well as two gauge bosons plus two Higgs fields. These decay modes constitute what we will call, from now

on, *non-standard* (Non-SM) Higgs decay modes, namely, those that do not appear when considering the SM Higgs boson. They could be important, for instance, if there is a significant fraction in the $h_2 \to h_1 h_1$ or $h_2 \to Z'Z'$ at LEP, like in the buried Higgs scenario [140]. In our setup we assumed that the decay width of the Z' into Standard Model particles is negligible, since its couplings to Standard Model particles are suppressed by a factor of ϵ_A with respect to the couplings of the Z. The decay width of a Higgs boson into two gauge bosons Z_1 and Z_2 is given by

$$\Gamma(H \to Z_1 Z_2) = \frac{g^2 m_H^3 g_{HZ_1Z_2}^2 S}{64\pi m_W^2} \quad \frac{m_Z^4}{m_{Z_1}^2 m_{Z_2}^2} \left[1 - \frac{(x_1+x_2)}{2} + \left(\frac{x_1 - x_2}{4}\right)^2\right]^{1/2} \times \left[1 + \frac{5}{8} x_1 x_2 + \frac{x_1^2 + x_2^2}{16} - \left(\frac{x_1+x_2}{2}\right)\right], \tag{2.21}$$

where $H = h_1, h_2$, $x_{1,2} = (2m_{Z_{1,2}}/m_H)^2$, $g_{HZ_1Z_2}$ can be read from table 2.1 and S is a symmetry factor, 1/2 if $Z_1 = Z_2$, 1 otherwise. The partial widths of the heavy Higgs boson into light ones is

$$\Gamma(h_2 \to h_1 h_1) = \frac{1}{32\pi m_{h_2}} \sqrt{1 - \frac{4m_{h_1}^2}{m_{h_2}^2}} |g_{h_2 h_1 h_1}|^2 , \tag{2.22}$$

where the trilinear Higgs coupling $g_{h_2 h_1 h_1}$ is given by

$$g_{h_2 h_1 h_1} = 2\big\{3 s_\alpha C_A \big(\lambda v s_\alpha - \lambda_D v_D C_A\big) - \frac{\epsilon_H}{4}\big[v C_A (3c_{2\alpha} - 1) + v_D s_\alpha (3 c_{2\alpha} + 1)\big]\big\} . \tag{2.23}$$

Due to the rescaling of the Higgs-to-Standard Model couplings the Higgs production cross sections are suppressed by a factor of s_α^2 for h_1 (C_A^2 for h_2). Consequently, in the case where one can neglect the non-SM decays, there is always one Higgs boson whose rate is suppressed at most by a factor of 1/2. The branching fractions into SM particles will be suppressed by a factor of $1 - \mathrm{Br}(h_i \to \text{non-SM})$. Therefore, the total rate for any Higgs boson into SM particles is always lower than in the SM by a factor of

$$g_{h_i WW}^2 \left(1 - \mathrm{Br}(h_i \to \text{non-SM})\right) . \tag{2.24}$$

2.3 Numerical Analysis: Parameter Scans and Constraints

2.3.1 Parameter scans and pre-LHC constraints

To explore the parameter space of the model a random parameter scan was performed using the CUBA-library [141]. We chose as input parameters the physical parameters m_1, m_2, the mixing angle α, g_D, $m_{Z'}$ and the kinetic mixing parameter ϵ_A with values in the ranges according to table 2.2. We focused on Higgs masses below 600 GeV since the LHC

m_1 [GeV]	m_2 [GeV]	α	$m_{Z'}$ [GeV]	g_D	ϵ_A
$[1; 400]$	$[1; 600]$	$[0; \pi]$	$[0; 1000]$	$[0; 1]$	$[0; 0.3]$

Table 2.2: Ranges of the parameter scan.

experiments have published exclusions in that mass range and the phenomenology of a heavy singlet Higgs has been studied elsewhere (see, for instance, ref [126]).

The potential parameters were computed using

$$\lambda = \frac{1}{4v^2}\left[m_1^2\left(1-c_{2\alpha}\right)+m_2^2\left(1+c_{2\alpha}\right)\right], \tag{2.25}$$

$$\lambda_D = \frac{1}{4v_D^2}\left[m_1^2\left(1+c_{2\alpha}\right)+m_2^2\left(1-c_{2\alpha}\right)\right], \tag{2.26}$$

$$\epsilon_H = \frac{1}{2vv_D}(m_2^2-m_1^2)\,s_{2\alpha}\,. \tag{2.27}$$

We also required the points to respect the positivity conditions, eq. (2.14), thereby ensuring the proper minimalisation of the potential. Motivated by the discussion of the electroweak phase transition in similar models (see, for example, [142] and references therein), we discarded points with nonperturbative potential parameters by requiring $\epsilon_H \leqslant 0.5$ and $\lambda,\, \lambda_D \leqslant 1$. This also limits the contribution of the invisible decay modes to the total width of the Higgs bosons such that their values stay within the validity of the narrow width approximation (i.e. $\Gamma_i^{\text{tot}}/m_i < .05$), which is required in order to interpret the exclusion limits set by collider data on the rates of the Higgs boson as the product of the production cross-section times branching ratio in a particular channel.

Constraints from direct searches were applied using `HiggsBounds 2.1.1` [143, 144], where points are excluded at the 95% confidence level. In the low-mass region (below 114.4 GeV) the main exclusion channels are the LEP searches for a Standard Model-like Higgs [145–147] and a Higgs-like scalar decaying completely invisibly [148–150]. In some cases the decay $h_2 \to h_1 h_1 \to 4b$ or 4τ was also constrained directly by the corresponding LEP MSSM searches [147]. In the high-mass region (120-200 GeV) the Tevatron searches were also used to bound the parameter space [151, 152].

Electroweak precision data also limit the parameter space of our model in a significant way [153, 154]. In order to assess the effect of a complete parameter fit, we used model independent bounds on the kinetic $Z\ -Z'$ - mixing [121] to constrain ϵ_A and computed the contribution of the extended gauge and Higgs sectors to the Peskin-Takeuchi S and T parameters [155] using FormCalc [156]. For the two Higgs bosons h_1 and h_2, it is given by

$$S = C_A^2 S^{\text{SM}}(m_1) + s_\alpha^2 S^{\text{SM}}(m_2), \tag{2.28}$$

where S^{SM} denotes the contribution of a Standard Model Higgs with respect to the reference mass $m_h = 120$ GeV (and analogously for the T-parameter). The tree-level contribution of the Z' to the oblique parameters is [157]

$$\alpha_{EW} S = 4c_W^2 s_W^2 \frac{c_W^2-\Delta}{(\Delta-1)^2}\epsilon_A^2, \quad \text{and} \quad \alpha_{EW} T = -s_W^2 \frac{\Delta}{(\Delta-1)^2}\epsilon_A^2, \tag{2.29}$$

which diverge as $m_{Z'} \to m_Z$. We are however confident that the formulas are valid as long as $|\frac{s_W \epsilon_A}{1-\Delta}| \ll 1$. Due to the constraints on ϵ_A that we implemented this condition is always fulfilled in our scan. Since we study the Higgs sector of this theory at the LHC, we were interested in how a Z' with suitably chosen properties can relax the upper mass limit on the Standard Model Higgs mass from the S and T parameter fit, which is the case when the tree level contributions are enhanced through $m_{Z'} \to m_Z$. We neglect loop contributions of the Z' via the ordinary photon and W,Z gauge boson self energies, since their size would be of order of the Standard Model gauge sector contributions to the neutral current amplitude, but suppressed by an additional factor of ϵ_A^2. In the threshold

Channel	Lum. (fb^{-1}) ATLAS	CMS	What we do	Mass range (GeV)	Ref.
$pp \to H \to WW$	1.7	1.5	Comb.	115-600	[162–164]
$pp \to H \to ZZ$	1.04–2.28	1.1–1.7	Comb.	120-600	[165–171]
$pp \to H \to \gamma\gamma$	1.08	1.7	Comb.	110-150	[172, 173]
$pp \to H \to \tau^+\tau^-$	1.06	1.6	Comb.	100-150	[174, 175]
$VH, H \to b\bar{b}$	–	1.1	CMS $\times$ 2	110-135	[176]
$qqH, H \to \tau^+\tau^-$	1	–	ATLAS $\times$ 2	110-130	[177]

Table 2.3: List of LHC channels used in this study. Here, H stands for either h_1 or h_2. The production mechanisms considered in pp are gluon-fusion, vector boson fusion, associated production with $Z, W, t\bar{t}$ and also $b\bar{b} \to H$. The cross sections at the LHC have been taken from ref [178]. See the main text for details.

region around $m_{Z'} = m_Z$ it is suppressed even further by the strong constraints on ϵ_A. We also neglected dark fermions, since their contribution would only enter the aforementioned at the two-loop level. We set $U = 0$ and required a parameter space point to lie inside the 2σ contour in the $S - T$-plane provided by the Gfitter collaboration [158–161].

2.3.2 LHC data and projections

In our analysis we include the current LHC data and future projections for the search channels listed in table 2.3. All of the searches use the most up-to-date LHC data with a total integrated luminosity between 1.04 - 2.28 fb^{-1} (depending on the search channel), except for the $qqH, H \to \tau^+\tau^-$ channel, for which we use the MonteCarlo 2010 sample [177], which provides a projection of the expected sensitivity of the current data-sample, since no LHC collaboration has presented yet updated data in this search channel. In the case of the associated production with a vector boson, with the Higgs decaying into bottom pairs, the current analysis was done using a cut based procedure that is able to exclude a Higgs boson with a rate of around 20 times the SM case [179]. The MC 2010 analysis was performed by taking advantage of boosted $b\bar{b}$ pairs [180], and the expected exclusion with 1 fb^{-1} of data for this case is around 6 times the SM [177]. We note that these channels are not able to probe points in our model, but, for the sake of completeness, we include them in our analysis.

We combine the results from ATLAS and CMS in the channels where both collaborations have presented data, following the prescription detailed in Refs. [181, 182] (see below). The *current exclusion* is obtained by using the observed limits reported by ATLAS and CMS. For channels where only one of the collaborations has presented data, we will base our current exclusion on that analysis. In the same case, we compute the *future projections* by doubling the expected result in an attempt to mimic the combination of both experiments and scaling the result by the expected total integrated luminosity using the prescription detailed below. Since the reach for SM-like Higgs bosons at CMS and ATLAS is similar, this approximation is expected to be reasonably accurate. Except in

the ZZ channel, all of the others involve, for a particular mass range, one definite final state. For the ZZ we also combine in quadrature the results for the a) four leptons, b) two leptons two quarks and c) two leptons plus two neutrinos, and d) two leptons plus two taus (CMS only) final state searches

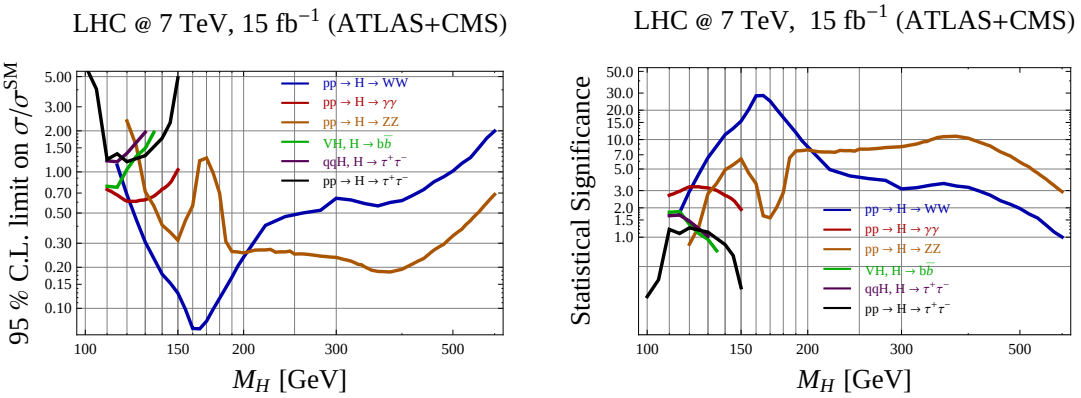

(a) (b)

Figure 2.1: LHC reach (a) and statistical significances (b) for the SM Higgs boson H with 15 fb^{-1}, combining both experiments. The color coding is as follows: WW (blue), ZZ (orange), $\gamma\gamma$ (red), $\tau\tau$ (black) , $VH, H \to b\bar{b}$ (green) and $qqH, H \to \tau^+\tau^-$ (purple).

Here we briefly review the procedure used to combine the experimental information. For each relevant channel we compute the following quantity:

$$Q(\mathcal{L}_0) = \frac{R_{\rm mod}}{R_{\rm exp}(\mathcal{L}_0)}\,, \tag{2.30}$$

where $R_{\rm mod}$ is the rate in this particular channel coming from our model, $R_{\rm exp}$ is the exclusion limit at the 95% C.L., at a reference total integrated luminosity $\mathcal{L}_0$. Eq. (2.30) is exactly the same definition used by HiggsBounds in order to set the 2σ exclusions: if $Q > 1$ the point is excluded at the 95% C.L.. We compute $R_{\rm exp}$ combining the results for each LHC experiment in inverse quadrature (see Refs. [181, 182]). In ref [132] this procedure was found to be more conservative than the combination performed by the ATLAS collaboration by 10-20 %[4]. While the quantity $R_{\rm mod}$ is a number that does not change, $R_{\rm exp}$ scales with the luminosity as $\mathcal{L}^{-1/2}$. Thus, defining $R_{\rm exp}(\mathcal{L}_0) = R_0$ and $Q_0 = R_{\rm mod}/R_0$, one has that

$$Q(\mathcal{L}_1) = \frac{R_{\rm mod}}{R_0}\sqrt{\frac{\mathcal{L}_1}{\mathcal{L}_0}} = Q_0\sqrt{\frac{\mathcal{L}_1}{\mathcal{L}_0}}\,. \tag{2.31}$$

In order to derive these equations, one is neglecting all systematic effects and also assumes that in each particular channel $B \gg S \gg 1$ holds, where B (S) are the number of background (signal) events for a particular channel. With these simplifications the expected statistical significance σ turns out to be $\sigma \approx 2\,Q$.

4. While the first version of this manuscript was under consideration, ATLAS and CMS presented the combination of their datasets in [183,184]. We have compared their results against our naive combinations, finding that the expected values differ by at most 10%, while for the observed values the discrepancy ranges from 30 to 50 %, but in those cases our naive combination turns out to be a conservative. A similar comparison is also shown in figure 2 of ref [185], where the SM combination is confronted against the experimental result, also finding a similar accuracy.

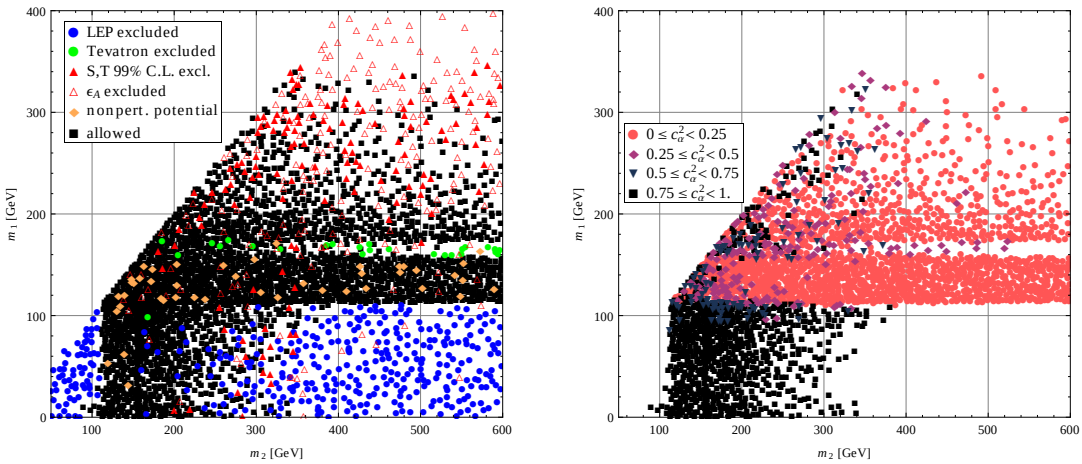

(a) (b)

Figure 2.2: Scanned points in the $m_1 - m_2$ plane. In the left panel (a) we show a representative sample of excluded along with allowed points, while in the right panel (b) we show only allowed points. In the left panel, we show the points excluded by LEP (blue), Tevatron (green), S- and T-parameters (red, filled), ϵ_A (red, empty) and perturbativity constraints (orange). The black points are allowed by all current collider data. In the right panel the color coding varies according to the value of c_α^2: red ($0 \le c_\alpha^2 < 0.25$), magenta ($0.25 \le c_\alpha^2 < 0.5$), blue ($0.5 \le c_\alpha^2 < 0.75$) and black ($0.75 \le c_\alpha^2 \le 1$).

As an illustration, we present in figure 2.1 the expected reach at the LHC and the statistical significance for the SM Higgs as a function of the Higgs mass in the channels described in table 2.3, assuming a total integrated luminosity of 15 fb^{-1}, which corresponds to the total integrated luminosity that can be collected by the end of 2012 if the instantaneous luminosity is kept at the current rate.

As one can see, the WW channel is setting the most stringent exclusion in the $120-200$ GeV range. For larger masses, the $H \to ZZ$ channel takes the leading role. For masses below 120 GeV one enters into the problematic range, where the WW channel becomes ineffective, and the diphoton requires $\mathcal{O}(10$ fb$^{-1})$ integrated luminosity in order to probe the SM Higgs. Moreover, as mentioned in section 2.2.2, the suppression factor for one of the Higgs bosons is at most 1/2, unless there is a significant *non-standard* branching ratio. This means that in the case of maximal mixing without significant extra-SM decay modes, at least one Higgs boson can be tested at the 2 (5) σ level if its mass lies in the 125-550 (140-190) GeV range.

2.4 Numerical Analysis: Results

In this section we present the results of the parameter scan as defined in section 2.3. In the left panel of figure 2.2 we study the impact of each experimental or theoretical bound on the parameter space of the model in the $m_1 - m_2$ plane. We plot points that are excluded by LEP (blue), Tevatron (green), S and T parameter (red, filled), ϵ_A (red, empty) and the requirement of perturbativity of the potential parameters (orange). It is clearly visible how the direct searches of LEP (blue) and Tevatron (green) constrain the region $m_1 < 114.4$ GeV and $m_i \approx 160 - 170$ GeV. The indirect bounds via the S and T

parameters (red, filled) and the constraints on kinetic mixing of the neutral massive gauge bosons (red, empty) mostly affect regions where one or both Higgs bosons are heavier than 155 GeV. As can be seen from equation (2.25), the perturbativity requirement $\lambda < 1$ places an upper bound $m_1 < \sqrt{2}v \approx 350$ GeV on the mass of the lighter Higgs boson (orange). However, points in that region tend to be excluded for other reasons before so that its most important effect is to prevent the decay width of either Higgs boson into $Z'Z'$ from becoming large enough to invalidate the narrow width approximation.

The black points evade all of the above constraints and are the focus of the study at hand. This subset is shown in the right panel of figure 2.2, where we have colored the points according to the rescaled squared coupling of h_2 to Standard Model particles, namely, to the particular value of c_α^2: red ($0 \leq c_\alpha^2 < 0.25$), magenta ($0.25 \leq c_\alpha^2 < 0.5$), blue ($0.5 \leq c_\alpha^2 < 0.75$) and black ($0.75 \leq c_\alpha^2 \leq 1$).

We focus first on the region where the mass of the ligher Higgs state h_1 is below the LEP limit of 114.4 GeV. Here, the h_1 coupling to Standard Model particles has to be significantly suppressed to avoid direct detection [5]. The heavier state h_2 can be lighter than 114.4 GeV at the same time if $h_2 \to h_1 h_1 \to$ SM is by far the dominant decay channel, in which case it can evade the constraints coming from the LEP searches for invisible decays of a Higgs-like scalar [6]. The decay $h_i \to ZZ'$ is sub-dominant (branching fraction below 1%) in this region as well as in the whole parameter space.

When $m_1 \lesssim 114$ GeV $\lesssim m_2 \lesssim 155$ GeV, the heavy Higgs state h_2 behaves largely as the Standard Model Higgs, except for possible non-standard decays. In turn, if m_2 is above 155 GeV, fine-tuning between the S and T parameter contributions of the extended bosonic sectors is needed in order to evade the constraints from electroweak precision tests. It is necessary that $m_{Z'} < m_Z$, and for a given point in the m_1-m_2-plane the allowed range for $m_{Z'}$ becomes smaller, the larger m_2 is.

When m_1 is above 114 GeV, there are no direct constraints on the mixing angle. The indirect constraints via the S and T parameter force the heavy Higgs to mostly decouple from the Standard Model for masses $m_2 \gtrsim 150$ GeV. Where the decay $h_2 \to h_1 h_1$ is possible, the corresponding branching fraction is always smaller than 0.5. $BR(h_2 \to Z'Z')$ can take any value, whereas $BR(h_1 \to Z'Z')$ decreases with growing m_2. The region where both Higgs masses are larger than 155 GeV is, again, the result of $m_{Z'} < m_Z$.

Let us now study how the LHC experiments will probe the parameter space with their main search channels for the Standard Model Higgs boson. Even though production rates and decay widths are never enhanced in this model, the parameter space is already probed efficiently. As it can be seen on the left panel of figure 2.3, the current dataset (1.04-2.28 fb^{-1}), shown in green, is able to exclude a vast majority of points in the region of $m_1 >$ 140 GeV, mostly due to the $h_1 \to WW/ZZ$ channels. If $m_1 < 114$ GeV, $h_2 \to WW/ZZ$ is probing values of m_2 above 135 GeV range. With 5 fb^{-1} (red points) one can exclude almost the complete region $m_1 > 130$ GeV except in the case that h_1 has small couplings to SM particles and at the same time a large branching fraction into $Z'Z'$ or other invisible particles. With 15 fb^{-1} of data (expected in 2012) the diphoton channel will start to probe

5. The parameter space points where $m_1 < 12$ GeV should be taken with care, since the LEP search in the $h_1 Z$, $h_1 \to b\bar{b}$ is cut-off at this value [147] and there are other low energy experiments that can probe this mass range more efficiently than the searches included in this study (see also [186] for an analysis of the LHC reach.) . The detailed analysis of this region is outside the scope of the present work.

6. Recent studies based on jet-substructure techniques show that the $h_2 \to h_1 h_1 \to 4j$ final states can be tested at the 5σ level at the 14 TeV LHC with $\mathcal{O}(10 - 100$ fb^{-1} of data [187–189], depending on the model under consideration, and on m_1 and m_2. Due to these reasons we decide not to include those analysis in the present work.

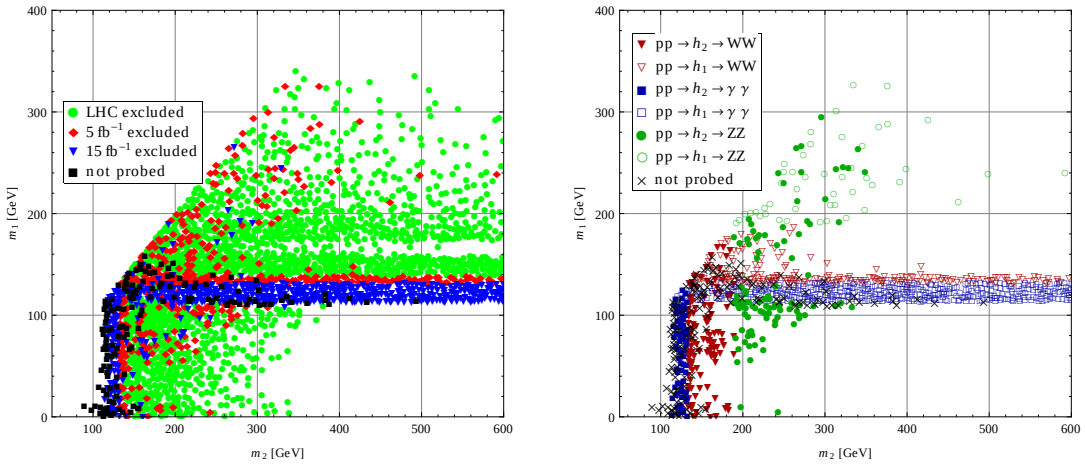

(a) (b)

Figure 2.3: (a) LHC 2σ exclusions for different scenarios and (b) most sensitive channels in the $m_1 - m_2$ plane. In the left panel, we show the points that have been excluded by the LHC with the current dataset (green), and also those that can be excluded after collecting 5 fb^{-1} (red) and 15 fb^{-1} (blue) of data. The black points will still be allowed by LHC data. In the right panel we remove the points excluded by the LHC today. Color coding varies according to the most sensitive channel to that particular point and filled (empty) shapes correspond to h_2 (h_1). The $pp \to h_i \to WW$ decay mode is shown in red, the diphoton channel in blue and the ZZ channel in green. The black points are not sensitive to the LHC search channels under consideration.

points in the 110-130 GeV range (blue points in the left plot). The region where both h_2 and h_1 are below the LEP limit (black points), and where the main decay mode for h_2 is into $h_1 h_1$, can not be tested with the channels used in this study, since the LHC collaborations have not presented dedicated searches for this kind of decays (one would typically look into $b\bar{b}b\bar{b}$, $\tau^+\tau^- b\bar{b}$ or even $\tau^+\tau^-\tau^+\tau^-$).

In figure 2.4 we show the 5σ discovery potential of the model in the $m_1 - m_2$ plane (left panel) and the rate suppression factor (2.24) for the most sensitive search channel as a function of the Higgs mass which is more sensitive for exclusion/discovery at the LHC (right panel).

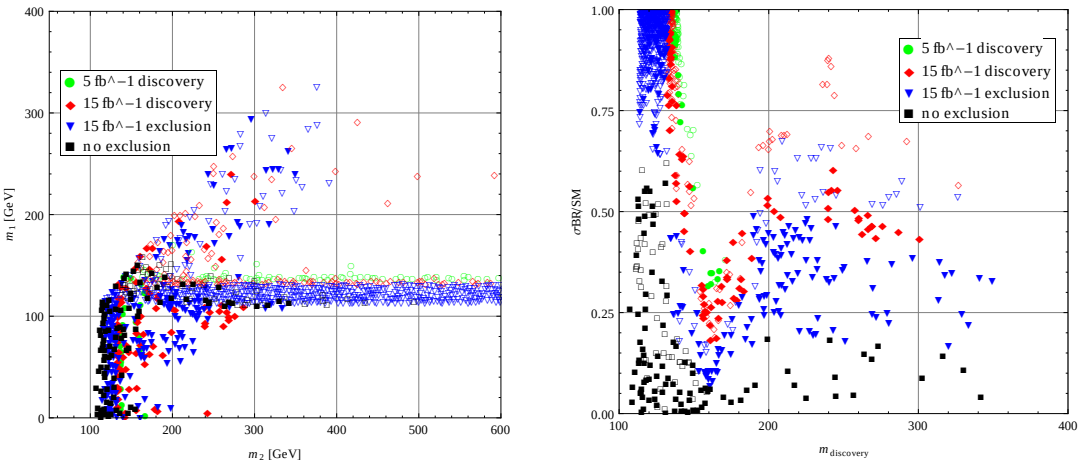

(a) (b)

Figure 2.4: Left panel: 5σ discovery potential with 5 fb^{-1} (green), 15 fb^{-1} (red), exclusion at 15 fb^{-1} (blue) and parameter space points outside of early LHC reach (black). Filled (empty) shapes correspond to the discovered or excluded particle being h_2 (h_1). Right panel: Rate suppression factor (2.24) at the LHC as a function of the mass of the Higgs more likely to be detected first.

From the left panel we see that a discovery with 15 fb^{-1} is only possible if either mass is larger than about 130 GeV. We have explicitly checked that the case where LHC discovers both Higgs states in the early run is only possible if the masses are in the range $130 \lesssim m_1 \lesssim 170$ GeV and $130 \lesssim m_2 \lesssim 260$ GeV and the mixing between the two states is sizable.

When a Higgs scalar with a lowered rate $\sigma \cdot BR$ than the Standard Model expectation is detected at the LHC it is a priori impossible to decide which of the two mass eigenstates has been discovered using above searches. Furthermore, more involved studies are needed to determine whether the origin of the rate suppression is the mixing between the states or decays invisible to the specific search channel, e.g. $h_i \to Z'Z'$ or $h_2 \to h_1 h_1$. From the right panel we see that after collecting 15 fb^{-1} of data, one can exclude a rate which is 0.6 (0.05) times the SM rate for $m_h \sim 130$ (160) GeV; for $m_h > 200$ GeV this value is 0.2. If a Higgs in the mass range of $180 \lesssim m_{\text{Discovery}} \lesssim 300$ GeV is discovered with a moderate rate suppression factor $\sigma \cdot BR/SM \approx 0.7$, it is likely that the detected particle is the lighter mass eigenstate h_1. Furthermore, the early discovery of a Higgs state with a mass larger than 155 GeV points toward $m'_Z < m_Z$. This is because it is likely that the first Higgs to be discovered is the one that couples more strongly to the Standard Model. If it is heavier

than 155 GeV, a Z' gauge boson with specific properties is needed to reconcile such a high Higgs mass with electroweak precision data.

2.5 Conclusions

In this chapter we have studied in detail the constraints on dark Higgs models at the 7 TeV LHC. In the scenario under consideration the usual SM Higgs boson (i.e the one responsible for electroweak symmetry breaking) mixes with a complex singlet that breaks an extra $U(1)_D$ gauge symmetry, which in turn mixes with the SM hypercharge $U(1)_Y$. The free parameters of this model are the masses of the two Higgs bosons m_1 and m_2, the cosine of the mixing angle c_α between them, the mass of the additional gauge boson $m_{Z'}$ with the kinetic mixing parameter ϵ_A and the coupling strength g_D. A parameter scan was performed and the effect of theoretical and experimental bounds from direct searches at LEP and Tevatron and electroweak precision data was studied.

The LHC analyses published at the time of preparation of this study (with luminosities between 1.04 and 2.28 fb^{-1}) were able to exclude Higgs masses above 140 GeV, save for a significant mixing between the two mass eigenstates, while with 5 fb^{-1} most of the points with the lightest Higgs mass above 130 GeV were excluded. Furthermore, we have found that the 7 TeV LHC with 15 fb^{-1} of total integrated luminosity will have probed most of the parameter space at the 2σ level.

The points that evaded these constraints correspond to two cases. The first of them is when either Higgs boson lies in the $115 - 130$ GeV range and there is some non-negligible mixing between the two mass eigenstates. For such masses the WW final state is not very useful, and if there is some mixing between h_1 and h_2 one can loosen the exclusion power of the $\gamma\gamma$ channel, which will rule out that mass range for the SM Higgs boson. However, we would like to point out that, according to projection on the SM Higgs that include combinations of the different low-mass sensitive channels, this region can in principle be accessed during the 7 TeV run.

The second case takes place when the Higgs rates are diminished due to a sizable mixing between the mass eigenstates, or if $h_2 \to h_1 h_1$ is kinematically open. For this region of parameter space one should perform a dedicated search of $h_2 \to h_1 h_1$ by looking at final states like $b\bar{b}b\bar{b}$, $\tau^+\tau^- b\bar{b}$ or even $\tau^+\tau^-\tau^+\tau^-$.

We would like to remark that the effectiveness of these bounds gets looser if there is an important partial width of any Higgs boson into other (not specified in this work) dark sector degrees of freedom (like the Dark Matter candidate). As a consequence, our results can either be interpreted as valid in a completion of the model where the aforementioned channel is not relevant, or also as the largest exclusion coverage one can get in parameter space.

We have also analyzed the possibility of discovering one or two Higgs bosons. We have found that, with 15 fb^{-1} one can discover one of the Higgs bosons of this scenario if their masses are larger than 130 GeV. If only one Higgs boson with a rate smaller than the SM Higgs is discovered, it would be impossible to tell *a priori* whether it is h_1 or h_2. Discovering both Higgs bosons will only happen if $m_2 \in [130, 260]$ GeV and $m_1 \in [130, 170]$ GeV. Such an observation would rule out some other models, like for instance the MSSM, since the lightest neutral Higgs boson can not have a mass well above 135 GeV. Finally, if the LHC should not see any Higgs signature after collecting 15 fb^{-1} of data then one can use that result to constrain the mixing between the two Higgs bosons and/or the invisible width. For the former case, a recent study using the $H \to ZZ \to 4l$

line-shape was presented in ref [190].

In 2011 and 2012 the LHC and the experiments have been performing exceptionally well and collected about 25fb^{-1} of data each and most of it at a collision energy of 8 instead of 7 TeV before their shutdown in the end of 2012. They have therefore surpassed the optimistic estimate of this study by far.

In December 2012 both the ATLAS and the CMS collaboration announced the discovery of a scalar particle that is consistent with the Standard Model Higgs boson with a collected luminosity of 4.7fb^{-1} each [191, 192]. Since then, more more than 20fb^{-1} additional data have been collected, analyzed and combined and been used to further strengthen the evidence that indeed the Higgs boson has been found. Up to date there are no significant deviations from the Standard Model expectations in all relevant channels. The most recent results by the ATLAS [193–198] and CMS [199–203] collaborations for the Higgs mass m_h and signal strength μ are:

$$\begin{aligned} \text{ATLAS:} \qquad m_h &= 125.5 \ \pm 0.2\,(\text{stat}) \ {}^{+.5}_{-.6}\,(\text{syst}) \ \text{GeV}\,, \\ \mu &= 1.43 \ \pm .16\,(\text{syst}) \ \pm .14\,(\text{sys})\,. \end{aligned}$$

$$\begin{aligned} \text{CMS:} \qquad m_h &= 125.7 \ \pm 0.3\,(\text{stat}) \ \pm 0.3(\text{syst}) \ \text{GeV}\,, \\ \mu &= 0.80 \ \pm 0.14\,, \end{aligned}$$

where the signal strength $\mu = \sigma/\sigma_S M$ is defined as the ratio of measured to Standard Model predicted total cross section.

Some slight enhancement of the signal in the search channel $H \to \gamma\gamma$ (still compatible with the Standard Model) in the ATLAS results [193] could point towards an enhanced decay width of the Higgs into two photons. If indeed this would be the case it would strongly disfavor a model like the present one where the event rates of a particular visible channel can only be lowered, either by the mixing in the Higgs sector or via invisible decays.

In a dedicated study $Z\,H \to l\,l\,+$ invisible the ATLAS collaboration was able to set an upper bound on the invisible branching ratio of 0.65 at the 95% C.L. [204]. This was combined with the other measurements from ATLAS, CMS and Tevatron in a recent study which found that the invisible branching ratio is smaller than 19 per cent at the 2σ level [205].

It may seem that the Higgs boson discovery and its (current) agreement with the Standard Model prediction disfavors the present model. However, many motivations for this extended Higgs sector require only small mixing and are therefore perfectly compatible with this result.

Furthermore, from a Bayesian standpoint, a large fraction of the randomly sampled parameter space points resulted in one of the two states being very similar to the SM-Higgs. It will now be interesting to determine whether the identified Higgs is the light or the heavy one, a task that will be very challenging. The most promising route for this would be to look for the decay of the heavier into two lighter Higgs bosons.

In a recent publication yet another motivation for such a class of models was found. In [206] the Higgs portal was used to generate the electroweak scale in a new way: In a hidden sector the breaking is generated radiatively via the Coleman-Weinberg mechanism and then transmitted to the Standard Model sector via the Higgs portal. In the SM, this mechanism does not work since it would result in a Higgs mass far below the gauge boson masses. However, in a dark sector a hierarchy like this is still possible, since in this sector there could be much heavier gauge bosons. Hence, this model could naturally explain the

smallness of the electroweak scale compared to the Planck-scale. With supersymmetry still evading discovery such alternatives to solving the hierarchy problem become more and more appealing.

The discovery of the Higgs and other successes of the LHC can now, in combination with direct detection experiments, be used to constrain Dark Matter models [207, 208]. Since there now exists an upper bound on the invisible branching fraction of the Higgs, a DM particle with mass smaller than 60 GeV communicating with the SM via Higgs exchange can be excluded [209]. More LHC data and results from ongoing Dark Matter detection experiments will be able to significantly reduce the allowed parameter space for singlet Higgs Dark Matter models [210]. The new results are also studied in the context of many other extended Higgs sector scenarios and strategies are devised for detecting these under the new circumstances, such as two-Higgs-doublet models [211].

At the moment the LHC is shut down and is undergoing reparation. When it will switch back on in 2015 to be running at higher energies the time for precision Higgs physics has come. As it has been discussed, this model is still very much alive and remains a valid contender among possible extensions of the Standard Model Higgs sector which is studied in similar studies than this one [212].

3

Algebraic Tools for Feynman Integrals

The computation of multi-loop amplitudes is very involved and becomes much more cumbersome with every additional external leg, loop or mass scale. Nevertheless, the resulting amplitude is often quite simple when written with the correct variables and functions. This is especially true for massless theories or theories which exhibit a large degree of symmetry, most notably planar $N = 4$-SYM.

In recent years much effort has been put into making use of the underlying analytical structure or the physical properties of the amplitude at hand in order to compute it more efficiently. A similar direction was the attempt to better understand the algebraic structure of the underlying building blocks of the amplitude, that is, the functions that are used to express these results analytically. They are called *Multiple Polylogarithms* (MPLs). This brought forward most notably the *symbol* formalism and its generalization, the *coproduct*. There exist countless identities among MPLs, making transformations among them complicated and cumbersome. The question whether a given result has in fact a much shorter representation is difficult to answer in general. These formalisms have been successfully applied to simplify existing results. It is an ongoing quest to "connect the dots" between these different directions and attempt to use these ideas to circumvent traditional integration altogether.

In this work we studied how the aforementioned tools can be used not only to simplify existing results but also to facilitate the computation of Feynman integrals the conventional way. As the number of mass scales in an integral increases, so does the complexity of the MPLs involved. A generalized algorithm for deriving required identities and transformations among them in an automated way and to provide a general framework for doing so for future applications is thus desirable and will be presented in this work.

The general idea is to translate an expression involving MPLs into a tensor space where all the complicated relations reduce to simple algebraic manipulations. After the desired manipulations the result is then translated back to the function space.

In the following section the MPLs are introduced and some of their properties studied. The symbol formalism is introduced in section 3.2 and its generalization, the coproduct, in section 3.3. Example applications are discussed in appendix D, which also illustrate the use of the developed computer algebra code. The Mathematica packages are described in

detail in appendix C.

3.1 Multiple Polylogarithms

Just as the name suggests are the Multiple Polylogarithms (MPLs) a "generalization of the generalization" of the logarithm. In mathematics they are studied in fields as diverse as, for example, algebraic topology or as volume functions of hyperbolic spaces and were already used in the early 20th century [1]. In physics they appear in the analytical computation of Feynman integrals when higher order corrections to physical observables are computed.

The multiple polylogarithms are defined by

$$\begin{aligned} G(a_1,\ldots,a_n;x) &= \int_0^x \frac{dt}{t-a_1} G(a_2,\ldots,a_n;t)\,, \\ &\text{with } G(x) = G(;x) = 1; \quad G(0) = \int_0^0 dt = 0\,. \end{aligned} \tag{3.1}$$

The $a_i \in \mathbb{C}$ are constants and are called the *index (vector)* $\vec{a}$ or *vector of singularities* whereas $x \in \mathbb{C}$ will be called the *argument* of the MPL in the following. The length of the index vector n is called the *(transcendental) weight* of the function. In the special case that the index vector consists of all zeroes $\vec{a} = \vec{0}_n = \{0,\ldots,0\}$, we define

$$G(\vec{0}_n, x) = \frac{1}{n!}\log^n x\,. \tag{3.2}$$

In mathematics a *transcendental* number is a number that is not the root of a polynomial equation with rational coefficients, or, the opposite to an algebraic number. While it is in general difficult to prove that a number is transcendental, it has been shown in the Lindemann-Weierstrass theorem that π is so indeed. In the context of repeated integrals it has been proven consistent and useful to define a *(degree of) transcendentality* of a function by the number of iterated integrations it contains, which in the case of MPLs corresponds to the length of the index vector. Therefore we will use the notion of weight and transcendentality interchangeably in the following. Since

$$\pi = i\log(-1-i\epsilon) = \int_1^{-1} \frac{1}{x-i\epsilon}\mathrm{d}x\,, \tag{3.3}$$

we have consistently that the transcendentality of π is 1.

In physics MPLs usually show up with the entries of the index vector chosen from a limited set,often called the *alphabet* of the problem under consideration. In the special case that $a_i \in -1,0,1$ these functions are called *Harmonic Polylogarithms (HPLs)* and were first studied in [213]. In multi-scale integrals the a_i often depend on another variable, e.g. $a_i \in \{0,1,z,1-z\}$, in which case they are called the *two-dimensional HPLs (2dHPLs)* and were studied first in [59]. In the present context, it is useful to think of the entries of the index vector as functions dependent on the kinematic variables of the process themselves, but nevertheless belonging to a finite set of possible relations. See, for example sections 5.3.3 and 5.4.1.

1. For an overview over the many fields of applications see the introduction of [67].

Some closed expressions for special index choices are, besides eq. (3.2), for $a \neq 0$,

$$\begin{aligned} G(\vec{a}_n; x) =& \frac{1}{n!} \log^n \left(1 - \frac{x}{a}\right) \quad \text{with } \vec{a}_n = \overbrace{(a, \ldots, a)}^{n \text{ times}} \\ G(\vec{0}_{n-1}, a; x) =& - \mathrm{Li}_n \left(\frac{x}{a}\right) , \\ G(\vec{0}_n, \vec{a}_p; x) =& (-1)^p S_{n,p} \left(\frac{x}{a}\right) , \end{aligned} \tag{3.4}$$

where $\mathrm{Li}_n(x)$ is the ordinary and $S_{n,p}(x)$ is the Nielsen polylogarithm. From the series representation (C.3) of the MPLs it can be seen that

$$\mathrm{Li}_n(1) = \zeta(n) \equiv \zeta_n , \tag{3.5}$$

where $\zeta(n)$ is the Rieman zeta function. Therefore, $\zeta(n)$ can be assigned the transcendentality n for integer values $n \in \mathbb{N}$. Up to weight three, MPLs can be expressed in terms of ordinary logarithms and polylogarithms. For example at weight two we have, for $0 \neq a \neq b$,

$$G(a, b; x) = \mathrm{Li}_2 \left(\frac{b-x}{b-a}\right) - \mathrm{Li}_2 \left(\frac{b}{b-a}\right) + \log \left(1 - \frac{x}{b}\right) \log \left(\frac{x-a}{b-a}\right) . \tag{3.6}$$

3.1.1 Properties

Let us study some analytical properties of the multiple polylogarithms. Numerical evaluation is based on its series representation and is briefly discussed in appendix C.2.

shuffle algebra

Repeated integrals form a shuffle algebra. This means, that the product of two MPLs of weights n_1, n_2 can be expressed in terms of functions of weight $n_1 + n_2$.

$$G(a_1, \ldots, a_{n_1}; x) G(a_{n_1+1}, \ldots, a_{n_1+n_2}; x) = \sum_{\sigma \in \Sigma(n_1, n_2)} G(a_{\sigma 1}, \ldots, a_{\sigma n_1+n_2}; x). \tag{3.7}$$

Formally, $\Sigma(n_1, n_2)$ is defined as the subset of the symmetric group $S_{n_1+n_2}$ defined by

$$\begin{aligned} &\Sigma(n_1,n_2) = \\ &\quad \left\{\sigma \in S_{n_1+n_2} | \sigma^{-1}(1) < \ldots < \sigma^{-1}(n_1) \text{ and } \sigma^{-1}(n_1+1) < \ldots < \sigma^{-1}(n_1+n_2)\right\} . \end{aligned} \tag{3.8}$$

In colloquial terms it is the set of all possibilities of riffle shuffling two decks of cards with n_1 and n_2 cards, which means that the respective order of the cards belonging to one of the original decks remains intact.

A consequence of this property is that the MPLs of a given weight with a certain set of indices are linearly dependent modulo products of lower weight functions. The shuffle property can be used to express $G(a_1, \ldots, a_j, 0, \ldots, 0; x)$, whose rightmost indices are zeros, as a sum over MPLs with the rightmost index unequal to zero and product of lower weight functions times powers of logarithms $G(0; x) = \log(x)$, therefore extracting its divergences at $x = 0$. The same is also true for endpoint singularities of type $G(b, \ldots, b, a_j, \ldots, a_n; x \to b)$.

scale invariance

If $a_n \neq 0$ we have that

$$G(a_1, \ldots, a_n; x) = G(\alpha a_1, \ldots, \alpha a_n; \alpha x) \text{ for } \alpha \in \mathbb{C}^* \,. \tag{3.9}$$

Therefore there is a certain redundancy in the definition of G, which plays a role in their numerical evaluation. If $a_n = 0$ we can use the shuffle relations to express it as a sum over MPLs whose rightmost index is different from zero plus a term $G(0; x)G(a_2, \ldots, a_n; x)$, thus 'extracting' this index.

cut structure

Using the scaling relation eq. (3.9), we can always rescale the argument to a positive real number. From the integral definition eq. (3.1) we can see that the MPL develops a branch cut whenever the integration variable exceeds an index that lies on the positive real axis as well. To determine the shape of the integration contour, an infinitesimally small imaginary part has to be given either to the integration variable or the the index in question. In this work, the integration variable carries this imaginary part.

Two problems arise often when having to deal with multiple polylogarithms. First, due to the large number of identities it is not abvious whether an expression involving these functions can in fact be expressed in a much simpler and shorter form. This often means to express the expression using logarithms and polylogarithms only.

Secondly, one often has to integrate over MPLs during the solution of a partial differential equation. This is trivial if the integral has the form of eq. (3.1) but not so if e.g. the integration variable contained in the index of the MPL. While for some sets of indices there exist so-called "interchange of argument identities" that can be used to exchange the variable in the argument with the one in the index, a general, possibly automated, way of dealing with these is desirable.

The *symbol calculus* and its generalization, the *coproduct*, posses the virtue that all expressions of arbitrary MPLs are translated into a certain tensor space where the complicated relations between these functions reduce to simple algebraic operations, therefore allowing for simplifications or the possibility of expressing the result in a desired form. With the formalism and its implementation presented here, these classes of problems can be tackled in an efficient way.

3.2 Symbol Calculus

The symbol formalism has been used in mathematics for more than twenty years, for example in [63,65] in the context of functional equations. It was introduced to the physics community only recently in [64] where it was shown to greatly simplify the two-loop $\mathcal{N} = 4$ Super Yang-Mills (SYM) theory six point remainder function computed in [214,215]. Since then, it was exploited mostly in the context of $\mathcal{N} = 4$ SYM, for example to obtain compact expressions for certain one-loop hexagon integrals in six dimensions [216–219], or to derive the symbol of certain multi-loop amplitudes by general considerations [70,215]. In a more phenomenological setting, the symbol was used for example in [220] to find representations of harmonic polylogarithms in terms or ordinary logarithms and polylogarithms for speedy numerical evaluation and in [221] to simplify the analytical result of two-loop integrals in top-quark pair production.

In [67], a prescription to obtain the symbol using the properties of a certain associated rooted decorated polygon was proposed and a general, systematized way to 'integrate' the symbol back to an analytical expression was given. This section will discuss this integration algorithm and describe how it can be used to simplify an expression. In addition, a second way to integrate the symbol will be introduced which was suggested by Claude Duhr and is useful when the size of the resulting expression is of no concern.

3.2.1 The symbol map

The symbol of a transcendental function F can be defined recursively [66]. If we have

$$F : \mathbb{C}^n \to \mathbb{C}, \quad x_k \mapsto F(x_k) \,, \tag{3.10}$$

whose total differential can be written as

$$\mathrm{d}F = \sum_i F_i(x_k) \mathrm{d}\log R_i(x_k) \,, \tag{3.11}$$

where R_i are rational functions, we can define the symbol of F recursively,

$$\mathcal{S}(F) = \sum_i \mathcal{S}(F_i) \otimes R_i \,, \tag{3.12}$$

where the the properties of the tensor product $\otimes$ will be discussed below. In the case of a multiple polylogarithm, we have, specializing for a moment to the case that all indices are mutually different and do not take particular values, for the total differential

$$dG(a_{n-1}, \ldots, a_1; a_n) = \sum_i^{n-1} G(a_{n-1}, \ldots \hat{a}_i, \ldots, a_i; a_n) \, \mathrm{d}\log\left(\frac{a_i - a_{1+1}}{a_i - a_{i-1}}\right) \,, \tag{3.13}$$

where the hat denotes an index that has been left out. In analogy to the above the symbol is then

$$\mathcal{S}(G(a_{n-1}, \ldots, a_1; a_n) = \sum_i^{n-1} \mathcal{S}(G(a_{n-1}, \ldots \hat{a}_i, \ldots, a_i; a_n)) \otimes \left(\frac{a_i - a_{1+1}}{a_i - a_{i-1}}\right) \,, \tag{3.14}$$

where we set $a_0 = 0$.

As it can be seen, the symbol map is a linear map that associates to every MPL of weight n an element in the n-fold tensor power in the vector space of one-forms. A different approach which defined the symbol as the sum over all possible maximal sets of arrows of the rooted polygon $P(a_1, \ldots, a_{n-1}, a_n)$ was given in [67] and its equivalence to 3.14 shown. But for the implementation in a computer algebra program the above definition is very suitable as it easily generalizes to arbitrary weight.

In the case that the a_i are degenerate, a careful regularization has do be performed [66]. However, for practical purposes a simple prescription to be detailed in the following section is sufficient.

3.2.2 Rules of symbol calculus

The rules to manipulate the tensors very much reflect the closeness to the differential, i.e. every factor a_i in $a_1 \otimes \ldots \otimes a_n$ can be seen as, but not quite like, as will be shortly shown, $\mathrm{d}\log$ term, that is

$$d\log a_i \equiv \frac{\mathrm{d}a_i}{a_i} \,. \tag{3.15}$$

Obviously, these rules are interesting and important in their own right; in the following section, they will be used to bring the symbol in a unique form in a sense to be defined later.

Distributivity

$$\begin{aligned} A \otimes (b_1 \cdot b_2) \otimes C =& A \otimes b_1 \otimes C + A \otimes b_2 \otimes C \,, \\ A \otimes b^n \otimes C =& n(A \otimes b \otimes C) \quad n \in \mathbb{Z} \,. \end{aligned} \tag{3.16}$$

where A and C are any tensors. Note that n multiplies the whole tensor rather than the first factor. Consequently we have

$$A \otimes 1 \otimes C = 0 \,. \tag{3.17}$$

Neglecting Torsion

In analogy to above, we set, with ρ_n a root of unity,

$$A \otimes \rho_n \otimes C = 0 \quad n \in \mathbb{Z} \,. \tag{3.18}$$

Shuffle Product

The symbol preserves the shuffle product of the MPLs. More precisely, the symbol of the product of two MPLs is mapped to the shuffle product of the two respective symbols, that is:

$$\mathcal{S}\left(G(a_1, \ldots, a_r; x) G(b_1, \ldots, b_s; y)\right) = \mathcal{S}\big(G(a_1, \ldots, a_r; x)\big) \text{ Ш } \mathcal{S}\big(G(b_1, \ldots, b_s; y)\big) \,, \tag{3.19}$$

where Ш is the shuffle product operator on two tensors defined by

$$(a_1 \otimes \ldots \otimes a_{n_1}) \text{ Ш } (a_{n_1+1} \otimes \ldots \otimes a_{n_1+n_2}) = \sum_{\sigma \in \Sigma(n_1, n_2)} a_{\sigma^{-1}(1)} \otimes \ldots \otimes a_{\sigma^{-1}(n_1+n_2)} \,. \tag{3.20}$$

Refined $d\log$ terms

One could be tempted, looking at the close relationship of the symbol to the total differential, to neglect all constant rational terms in equation (3.14). However, it is consistent and very useful to keep these terms, treating them in a completely analogous way, e.g.

$$A \otimes 9\sqrt{2}x^3 \otimes C = 2\, A \otimes 3 \otimes C + \frac{1}{2}\, A \otimes 2 \otimes C + 3\, A \otimes x \otimes C \,. \tag{3.21}$$

Regularization of degenerate indices

As mentioned above, equation 3.14 is only valid for mutually different indices a_i and a careful regularization has to be performed in the degenerate case. Whereas the construction of the symbol of [67] totally avoids these subtleties, the above definition can be used with the following trick:

1. In the last term of 3.14 apply the product rule already before assigning the a_k specific values, i.e.

$$\ldots \otimes \left(\frac{a_i - a_{1+1}}{a_i - a_{i-1}}\right) = \ldots \otimes (a_i - a_{1+1}) - \ldots \otimes (a_i - a_{i-1}) \ ; \tag{3.22}$$

2. Then plug in the values of the a_k of the specific MPL. Some of the tensor entries will now equal zero, which corresponds to a logarithmic divergence, but, carefully keeping them in the computation and during the manipulation of the symbol one sees that all the tensors containing such an entry cancel each other.

For example, at weight two we have

$$\begin{aligned} \mathcal{S}(G(b,b;c) = & \ \mathcal{S}(G(b;c)) \otimes \left(\tfrac{b-b}{b}\right) + \mathcal{S}(G(b;c)) \otimes \left(\tfrac{b-c}{b-b}\right) \\ = & -\mathcal{S}(G(b;c)) \otimes (b) + \mathcal{S}(G(b;c)) \otimes (b-c) \ . \end{aligned} \tag{3.23}$$

Elements in the kernel of the symbol map

The symbol of an expression does however contain less information than the original expression itself. For example,

$$\mathcal{S}(\pi^2) = S(\log^2(-1)) = (-1) \otimes (-1) = 0 \ . \tag{3.24}$$

Similarly, zeta values ζ_n are in the kernel of the symbol map. Since $\zeta_n = \mathrm{Li}_n(1)$ their symbol consists of factors 0, 1 only and is therefore equal to zero. In addition to that there are also combinations transcendental constants that have vanishing symbol. One relevant case is

$$\mathcal{S}\left(\mathrm{Li}_4\left(\frac{1}{2}\right) + \frac{1}{24}\log^4(2)\right) = 0 \ . \tag{3.25}$$

These elements of the kernel mentioned here are no means complete but cover the cases that were encountered in this work. The question of how to recover the information lost by the symbol map will be addressed in section 3.2.5.

3.2.3 Integration of symbols

Using these rules it is now relatively straightforward to compute the symbol of any combination of MPLs F_0 and to bring it to a form

$$\mathcal{S}(F_0) \equiv S = \sum_{i_1,\ldots,i_w} \widetilde{c}_{i_1\ldots i_w} \pi_{j_1} \otimes \ldots \otimes \pi_{j_w}. \tag{3.26}$$

with $\widetilde{c}_{i_1\ldots i_w}$ rational functions and the "elementary" tensors $\pi_i = \pi_i(x_1, \ldots, x_n)$ multiplicatively independent. This means that there exist no more relations of the form

$$\prod_{j=1}^{K} \pi_j^{r_j} = 1 \quad \text{for } r_j \in \mathbb{Z} \ . \tag{3.27}$$

In practice, arising polynomials in the variables x_i should be factored, sign ambiguities resolved and constants brought to a unique form. For example, factors like 2, 3, $2 \pm \sqrt{3}$ and $1 \pm \sqrt{3}$ can be expressed in function of 2, 3 and $2 + \sqrt{3}$ only. Similarly, it should be

checked whether complex numbers are a rational multiple of a root of unity, in which case they can be replaced by their absolute value. More precisely,

$$\pi_1 \otimes c \otimes \pi_3 = \pi_1 \otimes \left(|c|\frac{c}{|c|}\right) \otimes \pi_3 = \pi_1 \otimes |c| \otimes \pi_3 + \pi_1 \otimes \overbrace{\frac{c}{|c|}}^{=\rho_n} \otimes \pi_3 = \pi_1 \otimes |c| \otimes \pi_3 \ . \quad (3.28)$$

In the event that many different tensor product factors arise during the computation it is not always trivial to find all functional relations among them in order to write the symbol with the minimal set. In this work it has proven efficient to use the PSLQ algorithm [222] to find these relations in an automated way, which is described in appendix C.3.

It is now of interest to find a combination of simpler functions that has the same symbol than the expression before. These can for example be MPLs with a different set of indices but also logarithms and polylogarithms of more complicated arguments. The step of going from the symbol back to a expression is often called "integration" of a symbol in the literature.

First of all, let us quickly address the question whether every symbol can actually be integrated or conversely, whether every symbol is the symbol of a combination of MPLs. In [223] a necessary and sufficient condition for this was given, which can be written as,

$$\sum_{I=(i_1,\ldots,i_m)} \left[d\log\pi_{i_j} \wedge d\log\pi_{i_{j+1}}\right] \pi_{i_1} \otimes \ldots \hat{\pi}_{i_j} \otimes \hat{\pi}_{i_{j+1}} \otimes \ldots \otimes \pi_{i_m} = 0 \ , \quad (3.29)$$

where the hats again indicate left out tensor factors and $d\log\pi_{i_j} \wedge d\log\pi_{i_{j+1}}$ is the usual exterior product of two differential forms. With the relation between the symbol and the total differential, this is nothing other than the requirement that the total differential of the function vanishes

$$\mathrm{d}F = 0 \ . \quad (3.30)$$

Evidently this condition is always fulfilled in the case that a symbol of an expression involving MPLs is computed.

When trying to simplify an expression an important question is whether logarithms and polylogarithms, possibly of more complicated arguments, are sufficient to write down the amplitude. While this is always the case up to weight three, at weight four it was conjectured in [224] that this is only the case if the symbol vanishes under the action of the the operator

$$\delta(a\otimes b\otimes c\otimes d) = a\otimes b\otimes c\otimes d - a\otimes b\otimes d\otimes c - b\otimes a\otimes c\otimes d + b\otimes a\otimes d\otimes c - (a\leftrightarrow c, b\leftrightarrow d) \ . \quad (3.31)$$

However, this test tells us nothing about the nature of the arguments of the simple function that might be used to re-express the result in a shorter form. In principle, they could be any rational functions of the variables of the present problem. In general, experience and guesswork, motivated by physical constraints, can help at this step. In section 5.2 of [67] a procedure has been described how one can proceed even without this which will only be outlined here. The general idea is to take the set of elementary tensors of the symbol in question and extend it to a group (under multiplication of rational functions). A subset of the group elements are now the candidates for the function arguments. As an illustration, in the kinematical situation of the decay of a massive particle into three massless ones, described in 4.2, it has been found that the symbol of two-loop amplitudes only contains terms of the form

$$x_i, \ 1-x_i \qquad \text{for} \ \ x_i = x, y, z \ , \quad (3.32)$$

x_1	$1-x_1$	$1-1/x_1$
x_2	$1-x_2$	$1-1/x_2$
x_3	$1-x_3$	$1-1/x_3$
$-x_1/x_2$	$x_2/(1-x_3)$	$x_1/(1-x_3)$
$-x_2/x_3$	$x_3/(1-x_1)$	$x_2/(1-x_1)$
$-x_3/x_1$	$x_1/(1-x_2)$	$x_3/(1-x_2)$
$-x_1x_2/x_3$	$x_3/[(1-x_1)(1-x_2)]$	$x_1x_2/[(1-x_1)(1-x_2)]$
$-x_2x_3/x_1$	$x_1/[(1-x_2)(1-x_3)]$	$x_2x_3/[(1-x_2)(1-x_3)]$
$-x_3x_1/x_2$	$x_2/[(1-x_3)(1-x_1)]$	$x_3x_1/[(1-x_3)(1-x_1)]$

Table 3.1: Arguments of classical polylogarithms that can give rise to a symbol with entries drawn from the set in Eq. (3.32) under the constraint (4.6). Each line shows half an orbit of the S_3 action, the second half being obtained by inversion. All these functions are less than unity in the region defined by Eq. (4.6).

with the constraint $x+y+z=1$. The possible arguments are then given in table 3.1.

We now have almost all the ingredients to find the combination of functions F such that $\mathcal{S}(F)=S$. The general idea is to write down an ansatz using the previously determined 'basis' functions that span the vector space the symbol lives in. Let us suppose that the symbol in question is of 'pure' weight, i.e. consists of terms of weight w only. In the general case, one can always split the symbol into parts of pure weight and treat each of them separately. We write

$$S=\sum_i c_i\mathcal{S}(b_i^{(w)})+\sum_{\substack{i_1,i_2\\ w_1+w_2=w}} c_{i_1,i_2}\mathcal{S}\left(b_{i_1}^{(w_1)}b_{i_2}^{(w_2)}\right)+\ldots+\sum_{i_1,\ldots,i_w} c_{i_1\ldots i_w}\mathcal{S}\left(b_{i_1}^{(1)}\ldots b_{i_w}^{(1)}\right)\,, \quad (3.33)$$

where the exponent of functions $b^{(w)}$ indicates their weight and we choose that $w_i\leq w_{i+1}$. The $c_{i_1\ldots i_l}$ are the rational coefficients that we want to determine.

Equating our ansatz to 3.26 we realize that we have mapped our original problem of finding F such that $\mathcal{S}(F)=S$ to a the linear algebra problem of determining the coefficients c in function of the $\widetilde{c}$.

3.2.4 Projectors

Even though the problem can be in principle solved that way, the resulting system of linear equations can become quite large. Therefore it would be desirable to break the problem into smaller pieces to be solved separately. One way to do this is the use of projectors which select certain parts of the symbol which can then be integrated.

We define linear operators Π_w acting on elementary tensors of length $w\leq 1$:

$$\begin{aligned}\Pi_w(a_1\otimes\ldots\otimes a_w)=&\\ =&\frac{w-1}{w}\left[\Pi_{w-1}(a_1\otimes\ldots\otimes a_w-1)\otimes a_w-\Pi_{w-1}(a_2\otimes\ldots\otimes a_w)\otimes a_1\right],\ .\end{aligned} \quad (3.34)$$

with $\Pi_1=\mathrm{id}$.

It can then be shown that this operator maps to zero the part of a symbol S that can be written as the symbol of a linear combination of products of lower weight functions.

Applying this operator to our problem we now have

$$\Pi_w S = \sum_i c_i \Pi_w \mathcal{S}\left(b_i^{(w)}\right) \,, \tag{3.35}$$

which can be readily solved. We have therefore found the part of the symbol that cannot be written as a product of lower weight functions.

We would now like to proceed by induction in the same way with the other coefficients $c_{i_1 \ldots i_m}$. As it turns out [67], we can do this by a small extension of above projectors. We define tensor products of them $\Pi_{w_1} \otimes \ldots \otimes \Pi_{w_k}$ acting on tensors of weight $\sum_i w_i = w$, where the first projector Π_{w_1} acts on the first w_1 factors of the tensor product, and so on. Let consider partitions of w: If $\succ$ is the standard lexicographic order we can write the partitions

$$\begin{aligned}(w) \succ (w-1,1) \succ (w-2,2) \succ \ldots \succ (w - \lfloor \frac{w}{2} \rfloor, \lfloor \frac{w}{2} \rfloor) \succ (w-2,1,1) \succ \\ \succ \cdots \succ (2, \underbrace{1, \ldots, 1}_{w-2 \text{ slots}} \succ (\underbrace{1, \ldots, 1}_{w \text{ slots}}) \,,\end{aligned} \tag{3.36}$$

where $\lfloor x \rfloor$ denotes the largest integer $\leq x$. In an analogous manner there is a natural ordering of projection operators

$$\Pi_w \succ \Pi_{w-1} \otimes \Pi_1 \succ \Pi_{w-2} \otimes \Pi_2 \succ \cdots \succ \Pi_1 \otimes \ldots \otimes \Pi_1 \,. \tag{3.37}$$

At weight four these are, for example

$$\Pi_4 \succ \Pi_3 \otimes \Pi_1 \succ \Pi_2 \otimes \Pi_2 \succ \Pi_2 \otimes \Pi_1 \otimes \Pi_1 \succ \Pi_1 \otimes \Pi_1 \otimes \Pi_1 \otimes \Pi_1 \,. \tag{3.38}$$

As it can be shown, the images of these projectors each contain the ones of lower order. This means that a symbol that vanishes under the action of one projector vanishes also under the action of the previous ones. Additionally, a symbol which is zero under the action of the first i projectors still might not vanish under the action of the $(i+1)^{\text{th}}$. Therefore, we can proceed by induction and use these projectors to consecutively filter out different parts of the expression. Already having found the c_i, we compute

$$\begin{aligned}&\Pi_{w-1} \otimes \Pi_1 \left(S - \mathcal{S}\Big(\sum_i c_i b_i^{(w)} \Big) \right) = \\ &= \Pi_{w-1} \otimes \Pi_1 \left[\sum_{\substack{i_1, i_2 \\ w_1 + w_2 = w}} c_{i_1, i_2} \mathcal{S}\left(b_{i_1}^{(w_1)} b_{i_2}^{(w_2)} \right) + \ldots + \sum_{i_1, \ldots, i_w} c_{i_1 \ldots i_w} \mathcal{S}\left(b_{i_1}^{(1)} \ldots b_{i_w}^{(1)} \right) \right] \\ &= \sum_{\substack{i_1, i_2 \\ w_1 + w_2 = w}} c_{i_1, i_2} (\Pi_{w-1} \otimes \Pi_1) \mathcal{S}\left(b_{i_1}^{(w_1)} b_{i_2}^{(w_2)} \right) \,.\end{aligned} \tag{3.39}$$

We have sucessfully filtered the system and can now easily determine the c_{i_1, i_2}. The rest of the coefficients are determined this way by induction, leaving us with the sought after solution F for $\mathcal{S}(F) = \mathcal{S}(F_0)$.

3.2.5 Determining the parts in the kernel of the Symbol map

So far we have only found an expression which has the same symbol. We nevertheless have to determine the parts of the original expression that lie in the kernel of the symbol map, e.g. parts proportional to ζ values and some other constants (see section 3.2.2).

We again make an ansatz

$$F_0 - F = \sum_i \widetilde{c}_i \widetilde{k}_i + \sum_l \sum_{\substack{i_1,\ldots,i_l \\ w_1+\ldots+w_l=w}} c_{i_1\ldots i_l} k_{i_1\ldots i_l} b_{i_1}^{(w_1)} \ldots b_{i_l}^{w_l} \,, \tag{3.40}$$

where the b_i are the basis functions from the previous section, the k_i are generators from the kernel of the symbol map and the $\widetilde{c}_i$ and $c_{i_1\ldots i_l}$ are the rational constants to be determined. In principle it should be enough to evaluate this ansatz for specific values of the variables x_i, e.g. 0 or 1, and then obtain linear equations that can be solved for the sought-after constants. In the implementation presented in this work, however, this step is performed in a different way. The above ansatz is evaluated for random values for the x_i (in the correct analytical region) to very high precision using the GiNaC library [225] and then the PSLQ algorithm [222] is used to determine the $\widetilde{c}_i$ and $c_{i_1\ldots i_l}$. The PSLQ algorithm can be used to find integer relations, i.e. solutions to the equation

$$n_1 y_1 + n_2 y_2 + \ldots + n_k y_k = 0 \,. \tag{3.41}$$

where y_i are known transcendental numbers and the $n_i \in \mathbb{Z}$ are to be determined. It is briefly described in appendix C.3, where an example can be found as well. Adapting this to the present use case one can easily determine the part of F_0 in the kernel of the symbol map, albeit relying heavily on the precise numerical evaluation routines and the power of the PSLQ algorithm. With a growing number of basis function this task becomes increasingly difficult and time consuming.

3.2.6 Cut structure and imaginary parts

As it can be seen from the symbol rules and previous considerations, elementary tensors (a) and $(-a)$ are equivalent and therefore terms proportional to

$$\mathcal{S}(i\pi) = \mathcal{S}\left(\log(-1 + i\epsilon)\right) = 0 \tag{3.42}$$

vanish. Therefore, in an expression where the imaginary part has not been made explicit and can be simplified separately, all the information about it is lost by the symbol map. However, as it was pointed out in [68], the information about the cuts of an expression is encoded in the symbol in the very first factor of the tensor products. Employing a little trick, that will be justified more thoroughly in section 3.3.2, we can nevertheless keep the information about the imaginary part of the expression and compute its symbol.

1. When computing and simplifying the symbol we strictly keep the first entries of all the tensor products unchanged.
2. We interpret each of these entries as a logarithm and study whether they have to be analytically continued.
3. Where this is the case, we do so and interpret the part proportional to the imaginary part of the logarithm as the symbol of the complex part of our expression.

As illustration, let us suppose the symbol we compute contains a term

$$(-x) \otimes a_1 \otimes a_2 \, . \tag{3.43}$$

From the problem at hand we know $x > 0$ and therefore that $\log(-x)$ has to be analytically continued. Supposing that x possesses a small positive imaginary part we can continue the logarithm as

$$\log(-x) = \log(-x - i\epsilon) = \log(x) - i\pi \, . \tag{3.44}$$

In analogy we rewrite the above tensor product

$$(-x) \otimes a_1 \otimes a_2 = x \otimes a_1 \otimes a_2 - i\pi(a_1 \otimes a_2) \, . \tag{3.45}$$

This way we can sucessfully keep the information about the cut structure of our expression, extract its imaginary part and integrate it separately.

3.2.7 An alternative way to integrate the symbol

The algorithm described in section 3.2.4 is very useful when dealing with a low number of basis functions and when one is interested in writing the result using functions with complicated arguments. However, often we are not interested in obtaining a short form of our expression but rather express it as combination of MPLs with certain (simple) arguments. In this case an alternative way to integrate the symbol which will be described in the following can be used.

The general idea is to bring the symbol into a form from where information about the MPLs of the integrated version can be read off directly.

Let us suppose for the moment that the symbol of our expression F with weight n depends on one variable x and the symbol of the imaginary part will be ignored for the moment. We would like to integrate it as MPLs with x in the argument and constants in the index. First, similar to before, we need to bring the tensor product factors into a unique form which we choose this time as

$$\pi_i = \left(1 - \frac{x}{c_i}\right) \quad \text{or} \quad (c_i) \quad \text{with } c_i \in \mathbb{C}^* \, , \tag{3.46}$$

The algorithm is based on two observations. Firstly, it is a well known result that an expression in which all "shuffles have been eliminated" (i.e. products of MPLs with the same argument have been replaced by the sum of their shuffled GHPLs using (3.7)) is unique [213] in the sense that there is no alternative way of writing it using GHPLs of the same index set without using products of MPLs with the same argument. Secondly, it can be seen that the symbol of a generic MPL contains exactly one term of the form

$$\mathcal{S}(G(a_1, \ldots, a_n; x)) = \ldots + \left(1 - \frac{x}{a_n}\right) \otimes \ldots \otimes \left(1 - \frac{x}{a_1}\right) + \ldots \, , \tag{3.47}$$

whereas all the other terms contain at least one factor independent of x. Therefore, each term of that form present in the symbol comes from one MPL with x in the argument.

The idea is now to rewrite the symbol of the expression at hand in a way such that we can read off the terms of the form (3.47) and use them to construct the "shuffle free" part of the integrated expression. Then, in an analogous manner to the symbol integration using projectors before, we proceed iteratively. We subtract from the symbol $\mathcal{S}(F_0)$ which we seek to integrate the symbol of the newly found terms. The result should

now contain no more terms of form 3.47. In order to determine the parts proportional to $G(a_1, \ldots, a_{n-1}, x)\, \log(a_n)$ we now focus on the terms

$$\mathcal{S}(G(a_1, \ldots, a_{n-1}; x) \log a_n) = \ldots + (a_n) \otimes \left(1 - \frac{x}{a_{n-1}}\right) \otimes \ldots \otimes \left(1 - \frac{x}{a_1}\right) + \ldots \,, \quad (3.48)$$

and construct that part analogously. We then subtract that symbol from the "left over" symbol above.

Proceeding further we face a small subtlety: terms of the form

$$G(a_1, \ldots, a_{n-2}, x)\, \log(a_{n-1})\, \log(a_n)$$

produce two tensor products of the desired form due to the shuffle identities:

$$\begin{aligned} \mathcal{S}(G(a_1, \ldots, a_{n-2}; x) \log a_{n-1} \log a_n) = \\ = \ldots + (a_n) \otimes (a_{n-1}) \otimes \left(1 - \frac{x}{a_{n-1}}\right) \otimes \ldots \otimes \left(1 - \frac{x}{a_1}\right) \\ + (a_{n-1}) \otimes (a_n) \otimes \left(1 - \frac{x}{a_{n-1}}\right) \otimes \ldots \otimes \left(1 - \frac{x}{a_1}\right) + \ldots \,. \end{aligned} \quad (3.49)$$

We should therefore only pick products where the constant factors a_i in the beginning follow a certain order e.g.

$$a_i \otimes a_j \otimes \ldots \qquad \text{with } a_i <= a_j \quad (3.50)$$

to construct the next part of the result. In principle, also multiple polylogarithms with only constants in argument and index could produce such terms, e.g.

$$\mathcal{S}(G(-\frac{1}{2}, -1; 1)) = 2 \otimes 3 - 3 \otimes 2 \,, \quad (3.51)$$

but in the cases encountered in this work it was sufficient to only consider products of logarithms.

Repeating the above steps, all dependence of x can be integrated and only tensor products consisting of constant terms should be left. In the cases met in this work these consisted always of powers of logarithms of constants. These terms can again be integrated by using the ordered tensor products (in the sense of eq. (3.50) above) to construct the integrated expression.

In the case that the expression at hand depends on more than one variable, we can proceed in a completely analogous manner. For the case of two, x_1 and x_2, it is often desired to rewrite it in the form of MPLs

$$G(\{f_i(x_2)\}; x_1) \quad \text{and} \quad G(\{c_i\}; x_2) \quad c_i \in \mathbb{C} \,. \quad (3.52)$$

We cast the tensor product factors in $\mathcal{S}(F(x_1, x_2))$ into the form

$$\pi_i = \left(1 - \frac{x_1}{f_i(x_2)}\right) \quad \text{or} \quad \left(1 - \frac{x_2}{c_i}\right) \quad \text{or} \quad (c_i) \quad \text{with } c_i \in \mathbb{C}^* \,, \quad (3.53)$$

and focus on the terms containing factors dependent on x_1 first. We proceed exactly as above, i.e. at step $i \leq n$ we then pick the terms

$$\left(\bigotimes_{j=0}^{i-1} \left(1 - \frac{x_2}{c_j}\right)\right) \otimes \left(\bigotimes_{k=i}^{n} \left(1 - \frac{x_1}{f_k(x_2)}\right)\right) \quad (3.54)$$

which can be used to construct the parts proportional to

$$G(c_{i-1},\ldots,c_1;x_2)\,G(f_n(x_2),\ldots,f_i(x_2);x_1) \tag{3.55}$$

using the relation from equation (3.47). This way, we can integrate all tensor products containing x_1 first and are then left with a symbol depending on x_2 only, which can be treated as above.

3.2.8 Discussion and Conclusion

It has been shown that the symbol formalism provides a convenient framework to simplify a known expression involving MPLs in terms of a basis of chosen functions, once this one is known. However, the method has its shortfalls. Firstly, it is unsatisfactory that the symbol map loses much information which then has to be "guessed" in an additional step. Secondly, there is also a combinatorial problem. In many cases the number of basis functions need to be MPLs of a large set of indices, therefore enlarging the linear systems that have to be solved. This also makes the guessing of the part lost by the symbol map increasingly a time-consuming task, which becomes an important factor when the algorithm has to be applied many times as it was often the case in this work.

As a solution to the combinatorial problem and for the task of integrating a symbol in terms of MPLs of simple arguments an alternative way to integrate the symbol was described which avoids having to choose a basis of functions altogether.

A generalization of the symbol, the so-called coproduct, provides a remedy of the first problem. In the following chapter it will be shown how it can be used in a similar way as the symbol but allows to keep almost all information of the original expression.

3.3 The Coproduct of the Multiple Polylogarithms

As it has been mentioned in the previous section, the symbol formalism is a great tool to potentially simplify complicated expressions and to study whether such simplifications are possible. However, the fact that all information proportional to zeta values is lost is a serious problem. As we will show in this section, the coproduct as a generalization of the symbol alleviates this.

First, let us discuss some algebra basics. Then the coproduct will be introduced and the simplification procedure discussed.

3.3.1 An intuitive introduction of the coproduct

This section is a short review of the concepts presented in [68]. Its aim is not to give a precise introduction and definition of the required mathematical concepts but to provide the reader with an intuitive understanding of the coproduct.

Let us start by reviewing some definitions. As it is known from basic math, an *algebra* over a field $\mathbb{K}$ (usually $\mathbb{C}$ or $\mathbb{R}$) is a $\mathbb{K}$-vector space together with a map

$$\begin{aligned} m : \mathcal{A}\times\mathcal{A} &\to \mathcal{A} \\ (a,b) &\mapsto m(a,b)\equiv a\cdot b \end{aligned} \tag{3.56}$$

that is associative, posseses a unit ϵ and is compatible with the vector space structure of $\mathcal{A}$. We now observe that the multiple polylogarithms for a given set of indices equipped with the shuffle product form an algebra with the scalars being the rational numbers. Equation

(3.7) shows that the shuffle product preserves the weight. We can therefore deduce that this algebra is *graded*, that means that we can write the vector space as a direct sum

$$\mathcal{A} = \bigoplus_{n=0}^{\infty} \mathcal{A}_n \ , \tag{3.57}$$

such that the multiplication preserves the grading

$$\mathcal{A}_m \cdot \mathcal{A}_n \subset \mathcal{A}_{m+n} \ , \tag{3.58}$$

where $\mathcal{A}_n$ denotes the vector space of MPLs of weight n. We also observe that $\mathbb{K}$ is also embedded into $\mathcal{A}$ via $\mathcal{A}_0 = \mathbb{K}$.

Let us now add an additional structure: If we have two vector spaces U and V, then there is a unique vector space $U \otimes V$ called the *tensor product* of U and V. We then have that for every *bilinear* map β there is a unique *linear* map η such that

$$\beta(a, b) = \eta(a \otimes b) \ . \tag{3.59}$$

Since m is bilinear, we therefore have that there exists a linear map μ such that

$$a \cdot b = m(a, b) = \mu(a \otimes b) \ . \tag{3.60}$$

Since m is also associative we also have then for μ that

$$\mu(\mathrm{id} \otimes \mu) = \mu(\mu \otimes \mathrm{id}), \tag{3.61}$$

where $(\mathrm{id} \otimes \mu)$ acts on a tripple tensor product as

$$(\mathrm{id} \otimes \mu)(a \otimes b \otimes c) = \mathrm{id}(a) \otimes (\mu(b \otimes c)) \ . \tag{3.62}$$

Diagramatically, this tells us that we can choose whichever path in the following diagram (which is therefore *commutative*):

$$\begin{array}{ccc} \mathcal{A} \otimes \mathcal{A} \otimes \mathcal{A} & \xrightarrow{\mathrm{id} \otimes \mu} & \mathcal{A} \otimes \mathcal{A} \\ \downarrow{\scriptstyle \mu \otimes \mathrm{id}} & & \downarrow{\scriptstyle \mu} \\ \mathcal{A} \otimes \mathcal{A} & \xrightarrow{\mu} & \mathcal{A} \end{array} \tag{3.63}$$

The notion of the *coproduct* can now be introduced using familiar concepts. If we have vector spaces U, V, then there exist their dual vector spaces of one-forms U^* and V^*. A linear map $A : U \to V$ then induces a linear map $A^\dagger : V^* \to U^*$ in the opposite direction:

$$U \xrightarrow{A} V \quad \text{induces} \quad V^* \xrightarrow{A^\dagger} U^* \ . \tag{3.64}$$

Based on this observation we can derive a prescription for "dualizing" a commutative diagram:

1. replace each vector space by its dual,
2. replace each linear map by its dual and
3. reverse all the arrows in the diagram.

Similarly we part from a definition of an algebra $\mathcal{A}$ with multiplication $\mu : \mathcal{A} \otimes \mathcal{A} \to \mathcal{A}$ and can define a *coalgebra* $\mathcal{C}$ with *comultiplication* $\Delta \equiv \mu^\dagger : \mathcal{C} \to \mathcal{C} \otimes \mathcal{C}$. Dualizing the commutative diagram above we therefore have:

$$\begin{array}{ccc} \mathcal{C}\otimes\mathcal{C}\otimes\mathcal{C} & \xleftarrow{\mathrm{id}\otimes\Delta} & \mathcal{C}\otimes\mathcal{C} \\ \uparrow{\scriptstyle \Delta\otimes\mathrm{id}} & & \uparrow{\scriptstyle \Delta} \\ \mathcal{C}\otimes\mathcal{C} & \xleftarrow{\Delta} & \mathcal{C} \end{array} \tag{3.65}$$

Just like in the case with vector spaces, properties transcend from the product to the coproduct. Most importantly, *coassiociativity*:

$$(\mathrm{id}\otimes\Delta)\Delta = (\Delta\otimes\mathrm{id})\Delta\ . \tag{3.66}$$

In words: Associativity means that the order of multiplying together objects is irrelevant. Morally, applying the coproduct corresponds to "pulling apart" an object, and coassiociativity asserts that the order in which it is done is irrelevant. This therefore means that there is a unique way to iterate the coproduct

$$\mathcal{C} \xrightarrow{\Delta} \mathcal{C}\otimes\mathcal{C} \xrightarrow{\mathrm{id}\otimes\Delta} \mathcal{C}\otimes\mathcal{C}\otimes\mathcal{C} \xrightarrow{\mathrm{id}\otimes\mathrm{id}\otimes\Delta} \dots \tag{3.67}$$

Extending our notions once more, we define a *bialgebra*, an algebra that is a coalgebra at the same time, in other words a vector space equipped with a multiplication μ and a (coassiociative) comultiplication Δ. In this setting, μ and Δ are in general not hermitian conjugate to each other any more, but we require that they are compatible, that is

$$\Delta(a\cdot b) = \Delta(a)\cdot\Delta(b), \tag{3.68}$$

where the multiplication on the right hand side is defined as

$$(a_1\otimes a_2)\cdot(b_1\otimes b_2) \equiv (a_1\cdot b_1)\otimes(a_2\cdot b_2)\ . \tag{3.69}$$

This is equivalent with requiring that Δ is an algebra homomorphism.

A *Hopf algebra* $\mathcal{H}$ is a bialgebra which is also connected, that means that the field $\mathbb{K}$ is embedded into $\mathcal{H}$.

Let us study how the multiple polylogarithms can be promoted to a Hopf algebra.

3.3.2 The Hopf algebra of the multiple polylogarithms

It has been shown before that the multiple polylogarithms form an algebra together with the shuffle product which is graded by weight.

Let us introduce a different notation for the MPLs which allows the following formulas to be written in a much nicer form:

$$I(a_0;a_1,\dots,a_n;a_{n+1}) = \int_{a_0}^{a_{n+1}} \frac{dt}{t-a_n} I(a_0;a_1,\dots,a_{n-1};t)\ . \tag{3.70}$$

A we can see by comparison to equation (3.1) it is almost analogous to the standard definition, except that the lower integration boundary has become another variable and the order in the index vector has been reversed:

$$G(a_n,\dots,a_1;a_{n+1}) = I(0;a_1,\dots,a_n;a_{n+1})\ . \tag{3.71}$$

Note that I develops a logarithmic divergence in the limit that the first or the last indices indices agree, e.g. $I(a_0; a_0, a_1, \ldots, a_k; a_{k+1})$ or $I(a_0; a_1, \ldots, a_{n+1}; a_{n+1})$.

Since we can always choose the basis point of the integration it is easy to convert an integral $I(a_0; \ldots)$ with generic basis point a_0 to a combination of $I(0; \ldots) = G(\ldots)$: At weight one we have

$$I(a_0; a_1; a_2) = I(0; a_1; a2) - I(0; a_1; a_0) = G(a_1, a_2) - G(a_1; a_0). \tag{3.72}$$

At higher weights the relationship becomes more complicated due to the nestedness of the integration but requires no new concepts. For weight two we have

$$\begin{aligned} I(a_0; a_1, a_2; a_3) &= \int_{a_0}^{a_3} \frac{dt}{t - a_2} I(a_0; a_1; t) = \int_{a_0}^{a_3} \frac{dt}{t - a_2} \left[I(0; a_1; t) - I(0; a_1; a_0) \right] \\ &= I(0; a_1, a_2; a_3) - I(0; a_1, a_2; a_0) - I(0; a_1; a_0)[I(0; a_2; a_3) - I(0; a_2; a_0)] \\ &= G(a_2, a_1; a_3) - G(a_2, a_1; a_0) - G(a_1; a_0)[G(a_2; a_3) - G(a_2; a_0)] \,. \end{aligned} \tag{3.73}$$

The code that can produce this reduction for arbitrary weights can be found in the annexes of this work.

Let us now take the graded algebra formed by the multiple polylogarithms $\mathcal{H}$ equipped with the shuffle product.

$$\mathcal{H} = \bigoplus_{n=0}^{\infty} \mathcal{H}_n \tag{3.74}$$

Goncharov has defined a coproduct Δ on $\mathcal{H}$ and shown that it is compatible with its algebra structure. Since the rational numbers are embedded in $\mathcal{H}$ via $\mathcal{H}_0$, the GHPLs can thus be turned into a Hopf algebra [226]. The coproduct for mutually different indices a_i is given by

$$\begin{aligned} &\Delta(I(a_0; a_1, \ldots, a_n; a_{n+1})) = \\ &\sum_{0=i_1<i_2<\ldots<i_k<i_{k+1}=n} I(a_0; a_{i_1}, \ldots, a_{i_k}; a_{n+1}) \otimes \left[\prod_{p=0}^{k} I(a_{i_p}; a_{i_{p+1}}, \ldots a_{i_{p+1}-1}; a_{i_{p+1}}) \right] . \end{aligned} \tag{3.75}$$

It is a nontrivial statement that Δ is a genuine coproduct, i.e. that it fulfills coassiociativity and is an algebra homomorphism, both of which will not be shown here. When some indices are equal, regularization has to be performed which will be discussed in section 3.3.2. As an example, let us just quote here the coproduct of the ordinary (poly-)logarithm:

$$\begin{aligned} \Delta(\ln z) &= 1 \otimes \ln z + \ln z \otimes 1 \,, \\ \Delta(\mathrm{Li}_n(z)) &= 1 \otimes \mathrm{Li}_n(z) + \mathrm{Li}_n(z) \otimes 1 + \sum_{k=1}^{n-1} \mathrm{Li}_{n-k}(z) \otimes \frac{\ln^k z}{k!} \,. \end{aligned} \tag{3.76}$$

We observe that the coproduct Δ also "preserves the weight" in the sense below:

$$\mathcal{H} \xrightarrow{\Delta} \bigoplus_{p+q=n} \mathcal{H}_p \otimes \mathcal{H}_q \,, \tag{3.77}$$

where $\mathcal{H}_n$ denotes the space of MPLs of weight n. We can therefore write

$$\Delta = \sum_{p+q=n} \Delta_{p,q} \,, \tag{3.78}$$

where $\Delta_{p,q}$ is the operator whose image are the tensor products with the weights p, q in the respective factors. Let us also define the *reduced coproduct*

$$\Delta(a) = 1 \otimes a + a \otimes 1 + \Delta'(a) \; . \tag{3.79}$$

Any element that vanishes under the action of Δ' is called a *primitive element* of $\mathcal{H}$. It is now time to sketch the idea of how the coproduct can be used to simplify an expression. Let us suppose we have two identical expressions F_w and G_w of weight w which are in fact identical but take a different functional form and we would like to prove their equality. Evidently their coproducts but also the reduced coproduct must agree:

$$\Delta'(F_w) = \Delta'(G_w) \; . \tag{3.80}$$

This relation only involves functions of lower weight $w' < w$. If we know all functional relations among the MPLs involved at this weight we can use these to prove equality. In the contrary case, we apply the coproduct once more to one of the two factors in the tensor product to obtain a relation which involves only relations of even lower weight. Repeating this procedure for multiple times a whole tower of identities can be obtained. At weight four we have, for example,

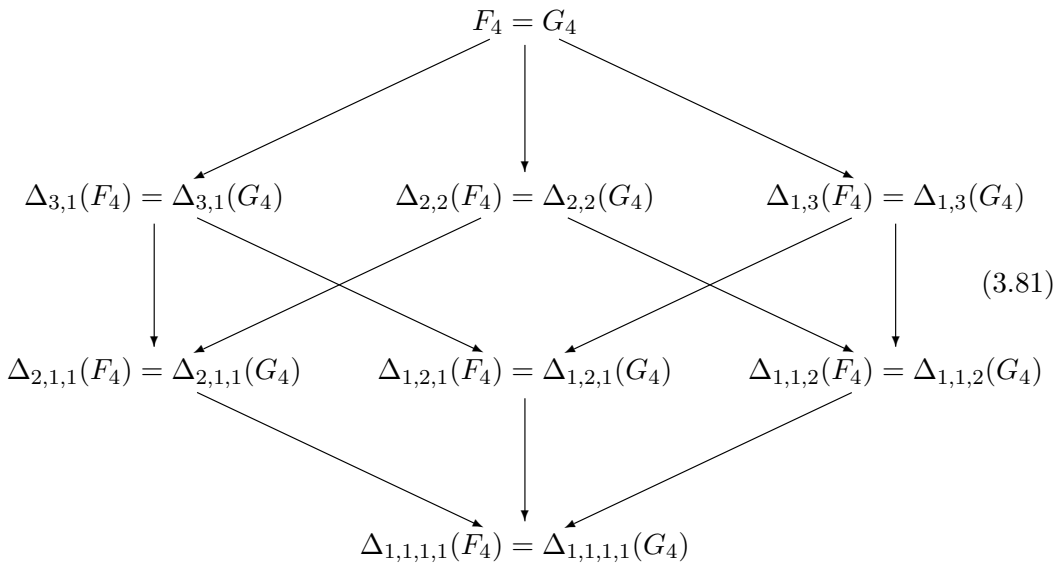

(3.81)

The idea is now to perform a "full decomposition" $\Delta_{1,\ldots,1}$ first, where all functions involved are of weight one, that is logarithms, for which all functional equations can be derived easily. It can be shown that his way we obtain the symbol of an expression, which will be discussed later. Therefore, requiring that two expressions have the same symbol is equivalent to requiring that they take the same form under the action of $\Delta_{1,\ldots,1}$. But one can still gain more information by applying the other operators $\Delta_{i_1,\ldots,i_k}$. Before showing how this can be done precisely, let us study a few more technical aspects of the coproduct.

The coproduct of ζ values

In section 3.2.5 we discussed that the symbol map maps zeta values to zero. Let us now study what happens to them under the action of the coproduct. Due to their definition we naively have, using equation (3.76),

$$\Delta(\zeta_n) = \Delta(\mathrm{Li}_n(1)) = 1 \otimes \zeta_n + \zeta_n \otimes 1 \,. \tag{3.82}$$

However, we know that the ζ_n for even n values are not independent but that they are all proportional to powers of ζ_2, for example

$$\zeta_4 = \frac{1}{15}\zeta_2^2 \tag{3.83}$$

Therefore,

$$\Delta(\zeta_4) = \frac{1}{15}\Delta(\zeta_2^2) = \frac{1}{15}[1 \otimes \zeta_n + \zeta_n \otimes 1] = \frac{1}{15}[1 \otimes \zeta_2^2 + \zeta_2^2 \otimes 1 + 2(\zeta_2 \otimes \zeta_2)] \,, \tag{3.84}$$

which contradicts 3.82 unless we set

$$\Delta(\zeta_2) = 0 \,. \tag{3.85}$$

In this case nothing would have been gained over the pure symbol approach. In [227] it was argued that it is consistent to define

$$\begin{aligned} \Delta(\zeta_2) &= \zeta_2 \otimes 1, \\ \Delta(\zeta_{2n}) &= \zeta_{2n} \otimes 1 \,, \quad n \in \mathbb{N} \,. \end{aligned} \tag{3.86}$$

which is compatible with the relationship of the ζ_n values for even n. Speaking precisely, this now defines the coproduct on the comodule over the Hopf algebra $\mathcal{H}$, but for our purposes this distinction is irrelevant.

In addition to that it was conjectured in [68] that we can also extend the above by setting

$$\Delta(\pi) = \pi \otimes 1 \,. \tag{3.87}$$

The two equations 3.86 and 3.87 lead us to render the definition of the coproduct more precise. It actually maps

$$\mathcal{H} \xrightarrow{\Delta} \mathcal{H} \otimes \mathcal{H}^\pi \xrightarrow{\Delta\otimes\mathrm{id}} \mathcal{H} \otimes \mathcal{H}^\pi \otimes \mathcal{H}^\pi \xrightarrow{\Delta\otimes\mathrm{id}\otimes\mathrm{id}} \mathcal{H} \otimes \mathcal{H}^\pi \otimes \mathcal{H}^\pi \otimes \mathcal{H}^\pi \xrightarrow{\Delta\otimes\mathrm{id}\otimes\mathrm{id}\otimes\mathrm{id}} \dots \tag{3.88}$$

where we have defined $\mathcal{H}^\pi$ as the quotient of $\mathcal{H}$ by the (two-sided) ideal generated by π, or, in lay-man's terms, that we drop all factors of π in the tensor products except in the first one.

A graphical rule for computation of the coproduct

For general harmonic polylogarithms there is a practical rule for computing the coproduct which produces all the terms in (3.75) [66, 226].

First, for a given MPL $I(a_0; a_1, \dots, a_n; a_{n+1})$ of weight n one draws a half-circle with the start- and end-point on opposite ends and the indices in between. For $n = 3$ this looks like:

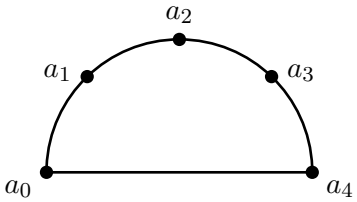

One then draws all possible polygons with the a_i at the corners (including the empty one) which have as baseline the connection $a_0 \leftrightarrow a_{n+1}$. For each of these pictures the indices that are on the corner of the polygon determine the arguments of I in the first factor of the tensor product, whereas the indices that are not on the polygons determine the second one. For weight three we find

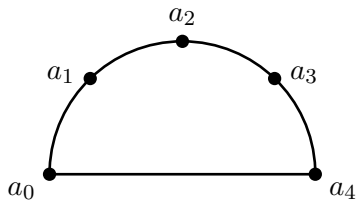

$1 \otimes I(a_0; a_1, a_2, a_3; a_4)$

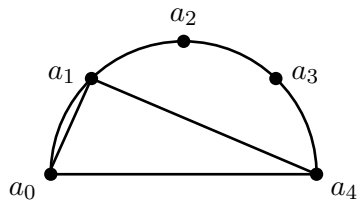

$I(a_0; a_1; a_4) \otimes I(a_1; a_2, a_3; a_4)$

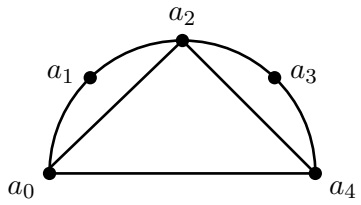

$I(a_0; a_2; a_4) \otimes (I(a_0; a_1; a_2) I(a_2, a_3; a_4))$

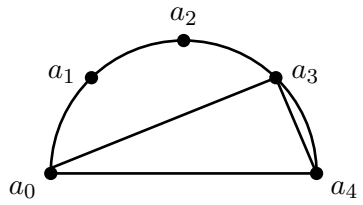

$I(a_0; a_3; a_4) \otimes I(a_0; a_1, a_2; a_3)$

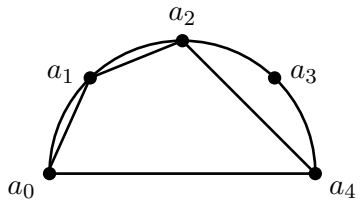

$I(a_0; a_1, a_2; a_4) \otimes I(a_2; a_3; a_4)$

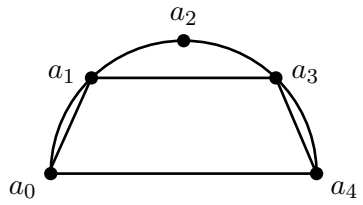

$I(a_0; a_1, a_3; a_4) \otimes I(a_1; a_2; a_3)$

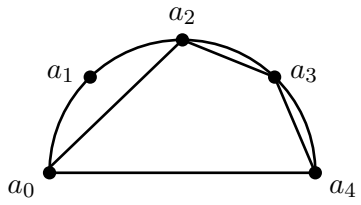

$I(a_0; a_2, a_3; a_4) \otimes I(a_0; a_1; a_2)$

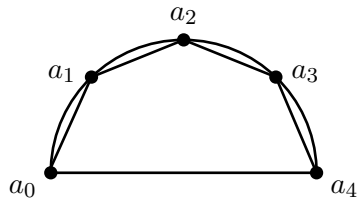

$I(a_0; a_1, a_2, a_3; a_4) \otimes 1$

The coproduct $\Delta(I(a_0; a_1, \ldots, a_n; a_{n+1})$ is then the sum over all these terms. The coproduct for $n = 4$ can be found in [68].

Regularization

The formula 3.75 is strictly only valid in the case that all the entries a_i are mutually different. In the case that some of them are equal, application of 3.75 yields divergent

terms in the coproduct. These divergences have to be regularized. In this work a slight modification of the procedure described in [68] has been used.

First, use the shuffle algebra to extract all divergences as powers of logarithmic divergences of type $I(a_i;a_j;a_j)$. For illustration, for $I(a_0,a_0,a_1,a_2;a_2)$ we have

$$\begin{aligned} I(a_0;a_0,&a_1,a_2;a_2) = \\ &= I(a_0;a_0;a_2)I(a_0;a_1,a_2;a_2) - I(a_0;a_1,a_0,a_2;a_2) - I(a_0;a_1,a_2,a_0;a_2) \\ &= I(a_0;a_0;a_2)(I(a_0;a_1;a_2)I(a_0;a_2;a_2) - I(a_0;a_2,a_1;a_2)) \\ &\quad - (I(a_0;a_2;a_2)I(a_0;a_1,a_0;a_2)) + I(a_0;a_2,a_1,a_0;a_2)\ . \end{aligned} \tag{3.89}$$

Then shift the integration bounds by a small amount $\epsilon > 0$ according to the rule

$$\begin{aligned} a_i &\to a_i(1-\epsilon) \quad a_i \neq 0 \\ a_i &\to \epsilon \quad a_i = 0\ . \end{aligned} \tag{3.90}$$

We then rewrite each of these divergences in terms of logarithms, extracting the divergent $\log\epsilon$ part. The possible cases are

$$\begin{aligned} I(a_0;a_0;a_1) &\to I(a_0(1-\epsilon);a_0;a_1(1-\epsilon)) = \log\epsilon + \log\left(1-\frac{a_1}{a_0}\right) \qquad 0 \neq a_0 \neq a_1\ , \\ I(0;0;a_1) &\to I(\epsilon;0;a_1(1-\epsilon)) = \log(a_1) - \log\epsilon \qquad a_1 \neq 0\ , \\ I(a_0;a_1;a_1) &\to I(a_0(1-\epsilon);a_1;a_1(1-\epsilon)) = \log\epsilon - \log\left(1-\frac{a_0}{a_1}\right) \qquad 0 \neq a_1 \neq a_0\ , \\ I(a_0;0;0) &\to I(a_0;0;\epsilon)) = \log\epsilon - \log(a_0) \qquad a_0 \neq 0\ . \end{aligned} \tag{3.91}$$

The regularization step now consist in discarding all the terms proportional to $\log\epsilon$. In the example above we obtain

$$\begin{aligned} I(a_0;a_0,a_1,a_2;a_2) &= I(a_0,a_2,a_1,a_0,a_2) - I(a_0,a_2,a_1,a_2)\log\left(1-\frac{a_2}{a_0}\right) \\ &+ \left(\log a_2 - \log a_0 - \log\left(1-\frac{a_2}{a_0}\right)\right)\left(I(a_0,a_1,a_2)\log\left(1-\frac{a_2}{a_0}\right) - I(a_0,a_1,a_0,a_2)\right)\ . \end{aligned} \tag{3.92}$$

The symbol as a limiting case of the coproduct

In [68] it was motivated that the maximal decomposition of the coproduct is indeed related to the symbol via

$$\mathcal{S} \equiv \Delta_{1,\ldots,1} \mod \pi\ . \tag{3.93}$$

That is, up to factors of π we have that

$$\begin{aligned} \mathcal{S}(F) &= \sum_{i_k} c_{i_1\ldots i_n} a_{i_1} \otimes_{\mathcal{S}} \ldots \otimes_{\mathcal{S}} a_{i_n} \\ &\sim \sum_{i_k} c_{i_1\ldots i_n} \log(a_{i_1}) \otimes_{\Delta} \ldots \otimes_{\Delta} \log(a_{i_n}) = \Delta_{1,\ldots,1}(F)\ , \end{aligned} \tag{3.94}$$

where we introduced the subscripts $\mathcal{S}$, Δ to underline the different nature of the two tensor products. We can now see the motivation for the statement in section 3.2.6: With the trick described there we basically restored the part of $\Delta_{1,\ldots,1}(F)$ proportional to π and interpreted it as symbol of lower weight.

3.3.3 Coproduct simplification procedure

We now have all the tools necessary to use the coproduct to do transformations of MPLs. As it was outlined previously, we work our way up through (3.81). Parting from an expression F_4, we first find the part of G_4 that has the same action under $\Delta_{1,\dots,1}$, i.e. the same symbol, using one of the techniques described in the previous chapter.

Then we reconstruct the parts of F that lie in $\mathcal{H}_{i_1\dots i_k}$ by applying the different operators $\Delta_{i_1\dots i_k}$ to the difference of the original expression and the expression integrated from previous steps. Again, we work from bottom up, e.g. at weight 3 we have the an ordering of operators

$$\Delta_{1,1,1} \succ \Delta_{2,1}, \Delta_{1,2} \ , \tag{3.95}$$

and at weight 4

$$\Delta_{1,1,1,1} \succ \Delta_{2,1,1}, \Delta_{1,1,2}, \Delta_{1,2,1} \succ \Delta_{3,1}, \Delta_{2,2}, \Delta_{1,3} \ . \tag{3.96}$$

which we apply in consecutive order.

In order to bring the expression to its unique form, i.e. everything is expressed in a unique set of MPLs, we need additional input. For example, let us suppose that the expression we want to re-express in a different set of MPLs contains $G(a,b,c;x)$. Computing

$$\begin{aligned}\Delta_{2,1,1}G(a,b,c;x) = {} & G(a,b;x)\otimes\log\left(1-\frac{b}{c}\right) + G(a,c;x)\otimes\log\left(1-\frac{a}{b}\right) \\ & - G(a,c;x)\otimes\log\left(1-\frac{c}{b}\right) - G(b,c;x)\otimes\log\left(1-\frac{b}{a}\right) + G(b,c;x)\otimes\log\left(1-\frac{x}{a}\right) \ ,\end{aligned} \tag{3.97}$$

we note that we now also need the identities re-expressing the lower weight functions $G(a,b;x)$, $G(a,c;x)$ and $G(b,c;x)$ as well as the limits $\log(1-b/c)$, $\log(1-a/b)$, $\log(1-c/b)$ and $\log(1-x/a)$. The lower weight identities have to be derived in a previous step whereas the limits have to be computed separately (see also the following example section). In principle, these could be ill-defined since we do not have a cut prescription how these limits should be taken. However, this ambiguity is only up to the imaginary part, i.e. parts proportional to π. As we can see in the definition of the coproduct, eq. (3.75), these limits only show up in the second factor, whereas the integration bounds of the first factor are the one of the original expression. Therefore we only need a cut prescription for the original expression.On the other hand we know that factors of π vanish everywhere but in the first factor of the tensor product, which allows us to ignore the ambiguous terms from taking these limits.

Applying all these identities, after lots of cancellations, we obtain a part of the original expression that would have been lost in the symbol map. At weight three, $\Delta_{2,1}$ yields the parts proportional to π^2, and at weight four

$$\begin{aligned} \Delta_{2,1,1} &\quad \text{yields parts } \propto \pi^2 \ , \\ \Delta_{3,1} &\quad \text{yields parts } \propto \zeta_3,\, i\pi^3 \ , \\ \Delta_{2,2} &\quad \text{yields parts } \propto \pi^2 \ , \\ \Delta_{1,3} &\quad \text{yields parts } \propto \zeta_3, \ . \end{aligned} \tag{3.98}$$

For example, let us suppose that we have an expression F of weight four whose integrated symbol is, also including the integrated symbol of the imaginary part, $F_{1,1,1,1}$. Applying

$\Delta_{2,1,1}$ to the difference and using all identities of lower weight needed yields

$$\Delta_{2,1,1}(F - F_{1,1,1,1}) = \sum c_{i_1 i_2} \pi^2 \otimes a_{i_1} \otimes a_{i_2}, \tag{3.99}$$

which can be integrated interpreting each summand as $\pi^2(a_{i_1} \otimes a_{i_2})$, i.e. as π^2 times a symbol of weight 2. There cannot be anything other than π^2 in the first factor since any other such factor would also have produced a contribution to the symbol of the expression. For the same reasons the operators $\Delta_{1,2,1}$ and $\Delta_{1,1,2}$ do not yield additional information. It was found that in the cases treated in this work the operators

$$\begin{aligned} \Delta_{1,2} \quad & \text{at weight 3 and} \\ \Delta_{1,2,1}, \Delta_{1,1,2}, \Delta_{2,2} \quad & \text{at weight 4} \end{aligned} \tag{3.100}$$

could be ignored for this reason [69].

Due to the symmetry of $\Delta(\zeta_3) = \zeta_3 \otimes 1 + 1 \otimes \zeta_3$ it was also not necessary to study the expression under the action of $\Delta_{1,3}$ either, once the result of the application of $\Delta_{3,1}$ was known. During the preparation of this work the only object encountered that did not obey this symmetry was one transcendental constant,

$$\theta_4 = \frac{\log^4 2}{24} + \mathrm{Li}_4\left(\frac{1}{2}\right) - \frac{1}{24}\pi^2 \log^2(2) + \frac{7}{8}\log(2)\zeta_3 \tag{3.101}$$

which vanishes under $\Delta_{3,1}$ but $\Delta_{1,3}(\theta_4) = \frac{7}{8}(\log(2) \otimes \zeta_3)$. Curiously, one obtains θ_4 when attempting to extend the familiar combination $\frac{\log^4(2)}{24} + \mathrm{Li}_4\left(\frac{1}{2}\right)$, which has vanishing symbol, to a constant that also vanishes under the action of $\Delta_{2,1,1}$ and $\Delta_{3,1}$.

The computations can be abbreviated even more. The zeta values in the first factors of the tensor product are always generated through the usage of the lower weight identities. After the simplifications everything in the first factor cancels except for said zeta values. It is therefore a safe procedure to anticipate these cancellations and replace a lower weight function *only* by its zeta value part. This speeds up computations tremendously.

In summary, it was found to be sufficient to only use the operators $\Delta_{1,1,1}$, $\Delta_{2,1}$ at weight three and $\Delta_{1,1,1,1}$, $\Delta_{2,1,1}$ and $\Delta_{3,1}$ at weight four for the computation and to leave determination of the prefactor of the constant θ_4 to the next step. This has the advantage of speeding up the computations considerably, since the action of fewer operators has to be computed. Furthermore, it also lowers the number of required additional identities that have to be computed separately. As it was shown in eq. (3.97), limit identities are needed in order to simplify all tensor product factors but the first ones. With above simplifications these identities are only needed at weight one where they become simple and can be computed automatically in many cases.

3.3.4 Reconstructing the primitive elements of the coproduct

After the previous steps we are almost done transforming the expression in the desired way. The only parts that we are still missing are the *primitive elements*, e.g. the elements a such that $\Delta'(a) = 0$. In the cases encountered during preparation of this work these were multiples of transcendental constants. They can again be derived evaluating the expression for a limit where the value of the original expression is known exactly. Alternatively, one can also evaluate both sides numerically to high precision and apply the PSLQ algorithm

on the difference to find the constants. In the cases treated in this work, we found the following constants to be sufficient:

$$\begin{aligned} \zeta_2 = \frac{\pi^2}{6} &\quad \text{at weight 2,} \\ \zeta_3 &\quad \text{at weight 3,} \\ \zeta_4 = \frac{\pi^4}{90},\ \theta_4 &\quad \text{at weight 4.} \end{aligned} \tag{3.102}$$

As mentioned above, θ_4 (3.101) does not vanish under the coproduct. Nevertheless it was the only expression ever encountered that was asymmetric under $\Delta_{1,3}$ and $\Delta_{3,1}$ and therefore it is the most efficient way to compute the contribution from the application of $\Delta_{1,3}$ after the contribution from $\Delta_{3,1}$ is known.

After this step the transformed expression has been constructed in its entirety. As it can be seen, the coproduct provides an extension of the symbol formalism which allows to keep almost all the information contained of the original expression and to keep the 'guessing' to a minimum. An example application of this algorithm can be found in Section 5.4.3 and in more detail in Appendix D.2.

3.4 Conclusion

Multiple polylogarithms have many interesting properties and have to be dealt with in an efficient way in current computations of collider observables. In this chapter we introduced them and discussed how they can be equipped with a Hopf algebra structure. This structure can be exploited to derive identities among them and to simplify results involving these functions. In the following chapters the algorithms are put to use in computations relevant for collider observables. More examples of their usage are found in appendix D.

4

Virtual Contributions to $gg \to Zg$, $gg \to Z\gamma$ at Next-to-leading Order

The original work in this chapter was done in collaboration with Thomas Gehrmann and Lorenzo Tancredi and appeared in [61].

4.1 Introduction

In section 1.1.4 it was discussed how the production of vector boson pairs at a hadron collider is induced by quark-antiquark annihilations at leading order. Including corrections from higher orders in the perturbative expansion in QCD, other processes will also contribute to vector boson final states. These contributions are suppressed by higher orders in the strong coupling constant α_s, but could receive a numerical enhancement through the relevant parton-parton luminosity. In particular, in high-energy proton-proton collisions at the LHC, gluon-induced higher-order processes can become of comparable importance to quark-induced processes due to the large gluon luminosity at invariant masses relevant to vector boson production.

Vector-boson production in gluon-gluon collisions is mediated through a quark loop, which vanishes for the exclusive $gg \to V$ vertex due to Furry's theorem. The gluon-gluon-induced subprocess becomes relevant for the production of vector boson pairs (WW, ZZ, $\gamma\gamma$ and $Z\gamma$), or for the production of a neutral vector boson and a gluon. The leading-order scattering amplitudes for these processes all involve a closed quark loop. The resulting gluon-induced contributions from one-loop squared [228–230] processes (that appear only at next-to-next-to-leading order in the formal perturbative expansion of the full process) were evaluated a long time ago [45, 231–235], and typically found to yield a contribution that amounts to 10–20% of the total cross section. Inclusion of these gluon-gluon subprocess contributions often results in an enhanced theoretical uncertainty on the prediction, since the one-loop squared process is effectively Born-level for this combination of partons. To stabilise these predictions, the computation of the next perturbative order in vector-boson pair production or vector-boson-plus-jet production in gluon fusion is required. Technically, such a calculation amounts to computing the corrections from single

real radiation or single virtual exchange to the Born processes. With the Born process itself being a one-loop amplitude, one thus requires the two-loop corrections to the relevant partonic amplitudes. Up to now, these were obtained [56] only for $gg \to \gamma\gamma$, where the NLO correction to the gluon-induced process was found to be sizeable and important in the stabilisation of the theoretical prediction for photon pair production [57, 236].

In this chapter, we derive in massless QCD the two-loop corrections to the helicity amplitudes relevant to the production of a Z-boson in association with either a real photon or a hadronic jet in gluon-gluon collisions: $gg \to Z\gamma$ and $gg \to Zg$. For these processes, the one-loop amplitudes involving an extra gluon in the final state can be obtained using by-now standard methods for the computation of one-loop multi-leg processes [237–242]. With the results derived here, a complete NLO calculation of $Z\gamma$ and Zj production in gluon fusion becomes thus feasible.

The chapter is structured as follows: in section 4.2, we fix the notation and discuss the basic helicity structure of the process under consideration. The general tensor structure of the amplitude is described in section 4.3 and expressed through helicity amplitudes in section 4.4. The calculation of the two-loop amplitudes, their renormalisation and infrared properties and their simplification are described in section 4.5. The two-loop helicity amplitudes are obtained in a closed analytic form and written, as far as possible, in terms of logarithms and polylogarithms as described in section 4.5.2 using the methods from chapter 3. We performed several non-trivial checks on the results, which are described in section 4.6. We conclude with an outlook in section 4.7. In Appendix A the leading order and some next-to-leading order analytical results are given in the form of helicity amplitudes in decay kinematics $V \to ggg$ and $V \to gg\gamma$. The full results for the one- and two-loop coefficients in all relevant kinematical regions in Mathematica readable format can be found in the sources of the arxiv-submission of [61].

4.2 Kinematics and notations

The production of a massive vector boson $V = (Z^0, \gamma^*)$ and a gluon (photon) through gluon-gluon fusion is related by crossing to the decay of a massive vector boson to three gluons (two gluons and a photon) and has the same kinematics as vector-boson-plus-jet production $q\bar{q} \to Vg$, $qg \to Vq$ and vector-boson-plus-photon production $q\bar{q} \to V\gamma$. Technically the calculation of the two-loop QCD corrections to the $gg \to Vg$ and $gg \to V\gamma$ amplitudes is thus similar to previous calculations for $3j$-production, vector-boson-plus-photon production and $H \to 3$ partons, which have been derived to two-loop accuracy in QCD [58, 243, 244].

In the following we will focus on the decay kinematics, while the crossings relevant for V-plus-jet and V-plus-photon production at hadron colliders will be discussed in section 4.4.3.

The relevant partonic subprocesses are:

$$\begin{aligned} &l^-(p_5) + l^+(p_6) \to V(q) \to g(p_1) + g(p_2) + g(p_3)\,, \\ &l^-(p_5) + l^+(p_6) \to V(q) \to g(p_1) + g(p_2) + \gamma(p_3)\,, \end{aligned} \tag{4.1}$$

where we included the production of the vector boson V through lepton-antilepton annihilation.

In the framework of massless QCD interchanging the virtual photon with a Z boson amounts only to a proper re-weighting of the final result. Moreover, note that we always assume massless fermions in the initial or final state.

The momentum of the vector boson is given by

$$q^\mu = p_1^\mu + p_2^\mu + p_3^\mu \ . \tag{4.2}$$

It is convenient to define the usual invariants

$$s_{12} = (p_1 + p_2)^2 \ , \qquad s_{13} = (p_1 + p_3)^2 \ , \qquad s_{23} = (p_2 + p_3)^2 \ , \tag{4.3}$$

which fulfil

$$q^2 = (p_1 + p_2 + p_3)^2 = s_{12} + s_{13} + s_{23} \equiv s_{123} \ , \tag{4.4}$$

as well as the dimensionless invariants

$$x = s_{12}/s_{123} \ , \qquad y = s_{13}/s_{123} \ , \qquad z = s_{23}/s_{123} \ , \tag{4.5}$$

which satisfy

$$x + y + z = 1 \ . \tag{4.6}$$

In the decay kinematics $V \to ggg/gg\gamma$, as in the $3j$ case, q^2 is time-like (hence positive) and all the s_{ij} are also positive, which implies that x, y, z all lie in the interval $[0; 1]$, with the above constraint $x + y + z = 1$.

The helicity amplitudes can be expressed as a product of a partonic current S_μ and a leptonic current L_μ:

$$A(p_5, p_6; g_1, g_2, b_3) = L^\mu(p_5; p_6) S_\mu(g_1; g_2; b_3) \tag{4.7}$$

where $g_i = g(p_i)$, and $b_3 = b(p_3)$ labels a generic massless gauge boson. In our case $b = g, \gamma$ in $V \to ggg$ and $V \to gg\gamma$ respectively.

The purely vectorial tree-level leptonic current reads:

$$L^\mu(p_5, p_6) = \bar{v}(p_6)\, \gamma^\mu\, u(p_5), \tag{4.8}$$

where in the case of an incoming lepton-antilepton pair $L_\mu(p_5^-, p_6^+)$ corresponds to a left-handed current, and $L_\mu(p_5^+, p_6^-)$ to a right-handed current:

$$L_L^\mu(p_5^-, p_6^+) = \bar{v}_+(p_6)\, \gamma^\mu\, u_-(p_5), \qquad L_R^\mu(p_5^+, p_6^-) = \bar{v}_-(p_6)\, \gamma^\mu\, u_+(p_5). \tag{4.9}$$

Only the partonic currents receive contributions from QCD radiative corrections, and they can be perturbatively decomposed as:

$$\begin{aligned} S_\mu(g_1; g_2; g_3) &= \sqrt{4\pi\alpha_s}\, d^{a_1 a_2 a_3} \left[\left(\tfrac{\alpha_s}{2\pi}\right) S_\mu^{(1)}(g_1; g_2; g_3) + \left(\tfrac{\alpha_s}{2\pi}\right)^2 S_\mu^{(2)}(g_1; g_2; g_3) + \mathcal{O}(\alpha_s^3) \right] , \\ S_\mu(g_1; g_2; \gamma_3) &= \sqrt{4\pi\alpha}\, \delta^{a_1 a_2} \left[\left(\tfrac{\alpha_s}{2\pi}\right) S_\mu^{(1)}(g_1; g_2; \gamma_3) + \left(\tfrac{\alpha_s}{2\pi}\right)^2 S_\mu^{(2)}(g_1; g_2; \gamma_3) + \mathcal{O}(\alpha_s^3) \right] , \end{aligned}$$

where we factored out the overall colour factors $\delta^{a_1 a_2}$, $d^{a_1 a_2 a_3}$.

The general form of the gauge boson coupling to fermions is:

$$\mathcal{V}_\mu^{V, f_1 f_2} = -i\, e\, \Gamma_\mu^{V, f_1 f_2} \qquad \text{with} \qquad e = \sqrt{4\pi\alpha}, \tag{4.10}$$

whose explicit form depends on the gauge boson, on the type of fermions and on their helicities:

$$\Gamma_\mu^{V, f_1 f_2} = L_{f_1 f_2}^V\, \gamma_\mu \left(\frac{1 - \gamma_5}{2} \right) + R_{f_1 f_2}^V\, \gamma_\mu \left(\frac{1 + \gamma_5}{2} \right) . \tag{4.11}$$

The left- and right-handed couplings are identical for a pure vector interaction, and are in general different if vector and axial-vector interactions contribute. Their values for a photon are

$$L^{\gamma^*}_{f_1 f_2} = R^{\gamma^*}_{f_1 f_2} = -e_{f_1}\,\delta_{f_1 f_2}, \tag{4.12}$$

while for a Z boson

$$L^{Z}_{f_1 f_2} = \frac{I_3^{f_1} - \sin^2\theta_w e_{f_1}}{\sin\theta_w \cos\theta_w}\,\delta_{f_1 f_2}\ , \qquad R^{Z}_{f_1 f_2} = -\frac{\sin\theta_w e_{f_1}}{\cos\theta_w}\,\delta_{f_1 f_2}\ . \tag{4.13}$$

The vector boson propagator can be written as:

$$P^V_{\mu\nu}(q,\xi) = \frac{i\,\Delta^V_{\mu\nu}(q,\xi)}{D_V(q)}, \tag{4.14}$$

where $\Delta^V_{\mu\nu}(q,\xi)$ and $D_V(q)$ are, respectively, the numerator and the denominator in the R_ξ gauge:

$$\Delta^V_{\mu\nu}(q,\xi) = \left(-g_{\mu\nu} + (1-\xi)\frac{q_\mu q_\nu}{q^2 - \xi M_V^2}\right), \tag{4.15}$$

$$D_Z(q) = \left(q^2 - M_Z^2 + i\Gamma_Z M_Z\right), \tag{4.16}$$

$$D_{\gamma^*}(q) = q^2. \tag{4.17}$$

In the narrow-width approximation we can simplify expression (4.16) to

$$D_Z(q) \approx i\Gamma_Z M_Z \qquad \text{and} \qquad q^2 = M_Z^2, \tag{4.18}$$

where M_Z is the mass of the Z boson, while Γ_Z is its decay width.

Since we do not consider any electroweak corrections, the vector boson V is always coupled to a fermion line which allows us to neglect the R_ξ dependence (or equivalently to put $\xi = 1$). A further consequence is that the total amplitude is proportional to the charge weighted sum over the quark flavours, such that all electroweak couplings can be collected into a multiplicative factor Q^b_V. With this notation we obtain for an incoming right-handed lepton-antilepton pair, for the different choices of $V = (\gamma^*, Z)$, and helicity configurations (h_1, h_2, h_3):

$$\mathcal{M}_V(p_5^+, p_6^-; g_1^{h_1}, g_2^{h_2}, b_3^{h_3}) = -i\,(4\pi\alpha)\,\frac{R^V_{f_5 f_6}\,Q^b_V}{D_V(p_5+p_6)}\,A_R^{(h_1\,h_2\,h_3)}(p_5,p_6;g_1,g_2,b_3), \tag{4.19}$$

In case of $V = \gamma^*$ we find

$$Q^g_{\gamma^*} = \textstyle\sum_q e_q, \tag{4.20}$$

$$Q^\gamma_{\gamma^*} = \textstyle\sum_q e_q^2, \tag{4.21}$$

where the sum runs over the quark flavours in the loop.

In the case of $V = Z$ we have a contribution from the vector component of the Z boson, which is given by

$$Q^g_Z = \tfrac{1}{2}\textstyle\sum_q (L^Z_{qq} + R^Z_{qq}), \tag{4.22}$$

$$Q^\gamma_Z = \tfrac{1}{2}\textstyle\sum_q (L^Z_{qq} + R^Z_{qq}) e_q, \tag{4.23}$$

but also a contribution involving its axial coupling. This contribution vanishes for $Z \to gg\gamma$ due to charge conjugation invariance, already before summing over the quark flavours in the loop. On the other hand, in the case of $Z \to ggg$ it vanishes only after summing over the quark flavours.

4.3 The general tensor structure

In order to extract the helicity amplitudes from a generic QCD process different approaches can be attempted. One possibility is to decompose the amplitude into linearly independent tensor structures, whose number and form are entirely determined by symmetry considerations and which are completely independent on the loop order we are interested in. The entire loop-dependence is then contained in the scalar coefficients which multiply the relevant tensor structures. In order to single out these coefficients we apply projectors defined in d-continuous dimensions directly on the Feynman-diagrammatic expression for the amplitude [58, 243–245].

Using Lorentz invariance one can show that there are 138 independent Lorentz structures which can contribute to the partonic current [245]:

$$\begin{aligned} S^{\mu\nu\rho\sigma} &= a_1 g^{\mu\nu} g^{\rho\sigma} + a_2 g^{\mu\rho} g^{\nu\sigma} + a_3 g^{\mu\sigma} g^{\nu\rho} \\ &\quad + \sum_{j_1,j_2=1}^{3} \Big(b^1_{j_1 j_2}\, g^{\mu\nu}\, p^\rho_{j_1}\, p^\sigma_{j_2} + b^2_{j_1 j_2}\, g^{\mu\rho}\, p^\nu_{j_1}\, p^\sigma_{j_2} + b^3_{j_1 j_2}\, g^{\mu\sigma}\, p^\nu_{j_1}\, p^\rho_{j_2} \\ &\qquad\qquad + b^4_{j_1 j_2}\, g^{\nu\rho}\, p^\mu_{j_1}\, p^\sigma_{j_2} + b^5_{j_1 j_2}\, g^{\nu\sigma}\, p^\mu_{j_1}\, p^\rho_{j_2} + b^6_{j_1 j_2}\, g^{\rho\sigma}\, p^\mu_{j_1}\, p^\nu_{j_2} \Big) \\ &\quad + \sum_{j_1,j_2,j_3,j_4=1}^{3} c_{j_1 j_2 j_3 j_4} p^\mu_{j_1}\, p^\nu_{j_2} p^\rho_{j_3}\, p^\sigma_{j_4}. \end{aligned} \tag{4.24}$$

Not all these tensors will be relevant for our computations. Defining the physical amplitude contracted with the external polatization vectors of the three massless on-shell bosons:

$$S_\mu(g_1; g_2; b_3) = S_{\mu\nu\rho\sigma}(p_1; p_2; p_3)\, \epsilon_1^\nu(g)\, \epsilon_2^\rho(g)\, \epsilon_3^\sigma(b), \tag{4.25}$$

we see that many of the structures do not contribute because of the transversality condition:

$$\epsilon_i \cdot p_i = 0, \qquad \text{with} \quad i = 1, 2, 3\,.$$

This reduces the number of independent tensors to 57. One way of proceeding is then to apply Ward identities for the massless bosons

$$S^{\mu\nu\rho\sigma}\, p_1^\nu\, \epsilon_2^\rho\, \epsilon_3^\sigma = S^{\mu\nu\rho\sigma}\, \epsilon_1^\nu\, p_2^\rho\, \epsilon_3^\sigma = S^{\mu\nu\rho\sigma}\, \epsilon_1^\nu\, \epsilon_2^\rho\, p_3^\sigma = 0. \tag{4.26}$$

which lowers the number of relevant structures down to 18. Applying finally current conservation for the massive boson

$$S^{\mu\nu\rho\sigma}\, \epsilon_1^\nu\, \epsilon_2^\rho\, \epsilon_3^\sigma\, p_4^\mu = 0. \tag{4.27}$$

further reduces the number of independent tensor coefficients to 14.

By requiring the amplitude to be invariant under the exchange of the three (two) gluons one can find further relations among these 14 coefficients with interchanged arguments. This allows to perform different checks on the final result (see section 4.6).

Once the tensor structure is known, one can compute d-dimensional projection operators that applied on $S_{\mu\nu\rho\sigma}$ extract each of the 14 coefficients. The tensors and the projectors contain a large number of individual terms. Therefore applying them to an amplitude in a Feynman-diagrammatic approach will in general result in a large number of contractions with a huge proliferation of terms.

Moreover, it must be noted that the basis of tensors is not unique, namely that any set of 14 tensors, obtained as independent linear combinations of those found above, can be chosen. Choosing suitable linear combinations of the above tensors can simplify their structure substantially.

For all these reasons we decided to follow a simplified approch, which nevertheless allows us to retain the full information on the process. It is well known that when performing a computation with a large number of external bosons a specific gauge choice can highly simplify the intermediate steps of the calculation, while gauge invariance ensures that the final result for the amplitude must be independent on the choice made. Following this idea, instead of imposing gauge invariance on the tensor structures, we chose to fix the gauge of the external particles in order to symplify the tensor structures as much as possible.

Naively one would expect the loss of gauge invariance on the tensors, together with the loss of part of the symmetry due to the gauge choice performed, to be a drawback of this approach. However, one can show that once these 14 coefficients are known, the full gauge-invariant tensor can be reconstructed. In particular one can find linear relations among the 14 coefficients obtained imposing the gauge fixing and the 14 coefficients of the gauge invariant tensor, as outlined in the following section.

4.3.1 The gauge-fixed tensor structure

Following the above reasoning, we replace the condition (4.26) with a gauge choice on the external on-shell bosons:

$$\epsilon_1 \cdot p_2 = \epsilon_2 \cdot p_3 = \epsilon_3 \cdot p_1 = 0. \tag{4.28}$$

This choice is arbitrary and could be substituted by any other set of gauge conditions. The advantage of this particular choice is to produce extremely compact tensor structures.

Fixing the gauge of the external bosons reduces the number of independent tensors to 18. Also in this case we impose current conservation (4.27) on the Z^0 and end up again with 14 tensor structures. As expected, the number of independent tensor structures obtained in this way is the same as for the gauge-independent tensor.

We decompose the parton current as

$$S^\mu(g_1, g_2, b_3) = \sum_{i=1}^{14} A_i^{(b)}\, T_i^\mu\,, \tag{4.29}$$

where the coefficients are functions of the mandelstam variables $A_i^{(b)} = A_i^{(b)}(s_{12}, s_{13}, s_{23})$ and their explicit values differ in general if b is a gluon or a photon.

Finally, the gauge-fixed tensors read:

$$T_1^\mu = \epsilon_1 \cdot p_3\, \epsilon_3 \cdot p_2\, \epsilon_2^\mu - \epsilon_2 \cdot p_1\, \epsilon_3 \cdot p_2\, \epsilon_1^\mu, \qquad T_2^\mu = \epsilon_1 \cdot p_3\, \epsilon_2 \cdot p_1\, \epsilon_3^\mu - \epsilon_2 \cdot p_1\, \epsilon_3 \cdot p_2\, \epsilon_1^\mu, \tag{4.30}$$

$$T_3^\mu = \epsilon_1 \cdot \epsilon_2 \left[\epsilon_3 \cdot p_2\, p_1^\mu - \frac{(s_{12} + s_{13})}{2}\, \epsilon_3^\mu\right], \tag{4.31}$$

$$T_4^\mu = \epsilon_1 \cdot \epsilon_2 \left[\epsilon_3 \cdot p_2\, p_2^\mu - \frac{(s_{12} + s_{23})}{2}\, \epsilon_3^\mu\right], \tag{4.32}$$

$$T_5^\mu = \epsilon_1 \cdot \epsilon_2 \left[\epsilon_3 \cdot p_2 \, p_3^\mu - \frac{(s_{13} + s_{23})}{2} \, \epsilon_3^\mu \right], \tag{4.33}$$

$$T_6^\mu = \epsilon_1 \cdot \epsilon_3 \left[\epsilon_2 \cdot p_1 \, p_1^\mu - \frac{(s_{12} + s_{13})}{2} \, \epsilon_2^\mu \right], \tag{4.34}$$

$$T_7^\mu = \epsilon_1 \cdot \epsilon_3 \left[\epsilon_2 \cdot p_1 \, p_2^\mu - \frac{(s_{12} + s_{23})}{2} \, \epsilon_2^\mu \right], \tag{4.35}$$

$$T_8^\mu = \epsilon_1 \cdot \epsilon_3 \left[\epsilon_2 \cdot p_1 \, p_3^\mu - \frac{(s_{13} + s_{23})}{2} \, \epsilon_2^\mu \right], \tag{4.36}$$

$$T_9^\mu = \epsilon_2 \cdot \epsilon_3 \left[\epsilon_1 \cdot p_3 \, p_1^\mu - \frac{(s_{12} + s_{13})}{2} \, \epsilon_1^\mu \right], \tag{4.37}$$

$$T_{10}^\mu = \epsilon_2 \cdot \epsilon_3 \left[\epsilon_1 \cdot p_3 \, p_2^\mu - \frac{(s_{12} + s_{23})}{2} \, \epsilon_1^\mu \right], \tag{4.38}$$

$$T_{11}^\mu = \epsilon_2 \cdot \epsilon_3 \left[\epsilon_1 \cdot p_3 \, p_3^\mu - \frac{(s_{13} + s_{23})}{2} \, \epsilon_1^\mu \right], \tag{4.39}$$

$$T_{12}^\mu = \epsilon_2 \cdot p_1 \, \epsilon_3 \cdot p_2 \left[\epsilon_1 \cdot p_3 \, p_1^\mu - \frac{(s_{12} + s_{13})}{2} \, \epsilon_1^\mu \right], \tag{4.40}$$

$$T_{13}^\mu = \epsilon_2 \cdot p_1 \, \epsilon_3 \cdot p_2 \left[\epsilon_1 \cdot p_3 \, p_2^\mu - \frac{(s_{12} + s_{23})}{2} \, \epsilon_1^\mu \right], \tag{4.41}$$

$$T_{14}^\mu = \epsilon_2 \cdot p_1 \, \epsilon_3 \cdot p_2 \left[\epsilon_1 \cdot p_3 \, p_3^\mu - \frac{(s_{13} + s_{23})}{2} \, \epsilon_1^\mu \right]. \tag{4.42}$$

The relations among the $A_i^{(b)}$ and the coefficients of the gauge invariant tensor can be found by performing on the latter the gauge fixing (4.28). This procedure obviously does not affect the scalar coefficients which multiply the tensor structures. One ends up then with 14 new tensor structures which can be related through linear combinations to those obtained fixing the gauge from the beginning. In this way the gauge invariant tensor can be fully reconstructed. We have verified this procedure by comparing our one-loop result with the literature [231, 232] where the results are given for an on-shell Z boson, and a different gauge choice is used (see section 4.6).

Once the tensor structure is known, one can obtain the coefficients $A_i^{(b)}$ by applying a set of projectors $P_\mu(A_i^{(b)})$ on the Feynman-diagrammatic expression of the amplitude defined such that

$$\sum_{spin} P^\mu(A_i^{(b)}) \, S_\mu(p_1, p_2, p_3) = A_i^{(b)}.$$

Note that the projection has to be performed in d dimensions, and that special care has to be taken in performing the polarization sums when applying the projectors on the single diagrams. In particular one has to consistently use a physical polarization sum which respects the gauge choice (4.28):

$$\sum_{spin} \epsilon_1^{*\mu}(p_1) \, \epsilon_1^\nu(p_1) = -g^{\mu\nu} + \frac{p_1^\mu \, p_2^\nu + p_1^\nu \, p_2^\mu}{p_1 \cdot p_2}, \tag{4.43}$$

$$\sum_{spin} \epsilon_2^{*\mu}(p_2)\,\epsilon_2^{\nu}(p_2) = -g^{\mu\nu} + \frac{p_2^{\mu}\,p_3^{\nu} + p_2^{\nu}\,p_3^{\mu}}{p_2 \cdot p_3}, \tag{4.44}$$

$$\sum_{spin} \epsilon_3^{*\mu}(p_3)\,\epsilon_3^{\nu}(p_3) = -g^{\mu\nu} + \frac{p_3^{\mu}\,p_1^{\nu} + p_3^{\nu}\,p_1^{\mu}}{p_3 \cdot p_1}. \tag{4.45}$$

The projectors themselves can be decomposed in the tensor basis and take the form:

$$P^{\mu}(A_j^{(b)}) = \sum_{j=1}^{14} X_i(A_j^{(b)})\,T_i^{*\mu} \tag{4.46}$$

where the $X_i(A_j^{(b)})$ are functions of d and the kinematical invariants s_{ij}.

4.4 Helicity amplitudes

By fixing the helicities of the external massless bosons the partonic current can be cast in the usual spinor helicity notation [246]. There are two independent helicity configurations in the $gggV$-case, and three independent helicity configurations in the $gg\gamma V$-case, from which all the others can be obtained. In the following we discuss separately the two cases.

4.4.1 $gggV$: The amplitude in spinor helicity notation

We start off considering the $gggV$-case. We choose as two independent helicity configurations (g_1^+, g_2^-, g_3^-) and (g_1^+, g_2^+, g_3^+). In order to include the spin-correlations with the leptonic decay products we contract the partonic current with the leptonic current L_μ for fixed helicities of the initial state leptons. This also helps to further simplify the result.

Consider the production of the vector boson V through lepton-antilepton annihilation:

$$l^-(p_5) + l^+(p_6) \longrightarrow V(q).$$

The leptonic currents (4.8) are

$$L_R^{\mu}(p_5^+, p_6^-) = [6\,|\gamma^{\mu}|\,5\rangle, \qquad L_L^{\mu}(p_5^-, p_6^+) = [5\,|\gamma^{\mu}|\,6\rangle = [L_R^{\mu}(p_5^+, p_6^-)]^*. \tag{4.47}$$

Performing the contraction and making use of Schouten identities and momentum conservation we end up with:

$$A_R^{(+--)}(p_5, p_6; g_1, g_2, g_3) = L_R^{\mu}(p_5^+, p_6^-)\,S_{\mu}(g_1^+, g_2^-, g_3^-) = \frac{1}{\sqrt{2}}\,\frac{\langle 2\,3\rangle}{\langle 1\,2\rangle\langle 1\,3\rangle[2\,3]}$$
$$\times\left\{\langle 2\,5\rangle\langle 3\,5\rangle[5\,6]\,\alpha_1(x,y,z) + \langle 2\,3\rangle\langle 2\,5\rangle[2\,6]\,\alpha_2(x,y,z) + \langle 2\,3\rangle\langle 3\,5\rangle[3\,6]\,\alpha_3(x,y,z)\right\}, \tag{4.48}$$

$$A_R^{(+++)}(p_5, p_6; g_1, g_2, g_3) = L_R^{\mu}(p_5^+, p_6^-)\,S_{\mu}(g_1^+, g_2^+, g_3^+) = \frac{1}{\sqrt{2}}$$
$$\times\left\{\frac{[1\,3]\langle 1\,5\rangle[1\,6]}{\langle 1\,2\rangle\langle 2\,3\rangle}\beta_1(x,y,z) + \frac{[2\,3]\langle 2\,5\rangle[2\,6]}{\langle 1\,2\rangle\langle 1\,3\rangle}\beta_2(x,y,z) + \frac{[2\,3]\langle 2\,5\rangle[1\,6]}{\langle 1\,2\rangle\langle 2\,3\rangle}\beta_3(x,y,z)\right\}, \tag{4.49}$$

where the coefficients α_i and β_i are linear combinations of the 14 tensor coefficients A_i. As an explicit example we write down the relations for the α_j:

$$\begin{aligned}\alpha_1(x,y,z) &= -(s_{12}+s_{13})\left[A_2+A_9+\frac{s_{12}}{2}A_{12}\right]-(s_{12}+s_{23})\left[A_1+A_{10}+\frac{s_{12}}{2}A_{13}\right]\\ &\quad-(s_{13}+s_{23})\left[A_{11}+\frac{s_{12}}{2}A_{14}\right], \qquad (4.50)\\ \alpha_2(x,y,z) &= -s_{12}\left[A_2+A_9+\frac{s_{12}}{2}A_{12}\right]-(s_{12}+s_{13}+s_{23})\left[A_1+A_{10}+\frac{s_{12}}{2}A_{13}\right]\\ &\quad-(s_{13}+s_{23})\left[A_{11}+\frac{s_{12}}{2}A_{14}\right], \qquad (4.51)\\ \alpha_3(x,y,z) &= s_{13}\left[A_2+A_9-A_{11}+\frac{s_{12}}{2}A_{12}-\frac{s_{12}}{2}A_{14}\right]. \qquad (4.52)\end{aligned}$$

The corresponding relations for the β_j are slightly longer and we do not reproduce them here for brevity. There are in total 16 different helicity configurations. From the above expressions for $A_R^{(+--)}(p_5,p_6;g_1,g_2,g_3)$ and $A_R^{(+++)}(p_5,p_6;g_1,g_2,g_3)$, all the other helicity amplitudes can be obtained by parity conjugation and permutations of the external legs. We find:

$$\begin{aligned}L_R^\mu(p_5^+,p_6^-)\,S_\mu(g_1^-,g_2^+,g_3^-) &= A_R^{(-+-)}(p_5,p_6;g_1,g_2,g_3) = A_R^{(+--)}(p_5,p_6;g_2,g_1,g_3)\,,\\ L_R^\mu(p_5^+,p_6^-)\,S_\mu(g_1^-,g_2^-,g_3^+) &= A_R^{(--+)}(p_5,p_6;g_1,g_2,g_3) = A_R^{(+--)}(p_5,p_6;g_3,g_2,g_1)\,,\\ L_R^\mu(p_5^+,p_6^-)\,S_\mu(g_1^+,g_2^+,g_3^-) &= A_R^{(++-)}(p_5,p_6;g_1,g_2,g_3) = [A_R^{(+--)}(p_6,p_5;g_3,g_2,g_1)]^*\,,\\ L_R^\mu(p_5^+,p_6^-)\,S_\mu(g_1^+,g_2^-,g_3^+) &= A_R^{(+-+)}(p_5,p_6;g_1,g_2,g_3) = [A_R^{(+--)}(p_6,p_5;g_2,g_1,g_3)]^*\,,\\ L_R^\mu(p_5^+,p_6^-)\,S_\mu(g_1^-,g_2^+,g_3^+) &= A_R^{(-++)}(p_5,p_6;g_1,g_2,g_3) = [A_R^{(+--)}(p_6,p_5;g_1,g_2,g_3)]^*\,,\\ L_R^\mu(p_5^+,p_6^-)\,S_\mu(g_1^-,g_2^-,g_3^-) &= A_R^{(---)}(p_5,p_6;g_1,g_2,g_3) = [A_R^{(+++)}(p_6,p_5;g_1,g_2,g_3)]^*.\end{aligned} \qquad (4.53)$$

The corresponding amplitudes for right-handed leptonic current can be obtained by simply interchanging $p_5 \leftrightarrow p_6$. Note that the complex conjugation operation has to be applied only on the spinor structures in (4.48) (4.49), and not on the coefficients α_j, β_j.

The unrenormalised helicity amplitude coefficients are vectors in colour space and have perturbative expansions:

$$\Omega_g^{\rm un} = \sqrt{4\pi\alpha_s}\,d^{a_1a_2a_3}\left[\left(\frac{\alpha_s}{2\pi}\right)\Omega_g^{(1),{\rm un}}+\left(\frac{\alpha_s}{2\pi}\right)^2\Omega_g^{(2),{\rm un}}+\mathcal{O}(\alpha_s^3)\right], \qquad (4.54)$$

for $\Omega_g = \alpha_i, \beta_i$. The dependence on (x,y,z) is again implicit.

4.4.2 $gg\gamma V$: The amplitude in spinor helicity notation

In the $gg\gamma V$-case there are three independent helicity configurations. Two of them can be chosen identical to those in the $gggV$-case, namely (g_1^+,g_2^-,γ_3^-) and (g_1^+,g_2^+,γ_3^+), the third is taken as (g_1^+,g_2^+,γ_3^-).

Fixing the helicities and contracting with the right-handed lepton current we have:

$$\begin{aligned}A_R^{(+--)}(p_5,p_6;g_1,g_2,\gamma_3) &= L_R^\mu(p_5^+,p_6^-)\,S_\mu(g_1^+,g_2^-,\gamma_3^-) = \frac{1}{\sqrt{2}}\,\frac{\langle 2\,3\rangle}{\langle 1\,2\rangle\langle 1\,3\rangle[2\,3]}\\ &\quad\times\Big\{\langle 2\,5\rangle\langle 3\,5\rangle[5\,6]\,\eta_1(x,y,z)+\langle 2\,3\rangle\langle 2\,5\rangle[2\,6]\,\eta_2(x,y,z)+\langle 2\,3\rangle\langle 3\,5\rangle[3\,6]\,\eta_3(x,y,z)\Big\},\end{aligned} \qquad (4.55)$$

$$A_R^{(+++)}(p_5,p_6;g_1,g_2,\gamma_3) = L_R^{\mu}(p_5^+,p_6^-)\,S_{\mu}(g_1^+,g_2^+,\gamma_3^+) = \frac{1}{\sqrt{2}} \times\left\{ \frac{[1\,3]\langle 1\,5\rangle[1\,6]}{\langle 1\,2\rangle\langle 2\,3\rangle}\theta_1(x,y,z) + \frac{[2\,3]\langle 2\,5\rangle[2\,6]}{\langle 1\,2\rangle\langle 1\,3\rangle}\theta_2(x,y,z) + \frac{[2\,3]\langle 2\,5\rangle[1\,6]}{\langle 1\,2\rangle\langle 2\,3\rangle}\theta_3(x,y,z) \right\}, \tag{4.56}$$

$$A_R^{(++-)}(p_5,p_6;g_1,g_2,\gamma_3) = L_R^{\mu}(p_5^+,p_6^-)\,S_{\mu}(g_1^+,g_2^+,\gamma_3^-) = \frac{1}{\sqrt{2}}\,\frac{[1\,2]}{\langle 1\,2\rangle[1\,3][2\,3]} \times\left\{ [1\,2][1\,6]\langle 1\,5\rangle\,\tau_1(x,y,z) + [1\,2][2\,6]\langle 2\,5\rangle\,\tau_2(x,y,z) + [1\,6][2\,6]\langle 6\,5\rangle\,\tau_3(x,y,z) \right\}. \tag{4.57}$$

From $A_R^{(+--)}(p_5,p_6;g_2,g_1,\gamma_3)$, $A_R^{(++-)}(p_5,p_6;g_1,g_2,\gamma_3)$ and $A_R^{(+++)}(p_5,p_6;g_1,g_2,\gamma_3)$ all the other helicity configurations can be obtained by parity and charge conjugation:

$$\begin{aligned} A_R^{(-+-)}(p_5,p_6;g_1,g_2,\gamma_3) &= A_R^{(+--)}(p_5,p_6;g_2,g_1,\gamma_3) \\ A_R^{(--+)}(p_5,p_6;g_1,g_2,\gamma_3) &= [A_R^{(++-)}(p_6,p_5;g_1,g_2,\gamma_3)]^* \\ A_R^{(+-+)}(p_5,p_6;g_1,g_2,\gamma_3) &= [A_R^{(+--)}(p_6,p_5;g_2,g_1,\gamma_3)]^* \\ A_R^{(-++)}(p_5,p_6;g_1,g_2,\gamma_3) &= [A_R^{(+--)}(p_6,p_5;g_1,g_2,\gamma_3)]^* \\ A_R^{(---)}(p_5,p_6;g_1,g_2,\gamma_3) &= [A_R^{(+++)}(p_6,p_5;g_1,g_2,\gamma_3)]^*. \end{aligned} \tag{4.58}$$

As before, the left-handed helicity amplitudes can be found by the exchange $p_5 \leftrightarrow p_6$, and the complex conjugation has to be performed only on the spinor structures and not on the coefficients η_j, θ_j, τ_j.

The unrenormalised helicity amplitude coefficients are vectors in colour space and have perturbative expansions:

$$\Omega_{\gamma}^{\text{un}} = \sqrt{4\pi\alpha}\,\delta^{a_1 a_2}\,\left[\left(\frac{\alpha_s}{2\pi}\right)\Omega_{\gamma}^{(1),\text{un}} + \left(\frac{\alpha_s}{2\pi}\right)^2 \Omega_{\gamma}^{(2),\text{un}} + \mathcal{O}(\alpha_s^3) \right], \tag{4.59}$$

for $\Omega_\gamma = \eta_i, \theta_i, \tau_i$. The dependence on (x,y,z) is again implicit.

4.4.3 Analytic continuation to the scattering kinematics

In order to compute the two-loop contributions to V-plus-jet and V-plus-photon production at hadron colliders, the helicity amplitudes must be continued to the appropriate kinematical situations.

The relevant partonic subprocesses are:

$$g(p_1) + g(p_2) \to g(-p_3) + V(q) \to g(-p_3) + l^+(p_5) + l^-(p_6)\,, \tag{4.60}$$

$$g(p_2) + g(p_3) \to g(-p_1) + V(q) \to g(-p_1) + l^+(p_5) + l^-(p_6)\,, \tag{4.61}$$

where the second crossing is required to fully account for all helicity combinations, and

$$g(p_1) + g(p_2) \to \gamma(-p_3) + V(q) \to \gamma(-p_3) + l^+(p_5) + l^-(p_6)\,. \tag{4.62}$$

With the notation above the definitions of the helicity amplitudes in terms of momentum spinors (4.48) (4.49) and (4.57) remain unchanged under crossing. Considering in fact an outgoing leptonic current defined as:

$$V(q) \longrightarrow l^+(p_5) + l^-(p_6) \tag{4.63}$$

with

$$L^\mu(p_5, p_6)\Big|_{out} = \bar{u}(p_6)\,\gamma^\mu\,v(p_5), \tag{4.64}$$

we find that:

$$L^\mu_R(p_5^+, p_6^-)\Big|_{in} = [6\,|\gamma^\mu|5\rangle = L^\mu_R(p_5^-, p_6^+)\Big|_{out}$$
$$L^\mu_L(p_5^-, p_6^+)\Big|_{in} = [5\,|\gamma^\mu|6\rangle = L^\mu_L(p_5^+, p_6^-)\Big|_{out}.$$

This means that the expressions for the helicity amplitudes defined in the two sections above remain unchanged provided that p_5 is now considered as the label of the antilepton and p_6 the one of the lepton.

Special care has to be taken in the analytic continuation of the helicity coefficients Ω_g and Ω_γ. In the kinematical situation in (4.60) and (4.62) q^2 remains time-like, but only s_{12} becomes positive:

$$q^2 > 0\,, \quad s_{12} > 0\,, \quad s_{13} < 0, \quad s_{23} < 0\,, \tag{4.65}$$

or, equivalently,

$$x > 0\,, \quad y < 0\,, \quad z < 0\,. \tag{4.66}$$

As shown in [247] (where this region is denoted as $(2a)_+$) and used for example in [58], this kinematical situation can be expressed by introducing new dimensionless variables

$$u_1 = -\frac{s_{13}}{s_{12}} = -\frac{y}{x}\,, \qquad v_1 = \frac{q^2}{s_{12}} = \frac{1}{x}\,, \tag{4.67}$$

which fulfil

$$0 \le u_1 \le v_1\,, \qquad 0 \le v_1 \le 1\,.$$

To account for all helicity combinations in the case of $gg \to gV$, also the kinematical situation (4.61) must be considered. In this case we have

$$q^2 > 0\,, \quad s_{12} < 0\,, \quad s_{13} < 0, \quad s_{23} > 0\,, \tag{4.68}$$

This can be treated with the following choice of variables [247] (this region is denoted as $(4a)_+$) :

$$u_2 = -\frac{s_{13}}{s_{23}} = -\frac{y}{z}\,, \qquad v_2 = \frac{q^2}{s_{23}} = \frac{1}{z}\,, \tag{4.69}$$

which fulfil again

$$0 \le u_2 \le v_2\,, \qquad 0 \le v_2 \le 1\,.$$

Note that the two kinematical regions (4.60) and (4.61) are turned each other by the permutation $p_1 \leftrightarrow p_3$, in particular one has:

$$u_1(p_1 \leftrightarrow p_3) = u_2$$
$$v_1(p_1 \leftrightarrow p_3) = v_2.$$

As shown in (4.53), in the $gggV$-case, in order to obtain all the different helicity configurations, we also need to exploit the Bose symmetry of the external gluons. It is now clear that whenever the permutation $p_1 \leftrightarrow p_3$ is performed, this only amounts to switching from region (4.60) to region (4.61).

The full results for the one- and two-loop coefficients in all relevant regions in Mathematica foramt can be found in the sources of the arxiv-submission of [61].

4.5 Outline of the calculation

The two-loop corrections to the coefficients Ω_b can be evaluated through a calculation of the relevant Feynman diagrams. The calculation proceeds as follows. The diagrams contributing to the process are produced using QGRAF [248]. In the $gggV$-case there are 12 diagrams at one loop and 264 at two loops, while in the $gg\gamma V$-case there are 8 diagrams at one and 138 at two loops. The tensor coefficients are evaluated analytically diagram by diagram applying the projectors defined above. As a result, one obtains the tensor coefficients in terms of thousands of planar and non-planar two-loop scalar integrals, which can be classified in two auxiliary topologies, one planar and the other non-planar [249]. In order to do so, one needs to perform both shifts in the integration variables and permutations on the external legs. All the routines needed for this purpose have been coded in FORM [250] and checked against the new automated shift-finder implemented in Reduze2 [251]. Through the usual IBP identities [252, 253] one can reduce independently all the integrals belonging to these two auxiliary topologies to a small set of master integrals. This reduction is performed using the Laporta algorithm [254] implemented in the Reduze code [251, 255]. All the masters for the topologies above are known as series in the parameter $\epsilon = (4-d)/2$ through a systematic approach based on the differential equation method [59, 60, 256]. The methods used for their computation are described in more detail in section 5.3.1, where they have been applied to previously unknown integrals. The masters are expressed as Laurent expansion in ϵ, with coefficients containing harmonic polylogarithms (HPLs, [213]) and two-dimensional harmonic polylogarithms (2dHPLs, [59, 60]). Numerical implementations of these functions are available [220, 225, 257–260]. For all the intermediate algebraic manipulations we have made extensive use of FORM [250] and Mathematica [261]. The two-loop unrenormalised helicity coefficients $\Omega_b^{(2),\mathrm{un}}$ can then be evaluated as linear combination of the tensor coefficients. The whole computation is performed in the euclidean non-physical region, where the amplitude is real. The final result is then analytically continued to the physical regions relevant for $Z + jet/\gamma$ production at LHC, as thoroughly discussed in [247] and in section 4.4.3.

4.5.1 UV Renormalisation and IR subtraction

Renormalisation of ultraviolet divergences is performed in the $\overline{\mathrm{MS}}$ scheme by replacing the bare coupling α_0 with the renormalised coupling $\alpha_s \equiv \alpha_s(\mu^2)$, evaluated at the renormalisation scale μ^2. Since there is no tree level contribution to the amplitude, we only need the one loop relation between the bare and renormalised couplings:

$$\alpha_0 \mu_0^{2\epsilon} S_\epsilon = \alpha_s \mu^{2\epsilon} \left[1 - \frac{\beta_0}{\epsilon} \left(\frac{\alpha_s}{2\pi} \right) + \mathcal{O}(\alpha_s^2) \right] , \tag{4.70}$$

where

$$S_\epsilon = (4\pi)^\epsilon e^{-\epsilon\gamma} \qquad \text{with Euler constant } \gamma = 0.5772\ldots$$

and μ_0^2 is the mass parameter introduced in dimensional regularisation to maintain a dimensionless coupling in the bare QCD Lagrangian density. β_0 is the first coefficient of the QCD β-function:

$$\beta_0 = \frac{11C_A - 4T_R N_F}{6}, \tag{4.71}$$

with the QCD colour factors

$$C_A = N, \qquad C_F = \frac{N^2-1}{2N}, \qquad T_R = \frac{1}{2}\,. \tag{4.72}$$

The renormalisation is performed at fixed scale $\mu^2 = q^2$. The renormalised helicity coefficients read:

$$\begin{aligned}\Omega_g^{(1)} &= S_\epsilon^{-1}\Omega_g^{(1),\mathrm{un}},\\ \Omega_g^{(2)} &= S_\epsilon^{-2}\Omega_g^{(2),\mathrm{un}} - \frac{3\beta_0}{2\epsilon}S_\epsilon^{-1}\Omega_g^{(1),\mathrm{un}}\,.\end{aligned} \tag{4.73}$$

$$\begin{aligned}\Omega_\gamma^{(1)} &= S_\epsilon^{-1}\Omega_\gamma^{(1),\mathrm{un}},\\ \Omega_\gamma^{(2)} &= S_\epsilon^{-2}\Omega_\gamma^{(2),\mathrm{un}} - \frac{\beta_0}{\epsilon}S_\epsilon^{-1}\Omega_\gamma^{(1),\mathrm{un}}\,.\end{aligned} \tag{4.74}$$

After performing ultraviolet renormalisation, the amplitudes still contain singularities, which are of infrared origin and will be analytically cancelled by those occurring in radiative processes of the same order. Catani [262] has shown how to organise the infrared pole structure of the one- and two-loop contributions renormalised in the $\overline{\mathrm{MS}}$-scheme in terms of the tree and renormalised one-loop amplitudes. The same procedure applies to the tensor coefficients. Since there is no tree level process contributing, their pole structure can be separated off as follows:

$$\begin{aligned}\Omega_b^{(1)} &= \Omega_b^{(1),\mathrm{finite}},\\ \Omega_b^{(2)} &= \boldsymbol{I}_b^{(1)}(\epsilon)\Omega_b^{(1)} + \Omega_b^{(2),\mathrm{finite}},\end{aligned} \tag{4.75}$$

where again $b = g, \gamma$.

In the two cases the operator $\boldsymbol{I}_b^{(1)}(\epsilon)$ is given by

$$\boldsymbol{I}_g^{(1)}(\epsilon) = -N\,\frac{e^{\epsilon\gamma}}{2\Gamma(1-\epsilon)}\left[\left(\frac{1}{\epsilon^2} + \frac{\beta_0}{N\,\epsilon}\right)(\mathtt{S}_{12} + \mathtt{S}_{13} + \mathtt{S}_{23})\right], \tag{4.76}$$

$$\boldsymbol{I}_\gamma^{(1)}(\epsilon) = -N\,\frac{e^{\epsilon\gamma}}{\Gamma(1-\epsilon)}\left[\left(\frac{1}{\epsilon^2} + \frac{\beta_0}{N\,\epsilon}\right)\mathtt{S}_{12}\right], \tag{4.77}$$

where, since we have set $\mu^2 = s_{123}$:

$$\mathtt{S}_{ij} = \left(-\frac{s_{123}}{s_{ij}}\right)^\epsilon \tag{4.78}$$

Note that on expanding $\mathtt{S}_{ij}$, imaginary parts are generated, depending on which kinematical configuration we are working in. In the decay kinematics $Z \to ggg\,/\,gg\gamma$ for example we have that all the s_{ij} become positive, so that all three terms will generate imaginary

parts whose sign is fixed by the small imaginary part $+i0$ of s_{ij}. On the other hand if we are interested in the scattering kinematics $gg \to Zg\,/\,Z\gamma$ only s_{12} or s_{13} become positive, with the usual $s_{ij} + i0$ prescription.

For the infrared factorisation of the two-loop results, the renormalised one-loop helicity amplitude coefficients are needed through to $\mathcal{O}(\epsilon^2)$. Their decomposition in colour structures is straightforward, namely the whole colour dependence is in the overall factors $d^{a_1a_2a_3}$ and $\delta^{a_1a_2}$ for $gggV$ and $gg\gamma V$ respectively.

$$\Omega_b^{(1),\text{finite}}(x,y,z) = a_{\Omega_b}(x,y,z)\,. \tag{4.79}$$

The expansion of the coefficients through to ϵ^2 yields HPLs and 2dHPLs up to weight 4. The explicit expressions are of considerable size, such that we only quote the ϵ^0-terms in the appendix. To this order, the coefficients had been derived previously [231, 232] in terms of logarithms and dilogarithms. The expressions through to $\mathcal{O}(\epsilon^2)$ in Mathematica format are appended to the arXiv submission of this article.

The finite two-loop remainder is obtained by subtracting the predicted infrared structure (expanded through to $\mathcal{O}(\epsilon^0)$) from the renormalised helicity coefficient. We further decompose it according to the colour structures as follows:

$$\Omega_b^{(2),\text{finite}}(x,y,z) = N\,A_{\Omega_b} + \frac{1}{N}\,B_{\Omega_b} + N_f\,C_{\Omega_b}.\,, \tag{4.80}$$

The helicity coefficients contain HPLs and 2dHPLs up to weight 4. The size of each helicity coefficient is comparable to the size of the helicity-averaged tree times two-loop matrix element for $3j$ production quoted in [249], and we decided not to include them here explicitly. The complete set of coefficients in Mathematica format is attached to the arXiv submission of this article.

4.5.2 Simplification using the Symbol formalism

After the computation of the amplitudes and subtraction of UV- and IR-divergences the Mathematica implementation of the algorithm described in section 3.2.3 to express the result as far as possible in logarithms and polylogarithms of functions of the kinematic invariants. The GiNaC libary was used to evaluate the 2dHPLs [263] and the implementation of the PSLQ algorithm contained in the arprec library [264] to find the parts mapped to zero by the symbol map. It was found that the symbol of the amplitudes depend only on terms of the form

$$x_i,\ 1 - x_i \qquad \text{for } \ x_i = x, y, z\,. \tag{4.81}$$

It is well known that up to transcendental weight three all multiple polylogarithms can be re-expressed in terms of logarithms and polylogarithms. In the present case it was found that the set of arguments for these functions listed in Table 3.1 was sufficient. However, for weight four this is not always the case. As it was mentioned before, there exists a conjecture which states that a combination of MPLs can be expressed in logarithms and polylogarithms if and only if its symbol fulfills the symmetry condition (3.31). In the present case, we found this condition in general not to be fulfilled and were also not able to express our result in logarithms and polylogarithms only. Nevertheless we reduced the number of required functions in all kinematic regions as far as possible, having to resort to 17 2dHPLs of weight four. The simplification procedure is described in detail in appendix D.1, which differs from the present case only insofar, as the basis did not contain any 2dHPLs.

In the past, surprising relations between certain QCD and N=4 SYM amplitudes have been found, for example in the case of $H \to ggg$ at two loops in the heavy-top-limit [68, 244, 265]. In the leading color part of the finite two-loop amplitude, the weight four contribution without a rational factor was found [265] to be helicity-independent and equal to the three-point form factor remainder function in planar N=4 SYM. In the present cases, however, no such relation could be observed. This feature can be understood from the fact that, in contrast to the Higgs amplitudes, no purely gluonic contribution is present here, due to the internal quark loop coupling to the vector boson.

4.6 Checks on the result

Several non-trivial checks were applied to validate our results.

1. As a first check we computed all 14 tensor coefficients in (4.29) at one-loop order for the $gggV$-case, and we verified that we can reproduce the results in [231, 232] up to order $O(\epsilon^0)$. Performing this check was not entirely trivial. In [231, 232] the results for the one-loop helicity amplitudes are given in the case of an on-shell Z with a fixed polarization. Moreover, the amplitudes for different helicity configurations are given choosing an explicit representation for the polarization vectors of the external particles. This representation does not respect the gauge choice performed in (4.28), so that we cannot naively start from our tensor structure and fix the polarization vectors in the same way to reproduce their result. Nevertheless, as explained in section 4.3, the full gauge-invariant tensor can be fully reconstructed taking suitable linear combinations of the tensor coefficients of the gauge-fixed tensor. Once the gauge-invariant tensor is known, one can then use the explicit representation of the polarization vectors given in [231, 232] and demonstrate the analytic agreement of the expressions.
2. We computed all the 14 tensor coefficients both at one-loop and at two-loop order, in the $gggV$- and in the $gg\gamma V$-case. Following the procedure outlined in section 4.3, we obtained the 14 coefficients of the gauge invariant tensor for both processes, and we verified that they respect the expected symmetry relations under permutation of the external gluons.
3. The IR singularity structure of our results agrees with the prediction of Catani formula [262], see section 4.5.1.
4. We compared the helicity amplitudes $\Omega_b^{(1)}$ for the $gggV$- and the $gg\gamma V$-case. We verified the following identities for the one-loop amplitude coefficients:

$$\begin{aligned} 2\, a_{\alpha_j}(x,y,z) &= a_{\eta_j}(x,y,z), \\ 2\, a_{\beta_j}(x,y,z) &= a_{\theta_j}(x,y,z). \qquad j = 1,2,3\,. \end{aligned} \tag{4.82}$$

5. Finally, we performed the same comparison at two-loop order, finding:

$$\begin{aligned} 2\, B_{\alpha_j}(x,y,z) &= B_{\eta_j}(x,y,z), \\ 2\, B_{\beta_j}(x,y,z) &= B_{\theta_j}(x,y,z), \qquad j = 1,2,3\,, \end{aligned} \tag{4.83}$$

which follow from the structure of the underlying two-loop diagrams. The subleading colour coefficients B are unaffected by renormalisation and infrared subtraction. No relation of this type can be found for the coefficients C_{Ω_b}, which are determined purely from renormalisation counterterms and IR subtraction, which differ in the cases $b = g, \gamma$.

4.7 Conclusions and Outlook

In this chapter we presented the two-loop corrections to the helicity amplitudes for the processes $gg \to Vg$ and $gg \to V\gamma$. We performed the calculation in dimensional regularisation by applying d-dimensional projection operators to the most general tensor structure of the amplitude. We showed how an explicit gauge choice can reduce considerably the complexity of the basic tensor structures appearing while retaining the full information on the gauge-invariant amplitudes. We expressed our results in terms of dimensionless helicity coefficients, which multiply four-dimensional spinor structures. We extracted the infrared singularities by means of an infrared factorisation formula and provide compact analytic expressions for the finite part of the two-loop helicity coefficients in all relevant kinematical regions. Albeit the fact that the symbol formalism did not greatly simplify the result it used to rewrite the amplitude in terms of logarithms and polylogarithms as much as possible. We were also able to show this way that there exists no naive connection between this and a related N=4 SYM amplitude.

The matrix elements derived here contribute to the NLO corrections to the gluon-induced production of $Z\gamma$ and $Z + j$ final states at the LHC. Viewed in an expansion in the strong coupling constant, these contributions are formally $\mathrm{N^3LO}$ as far as the reactions $pp \to V\gamma + X$, $pp \to Vj + X$ are concerned. However, due to the large gluon-gluon luminosity at the LHC, these contributions could be comparable in size with the NNLO corrections to $q\bar{q} \to Vg$, $qg \to Vq$ and $q\bar{q} \to V\gamma$. Their inclusion will also help to stabilise the substantial scale dependence of the gluon-induced subprocesses, which were known only at Born-level up to now.

5

Two-Loop Master Integrals for $q\bar{q} \to VV$: the Planar Topologies

The original work in this chapter was done in collaboration with Thomas Gehrmann and Lorenzo Tancredi and appeared in [62].

5.1 Introduction

Vector boson pair production ($\gamma\,\gamma$, $Z\,\gamma\,/\,W\,\gamma$, $Z\,Z$, $W\,W$, $W\,Z$) is a key process in studying the dynamics of the electroweak theory at the LHC. It enters as background not only for Higgs production, but also for many other new-physics searches. It offers in fact a large number of observables which allow precise tests of the electroweak symmetry-breaking and in general of the non-abelian gauge structure of the group $SU(2) \times U(1)$, for example of the triple gauge-boson couplings. With large production rates to be expected from the future data taking at the LHC, vector boson pair production processes will become electroweak precision observables. The high experimental precision must be matched by a comparably high accuracy of the theoretical predictions, typically requiring next-to-leading order (NLO) electroweak and next-to-next-to-leading order (NNLO) QCD corrections.

At present large parts of the NLO electroweak corrections [13,31,32,266] and the NLO massless QCD corrections [38, 39, 267–269] are known for vector boson pair production, usually including the vector boson decays to leptons. The massless NNLO QCD corrections are known only for $\gamma\,\gamma$ production [57].

A full NNLO computation requires three different ingredients: the two-loop double-virtual corrections to the partonic $2 \to 2$ process, the one-loop real-virtual corrections to the $2 \to 3$ process for the production of the vector boson pair plus an additional parton, and the tree-level corrections to the $2 \to 4$ process involving two extra partons.

In the case of vector boson pair production, the $2 \to 3$ and $2 \to 4$ ingredients have already been known in the literature for some time in the context of NLO calculations with higher final-state multiplicity [47–50, 52, 53, 270, 271]. On the other hand, the two-loop parton-level matrix elements are known only for $\gamma\,\gamma$ [56] and $V\,\gamma$ production [58,61].

Finally, in the case of $W\,W$ production the two-loop virtual corrections are known in the high-energy approximation [272].

The computation of the two-loop matrix elements for two massive vector boson production is still an outstanding task and it constitutes the bottleneck for having a complete NNLO description of the process. When computing two-loop corrections to four-point functions in quantum field theory a large number of apparently different integrals appears. In particular, increasing the number of loops and/or the number of external legs, more and more different scales are added, increasing the complexity of analytically evaluating the integrals.

In the framework of dimensional regularization, many powerful techniques have been developed in order to make the computation of two-loop corrections to three- and four-point functions feasible. Employing integration-by-parts (IBPs), Lorentz and symmetry identities [252, 253] a large number of relations among the integrals can be established. The latter turn out to be simple linear equations which involve the integrals and only rational functions of the invariants and of the dimensional regularization parameter d. Solving this system of equations allows one to express most of the integrals in terms of a relatively small subset of irreducible integrals, the so-called Master Integrals (MIs).

In non-trivial applications to two-loop corrections to four-point functions the system of equations can easily grow to include tens or hundreds of thousands of equations, so that one must resort to the use of computer algebra. In the last years many public and private implementations for the automatic reduction to master integrals using the Laporta algorithm [254] have become available [251, 255, 273, 274]. Symmetry relations can often give new equations that must be consistently included in the system in order to ensure a full reduction to a minimal set of MIs.

Once the reduction is completed, we are left with the problem of computing the MIs. While, quite in general, there exists no algorithm that allows to compute two-loop corrections to four-point functions with arbitrary configuration of external and internal masses, the differential equation method [256, 275–277] has proven to be very powerful in a large number of computations, including two-loop four-point functions with massless and massive internal propagators [59, 60, 278–281]. In this method, differential equations for the integrals under consideration are derived at the basis of the integrands. The master integrals are then determined by solving these differential equations, matched to appropriate boundary conditions (that usually correspond to integrals in special points or with fewer scales). In order to determine those boundary conditions and to perform necessary transformations on the differential equations, techniques that make use of the algebraic structure of the underlying functions are used extensively [68, 69, 282].

In this paper we make use of the differential equations method to compute all MIs appearing in the reduction of planar two-loop four-point functions with two legs off-shell with the same mass. These masters constitute a fundamental ingredient towards the computation of the two-loop QCD corrections to $q\,\bar{q} \to Z\,Z\,/\,W\,W$ and $g\,g \to Z\,Z\,/\,W\,W$. In all steps of the computation we made extensive use of FORM [283] and Mathematica [261].

The chapter is organized as follows. In section 5.2 we discuss the notation and the method employed. The method is further explained in section 5.3, where we describe the MIs that appear in the reduction of planar two-loop corrections to four-point functions with two adjacent massive legs. In section 5.4 we focus on the MIs needed for the two-loop corrections to four-point functions with two non-adjacent massive legs. Extensive analytical and numerical checks to validate the results are documented in Section 5.5. We conclude in Section 5.6. The results can be found in appendix B and in mathematica

format in the attached files to [62].

5.2 Definitions, Notation and Method

Four-point functions depend in general on three linearly independent momenta, which we will call p_1, p_2 and q_1. In the scattering kinematics the fourth momentum is given by $q_2 = p_1 + p_2 - q_1$. We take two of the momenta on-shell and the remaining two momenta off-shell at the same invariant mass, such that

$$p_1^2 = p_2^2 = 0, \qquad q_1^2 = q_2^2 = Q^2, \tag{5.1}$$

where for physical applications Q^2 represents the mass of the vector boson.

We define the usual Mandelstam variables as:

$$s = (p_1 + p_2)^2\,, \quad t = (p_1 - q_1)^2\,, \quad u = (p_2 - q_1)^2 \quad \text{with} \quad s + t + u = 2\,Q^2. \tag{5.2}$$

In the physical region relevant for vector boson pair production we have

$$Q^2 > 0\,, \quad s > 4\,Q^2\,, \quad t < 0\,, \quad u < 0\,,$$

and the MIs are complex-valued functions.

In the general case of four-point functions there are up to six independent invariants which can be identified with the scalar products among the three external momenta:

$$s_1 = p_1^2\,, \quad s_2 = p_2^2\,, \quad s_3 = q_1^2\,, \quad s_4 = p_1 \cdot p_2\,, \quad s_5 = p_1 \cdot q_1\,, \quad s_6 = p_2 \cdot q_1\,. \tag{5.3}$$

Using the kinematical constrains in (5.1) they reduce to the three independent invariants in (5.2). Due to Lorentz invariance all integrals can only depend on combinations of the latter.

Feynman integrals can be classified in terms of their topology, i.e. in terms of the propagator denominators appearing in them. Any integral with the same set of denominators raised to any powers and involving any combination of scalar products among external and internal momenta in the numerator belongs to the same topology. Starting from those integrals with the largest number of denominators, we can define their sub-topologies as all possible sets of denominators that can be built removing one or more denominators. For each topology one can derive a set of IBP identities, Lorentz invariance identities and (sometimes) symmetry relations which allow to express all integrals belonging to that topology in terms of a small number of MIs.

Once the MIs have been identified, we can derive differential equations for them with respect to the external invariants (5.3) as follows. Starting from their very definition, one can easily see that the derivatives in the invariants can be expressed by suitable combinations of derivatives in the external momenta. Let us consider for simplicity the case where all integrals in one given topology are reduced to one single MI. Differentiating the MI with respect to any of the external invariants will generate a linear combination of new integrals, all with the same subset of denominators as the starting integral, but in general raised to different powers. Using the IBP identities all these integrals can be reduced again to the MI itself plus integrals from its sub-topologies, which in a bottom-up approach are considered as known. We are thus left with a single first order non-homogeneous differential equation for the MI in each of the external invariants.

Equipped with a suitable boundary condition, the differential equation can be easily integrated by means of Euler's method of the variation of constants. This reduces the

problem of performing one or more loop integrations to a single one-dimensional integration. In most cases a boundary condition can be found studying the behavior of the integrals in some well defined kinematical limit where the integral is known to be regular.

The method immediately generalizes to the case where N master integrals are present. The single first order differential equation will be in general substituted by a system of N coupled differential equations for the N master integrals, which can in turn be rephrased as a N-th order differential equation for any of the masters. Finding the solution to a N-th order differential equation requires fixing N boundary conditions. Even though no general method is available for solving a system of N coupled differential equations with non-constant coefficients, experience shows that by an appropriate choice of the basis of master integrals the system can usually be diagonalized (or at least put in triangular form in the limit $d \to 4$), allowing a recursive solution by direct integration. A proposal towards systematizing the computation of master integrals from differential equations has been put forward recently in [284]. Especially for topologies with more than one master integral, finding boundary conditions is in general a non-trivial task and represents often the bottleneck of the whole procedure.

5.2.1 Auxiliary topologies and reduction to Master Integrals

Two-loop corrections to four-point functions involve integrals with up to seven different propagators and up to nine independent scalar products among the external and the loop momenta in the numerator. This implies that two out of the nine scalar products are irreducible, namely they cannot be rewritten as linear combinations of the seven denominators. One way to perform a complete reduction is then to define a larger set of nine denominators, that we will refer to as auxiliary topology. In the case of pair production of equal-mass vector bosons, three independent auxiliary topologies are needed in order to account for all the integrals appearing.

We define two planar topologies, named **Topo A** and **Topo B**, needed to represent respectively the double-boxes with adjacent and non-adjacent off-shell legs. A third topology, named **Topo C**, is sufficient to represent all non-planar integrals. We choose the propagators of the three topologies as listed in Table 5.1. The reduction to MIs of the three auxiliary topologies above has been performed using Reduze1 and Reduze2 [251,255].

Topo A	**Topo B**	**Topo C**
k^2	k^2	k^2
l^2	l^2	l^2
$(k-l)^2$	$(k-l)^2$	$(k-l)^2$
$(k-p_1)^2$	$(k-p_1)^2$	$(k-p_1)^2$
$(l-p_1)^2$	$(l-p_1)^2$	$(l-p_1)^2$
$(k-p_1-p_2)^2$	$(k-p_1+q_1)^2$	$(k-p_1-p_2)^2$
$(l-p_1-p_2)^2$	$(l-p_1+q_1)^2$	$(k-l-q_1)^2$
$(k-p_1-p_2+q_1)^2$	$(k-p_1-p_2+q_1)^2$	$(l-p_1-p_2+q_1)^2$
$(l-p_1-p_2+q_1)^2$	$(l-p_1-p_2+q_1)^2$	$(k-l-p_1-p_2)^2$

Table 5.1: Propagators in the three different auxiliary topologies used to represent all two-loop 4-point integrals with two massless and two massive legs with the same mass.

We refer to the MIs in these topologies as $\mathcal{I}_n^{(T)}$, where T is the auxiliary topology (A,

B or C), while n is a decimal number which corresponds to the selection of propagator momenta that appear as denominators in the integral. Any integral is first mapped to one of the topologies above. Its set of denominators is then identified with a binary number, containing a 1 for each propagator momentum appearing in the integral, and a 0 for those momenta not appearing as propagators. The minimum binary number to which the integral can be mapped in the topology under consideration is then converted to a decimal number and used as label for the integral itself. To give an explicit example consider the following integral belonging to **Topo A**:

$$\int \frac{d^dk}{(2\pi)^d}\frac{d^dl}{(2\pi)^d}\frac{1}{l^2(k-l)^2(k-p_1)^2(k-p_1-p_2+q_1)^2}.$$

The binary number associated to its denominators is $010001110 = 142$, so that with the definitions above this integral will be labeled as $\mathcal{I}^{(A)}_{142}$. In the following we will often use the terminology *sector 'n'* interchangeably with that of *topology 'n'*, referring to the set of all those integrals whose label according to this procedure is *'n'*.

With the Mandelstam variables defined above, one can see from the arrangement of the momenta in the three topologies that the planar integrals belonging to **Topo A** have cuts only in s and u while those belonging to **Topo B** have cuts only in t and u. On the other hand, as it is well known [285], the non-planar integrals belonging to **Topo C** are expected to have cuts in all three Mandelstam variables. In what follows we will focus on the explicit evaluation of the Master Integrals that emerge from the reduction of the two planar topologies, referring to a future work for the computation of the non-planar master integrals belonging to **Topo C**.

The arrangement of the cuts in the two planar topologies suggests that, in order to express the final results in compact form, the natural variables should be (s,u) for **Topo A** and (t,u) for **Topo B**. The kinematical constraints are those that determine the analyticity structure of the scattering amplitude and hence of the functions used to describe the result. In the following two sub-sections we describe separately the kinematics for vector boson pair production in the two different sets of variables.

5.2.2 Kinematics and analytic continuation in s, u

In the physical region we have $Q^2 > 0$ and $s > 4\,Q^2$. Using s and u as independent variables we can express the kinematical constrains in u in function of s and Q^2. In the center-of-mass frame of p_1, p_2 we find

$$u = Q^2 - \frac{s}{2}\left[1 - \sqrt{1-\frac{4Q^2}{s}}\cos\theta\right], \tag{5.4}$$

where θ is the angle between $\vec{p}_2$ and $\vec{q}_1$. In Fig. 5.1 we show the kinematical plane in s, u.

It is convenient to introduce the dimensionless variables

$$s = M^2\frac{(1+\xi)^2}{\xi}, \quad u = -M^2\zeta, \quad Q^2 = M^2, \tag{5.5}$$

in which the physical region is given by

$$M^2 > 0, \qquad 0 < \xi \leq 1, \qquad \xi \leq \zeta \leq \frac{1}{\xi}.$$

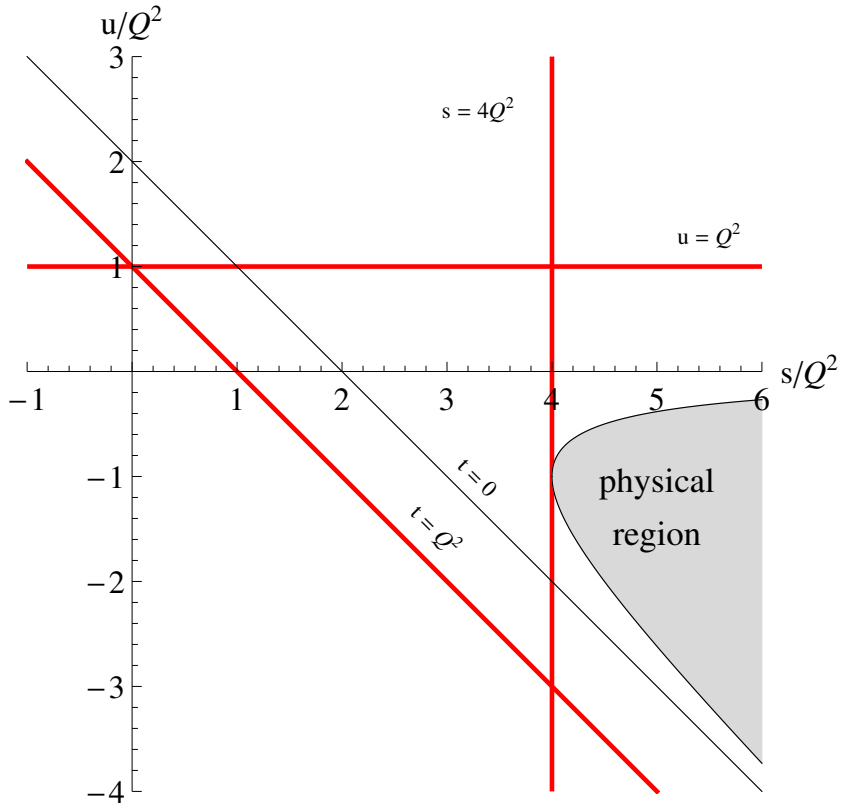

Figure 5.1: Dalitz plot for the $2 \to 2$ scattering kinematics.

With the parametrization above we obtain:

$$t = 2Q^2 - s - u = -M^2 \left(\frac{1+\xi^2}{\xi} - \zeta \right) < 0\,. \tag{5.6}$$

In the physical region all integrals with a cut in s and Q^2 will be complex-valued. They can be expressed as analytical continuations of real-valued functions defined in a non-physical region where $s < 0$, $u < 0$ and $Q^2 < 0$, expressed as:

$$s = -m^2 \frac{(1+x)^2}{x} < 0\,, \qquad u = -m^2 z < 0\,, \qquad Q^2 = -m^2 < 0\,, \tag{5.7}$$

with

$$x = \frac{\sqrt{s} - \sqrt{s-4Q^2}}{\sqrt{s} + \sqrt{s-4Q^2}}\,, \qquad z = \frac{u}{Q^2}. \tag{5.8}$$

Now taking

$$m^2 > 0\,, \quad 0 < x < 1\,, \quad z > 0\,,$$

all MIs are real functions of the dimensionless variables x and z.

The analytic continuation to the physical region can be obtained as:

$$m^2 \to -M^2 - i\eta\,, \quad x \to \xi\,, \quad z \to -\zeta + i\,\eta \tag{5.9}$$

such that the Mandelstam variables which become positive acquire the correct imaginary part

$$s = M^2\frac{(1+\xi)^2}{\xi} + i\eta\,, \qquad u = -M^2\zeta\,, \qquad Q^2 = M^2 + i\eta\,. \tag{5.10}$$

In this context, a subtle issue about the analytical continuations should be recalled [247, 285]. If one tries to express all three Mandelstam variables s, t, u in terms of x, z and m^2 only, one easily realizes that no real value of x, z and m^2 can make at the same time $s < 0$, $t < 0$, $u < 0$, $Q^2 < 0$. For example with our choice we find:

$$\begin{aligned} &s = -m^2\frac{(1+x)^2}{x} < 0\,, \qquad u = -m^2 z < 0\,, \qquad Q^2 = -m^2 < 0\,, \\ &t = +m^2\left(\frac{1+x^2}{x} + z\right) > 0\,, \qquad \text{with} \quad x, z \in \mathbb{R}^+ \end{aligned} \tag{5.11}$$

which means that if we tried to express in x and z MIs with a cut in t, they would have an imaginary part different from zero. One could argue that this comes from having imposed the on-shell condition $s + t + u = 2Q^2$. This problem could be avoided by giving up the on-shell condition, i.e. computing the MIs *off-shell*, however at the expense of introducing one more independent scale in the computation.

This particular choice of variables was motivated by the cut structure of the first planar topology, and will be used only for representing the integrals in this topology in a compact form.

5.2.3 Kinematics and analytic continuation in t, u

Using t, u and Q^2 as independent variables we can repeat the reasoning above. Defining:

$$t = -\frac{M^2}{w}\,, \quad u = -M^2 v\,, \quad Q^2 = M^2\,, \tag{5.12}$$

the physical region is given by

$$M^2 > 0\,, \qquad 0 < v < \infty\,, \qquad 0 < w < v\,,$$

with

$$s = 2Q^2 - t - u = M^2\left(2 + v + \frac{1}{w}\right) > 0\,. \tag{5.13}$$

In order to make all integrals in **Topo B** real functions we define a non-physical region where $Q^2 < 0$, $t < 0$, $u < 0$:

$$t = -m^2 y < 0\,, \qquad u = -m^2 z < 0\,, \qquad Q^2 = -m^2 < 0\,, \tag{5.14}$$

with

$$y = \frac{t}{Q^2}\,, \qquad z = \frac{u}{Q^2}\,. \tag{5.15}$$

Taking now

$$m^2 > 0\,, \quad z > 0\,, \quad y > 0\,, \quad \text{with} \quad y + z < 1\,,$$

all MIs are real functions of y and z.

In continuing to the physical region only Q^2 becomes positive, while t and u remain negative. The analytic continuation can be obtained through:

$$m^2 \to -M^2 - i\eta\,, \quad y \to -1/w + i\eta\,, \quad z \to -v + i\,\eta \tag{5.16}$$

which gives

$$t = -\frac{M^2}{w}\,, \quad u = -M^2\,v\,, \quad Q^2 = M^2 + i\eta\,. \tag{5.17}$$

Note that even though t and u remain negative we still need to fix an imaginary part for y and z, which is determined as:

$$y \to \frac{t}{Q^2 + i\eta} = \frac{t}{Q^2} + i\eta = -\frac{1}{w} + i\,\eta\,, \tag{5.18}$$

$$z \to \frac{u}{Q^2 + i\eta} = \frac{u}{Q^2} + i\eta = -v + i\,\eta\,. \tag{5.19}$$

5.3 Topo A

In the following section we will focus on the first planar topology, **Topo A**. We will use this first case also to describe all details of the differential equation method. As discussed above, the first planar topology has cuts in s and u, so that we expect the MIs to be naturally expressed in functions of these two Mandelstam variables. We can then get rid of t using $s + t + u = 2Q^2$ and exploit what we know *a priori* deriving directly differential equations for the MIs in s, u and Q^2.

In the next sections we derive the differential operators and we work out explicitly a one-loop example, which will also allow us to discuss the method in detail. The common normalization factor of all master integrals is

$$S_\epsilon = \left[(4\pi)^\epsilon \frac{\Gamma(1+\epsilon)\,\Gamma^2(1-\epsilon)}{\Gamma(1-2\epsilon)}\right]. \tag{5.20}$$

5.3.1 Differential equations

In order to derive the differential equations in s and u we choose the following set of invariants as linear combinations of (5.3):

$$s_1 = p_1^2\,, \quad s_2 = p_2^2\,, \quad s_3 = q_1^2 - q_2^2\,, \quad s_4 = q_1^2\,, \quad s_5 = (p_1+p_2)^2\,, \quad s_6 = (p_2 - q_1)^2,$$

with these definitions, applying the on-shell conditions we find:

$$s_1 = 0\,, \quad s_2 = 0\,, \quad s_3 = 0\,, \quad s_4 = Q^2\,, \quad s_5 = s\,, \quad s_6 = u.$$

Expressing the derivatives with respect to the three non-zero invariants as linear combinations of derivatives with respect to the external momenta we obtain:

$$s\,\frac{\partial}{\partial s} = \frac{s}{Q^4 - 2uQ^2 + u^2 + su}\left\{\frac{(Q^4 - 2uQ^2 + u^2 + 2su)}{2s}\,p_1^\mu \frac{\partial}{\partial\, p_1^\mu}\right.$$

$$+\frac{(u-Q^2)}{2}\left[\frac{(s+u-Q^2)}{s}p_2^\mu\frac{\partial}{\partial p_1^\mu}-q_1^\mu\frac{\partial}{\partial p_1^\mu}\right]\Bigg\},$$

$$u\frac{\partial}{\partial u}=\frac{u}{Q^4-2uQ^2+u^2+su}\Bigg\{\frac{(u-Q^2)}{2}\left[p_1^\mu\frac{\partial}{\partial p_1^\mu}-p_1^\mu\frac{\partial}{\partial p_2^\mu}\right]$$
$$+\frac{(s+u-Q^2)}{2}\left[p_2^\mu\frac{\partial}{\partial p_2^\mu}-p_2^\mu\frac{\partial}{\partial p_1^\mu}\right]+\frac{s}{2}\left[q_1^\mu\frac{\partial}{\partial p_1^\mu}-q_1^\mu\frac{\partial}{\partial p_2^\mu}\right]\Bigg\},$$

$$Q^2\frac{\partial}{\partial Q^2}=\frac{Q^2}{Q^4-2uQ^2+u^2+su}\Bigg\{\frac{(Q^4-2uQ^2+u^2+2su)}{2s}p_1^\mu\frac{\partial}{\partial q_1^\mu}$$
$$+\frac{(u-Q^2)}{2}\left[\frac{(s+u-Q^2)}{s}p_2^\mu\frac{\partial}{\partial q_1^\mu}-q_1^\mu\frac{\partial}{\partial q_1^\mu}-p_1^\mu\frac{\partial}{\partial p_1^\mu}\right]$$
$$+\frac{(s+u-Q^2)}{2}p_2^\mu\frac{\partial}{\partial p_1^\mu}-\frac{s}{2}q_1^\mu\frac{\partial}{\partial p_1^\mu}\Bigg\}. \tag{5.21}$$

We recall here that, due to Lorentz invariance identities [256], these relations are not unique. Scalar Feynman integrals, in fact, must be Lorentz invariant. This implies that given any integral $I(s_j)$ the following relation must be fulfilled:

$$\left\{\left(p_1^\mu\frac{\partial}{\partial p_1^\nu}-p_1^\nu\frac{\partial}{\partial p_1^\mu}\right)+\left(p_2^\mu\frac{\partial}{\partial p_2^\nu}-p_2^\nu\frac{\partial}{\partial p_2^\mu}\right)+\left(q_1^\mu\frac{\partial}{\partial q_1^\nu}-q_1^\nu\frac{\partial}{\partial q_1^\mu}\right)\right\}I(s_j)=0. \tag{5.22}$$

Contracting (5.22) with any antisymmetric combination of the external momenta we find relations which connect the different derivative operators when applied on a Feynman integral. Having three independent external momenta we can build up three antisymmetric combinations:

$$p_1^\mu p_2^\nu-p_1^\nu p_2^\mu\,,\qquad p_1^\mu q_1^\nu-p_1^\nu q_1^\mu\,,\qquad p_2^\mu q_1^\nu-p_2^\nu q_1^\mu.$$

Starting from the 6 scalar products in (5.3), the three Lorentz invariance relations state what we already know, i.e. that only three of them are really independent. As an explicit example, upon contracting (5.22) with $p_1^\mu p_2^\nu-p_1^\nu p_2^\mu$ we find

$$\left\{s\left[p_1^\mu\frac{\partial}{\partial p_1^\mu}-p_2^\mu\frac{\partial}{\partial p_2^\mu}-p_2^\mu\frac{\partial}{\partial q_1^\mu}\right]+(u-Q^2)\left[p_1^\mu\frac{\partial}{\partial q_1^\mu}-p_2^\mu\frac{\partial}{\partial q_1^\mu}\right]\right\}I(s_j)=0.$$

Furthermore, the differential operators (5.21) when applied on a Feynman integral are not independent due to the scaling properties of the integrals. Assuming for the mass dimension of the integral

$$I(\lambda^2 s,\lambda^2 t,\lambda^2 u)=\lambda^\alpha I(s,t,u) \tag{5.23}$$

one finds the Euler scaling relation

$$\left(s\frac{\partial}{\partial s}+u\frac{\partial}{\partial u}+Q^2\frac{\partial}{\partial Q^2}\right)I(s,t,u)=\frac{\alpha}{2}I(s,t,u)\,. \tag{5.24}$$

5.3.2 A one-loop example

As illustration of the method let us consider the one-loop triangle with three legs off-shell. The example is interesting for at least two different reasons. First, it appears naturally as sub-topology of some of the two-loop integrals considered in the following. Second, in spite of its simplicity, it will also allow us to discuss some of the features of the computation of the more involved two-loop integrals.

We consider the one-loop triangle with three legs off-shell, two of which with the same mass. With our notation it is a function of the ratio $\tilde{s} = s/Q^2$ and can be defined as:

$$\mathcal{T}(\tilde{s}) = \quad \text{ 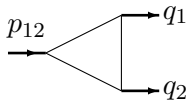 } \quad = \int \frac{d^dk}{(2\pi)^d} \frac{1}{k^2(k-q_1)^2(k-p_1-p_2)^2} \tag{5.25}$$

We define also the one-loop bubble, which is its only sub-topology, as:

$$\mathcal{B}(p^2) = \quad \text{ 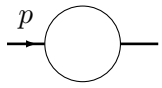 } \quad = \int \frac{d^dk}{(2\pi)^d} \frac{1}{k^2(k-p)^2}. \tag{5.26}$$

Applying the differential operators (5.21) directly on the definition (5.25), and using the IBPs to re-express the resulting integrals in terms of the master $T(\tilde{s})$ itself and the bubbles, we find:

$$s\,\frac{\partial}{\partial s}\mathcal{T}(\tilde{s}) = -\left[\frac{d-2}{2} + \frac{2Q^2(d-3)}{s-4Q^2}\right]\mathcal{T}(\tilde{s}) + \frac{2\,(d-3)}{s-4Q^2}\left[\,\mathcal{B}(Q^2) - \mathcal{B}(s)\,\right], \tag{5.27}$$

$$u\,\frac{\partial}{\partial u}\mathcal{T}(\tilde{s}) = 0\,, \tag{5.28}$$

$$Q^2\,\frac{\partial}{\partial Q^2}\mathcal{T}(\tilde{s}) = \left[d-4+\frac{2Q^2(d-3)}{s-4Q^2}\right]\mathcal{T}(\tilde{s}) + \frac{2(d-3)}{s-4Q^2}\left[\mathcal{B}(s) - \mathcal{B}(Q^2)\,\right]. \tag{5.29}$$

Note that summing the three equation we find the expected Euler scaling-relation:

$$\left(s\,\frac{\partial}{\partial s} + u\,\frac{\partial}{\partial u} + Q^2\,\frac{\partial}{\partial Q^2}\right)T(\tilde{s}) = \frac{(d-6)}{2}\,T(\tilde{s})\,. \tag{5.30}$$

We focus now on the differential equation in s and we attempt to solve it as a series expansion in $\epsilon = (4-d)/2$. Since the one-loop bubble develops a $1/\epsilon$ pole,

$$\begin{aligned}\mathcal{B}(p^2) &= i\left(\frac{S_\epsilon}{16\pi^2}\right)(-p^2)^{-\epsilon}\,\frac{1}{\epsilon(1-2\epsilon)} \\ &= i\left(\frac{S_\epsilon}{16\pi^2}\right)(-p^2)^{-\epsilon}\left[\frac{1}{\epsilon} + 2 + 4\,\epsilon + \mathcal{O}(\epsilon^2)\right],\end{aligned}$$

we should consistently expand also the function $\mathcal{T}(\tilde{s})$ starting from $1/\epsilon$,

$$\mathcal{T}(\tilde{s},\epsilon) = i\left(\frac{S_\epsilon}{16\pi^2}\right)(-Q^2)^{-\epsilon}\left[\frac{1}{\epsilon}\,\mathcal{T}^{(-1)}(\tilde{s}) + \mathcal{T}^{(0)}(\tilde{s}) + \epsilon\,\mathcal{T}^{(1)}(\tilde{s}) + \mathcal{O}(\epsilon^2)\right]. \tag{5.31}$$

Inserting the expansions on both sides of the differential equation and keeping only the first two terms in the expansion we get the following differential equations for the Laurent coefficients of the first two orders:

$$\frac{\partial}{\partial s}\mathcal{T}^{(-1)}(\tilde{s}) = -\frac{1}{2}\left[\frac{1}{s}+\frac{1}{s-4Q^2}\right]\mathcal{T}^{(-1)}(\tilde{s})\,, \tag{5.32}$$

$$\begin{aligned}\frac{\partial}{\partial s}\mathcal{T}^{(0)}(\tilde{s}) = &-\frac{1}{2}\left[\frac{1}{s}+\frac{1}{s-4Q^2}\right]\mathcal{T}^{(0)}(\tilde{s})\\ &+\frac{1}{s-4Q^2}\,\mathcal{T}^{(-1)}(\tilde{s})+\frac{1}{2Q^2}\left[\frac{1}{s}-\frac{1}{s-4Q^2}\right]\left(\ln\left(-Q^2-i\,\eta\right)-\ln\left(-s-i\,\eta\right)\right)\,,\end{aligned} \tag{5.33}$$

where η is a small positive real number which comes from the usual prescription

$$s \to s+i\eta\,, \quad Q^2 \to Q^2+i\eta\,.$$

Note that the homogeneous part of the equation is the same at any order in ϵ.

Since in the equation for order $\mathcal{T}^{(n)}(s)$ the previous orders appear as inhomogeneous terms, we must solve the equation bottom up in ϵ starting from the leading singularity term. At order $1/\epsilon$ the equation is purely homogeneous and its solution is easily found as

$$\mathcal{T}^{(-1)}(\tilde{s}) = \frac{C^{(-1)}}{\sqrt{s\,(s-4Q^2)}}\,, \tag{5.34}$$

where $C^{(j)}$ is the integration constant at order ϵ^j.

Upon matching this solution with an appropriate boundary condition one finds that in this particular case $C^{(-1)}=0$, so that

$$\mathcal{T}^{(-1)}(\tilde{s}) = 0\,.$$

Inserting this result into (5.33) we find a linear first-order non-homogeneous differential equation for $\mathcal{T}^{(0)}(\tilde{s})$, which can be solved using Euler's method of the variation of the constants:

$$\mathcal{T}^{(0)}(\tilde{s}) = \frac{2}{\sqrt{s\,(s-4Q^2)}}\left\{\int ds\,\frac{1}{\sqrt{s\,(s-4Q^2)}}\left[\,\ln\left(-s-i\,\eta\right)-\ln\left(-Q^2-i\,\eta\right)\right]+C^{(0)}\right\} \tag{5.35}$$

The square root $\sqrt{s\,(s-4Q^2)}$ shows up in all computations of three- and four-point functions with respectively 3 and 2 legs off-shell (see for example [286–288]) and physically it represents the threshold for the production of the two massive particles of equal masses Q^2.

In general, integrating a square root with a combination of (poly-)logarithmic functions can be a quite non-trivial task and we expect the integrals to become more and more involved as the order in ϵ increases. Nevertheless, as it is well known, in this specific case one can get rid of the square-root through the usual Landau variable ξ defined above. In order to obtain a real result we use the parametrization defined in section 5.2.2 as function of x, z finding:

$$s \to -m^2\frac{(1+x)^2}{x}\,, \qquad ds \to m^2\frac{(1-x^2)}{x^2}\,dx\,, \qquad \text{with} \quad Q^2=-m^2\,, \tag{5.36}$$

so that

$$\int ds \frac{1}{\sqrt{s\,(s-4Q^2)}} \to \int \frac{dx}{x}\,.$$

The arguments of the logarithms are now positive so that the explicit imaginary part can be dropped and we obtain:

$$\mathcal{T}^{(0)}(x) = -\frac{2\,x}{m^2\,(1-x^2)} \left\{ \int dx \left[\frac{\ln(x)}{x} - 2\,\frac{\ln(1+x)}{x} \right] + C^{(0)} \right\}, \tag{5.37}$$

which can be now easily integrated in terms of HPLs [213]. Fixing the boundary condition we find:

$$\mathcal{T}^{(0)}(x) = -\frac{2\,x}{m^2\,(1-x^2)} \left\{ G(0,0,x) - 2\,G(0,-1,x) + \frac{\pi^2}{6} \right\}. \tag{5.38}$$

Iterating this procedure one can compute the function $\mathcal{T}(\tilde{s})$ up to any order in ϵ.

Given the result in the non-physical region, the analytic continuation to the physical region can be achieved as described above, i.e. with

$$m^2 \to -M^2 - i\eta\,, \quad x \to \xi$$

which has to be consistently performed also on the pre-factors in (5.31).

5.3.3 GHPLs as functions of (x, z)

Proceeding as outlined in the case of the one-loop triangle, we can derive the set of differential equations in (x, z) fulfilled by the MIs in **Topo A**. By direct inspection of the denominators in the differential equations we can read off what the alphabet of all possible indices appearing in the GHPLs will be. We find that in the non-physical region only the following functions can appear:

$$\begin{aligned} &G(a_1,\ldots,a_n;x) \quad \text{with } a_i \in \{0,\pm 1,-c,-\bar{c}\}\,, \\ &G(a_1,\ldots,a_n;z) \quad \text{with } a_i \in \{0,1,-x,-\frac{1}{x},-I_x,-\frac{1}{I_x}\}\,. \end{aligned} \tag{5.39}$$

where

$$\begin{aligned} c &= \frac{1}{2}\left(1+i\sqrt{3}\right)\,, \\ I_\alpha &= \frac{\alpha}{1+\alpha+\alpha^2}\,. \end{aligned} \tag{5.40}$$

After analytical continuation to the physical region (5.9) this becomes:

$$\begin{aligned} &G(a_1,\ldots,a_n;\xi) \quad \text{with } a_i \in \{0,\pm 1,-c,-\bar{c}\}\,, \\ &G(a_1,\ldots,a_n;\zeta) \quad \text{with } a_i \in \{0\,,\,-1\,,\,\xi\,,\,\frac{1}{\xi}\,,\,I_\xi\,,\,\frac{1}{I_\xi}\}\,. \end{aligned} \tag{5.41}$$

Note that this does not imply that *all* indices in (5.41) will necessarily be needed in order to represent the physical result, it only provides us with the largest set possible of allowed indices. Nevertheless, by direct computation we verified that indeed the full set of indices is needed in order to represent all MIs up to transcendentality 4.

5.3.4 Master Integrals

We list here all the genuine 2-loop master integrals that appear in the reduction, giving an explicit form in terms of propagators for those topologies that have more than one master. In order to write down the integrals we introduce the following notation for the momenta:

$$p_{12} = p_1 + p_2\,, \qquad p_{13} = p_1 - q_1\,, \qquad p_{23} = p_2 - q_1\,, \qquad p_{123} = p_1 + p_2 - q_1\,.$$

One-scale integrals

There are three trivial one-scale topologies, whose values can be computed directly from their Feynman parameters representation and have been known for a long time. We have

$\mathcal{I}^{(A)}_{38}(s) =$ 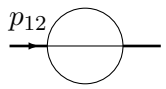

$\mathcal{I}^{(A)}_{53}(s) =$ 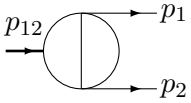

(5.42)

$$\mathcal{I}^{(A)}_{134}(Q^2) = \mathcal{I}^{(A)}_{38}(Q^2) \qquad \mathcal{I}^{(A)}_{148}(u) = \mathcal{I}^{(A)}_{38}(u) \tag{5.43}$$

Two-Scale integrals

All seven two-scale vertex functions have already been computed in [59, 60] for two off-shell legs and in [289, 290] for three off-shell legs. In the latter papers all three-point functions with three different external masses have been computed. In the context of this work we recomputed the planar ones in the case of two equal masses. Note that they can all be conveniently expressed as functions of one of the two ratios $\tilde{s} = s/Q^2$ and $\tilde{u} = u/Q^2$.

Among the irreducible topologies with four denominators two have a single master integral:

$\mathcal{I}^{(A)}_{142}(\tilde{u}) =$ 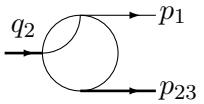

$\mathcal{I}^{(A)}_{149}(\tilde{u}) =$ 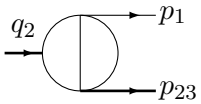

(5.44)

while two have two master integrals each. We choose the following basis:

$\mathcal{I}^{(A)}_{166,1}(\tilde{s}) =$ 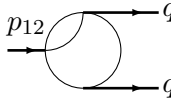

$= \int \frac{d^dk}{(2\pi)^d}\frac{d^dl}{(2\pi)^d}\frac{1}{l^2(k-l)^2(k-p_{12})^2(k-p_{123})^2}\,,$ (5.45)

$\mathcal{I}^{(A)}_{166,2}(\tilde{s}) =$ 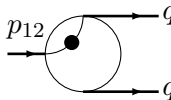

$= \int \frac{d^dk}{(2\pi)^d}\frac{d^dl}{(2\pi)^d}\frac{1}{l^2(k-l)^4(k-p_{12})^2(k-p_{123})^2}$ (5.46)

and

$\mathcal{I}^{(A)}_{198,1}(\tilde{s}) =$ 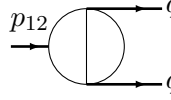

$= \int \frac{d^dk}{(2\pi)^d}\frac{d^dl}{(2\pi)^d}\frac{1}{l^2(k-l)^2(l-p_{12})^2(k-p_{123})^2}\,,$ (5.47)

$\mathcal{I}^{(A)}_{198,2}(\tilde{s}) =$ 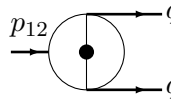

$= \int \frac{d^dk}{(2\pi)^d}\frac{d^dl}{(2\pi)^d}\frac{1}{l^2(k-l)^4(l-p_{12})^2(k-p_{123})^2}\,.$ (5.48)

Finally, there are three different irreducible two-scale topologies with 5 denominators, all with one single master integral:

$\mathcal{I}^{(A)}_{398}(\tilde{u}) =$ 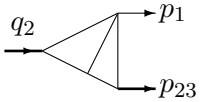

, (5.49)

$\mathcal{I}^{(A)}_{199}(\tilde{s}) =$ 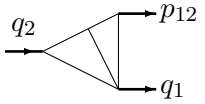

, $\mathcal{I}^{(A)}_{422}(\tilde{s}) =$ 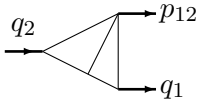

. (5.50)

Three-Scale Integrals

We found eight nontrivial three-scale topologies which depend on both ratios $(\tilde{s}, \tilde{u})$.

There are four irreducible topologies with 5 denominators, out of which two have one master integral:

$\mathcal{I}^{(A)}_{174} =$ 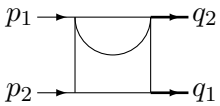

, $\mathcal{I}^{(A)}_{214} =$ 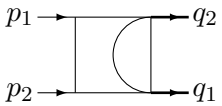

, (5.51)

and two have two master integrals each, that we choose to be:

$$\mathcal{I}^{(A)}_{181,1} = \quad \text{ 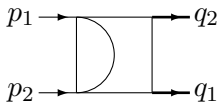 }$$

$$= \int \frac{d^dk}{(2\pi)^d} \frac{d^dl}{(2\pi)^d} \frac{1}{k^2(k-l)^2(l-p_1)^2(k-p_{12})^2(k-p_{123})^2}\,, \tag{5.52}$$

$$\mathcal{I}^{(A)}_{181,2} = \quad \text{ 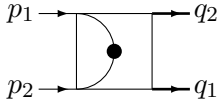 }$$

$$= \int \frac{d^dk}{(2\pi)^d} \frac{d^dl}{(2\pi)^d} \frac{1}{k^2(k-l)^4(l-p_1)^2(k-p_{12})^2(k-p_{123})^2}\,, \tag{5.53}$$

$$\mathcal{I}^{(A)}_{182,1} = \quad \text{ 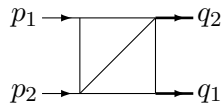 }$$

$$= \int \frac{d^dk}{(2\pi)^d} \frac{d^dl}{(2\pi)^d} \frac{1}{l^2(k-l)^2(l-p_1)^2(k-p_{12})^2(k-p_{123})^2}\,, \tag{5.54}$$

$$\mathcal{I}^{(A)}_{182,2} = \quad \text{ 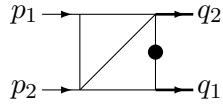 }$$

$$= \int \frac{d^dk}{(2\pi)^d} \frac{d^dl}{(2\pi)^d} \frac{1}{l^2(k-l)^2(l-p_1)^2(k-p_{12})^2(k-p_{123})^4}\,. \tag{5.55}$$

The two irreducible 6-denominator topologies have both one single master integral:

$\mathcal{I}^{(A)}_{215} =$ 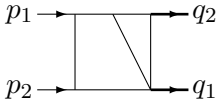

, $\mathcal{I}^{(A)}_{430} =$ 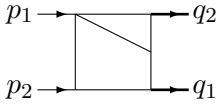

. (5.56)

Finally there are two irreducible 7-denominator topologies, one with three master integrals:

$$\mathcal{I}^{(A)}_{247,1} = \quad \text{ 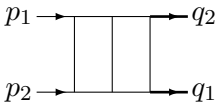 }$$

$$= \int \frac{d^dk}{(2\pi)^d}\frac{d^dl}{(2\pi)^d}\frac{1}{k^2l^2(k-l)^2(l-p_1)^2(k-p_{12})^2(l-p_{12})^2(k-p_{123})^2}\,, \quad (5.57)$$

$$\mathcal{I}^{(A)}_{247,2} = \quad \text{ 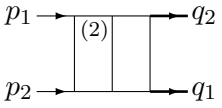 }$$

$$= \int \frac{d^dk}{(2\pi)^d}\frac{d^dl}{(2\pi)^d}\frac{(k-p_1)^2}{k^2l^2(k-l)^2(l-p_1)^2(k-p_{12})^2(l-p_{12})^2(k-p_{123})^2}\,, \quad (5.58)$$

$$\mathcal{I}^{(A)}_{247,3} = \quad \text{ 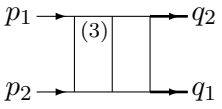 }$$

$$= \int \frac{d^dk}{(2\pi)^d}\frac{d^dl}{(2\pi)^d}\frac{(l-p_{123})^2}{k^2l^2(k-l)^2(l-p_1)^2(k-p_{12})^2(l-p_{12})^2(k-p_{123})^2} \quad (5.59)$$

and one with two master integrals:

$$\mathcal{I}^{(A)}_{446,1} = \quad \text{ 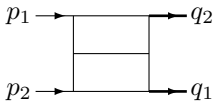 }$$

$$= \int \frac{d^dk}{(2\pi)^d}\frac{d^dl}{(2\pi)^d}\frac{1}{l^2(k-l)^2(k-p_1)^2(l-p_1)^2(k-p_{12})^2(k-p_{123})^2(l-p_{123})^2}\,, \quad (5.60)$$

$$\mathcal{I}^{(A)}_{446,2} = \quad \text{ 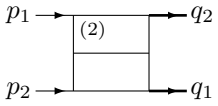 }$$

$$= \int \frac{d^dk}{(2\pi)^d}\frac{d^dl}{(2\pi)^d}\frac{k^2}{l^2(k-l)^2(k-p_1)^2(l-p_1)^2(k-p_{12})^2(k-p_{123})^2(l-p_{123})^2}\,. \quad (5.61)$$

As it is well known the basis is not unique. The choice that we made was only motivated by the fact that with it we obtain systems of differential equations that decouple in $d \to 4$ and allow a direct integration of the MIs.

The results for the masters computed in the non-physical region up to weight 3 can be found in Appendix B.1. The full result up to weight 4 and the analytical continuation to the physical region relevant for vector boson pair production is attached to the arXiv submission of this paper. In addition, we also provide the one-loop $\times$ one-loop integrals required for the full reduction in the same set of variables. Their naming convention follows the same scheme outlined in section 5.2.1.

5.4 Topo B

We consider now the second topology which collects all planar masters with two non-adjacent massive legs. As already discussed, **Topo B** has cuts in t and u. This suggests as first attempt to try to derive and solve the differential equations in these variables.

The kinematics and the analytical continuation to the proper physical region has been described in section 5.2.3.

Proceeding in the same way as outlined in section 5.3 we start from the following set of invariants:

$$s_1 = p_1^2\,, \quad s_2 = p_2^2\,, \quad s_3 = q_1^2 - q_2^2\,, \quad s_4 = q_1^2\,, \quad s_5 = (p_1 - q_1)^2\,, \quad s_6 = (p_2 - q_1)^2,$$

where, applying the on-shell conditions we find:

$$s_1 = 0\,, \quad s_2 = 0\,, \quad s_3 = 0\,, \quad s_4 = Q^2\,, \quad s_5 = t\,, \quad s_6 = u.$$

All the discussion done for **Topo A** applies also here, but for brevity we omit the explicit form of the differential operators in this case.

As discussed already in section 5.3, the kinematics for vector boson pair production generates naturally the square root $\sqrt{s(s-4Q^2)}$. This means that, if in order to highlight the symmetries of this topology we choose not to use the Landau variable (5.36), we can expect that in turn there will appear this same square root in the homogeneous solutions of some of the differential equations. On the other hand, introducing the Landau variable would oblige us to get rid of either t or u in favor of s, and so to give up the symmetry in (t, u).

Nevertheless, limiting ourselves to considering only the MIs in **Topo B**, because of their cut structure, this square root appears in only one single master integral. As it will be discussed in more detail below, this integral belongs to sector 213 which has five denominators and is reduced to four MIs. This could easily generate a problem since, in the differential equation approach, the integral can be expected to affect the differential equations of the other three MIs of its sector, plus all the topologies with a larger number of denominators that contain it as sub-topology. In spite of that, by direct computation we found that with an appropriate choice of the basis, the integral above "decouples" from the rest of the integrals in its sector and also from all the integrals with a larger number of denominators, in a sense more clearly specified below. This allows us to compute all the other integrals in **Topo B** without having to explicitly carry out the integration of this integral. The computation of this last integral has been performed in the physical region reintroducing the Landau variable ξ as described in the following.

5.4.1 GHPLs as functions of (y, z)

As for **Topo A**, the alphabet of indices for the GHPLs needed to describe all MIs in **Topo B** can be read off directly from the differential equations. By direct inspection we find that all integrals except one can be written through the following set of GHPLs:

$$\begin{aligned} &G(a_1, \ldots, a_n; z) \quad \text{with } a_i \in \{0, 1, 2\}\,, \\ &G(a_1, \ldots, a_n; y) \quad \text{with } a_i \in \{0, 1, 2 - z, \frac{1}{z}\}\,, \end{aligned} \tag{5.62}$$

which becomes after analytical continuation (5.16)

$$\begin{aligned} &G(a_1, \ldots, a_n; v) \quad \text{with } a_i \in \{0, -1, -2\}\,, \\ &G(a_1, \ldots, a_n; w) \quad \text{with } a_i \in \{0, -1, v, -\frac{1}{2+v}\}\,. \end{aligned} \tag{5.63}$$

One of the MIs, $\mathcal{I}^{(B)}_{213,1}$, had to be integrated in ξ and ζ (see section 5.4.3). Again, we can predict the full set of indices needed to describe the result deriving the differential equations

fulfilled by the MI in these variables. In order to gain a more thorough understanding, instead of doing it only for this MI, we derived the differential equations in (ξ, ζ) for the full set of MIs in **Topo B**. We find that they can be expressed through the following set of GHPLs:

$$\begin{aligned} &G(a_1, \ldots, a_n; \xi) \quad \text{with } a_i \in \{0, -1, \pm i, -c, -\bar{c}\}\,, \\ &G(a_1, \ldots, a_n; \zeta) \quad \text{with } a_i \in \left\{0, -1, \xi, \frac{1}{\xi}, \frac{1}{I_\xi}, \frac{1}{J_\xi}\right\}\,. \end{aligned} \tag{5.64}$$

Note the appearance of the additional indices

$$\begin{aligned} &\frac{1}{J_\xi} = \frac{1+\xi^2}{\xi}\,, \quad \text{in GHPLs with argument } \zeta\,, \\ &\pm i\,, \quad \text{in GHPLs with argument } \xi\,, \end{aligned} \tag{5.65}$$

compared to the alphabet of **Topo A**, eq. (5.41). These indices are indeed needed in order to describe the cut in t using instead s and u (expressed through ξ and ζ) as independent variables.

5.4.2 Master Integrals

As for the first topology, a catalog of all master integrals appearing in the reduction of this topology can be established. Since all one- and two-scale integrals are identical to those appearing in **Topo A** up to a permutation of the external legs, we do not give their explicit expressions here for brevity. Nevertheless, depending on which set of variables we choose to express these MIs in, the identities to perform the transformation can be highly nontrivial. In the differential equation method, in order to derive a sensible differential equation for a MI we need to express all its sub-topologies in the same set of variables. We introduce then a notation for these masters and give their explicit expression. In appendix B the variables used are the ones that produce the most compact expressions; the results in all sets of variables can be obtained by the authors.

One-scale Integrals

The one-scale integrals needed for the full reduction of **Topo B** are simply

$$\mathcal{I}^{(A)}_{38}(t)\,, \quad \mathcal{I}^{(A)}_{38}(u)\,. \tag{5.66}$$

Two-scale Integrals

The two-scale integrals needed are

$$\mathcal{I}^{(A)}_{149}(u)\,, \quad \mathcal{I}^{(A)}_{142}(u)\,,$$

$$\mathcal{I}^{(B)}_{46}(t) = \mathcal{I}^{(A)}_{149}(u \leftrightarrow t)\,, \qquad \mathcal{I}^{(B)}_{53}(t) = \mathcal{I}^{(A)}_{142}(u \leftrightarrow t)\,. \tag{5.67}$$

$$\mathcal{I}^{(B)}_{110}(t) = \mathcal{I}^{(A)}_{398}(u \leftrightarrow t)\,. \tag{5.68}$$

Three-scale Integrals

We find three irreducible 5-denominator topologies, two with one single master integral:

$\mathcal{I}^{(B)}_{174} =$ 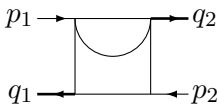 , $\mathcal{I}^{(B)}_{182} =$ 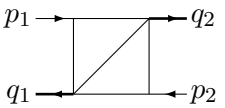 , (5.69)

and one with four master integrals. We choose them as:

$\mathcal{I}^{(B)}_{213,1} =$ 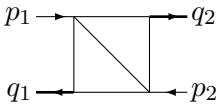

$$= \int \frac{d^dk}{(2\pi)^d} \frac{d^dl}{(2\pi)^d} \frac{1}{k^2(k-l)^2(l-p_1)^2(l-p_{13})^2(k-p_{123})^2} , \tag{5.70}$$

$\mathcal{I}^{(B)}_{213,2} =$ 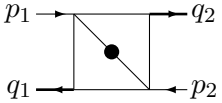

$$= \int \frac{d^dk}{(2\pi)^d} \frac{d^dl}{(2\pi)^d} \frac{1}{k^2(k-l)^4(l-p_1)^2(l-p_{13})^2(k-p_{123})^2} , \tag{5.71}$$

$\mathcal{I}^{(B)}_{213,3} =$ 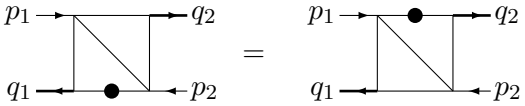

$$= \int \frac{d^dk}{(2\pi)^d} \frac{d^dl}{(2\pi)^d} \frac{1}{k^2(k-l)^2(l-p_1)^2(l-p_{13})^4(k-p_{123})^2} , \tag{5.72}$$

$\mathcal{I}^{(B)}_{213,4} =$ 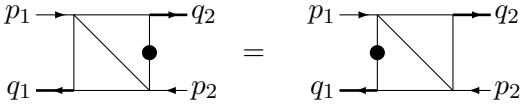

$$= \int \frac{d^dk}{(2\pi)^d} \frac{d^dl}{(2\pi)^d} \frac{1}{k^2(k-l)^2(l-p_1)^2(l-p_{13})^2(k-p_{123})^4} , \tag{5.73}$$

Note that, in the case of sector 213, a naive reduction using only IBP identities would indeed produce five independent MIs. Nevertheless, using the symmetry relations of the topology under shift of the integration variables we realize that one of these masters can be re-expressed as linear combination of the others, leaving four independent MIs. Our choice for the basis of MIs makes this symmetry manifest. This is an explicit example of a case where symmetry relations do contribute to reduce the number of independent masters. The consistent inclusion of symmetry relations in the reduction to MIs has been recently automated inside Reduze2.

There is only one irreducible 6-denominator topology, with one single master integral

$\mathcal{I}^{(B)}_{215} =$ 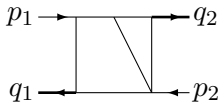 . (5.74)

Finally, we find only one irreducible 7-denominator topology, with two master integrals,

$\mathcal{I}^{(B)}_{247,1} =$ 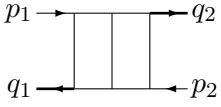

$$= \int \frac{d^dk}{(2\pi)^d} \frac{d^dl}{(2\pi)^d} \frac{1}{k^2 l^2 (k-l)^2 (l-p_1)^2 (k-p_{13})^2 (l-p_{13})^2 (k-p_{123})^2}\,, \quad (5.75)$$

$\mathcal{I}^{(B)}_{247,2} =$

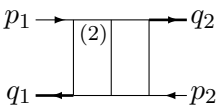

$$= \int \frac{d^dk}{(2\pi)^d} \frac{d^dl}{(2\pi)^d} \frac{(k-p_1)^2}{k^2 l^2 (k-l)^2 (l-p_1)^2 (k-p_{13})^2 (l-p_{13})^2 (k-p_{123})^2}\,. \quad (5.76)$$

We want to stress here also another aspect. Very often in the case of a sector with a large number of masters, an appropriate choice of basis also helps simplify substantially the identities needed to express all integrals of that topology through the set of masters themselves. In treating four-point functions the reduction identities often attain an enormous size, and we found that using this basis helped speed up considerably the intermediate stages of the computations.

In Appendix B.2 we report the results for all masters except $\mathcal{I}^{B}_{(213,1)}$ computed in the non-physical region up to weight 3. This last integral has been computed in the physical region, as discussed below. Since its expansion starts only at weight 4, we decided to include its explicit expression in the same Appendix. The full result up to weight 4 and the analytic continuation to the physical region relevant for vector boson pair production for all MIs is attached to the arXiv submission of this paper. In addition, we also provide the one-loop × one-loop integrals required for the full reduction in the same set of variables. Their naming convention follows the same scheme outlined in section 5.2.1.

5.4.3 The computation of the 4 MIs in sector 213.

In the following section we describe in detail the computation of the four masters in sector 213. We use for the 4 MIs the following notation:

$$M_j(y,z,\epsilon) = \mathcal{I}^{(B)}_{213,j} \quad \text{with} \quad j = 1,2,3,4$$

where we made explicit the dependence on y, z and on the dimensional regulator ϵ. Although the symmetries of **Topo B** would favor the choice of (y, z) as variables, one of the masters in this sector could not be expressed explicitly in terms of standard GHPLs only using these variables and required hence a special treatment.

Deriving the differential equations satisfied by the four MIs in (y, z) we find a system of four coupled differential equations. With the choice described above the system assumes a triangular form in the limit $d \to 4$, allowing at least in principle its solution as series expansion in $\epsilon = (4-d)/2$. Due to the symmetry of the sector under the exchange $y \leftrightarrow z$ we can limit the discussion to the system of equations in $\partial/\partial y$. Also, for the sake of argument, we look just at its homogeneous part. Highlighting the dependence on ϵ the system takes the symbolic form

$$\begin{aligned}
\frac{\partial}{\partial y} M_1 &= a_{11}\, M_1 + a_{12}\, M_2 + a_{13}\, M_3 + a_{14}\, M_4 \\
\frac{\partial}{\partial y} M_2 &= a_{22}\, M_2 + \epsilon\, [a_{23}\, M_3 + a_{24}\, M_4] \\
\frac{\partial}{\partial y} M_3 &= \epsilon^2\, [a_{31}\, M_1] + \epsilon\, [a_{32}\, M_2 + a_{33}\, M_3 + a_{34}\, M_4] \\
\frac{\partial}{\partial y} M_4 &= \epsilon^2\, [a_{41}\, M_1] + \epsilon\, [a_{42}\, M_2 + a_{43}\, M_3] + a_{44}\, M_4
\end{aligned} \quad (5.77)$$

where both the M_j and the a_{ij} are functions of (y, z) and of the regularization parameter ϵ, such that the a_{ij} do not have any poles in $1/\epsilon$. The triangular form in $\epsilon \to 0$ is easy to see. In particular the equations for masters M_2, M_3, M_4 are decoupled from that for M_1 and from each other in this limit. Our strategy will then be that of expanding both sides of the equations in ϵ and attempt a solution in a bottom up approach. Upon expanding in ϵ one obtains, order by order, a system of four differential equations in triangular form. At order ϵ^n the system takes the form

$$\begin{aligned}
\frac{\partial}{\partial y} M_1^{(n)}(y,z) &= \frac{1}{2}\left[\frac{1}{2-y-z} - \frac{1}{2+y+z}\right] M_1^{(n)}(y,z) \\
&+ \left[\frac{m^2(1-yz)}{(2+y+z)(2-y-z)}\right] M_2^{(n)}(y,z) \\
&- \left[\frac{m^2(1-y)(z^2+4yz-5)}{(1-yz)(2+y+z)(2-y-z)}\right] M_3^{(n)}(y,z) \\
&+ \left[\frac{m^2(1-z)(z^2-2yz+1)}{(1-yz)(2+y+z)(2-y-z)}\right] M_4^{(n)}(y,z) + N_1^{(n)}(y,z)\,, \\
\frac{\partial}{\partial y} M_2^{(n)}(y,z) &= \left[\frac{z}{1-yz}\right] M_2^{(n)}(y,z) + N_2^{(n)}(y,z)\,, \\
\frac{\partial}{\partial y} M_3^{(n)}(y,z) &= \left[\frac{1}{1-y}\right] M_3^{(n)}(y,z) + N_3^{(n)}(y,z)\,, \\
\frac{\partial}{\partial y} M_4^{(n)}(y,z) &= N_4^{(n)}(y,z)\,,
\end{aligned}$$

where the $N_j^{(n)}(y,z)$ is the non-homogeneous term of the equation for M_j at order ϵ^n. Note that the homogeneous part of the system is independent on the order of the expansion, while the non-homogeneous terms do depend on n.

At order n we start integrating the last three equations and fixing the boundary condition to determine the exact solution for $M_2^{(n)}$, $M_3^{(n)}$ and $M_4^{(n)}$. The result of the integration must then be used as input to derive a first order differential equation for $M_1^{(n)}$. If we are able to integrate this equation and to fix the boundary condition, we can use the result as input for the equations of $M_2^{(n+1)}$, $M_3^{(n+1)}$, $M_4^{(n+1)}$ proceeding bottom up from ϵ^{-4} (the first relevant order for the expansion) to any desired order.

One complication arises. The homogeneous equation for $M_1^{(n)}(y,z)$ reads

$$\frac{\partial H_1^{(n)}(y,z)}{\partial y} = \frac{1}{2}\left[\frac{1}{2-y-z} - \frac{1}{2+y+z}\right] H_1^{(n)}(y,z)\,,$$

so that its solution contains a square root, which for $(y,z) > 0$ and $y + z < 1$ reads

$$H_1^{(n)}(y,z) = \frac{1}{\sqrt{(2-y-z)(2+y+z)}}.$$

Re-written in terms of s and Q^2, this is exactly the square-root described in section 5.3. The presence of this square-root tells us that if we want to express the result in terms of (y,z) we need to introduce a new set of generalized polylogarithms that may contain also non-rational integrating factors (see for example [286]). The algebraic properties of these functions are much less well understood than those of GHPLs, and no numerical

implementation exists for them. By studying $M_1(y,z)$ one easily realizes that the master has no divergences for $\epsilon \to 0$ so that its expansion starts only at order ϵ^0

$$M_1(y,z,\epsilon) = M_1^{(0)}(y,z) + \mathcal{O}(\epsilon)\,.$$

From the ϵ dependence of the system in (5.77) we see that $M_1(y,z)$ can then enter as non-homogeneous term in the equations for M_2, M_3 and M_4 only starting at order ϵ^2. Since we are interested in the expression for the masters up to transcendentality 4, which corresponds in this case to computing them up to order ϵ^0, the explicit value of $M_1^{(0)}(y,z)$ is never required. Note that the same kind of cancellation takes place also for the integrals with larger number of denominators, $\mathcal{I}^{(B)}_{215}$, $\mathcal{I}^{(B)}_{247,1}$ and $\mathcal{I}^{(B)}_{247,2}$. By direct inspection of their differential equations we see that both topologies contain only M_2, M_3 and M_4 as sub-topologies, while M_1 never contributes (at any order in ϵ!).

In order to compute M_1 we proceed in the following way. We use the explicit results for M_2, M_2 and M_3 to obtain two linear first order differential equations for M_1 in y and z. These are then continued to the Minkowski region as outlined in section 5.2.3. We then re-interpret the equations given in v, w as equation given in $v = \zeta$ and $w = w(\xi,\zeta)$ and obtain

$$\frac{\partial M_1}{\partial \zeta} = \frac{\partial M_1}{\partial v}\frac{\partial v}{\partial \zeta} + \frac{\partial M_1}{\partial \frac{1}{w}}\frac{\partial \frac{1}{w}}{\partial \zeta}\,. \tag{5.78}$$

Since we have the following relations in the physical region

$$v = \zeta\,, \qquad \frac{1}{w} = \frac{1+\xi^2}{\xi} - \zeta\,, \tag{5.79}$$

we find, using the analytically continued differential equations as input,

$$\begin{aligned}
\frac{\partial M_1}{\partial \zeta} = \frac{1}{(\xi-\zeta)(\frac{1}{\xi}-\zeta)} \Bigg\{ & 2G\left(-1,\frac{1}{\zeta},0;\frac{1+\xi^2}{\xi}-\zeta\right) - 2G\left(-1,-1,0;\frac{1+\xi^2}{\xi}-\zeta\right) \\
& + 2G\left(-1,-1,0;\zeta\right) + 2G\left(0,-1,0;\frac{1+\xi^2}{\xi}-\zeta\right) - 2G\left(0,-1,0;\zeta\right) \\
& - G\left(0,\frac{1}{\zeta},0;\frac{1+\xi^2}{\xi}-\zeta\right) + G\left(0;\zeta\right)\Bigg[2G\left(-1,\frac{1}{\zeta};\frac{1+\xi^2}{\xi}-\zeta\right) \\
& \qquad -2G\left(-1;\frac{1+\xi^2}{\xi}-\zeta\right)G\left(-1,0;\zeta\right) - G\left(0,\frac{1}{\zeta};\frac{1+\xi^2}{\xi}-\zeta\right)\Bigg] \\
& + \frac{\pi^2}{6}\left[2G\left(-1;\frac{1+\xi^2}{\xi}-\zeta\right) - 2G\left(-1;\zeta\right) - G\left(0;\frac{1+\xi^2}{\xi}-\zeta\right) + G\left(0;\zeta\right)\right] \\
& - 2\pi\, i\,\Bigg[G\left(-1;\frac{1+\xi^2}{\xi}-\zeta\right)G\left(-1;\zeta\right) + G\left(-1,-1;\frac{1+\xi^2}{\xi}-\zeta\right) - G\left(-1,-1;\zeta\right) \\
& - 2G\left(-1,\frac{1}{\zeta};\frac{1+\xi^2}{\xi}-\zeta\right) - G\left(0,-1;\frac{1+\xi^2}{\xi}-\zeta\right) + G\left(0,-1;\zeta\right) \\
& + G\left(0,\frac{1}{\zeta};\frac{1+\xi^2}{\xi}-\zeta\right)\Bigg]\Bigg\} + \mathcal{O}(\epsilon)\,.
\end{aligned} \tag{5.80}$$

The $\mathcal{O}(\epsilon)$ part is not reproduced here but is nevertheless needed for fixing the boundary condition. The integration of the differential equation becomes trivial if all the ζ dependence of the GHPLs is in their argument. With the procedure described in section 3.3.3,

we can rewrite all the functions where this is not the case in terms of GHPLs of ξ and ζ. For example, we obtain

$$\begin{aligned} G\left(-1, \frac{1}{\zeta}; \frac{1+\xi^2}{\xi} - \zeta\right) =& G\left(0, \frac{1}{\xi}; \zeta\right) + G\left(0, \xi; \zeta\right) + G\left(\frac{1}{I_\xi}, \frac{1}{\xi}; \zeta\right) + G\left(\frac{1}{I_\xi}, \xi; \zeta\right) \\ & - G\left(-1, \frac{1}{\xi}; \zeta\right) - G\left(-1, \xi; \zeta\right) + G\left(-1, \frac{1}{I_\xi}; \zeta\right) \\ & + G\left(-1; \zeta\right)\left(-G\left(0; \xi\right) + G\left(-c; \xi\right) + G\left(-\bar{c}; \xi\right)\right) \ . \end{aligned} \tag{5.81}$$

In transforming the individual GHPLs independently we find that an apparently larger set of functions is needed:

$$\begin{aligned} & G(a_1, \ldots, a_n; \zeta) \quad \text{with } a_i \in \left\{-2, -1, 0, \frac{1}{\xi}, \xi, \frac{1}{I_\xi}, \frac{1}{J_\xi}\right\} \ , \\ & G(a_1, \ldots, a_n; \xi) \quad \text{with } a_i \in \{-1, 0, \pm i, -c, -\bar{c}\} \ . \end{aligned} \tag{5.82}$$

The appearance of index -2 is surprising since, as explained in section 5.4.1, no denominator $1/(\zeta+2)$ appears in the differential equations. Nevertheless, putting everything together all GHPLs with index -2 cancel, as expected, so that only the set described in section 5.4.1 survives. This cancellation gives a confirmation of the consistency of our procedure. Once equation (5.80) is put in this form, we can determine the primitive of M_1 by straightforward integration using the very definition of GHPLs.

In order to fix the boundary condition we require M_1 to be regular in $\zeta = \xi$. By multiplying equation (5.80) with $(\zeta - \xi)$ and taking the limit $\zeta \to \xi$ we obtain the value of $M_1(\xi, \zeta = \xi)$ from the $\mathcal{O}(\epsilon)$ part. The required limit identities can again be derived using the procedure from section 3.3.3. As for the other master integrals, the explicit result is provided with the arXiv submission of this paper.

5.5 Checks on the results

Many non-trivial checks have been performed in order to validate our result. As already stated above, all triangle topologies had been already computed in [289, 290], in the more general case of three different external masses. We compared our results in the Euclidean region numerically to those in [289, 290], finding perfect agreement.

We have used FIESTA [291] and SecDec2 [292] in order to check numerically all the double-box topologies in **Topo A** and **Topo B**, except for $\mathcal{I}^{(B)}_{213,1}$, in the non-physical region, where all integrals are real, finding agreement in different phase space points.

Recently a new version of SecDec has been released [293], which has been successfully used to perform accurate numerical evaluation of planar and non-planar double boxes also in the physical region. Using it we could then perform a full check in different phase space points of $\mathcal{I}^{(B)}_{213,1}$ finding again agreement with our result.

In the same way we could also check our analytic continuation procedure evaluating with SecDec2 numerically most of the masters in **Topo A** and **Topo B** also in the physical region, even though the numerical evaluation in this region is computationally much more demanding.

5.6 Conclusions

The precise interpretation of upcoming LHC results on vector boson pair production will require the computation of NNLO QCD corrections to this process, currently known

only to NLO. Besides already known contributions with higher final state multiplicity and a lower number of loops, this calculation requires the two-loop corrections to vector boson pair production matrix elements. Using the integration-by-parts (IBP) technique, the Feynman integrals appearing in these matrix elements can be expressed as a linear combination of a small set of so-called master integrals.

In this chapter, we considered the integrals relevant to the two-loop corrections for the production of massive equal-mass gauge bosons: $q\bar{q} \to VV$. For the application of the IBP technique, the integrals could be assigned to one of the three auxiliary topologies relevant to this process. Two of these auxiliary topologies contain only planar master integrals, which are the main focus here. We derived differential equations in the external Mandelstam invariants for all integrals, starting at the integrand level. The integrals are then computed by solving these differential equations, matched to appropriate boundary conditions in special kinematical points.

The master integrals are expressed in terms of generalized harmonic polylogarithms (GHPLs), which appear widely in analytical calculations of Feynman integrals. In the course of deriving these integrals from the differential equations, three types of manipulations have to be performed repeatedly: variable transformations, determination of limiting behavior in special points and analytical continuation. The computer algebra automation of these operations relies heavily on the algebraic properties of the GHPLs. The recently developed coproduct formalism [68, 69] was used to perform most of the transformations on GHPLs.

We obtained analytical results for all massless planar two-loop four-point functions with two off-shell legs of equal invariant mass. The resulting expressions prior to analytical continuation to the physical region are fairly compact, and the pole parts of all integrals are documented in this chapter. The finite pieces, as well as the analytical continuation of the integrals are more lengthy, and are enclosed with the arXiv submission of [62]. The newly derived master integrals will allow us to calculate the planar (for example leading-color) two-loop corrections to the amplitudes for $q\bar{q} \to VV$. This work, as well as the computation of the non-planar master integrals, is in progress.

6 Conclusions and Outlook

In this thesis two different topics in particle physics phenomenology were treated. It was shown how the early LHC could be used to constrain the parameter space of the Standard Model Higgs sector extended with a dark Higgs and a dark gauge boson. This class of models is well motivated in the context of Dark Matter models. While the Higgs boson has been discovered and its properties seem to be very similar to the Standard Model predictions there is still ample parameter space to accommodate this model in the region where it is best motivated.

The second part of this thesis dealt with the computation of two-loop contributions to the production of two gauge bosons at hadron colliders. This class of processes is an important background for Higgs searches and can be used to constrain physics beyond the Standard Model indirectly. In order to do this precise predictions of the Standard Model differential cross sections are necessary.

The two-loop virtual contributions to the process $g\,g \to Z\,g/\gamma$ were computed using previously known integrals and the results were written, where possible, in terms of logarithms and polylogarithms with the help of the symbol formalism. The symbol formalism and its extension, the coproduct, exploit the algebraic structure of the multiple polylogarithms and can be used to make transformations among this class of functions trivial.

Furthermore, the two-loop planar master integrals for the production of equal-mass massive particles were computed using the method of differential equations. During the computation various transformations and limits on multiple polylogarithms had to be computed. This was achieved using the coproduct of the multiple polylogarithms together with an alternative method to integrate the symbol. The completion of these integrals constitutes an important step toward the computation of the two-loop amplitude of the production of W and Z boson pairs at the LHC.

The algorithms for the usage of the coproduct and symbol formalism were presented and their implementation in `mathematica` described in the documentation and using examples.

The computation of multi-loop amplitudes is an ongoing challenge and is hoped to yield new theoretical insights as well. The presented code is likely to help in this endeavor.

The next step will be the computation of the planar amplitudes for $q\,\bar{q} \to Z\,Z$, $W\,W$ and $g\,g \to Z\,Z$, $W\,W$. It remains to be seen whether the inclusion of the light scattering process (two photons in the initial state) is also a goal worthy of pursuit.

All the necessary tools for the computation of the non-planar integrals of the same topology should now be available. Evidently, they are required for a full description of massive vector boson pair production processes at the LHC.

At this stage the last diboson process the last missing process will be the production of $q_1\,q_2 \to W\,Z$. The two-loop integrals required for this amplitude exhibits additional complications due to the different masses in the final state. It remains to be seen and will be exciting to find out whether these newly available tools can help in the computation of its master integrals.

A

Some results of $Z \to ggg$ and related processes

The full results for the one- and two-loop coefficients in all relevant regions in Mathematica format can be found in the sources of the arxiv-submission of [61].

A.1 One-loop helicity amplitudes

A.1.1 $V \to ggg$ at one loop

We reproduce the leading order $O(\epsilon^2)$ for $V \to ggg$ in the decay kinematics defined in equation (4.1). The coefficients a_{Ω_i} defined in equation (4.79) are related to the α_i, β_i defined in equations (4.48) and (4.49), respectively.

$$\begin{aligned} a_{\alpha_1}(x,y,z) = {} & 2x\left(\frac{1}{1-x}-\frac{2}{z}\right)\log(x) + 2y\left(\frac{1}{1-y}-\frac{2}{z}\right)\log(y) \\ & - 2\left(\frac{(1-x)x+(1-y)y}{z^2}\right)\Bigg[\frac{\pi^2}{6} + \log(x)\log(y) \\ & \qquad - \left(\log(1-x)\log(x) + \mathrm{Li}_2(x)\right) \\ & \qquad - \left(\log(1-y)\log(y) + \mathrm{Li}_2(y)\right)\Bigg], \end{aligned} \tag{A.1}$$

$$\begin{aligned} a_{\alpha_2}(x,y,z) = {} & 2y\left(\frac{1}{1-y}-\frac{1}{z}\right) - \frac{2x(2y+z)}{z^2}\log(x) - \frac{2xy(z+(1-y)(2y+z))}{(1-y)^2z^2}\log(y) \\ & + 2\left(-\frac{x\left(2y^2+2yz+z^2\right)}{z^3}\right)\Bigg[\frac{\pi^2}{6} + \log(x)\log(y) \\ & \qquad - \left(\log(1-x)\log(x) + \mathrm{Li}_2(x)\right) \\ & \qquad - \left(\log(1-y)\log(y) + \mathrm{Li}_2(y)\right)\Bigg], \end{aligned} \tag{A.2}$$

$$a_{\alpha_3}(x,y,z) = -a_{\alpha_2}(y,x,z)\,, \tag{A.3}$$

$$\begin{aligned} a_{\beta_1}(x,y,z) = -2\left(1-\frac{1}{y}\right)\,, \quad a_{\beta_2}(x,y,z) = -2\left(1-\frac{1}{z}\right)\,, \\ a_{\beta_3}(x,y,z) = -4\,. \end{aligned} \tag{A.4}$$

A.1.2 $V \to gg\gamma$ at one loop

At one loop, the amplitude is related to $V \to ggg$ as follows:

$$\begin{aligned} a_{\eta_i}(x,y,z) &= 2\,a_{\alpha_i}(x,y,z) \quad \text{for}\, i = 1,2,3\,, \\ a_{\theta_i}(x,y,z) &= 2\,a_{\beta_i}(x,y,z) \quad \text{for}\, i = 1,2,3\,, \end{aligned} \tag{A.5}$$

$$\begin{aligned} a_{\tau_1}(x,y,z) = 2\,a_{\alpha_3}(z,y,x)\,, \quad a_{\tau_2}(x,y,z) = 2\,a_{\alpha_2}(z,y,x)\,, \\ a_{\tau_3}(x,y,z) = 2\,a_{\alpha_1}(z,y,x)\,. \end{aligned} \tag{A.6}$$

A.2 Two-loop amplitudes: all-plus helicity coefficients

Due to the length of the resulting expressions only the all-plus $(g_1^+, g_2^+, g_3^+/\gamma_3^+)$ helicity amplitudes of both processes in the decay region are reproduced. These are considerably shorter than the other helicity combinations and contain only functions up to transcendental weight two.

A.2.1 $V \to ggg$ at two loops

The coefficients A_i, B_i and C_i defined in equation (4.80) for the (g_1^+, g_2^+, g_3^+) helicity configuration are:

$$\begin{aligned} A_{\beta_1}(x,y,z) = &-\frac{1}{27}\left(27\left(3-\frac{1}{1-x}-\frac{1}{y}-\frac{1}{1-z}\right)-\frac{4z}{x}-\frac{4z^2}{x^2}\right. \\ &\left.+x^2\left(-\frac{4}{z^2}-\frac{4z}{y^3}\right)+\frac{4x}{z}\left(-1-\frac{z^3}{y^3}\right)\right)-\frac{11}{2}\left(1-\frac{1}{y}\right)i\pi \\ &-\frac{1}{12}\left(\frac{3(1-y)}{xy}-\frac{2(-1+2y)}{y^2}+\frac{3(1-y)}{yz}+\frac{14(1-y)z}{y^3}-\frac{14z^2}{y^3}\right)\pi^2 \\ &+\frac{1}{6}\left(11+\frac{6}{(1-x)^2}-\frac{6}{1-x}-\frac{42x+11y}{y^2}\right)\log(x)+\frac{1}{6}\left(11-\frac{47}{y}\right)\log(y) \\ &+\frac{1}{6}\left(11+\frac{-42+42x+31y}{y^2}+\frac{6}{(1-z)^2}-\frac{6}{1-z}\right)\log(z) \\ &-\frac{1}{2}\left(\frac{2}{y}+\frac{3x}{yz}\right)\log(x)\log(y)-\frac{1}{2}\left(\frac{2}{y}+\frac{3z}{xy}\right)\log(y)\log(z) \\ &-\left(\frac{7(1-x)x}{y^3}+\frac{1}{y^2}-\frac{7x}{y^2}-\frac{1}{y}\right)\log(x)\log(z) \\ &+\frac{1}{2}\left(\frac{2(1-7z)}{y^2}-\frac{3}{z}+\frac{3(1-z)}{yz}+\frac{14(1-z)z}{y^3}\right) \end{aligned}$$

$$\times \left(\log(1-x)\log(x)+\mathrm{Li}_2(x)\right)$$
$$+\frac{1}{2}\left(\frac{4}{y}+\frac{3x}{yz}+\frac{3z}{xy}\right)\left(\log(1-y)\log(y)+\mathrm{Li}_2(y)\right)$$
$$-\frac{1}{2}\left(\frac{14x^2}{y^3}-\frac{14x(1-y)}{y^3}-\frac{3(1-y)}{xy}+\frac{-2+3y}{y^2}\right)$$
$$\times \left(\log(1-z)\log(z)+\mathrm{Li}_2(z)\right)\,, \quad \text{(A.7)}$$

$$\begin{aligned}
A_{\beta_2}(x,y,z) =& -\frac{1}{27}\left(\frac{27}{1-x}+\frac{27}{1-y}-\frac{4y}{x}-\frac{4y^2}{x^2}+x^2\left(-\frac{4}{y^2}-\frac{4y}{z^3}\right)\right.\\
&\left.+\frac{4x}{y}\left(-1-\frac{y^3}{z^3}\right)-\frac{54}{z}\right)-\frac{11}{2}\left(1-\frac{1}{z}\right)i\pi\\
&-\frac{1}{12}\left(\frac{x^2(14+y(-58+45y))}{y^2z^2}+\frac{14x^3(-2+3y)}{y^2z^2}-\frac{2(1-y)y(-8+21y)}{xz^2}\right.\\
&\left.-\frac{4x(1-y)(-4+5y)}{yz^2}+\frac{3(2+3y(-4+5y))}{z^2}+\frac{14(1-y)^2y^2}{x^2z^2}+\frac{14x^4}{y^2z^2}\right)\pi^2\\
&-\frac{1}{6}\left(\frac{53x}{z}+\frac{42x^2}{yz}-\frac{(-47-53(-2+x)x)y}{(1-x)^2z}\right)\log(x)\\
&+\frac{1}{6}\left(-\frac{53y}{z}-\frac{42y^2}{xz}-\frac{x(47+53(-2+y)y)}{(1-y)^2z}\right)\log(y)\\
&-\frac{1}{6}\left(31+\frac{42x}{y}+\frac{42y}{x}+\frac{11}{z}\right)\log(z)\\
&-\frac{1}{2}\left(\frac{x^2}{z^2}+\frac{x(2-12y)}{z^2}+\frac{y(2+y)}{z^2}\right)\log(x)\log(y)\\
&-\frac{1}{2}\left(1+\frac{14(1-z)^2}{y^2}-\frac{2(1-z)(-1+7z)}{yz}\right)\log(x)\log(z)\\
&-\frac{1}{2}\left(1+\frac{14y^2}{x^2}+\frac{-2+14y+\frac{2}{z}}{x}\right)\log(y)\log(z)\\
&+\frac{1}{2}\left(\frac{14(1-z)^2}{y^2}+\frac{14y^2}{z^2}-\frac{14y(1-z)}{z^2}-\frac{2(1-z)(-1+7z)}{yz}\right.\\
&\left.+\frac{3+2(-2+z)z}{z^2}\right)\left(\log(1-x)\log(x)+\mathrm{Li}_2(x)\right)\\
&+\frac{1}{2}\left(\frac{14(1-z)^2}{x^2}+\frac{14x^2}{z^2}-\frac{14x(1-z)}{z^2}-\frac{2(1-z)(-1+7z)}{xz}\right.\\
&\left.+\frac{3+2(-2+z)z}{z^2}\right)\left(\log(1-y)\log(y)+\mathrm{Li}_2(y)\right)\\
&-\left(\frac{1-x}{x}-\frac{7x^2}{y^2}+\frac{x(-8+7x)}{(1-x)y}-\frac{7y}{x}-\frac{7y^2}{x^2}-\frac{1}{(1-x)xz}\right)\\
&\times \left(\log(1-z)\log(z)+\mathrm{Li}_2(z)\right)\,,
\end{aligned} \quad \text{(A.8)}$$

$$A_{\beta_3}(x,y,z) = -\frac{1}{27}\left(81-\frac{8y^2}{z^2}-\frac{8z}{y}+\frac{8(1-z)z}{y^2}+\frac{8y}{z^2}\left(1-z+\frac{z^3}{x^2}\right)\right)-11i\pi$$

$$
\begin{aligned}
&- \frac{1}{12}\left(3 - \frac{5}{x} - \frac{14(1-x)x}{y^2} + \frac{-5+14x}{y} - \frac{14(1-x)y}{x^2}\right.\\
&\qquad \left. + \frac{14y^2}{x^2} - \frac{14(1-x)x}{z^2} - \frac{5-14x}{z}\right)\pi^2\\
&+ \frac{1}{3}\left(32 - \frac{3}{1-x} + \frac{21(1-x)x}{yz}\right)\log(x)\\
&+ \frac{1}{3}\left(32 - \frac{3}{1-y} + \frac{21(1-y)y}{xz}\right)\log(y)\\
&+ \frac{1}{3}\left(32 - \frac{3}{1-z} + \frac{21(1-z)z}{xy}\right)\log(z)\\
&- \frac{1}{2}\left(\frac{14x^2}{z^2} - \frac{14x(1-z)}{z^2} + \frac{-5+z}{z}\right)\log(x)\log(y)\\
&- \frac{1}{2}\left(1 - \frac{14(1-z)z}{y^2} + \frac{-5+14z}{y}\right)\log(x)\log(z)\\
&- \frac{1}{2}\left(1 - \frac{14(1-y)y}{x^2} + \frac{-5+14y}{x}\right)\log(y)\log(z)\\
&+ \frac{1}{2}\left(2 - \frac{(1-x)}{y^2z^2}\left(14(1-x)^2x - (1-x)(-5+42x)y + (-5+42x)y^2\right)\right)\\
&\qquad \times \left(\log(1-x)\log(x) + \mathrm{Li}_2(x)\right)\\
&+ \frac{1}{2}\left(2 - \frac{(1-y)}{x^2z^2}\left(14(1-y)^2y - (1-y)(-5+42y)z + (-5+42y)z^2\right)\right)\\
&\qquad \times \left(\log(1-y)\log(y) + \mathrm{Li}_2(y)\right)\\
&+ \frac{1}{2}\left(\frac{14x^2}{y^2} - \frac{14x(1-y)}{y^2} - \frac{14(1-y)y}{x^2} + \frac{-5+2y}{y} + \frac{-5+14y}{x}\right)\\
&\qquad \times \left(\log(1-z)\log(z) + \mathrm{Li}_2(z)\right)\,,
\end{aligned}
\tag{A.9}
$$

$$
\begin{aligned}
B_{\beta_1}(x,y,z) =& \frac{1}{1-x} + \frac{1}{y} + \frac{1}{1-z} - 3\\
&+ \frac{1}{12}\left(\frac{2}{y} - \frac{1-y}{xy} - \frac{1-y}{yz} - \frac{2(1-y)z}{y^3} + \frac{2z^2}{y^3}\right)\pi^2\\
&+ \left(\frac{x}{(1-x)^2} - \frac{x}{y^2}\right)\log(x) - \left(\frac{z}{y^2} - \frac{z}{(1-z)^2}\right)\log(z)\\
&- \frac{1}{2}\left(\frac{x}{yz}\right)\log(x)\log(y) - \left(\frac{xz}{y^3}\right)\log(x)\log(z)\\
&- \frac{1}{2}\left(\frac{z}{xy}\right)\log(y)\log(z)\\
&+ \frac{1}{2}\left(\frac{x}{yz} + \frac{2xz}{y^3}\right)\left(\log(1-x)\log(x) + \mathrm{Li}_2(x)\right)\\
&+ \frac{1}{2}\left(\frac{x}{yz} + \frac{z}{xy}\right)\left(\log(1-y)\log(y) + \mathrm{Li}_2(y)\right)\\
&- \frac{1}{2}\left(-\frac{2xz}{y^3} - \frac{z}{xy}\right)\left(\log(1-z)\log(z) + \mathrm{Li}_2(z)\right)\,,
\end{aligned}
\tag{A.10}
$$

$$
\begin{aligned}
B_{\beta_2}(x,y,z) = &-\frac{1}{1-x}-\frac{1}{1-y}+\frac{2}{z}\\
&-\frac{1}{12}\left(3+\frac{2x^2}{y^2}+\frac{2x}{y}+\frac{2y}{x}+\frac{2y^2}{x^2}+\frac{1-2(1-x)x}{z^2}-\frac{2(1-x)}{z}\right)\pi^2\\
&-\left(\frac{2x}{(1-x)^2}-\frac{x}{z}+\frac{x^2z}{(1-x)^2y}\right)\log(x)-\left(1+\frac{x}{y}+\frac{y}{x}\right)\log(z)\\
&+\left(1-\frac{1}{(1-y)^2}+y\left(-\frac{y}{x(1-y)}+\frac{1}{z}\right)\right)\log(y)\\
&-\frac{1}{2}\left(\frac{x^2}{z^2}+\frac{y^2}{z^2}\right)\log(x)\log(y)-\frac{1}{2}\left(1+\frac{2x^2}{y^2}+\frac{2x}{y}\right)\log(x)\log(z)\\
&-\frac{1}{2}\left(1+\frac{2y}{x}+\frac{2y^2}{x^2}\right)\log(y)\log(z)\\
&+\frac{1}{2}\left(2+\frac{2x(1-z)}{y^2}+\frac{1-2(1-x)x}{z^2}-\frac{2(1-x)}{z}\right)\\
&\qquad\times\left(\log(1-x)\log(x)+\mathrm{Li}_2(x)\right)\\
&+\frac{1}{2}\left(2+\frac{2y}{x}+\frac{2y^2}{x^2}+\frac{1-2(1-x)x}{z^2}-\frac{2(1-x)}{z}\right)\\
&\qquad\times\left(\log(1-y)\log(y)+\mathrm{Li}_2(y)\right)\\
&+\left(1+\frac{x^4+x^3y+xy^3+y^4}{x^2y^2}\right)\left(\log(1-z)\log(z)+\mathrm{Li}_2(z)\right)\,, \qquad \text{(A.11)}
\end{aligned}
$$

$$
\begin{aligned}
B_{\beta_3}(x,y,z) = &-3-\frac{1}{12}\left(3-\frac{1}{x}-\frac{2(1-x)x}{y^2}+\frac{-1+2x}{y}-\frac{2(1-x)y}{x^2}\right.\\
&\qquad\left.+\frac{2y^2}{x^2}-\frac{2(1-x)x}{z^2}-\frac{1-2x}{z}\right)\pi^2\\
&-\left(\frac{x}{1-x}-\frac{x}{y}-\frac{x}{z}\right)\log(x)+\left(\frac{y}{x}+\frac{xy}{(1-y)z}\right)\log(y)\\
&+\left(\frac{1-x}{y}-\frac{1}{1-z}+\frac{z}{x}\right)\log(z)\\
&+\frac{1}{2}\left(\frac{(1-x)x}{z^2}+\frac{(1-y)y}{z^2}\right)\log(x)\log(y)\\
&-\frac{1}{2}\left(1-\frac{2(1-z)z}{y^2}+\frac{-1+2z}{y}\right)\log(x)\log(z)\\
&-\frac{1}{2}\left(1-\frac{2(1-y)y}{x^2}+\frac{-1+2y}{x}\right)\log(y)\log(z)\\
&+\frac{1}{2}\left(2-\frac{1}{y^2z^2}\left((1-x)\left(2(1-x)^2x+y+x(-7+6x)y+(-1+6x)y^2\right)\right)\right)\\
&\qquad\times\left(\log(1-x)\log(x)+\mathrm{Li}_2(x)\right)\\
&+\frac{1}{2}\left(2-\frac{1}{x^2z^2}\left((1-y)\left(2(1-y)^2y+z+y(-7+6y)z+(-1+6y)z^2\right)\right)\right)\\
&\qquad\times\left(\log(1-y)\log(y)+\mathrm{Li}_2(y)\right)
\end{aligned}
$$

$$+\frac{1}{2}\left(\frac{2x^2}{y^2}-\frac{2x(1-y)}{y^2}-\frac{2(1-y)y}{x^2}+\frac{-1+2y}{x}+\frac{-1+2y}{y}\right) \times\left(\log(1-z)\log(z)+\mathrm{Li}_2(z)\right), \tag{A.12}$$

$$C_{\beta_1}(x,y,z)=\frac{1}{3}\left(1-\frac{1}{y}\right)\left(3i\pi-\log(x)-\log(y)-\log(z)\right), \tag{A.13}$$

$$C_{\beta_2}(x,y,z)=\frac{1}{3}\left(1-\frac{1}{z}\right)\left(3i\pi-\log(x)-\log(y)-\log(z)\right), \tag{A.14}$$

$$C_{\beta_3}(x,y,z)=\frac{2}{3}\left(3i\pi-\log(x)-\log(y)-\log(z)\right). \tag{A.15}$$

A.2.2 $V \to gg\gamma$ at two loops

The coefficients for the $(g_1^+, g_2^+, \gamma_3^+)$ helicity configuration are as follows:

$$\begin{aligned}
A_{\theta_1}(x,y,z) =& -\frac{2}{81}\left(81-\frac{81}{1-x}+\frac{8(1-y)}{z^2}\left(-x-\frac{z^3}{x^2}+\frac{z^3}{y^2}-\frac{(1-z)z^3}{y^3}\right)\right)\\
&-\frac{22}{3}\left(1-\frac{1}{y}\right)i\pi+\frac{1}{6}\left(-\frac{2(1-y)}{xy}-\frac{2(1-y)}{yz}+\frac{(-9+5y)z}{y^3}+\frac{9z^2}{y^3}\right)\pi^2\\
&+\frac{1}{3}\left(22+\frac{6}{(1-x)^2}-\frac{6}{1-x}-\frac{27x+22y}{y^2}\right)\log(x)\\
&-9\frac{1}{y}\log(y)-9\frac{z}{y^2}\log(z)-2\left(\frac{z}{xy}\right)\log(y)\log(z)\\
&-2\left(\frac{2}{y}+\frac{x}{yz}\right)\log(x)\log(y)-\left(\frac{9xz}{y^3}+\frac{4z}{y^2}\right)\log(x)\log(z)\\
&-\left(\frac{2}{z}+\frac{5z}{y^2}-\frac{9(1-z)z}{y^3}-\frac{2(1+z)}{yz}\right)\left(\log(1-x)\log(x)+\mathrm{Li}_2(x)\right)\\
&+2\left(\frac{(1-y)^2}{xyz}\right)\left(\log(1-y)\log(y)+\mathrm{Li}_2(y)\right)\\
&-\left(-\frac{9xz}{y^3}-\frac{4z}{y^2}-\frac{2z}{xy}\right)\left(\log(1-z)\log(z)+\mathrm{Li}_2(z)\right),
\end{aligned} \tag{A.16}$$

$$\begin{aligned}
A_{\theta_2}(x,y,z) =& -\frac{2}{81}\left(-\frac{8y}{x}-\frac{8y^2}{x^2}+x^2\left(-\frac{8}{y^2}-\frac{8y}{z^3}\right)+\frac{8x\left(-1-\frac{y^3}{z^3}\right)}{y}-\frac{81y}{(1-x)z}\right)\\
&-\frac{1}{6}\left(4+\frac{9x^2}{y^2}+\frac{12x}{y}+\frac{8y}{x}+\frac{8y^2}{x^2}-\frac{-1+(8-9x)x}{z^2}+\frac{2(-1+6x)}{z}\right)\pi^2\\
&-\frac{1}{3}\left(\frac{46x}{z}+\frac{27x^2}{yz}+\frac{2(20+23(-2+x)x)y}{(1-x)^2z}\right)\log(x)-\frac{22}{3}\left(1-\frac{1}{z}\right)i\pi\\
&+\left(-\frac{9x}{z}-\frac{8y}{z}-\frac{8y^2}{xz}\right)\log(y)-\left(8+\frac{9x}{y}+\frac{8y}{x}\right)\log(z)\\
&+\left(\frac{2(-2+x)x}{z^2}+\frac{10xy}{z^2}-\frac{y^2}{z^2}\right)\log(x)\log(y)
\end{aligned}$$

$$
\begin{aligned}
&- \left(1 - \frac{3x(-4+x+4z)}{y^2}\right) \log(x)\log(z) \\
&- 2\left(\frac{(x+2y)^2}{x^2}\right) \log(y)\log(z) \\
&+ \left(2 - \frac{-1+(8-9x)x}{z^2} - \frac{2-12x}{z} - \frac{3x(-4+x+4z)}{y^2}\right) \\
&\qquad \times (\log(1-x)\log(x) + \mathrm{Li}_2(x)) \\
&+ \left(\frac{8y(1-z)}{x^2} + \frac{2+y(-10+9y)}{z^2} + \frac{6y}{z}\right) (\log(1-y)\log(y) + \mathrm{Li}_2(y)) \\
&+ \left(\frac{9x}{y^2} + \frac{3}{y} + \frac{8y}{x^2} - \frac{9xz}{y^2} - \frac{3z}{y} - \frac{8yz}{x^2}\right) (\log(1-z)\log(z) + \mathrm{Li}_2(z)) \,,
\end{aligned} \tag{A.17}
$$

$$
\begin{aligned}
A_{\theta_3}(x,y,z) = &- \frac{2}{81}\left(81 + \frac{16\left(-y^4 - yz^3 + (1-z)z^3 + y^3\left(1 - z + \frac{z^3}{x^2}\right)\right)}{y^2 z^2}\right) - \frac{44}{3} i\pi \\
&+ \frac{1}{6}\left(2 + \frac{2}{y} + \frac{8(1-y)y}{x^2} - \frac{-2+8y}{x} + \frac{9(1-y)y}{z^2} + \frac{2-6y}{z}\right. \\
&\qquad \left. + \frac{(9-6y)z}{y^2} - \frac{9z^2}{y^2}\right)\pi^2 + \frac{1}{3}\left(68 - \frac{6}{1-x} + \frac{27(1-x)x}{yz}\right)\log(x) \\
&+ \left(9 + \frac{8y}{x} + \frac{9y}{z}\right)\log(y) + \left(\frac{9(1-x)}{y} + \frac{8z}{x}\right)\log(z) \\
&+ \left(-\frac{9x^2}{z^2} + \frac{x(9-12z)}{z^2} - \frac{-5+z}{z}\right)\log(x)\log(y) \\
&+ \left(-\frac{9x^2}{y^2} + \frac{x(9-12y)}{y^2} - \frac{-5+y}{y}\right)\log(x)\log(z) \\
&- 2\left(1 - \frac{4(1-y)y}{x^2} + \frac{-1+4y}{x}\right)\log(y)\log(z) \\
&+ \left(2 + \frac{(1-x)\left(-9(1-x)^2 x + 5(1-x)(-1+6x)y + 5(1-6x)y^2\right)}{y^2 z^2}\right) \\
&\qquad \times (\log(1-x)\log(x) + \mathrm{Li}_2(x)) \\
&- \left(\frac{2-3x}{x} + \frac{9(1-x)x}{z^2} + \frac{5-12x}{z} + \frac{8(1-x)z}{x^2} - \frac{8z^2}{x^2}\right) \\
&\qquad \times (\log(1-y)\log(y) + \mathrm{Li}_2(y)) \\
&- \left(\frac{2-3x}{x} + \frac{9(1-x)x}{y^2} + \frac{5-12x}{y} + \frac{8(1-x)y}{x^2} - \frac{8y^2}{x^2}\right) \\
&\qquad \times (\log(1-z)\log(z) + \mathrm{Li}_2(z)) \,,
\end{aligned} \tag{A.18}
$$

$$
B_{\theta_i}(x,y,z) = 2B_{\beta_i}(x,y,z) \quad \text{for } i = 1,2,3\,, \tag{A.19}
$$

$$
C_{\theta_1}(x,y,z) = \frac{4}{3}\left(1 - \frac{1}{y}\right)(i\pi - \log(x)) \,, \tag{A.20}
$$

$$C_{\theta_2}(x,y,z) = \frac{4}{3}\left(1-\frac{1}{z}\right)(i\pi - \log(x)) \ , \tag{A.21}$$

$$C_{\theta_3}(x,y,z) = \frac{8}{3}(i\pi - \log(x)) \ . \tag{A.22}$$

B

Two-loop Planar Four Point Functions with Two Equal-mass Legs

B.1 Master Integrals: Topo A

In this appendix we give the analytic expressions for the relevant genuine two-loop boxes that appear in the reduction of **Topo A**, classified with respect to the number of denominators. We write explicitly the results up to weight three, while the full result up to weight four can be found attached to the arXiv submission of [62] readable using Mathematica or FORM. All triangle topologies were derived previously in the literature [59, 60, 289, 290]; they are also included in the the arXiv submission of [62], where they are expressed in the same functional basis as the box integrals derived here.

The common normalisation factor of all master integrals is

$$S_\epsilon = \left[(4\pi)^\epsilon \frac{\Gamma(1+\epsilon)\,\Gamma^2(1-\epsilon)}{\Gamma(1-2\epsilon)} \right] . \tag{B.1}$$

5-denominator integrals

$$\mathcal{I}^{(A)}_{174} = \left(\frac{S_\epsilon}{16\pi^2} \right)^2 \frac{(m^2)^{-2\epsilon-1}}{(1-z)} \sum_{n=-2}^{0} \epsilon^n \, f^{(174)}_n(x,z) + \mathcal{O}(\epsilon) \,, \tag{B.2}$$

with

$$\begin{aligned}
f^{(174)}_{-2}(x,z) &= G(0,z) \,, \\
f^{(174)}_{-1}(x,z) &= -\frac{\pi^2}{6} - 2G(-1,x)G(0,z) + G(0,x)G(0,z) + 2G(0,z) - 2G(0,0,z) + G(1,0,z) \,, \\
f^{(174)}_{0}(x,z) &= \zeta_3 - \frac{\pi^2}{3} - 1/6G(-1/x,z)\pi^2 - G(-1/x,0,0,z) + 2G(-1/x,1,0,z) - 1/2G(-x,z)\pi^2 \\
&\quad - G(-x,0,0,z) + 2G(-x,1,0,z) + G(-1,x)\pi^2 - 2G(-1,x)G(-1/x,0,z) \\
&\quad - 2G(-1,x)G(-x,0,z) - 4G(-1,x)G(0,z) + 6G(-1,x)G(0,0,z) \\
&\quad - 2G(-1,x)G(1,0,z) + 8G(-1,-1,x)G(0,z) - 4G(-1,0,x)G(0,z) - 2/3G(0,x)\pi^2
\end{aligned}$$

$$
\begin{aligned}
&+ G(0,x)G(-1/x,0,z) + G(0,x)G(-x,0,z) + 2G(0,x)G(0,z) + G(0,x)G(1,0,z)\\
&+ 4G(0,z) + 2/3G(0,z)\pi^2 - 2G(0,-1,x)G(-1/x,z) + 2G(0,-1,x)G(-x,z)\\
&- 4G(0,-1,x)G(0,z) + G(0,0,x)G(-1/x,z) - G(0,0,x)G(-x,z) + 2G(0,0,x)G(0,z)\\
&- 4G(0,0,z) - 3G(0,0,z)G(0,x) + 2G(0,0,-1,x) - G(0,0,0,x) + 5G(0,0,0,z)\\
&- 4G(0,1,0,z) - 1/6G(1,z)\pi^2 + 2G(1,0,z) - 2G(1,0,0,z) + G(1,1,0,z)\,.
\end{aligned}
$$

$$
\mathcal{I}^{(A)}_{214} = \left(\frac{S_\epsilon}{16\pi^2}\right)^2 \frac{x\,(m^2)^{-2\epsilon-1}}{(1+x)^2} \sum_{n=-3}^{0} \epsilon^n\, f^{(214)}_n(x,z) + \mathcal{O}(\epsilon)\,, \tag{B.3}
$$

with

$$
\begin{aligned}
f^{(214)}_{-3}(x,z) &= 1\,,\\
f^{(214)}_{-2}(x,z) &= 2 - 2G(-1,x) + G(0,x) - G(0,z)\,,\\
f^{(214)}_{-1}(x,z) &= 4 + \frac{\pi^2}{3} - 4G(-1,x) + 2G(-1,x)G(0,z) + 4G(-1,-1,x) - 2G(-1,0,x) + 2G(0,x)\\
&\quad - G(0,x)G(0,z) - 2G(0,z) - 2G(0,-1,x) + G(0,0,x) + 3G(0,0,z) - 2G(1,0,z)\,,\\
f^{(214)}_{0}(x,z) &= 8 - 6\zeta_3 + \frac{2}{3}\pi^2 + 1/6G(-1/x,z)\pi^2 + G(-1/x,0,0,z) - 2G(-1/x,1,0,z)\\
&\quad + 1/2G(-x,z)\pi^2 + G(-x,0,0,z) - 2G(-x,1,0,z) - 8G(-1,x) - 2/3G(-1,x)\pi^2\\
&\quad + 2G(-1,x)G(-1/x,0,z) + 2G(-1,x)G(-x,0,z) + 4G(-1,x)G(0,z)\\
&\quad - 6G(-1,x)G(0,0,z) + 8G(-1,-1,x) - 4G(-1,-1,x)G(0,z) - 8G(-1,-1,-1,x)\\
&\quad + 4G(-1,-1,0,x) - 4G(-1,0,x) + 2G(-1,0,x)G(0,z) + 4G(-1,0,-1,x)\\
&\quad - 2G(-1,0,0,x) + 4G(0,x) + 2/3G(0,x)\pi^2 - G(0,x)G(-1/x,0,z) - G(0,x)G(-x,0,z)\\
&\quad - 2G(0,x)G(0,z) - 4G(0,z) - G(0,z)\pi^2 - 4G(0,-1,x) + 2G(0,-1,x)G(-1/x,z)\\
&\quad - 2G(0,-1,x)G(-x,z) + 2G(0,-1,x)G(0,z) + 4G(0,-1,-1,x) - 2G(0,-1,0,x)\\
&\quad + 2G(0,0,x) - G(0,0,x)G(-1/x,z) + G(0,0,x)G(-x,z) - G(0,0,x)G(0,z)\\
&\quad + 6G(0,0,z) + 3G(0,0,z)G(0,x) - 6G(0,0,-1,x) + 3G(0,0,0,x) - 9G(0,0,0,z)\\
&\quad + 6G(0,1,0,z) - 4G(1,0,z) + 4G(1,0,0,z)\,.
\end{aligned}
$$

Sector 181 has 2 MIs, which read:

$$
\mathcal{I}^{(A)}_{181,1} = \left(\frac{S_\epsilon}{16\pi^2}\right)^2 \frac{x\,(m^2)^{-2\epsilon-1}}{(1-x^2)} \sum_{n=-1}^{0} \epsilon^n\, f^{(181,1)}_n(x,z) + \mathcal{O}(\epsilon)\,, \tag{B.4}
$$

with

$$
\begin{aligned}
f^{(181,1)}_{-1}(x,z) &= \frac{\pi^2}{3} - 4G(0,-1,x) + 2G(0,0,x)\,,\\
f^{(181,1)}_{0}(x,z) &= 4\zeta_3 + \frac{2}{3}\pi^2 + 1/6G(-1/x,z)\pi^2 + G(-1/x,0,0,z) - 2G(-1/x,1,0,z)\\
&\quad - 1/2G(-x,z)\pi^2 - G(-x,0,0,z) + 2G(-x,1,0,z) + 2G(-1,x)G(-1/x,0,z)\\
&\quad - 2G(-1,x)G(-x,0,z) - 2/3G(0,x)\pi^2 - G(0,x)G(-1/x,0,z) + G(0,x)G(-x,0,z)\\
&\quad - 8G(0,-1,x) + 2G(0,-1,x)G(-1/x,z) + 2G(0,-1,x)G(-x,z) + 16G(0,-1,-1,x)\\
&\quad - 8G(0,-1,0,x) + 4G(0,0,x) - G(0,0,x)G(-1/x,z) - G(0,0,x)G(-x,z)\\
&\quad + 4/3G(1,x)\pi^2 - 16G(1,0,-1,x) + 8G(1,0,0,x)\,.
\end{aligned}
$$

and

$$\mathcal{I}^{(A)}_{181,2} = \left(\frac{S_\epsilon}{16\pi^2}\right)^2 \frac{x\,(m^2)^{-2\epsilon-2}}{z(1+x)^2} \sum_{n=-3}^{0} \epsilon^n\, f_n^{(181,2)}(x,z) + \mathcal{O}(\epsilon)\,, \tag{B.5}$$

with

$$\begin{aligned}
f_{-3}^{(181,2)}(x,z) &= \frac{1}{4}\,,\\
f_{-2}^{(181,2)}(x,z) &= 1/2G(0,x) - G(-1,x) - G(0,z)\,,\\
f_{-1}^{(181,2)}(x,z) &= \frac{7}{12}\pi^2 + 4G(-1,x)G(0,z) + 4G(-1,-1,x) - 2G(-1,0,x) - 2G(0,x)G(0,z)\\
&\quad - 2G(0,-1,x) + G(0,0,x) + 4G(0,0,z) - 3G(1,0,z)\,,\\
f_{0}^{(181,2)}(x,z) &= -4\zeta_3 + 1/2G(-1/x,z)\pi^2 + 3G(-1/x,0,0,z) - 6G(-1/x,1,0,z) + 3/2G(-x,z)\pi^2\\
&\quad + 3G(-x,0,0,z) - 6G(-x,1,0,z) - 7/3G(-1,x)\pi^2 + 6G(-1,x)G(-1/x,0,z)\\
&\quad + 6G(-1,x)G(-x,0,z) - 16G(-1,x)G(0,0,z) - 16G(-1,-1,x)G(0,z)\\
&\quad - 16G(-1,-1,-1,x) + 8G(-1,-1,0,x) + 8G(-1,0,x)G(0,z) + 8G(-1,0,-1,x)\\
&\quad - 4G(-1,0,0,x) + 7/6G(0,x)\pi^2 - 3G(0,x)G(-1/x,0,z) - 3G(0,x)G(-x,0,z)\\
&\quad - 7/3G(0,z)\pi^2 - 1/2G(1,z)\pi^2 + 6G(0,-1,x)G(-1/x,z) - 6G(0,-1,x)G(-x,z)\\
&\quad + 8G(0,-1,x)G(0,z) + 8G(0,-1,-1,x) - 4G(0,-1,0,x) - 3G(0,0,x)G(-1/x,z)\\
&\quad + 3G(0,0,x)G(-x,z) - 4G(0,0,x)G(0,z) + 8G(0,0,z)G(0,x) - 4G(0,0,-1,x)\\
&\quad + 2G(0,0,0,x) - 16G(0,0,0,z) + 12G(0,1,0,z) + 6G(1,0,0,z) + 3G(1,1,0,z)\,.
\end{aligned}$$

Sector 182 has 2 MIs, which read:

$$\mathcal{I}^{(A)}_{182,1} = \left(\frac{S_\epsilon}{16\pi^2}\right)^2 \frac{x\,(m^2)^{-2\epsilon-1}}{(1+x+x^2+x\,z)} \sum_{n=-1}^{0} \epsilon^n\, f_n^{(181,1)}(x,z) + \mathcal{O}(\epsilon)\,, \tag{B.6}$$

with

$$\begin{aligned}
f_{0}^{(182,1)}(x,z) &= -2\zeta_3 + 1/6G(-1/x,z)\pi^2 + G(-1/x,0,0,z) - 2G(-1/x,1,0,z) + 1/2G(-x,z)\pi^2\\
&\quad + G(-x,0,0,z) - 2G(-x,1,0,z) - 1/3G(-1,x)\pi^2 + 2G(-1,x)G(-1/x,0,z)\\
&\quad + 2G(-1,x)G(-x,0,z) - 2G(-1,x)G(1,0,z) + 2/3G(0,x)\pi^2 - G(0,x)G(-1/x,0,z)\\
&\quad - G(0,x)G(-x,0,z) + G(0,x)G(1,0,z) + 2G(0,-1,x)G(-1/x,z)\\
&\quad - 2G(0,-1,x)G(-x,z) - G(0,0,x)G(-1/x,z) + G(0,0,x)G(-x,z) - 6G(0,0,-1,x)\\
&\quad + 3G(0,0,0,x) - 1/6G(1,z)\pi^2 - G(1,0,0,z) + G(1,1,0,z)\,.
\end{aligned}$$

and

$$\mathcal{I}^{(A)}_{182,2} = \left(\frac{S_\epsilon}{16\pi^2}\right)^2 \frac{(m^2)^{-2\epsilon-2}}{(1-z)} \sum_{n=-2}^{0} \epsilon^n\, f_n^{(181,2)}(x,z) + \mathcal{O}(\epsilon)\,, \tag{B.7}$$

with

$$\begin{aligned}
f_{-2}^{(182,2)}(x,z) &= G(0,z)\,,\\
f_{-1}^{(182,2)}(x,z) &= \frac{\pi^2}{6} + 2G(-1,x)G(0,z) - G(0,x)G(0,z) - G(0,0,z) - G(1,0,z)\,,\\
f_{0}^{(182,2)}(x,z) &= -2\zeta_3 + 1/2G(-1/x,z)\pi^2 + 3G(-1/x,0,0,z) - 6G(-1/x,1,0,z) + 3/2G(-x,z)\pi^2\\
&\quad + 3G(-x,0,0,z) - 6G(-x,1,0,z) - 5/3G(-1,x)\pi^2 + 6G(-1,x)G(-1/x,0,z)\\
&\quad + 6G(-1,x)G(-x,0,z) - 8G(-1,x)G(0,0,z) - 2G(-1,x)G(1,0,z)
\end{aligned}$$

$$
\begin{aligned}
&- 8G(-1,-1,x)G(0,z) + 4G(-1,0,x)G(0,z) + 4/3G(0,x)\pi^2 - 3G(0,x)G(-1/x,0,z)\\
&- 3G(0,x)G(-x,0,z) + G(0,x)G(1,0,z) - 7/6G(0,z)\pi^2 + 6G(0,-1,x)G(-1/x,z)\\
&- 6G(0,-1,x)G(-x,z) + 4G(0,-1,x)G(0,z) - 3G(0,0,x)G(-1/x,z)\\
&+ 3G(0,0,x)G(-x,z) - 2G(0,0,x)G(0,z) + 4G(0,0,z)G(0,x) - 6G(0,0,-1,x)\\
&+ 3G(0,0,0,x) - 2G(0,0,0,z) + 7G(0,1,0,z) - 1/6G(1,z)\pi^2 + G(1,0,0,z)\\
&+ G(1,1,0,z)\,.
\end{aligned}
$$

6-denominator integrals

Two topologies with 6 denominators have one single MI:

$$
\mathcal{I}^{(A)}_{215} = \left(\frac{S_\epsilon}{16\pi^2}\right)^2 \frac{x\,(m^2)^{-2\epsilon-2}}{(1+x)^2(1-z)} \sum_{n=-3}^{-1} \epsilon^n\, f^{(215)}_n(x,z) + \mathcal{O}(\epsilon^0)\,, \tag{B.8}
$$

with

$$
\begin{aligned}
f^{(215)}_{-3}(x,z) &= -\frac{1}{2}G(0,z)\,,\\
f^{(215)}_{-2}(x,z) &= -\frac{\pi^2}{6} + G(0,0,z) + G(1,0,z)\\
f^{(215)}_{-1}(x,z) &= -2\zeta_3 - 1/6G(-1/x,z)\pi^2 - G(-1/x,0,0,z) + 2G(-1/x,1,0,z) - 1/2G(-x,z)\pi^2\\
&\quad - G(-x,0,0,z) + 2G(-x,1,0,z) + 2/3G(-1,x)\pi^2 - 2G(-1,x)G(-1/x,0,z)\\
&\quad - 2G(-1,x)G(-x,0,z) + 2G(-1,x)G(0,0,z) + 4G(-1,-1,x)G(0,z)\\
&\quad - 2G(-1,0,x)G(0,z) - 1/2G(0,x)\pi^2 + G(0,x)G(-1/x,0,z) + G(0,x)G(-x,0,z)\\
&\quad - 2G(0,-1,x)G(-1/x,z) + 2G(0,-1,x)G(-x,z) - 2G(0,-1,x)G(0,z)\\
&\quad + G(0,0,x)G(-1/x,z) - G(0,0,x)G(-x,z) + G(0,0,x)G(0,z) - G(0,0,z)G(0,x)\\
&\quad + 2G(0,0,-1,x) - G(0,0,0,x) - G(0,0,0,z) - G(0,1,0,z) + 1/3G(1,z)\pi^2\\
&\quad - 2G(1,0,0,z) - 2G(1,1,0,z) + 1/6G(0,z)\pi^2\,.
\end{aligned}
$$

$$
\mathcal{I}^{(A)}_{430} = \left(\frac{S_\epsilon}{16\pi^2}\right)^2 \frac{x\,(m^2)^{-2\epsilon-2}}{(x+z(1+x+x^2))} \sum_{n=-1}^{-1} \epsilon^n\, f^{(430)}_n(x,z) + \mathcal{O}(\epsilon^0)\,, \tag{B.9}
$$

with

$$
\begin{aligned}
f^{(430)}_{-1}(x,z) &= \zeta_3 + 1/6G(-1/x,z)\pi^2 + G(-1/x,0,0,z) - 2G(-1/x,1,0,z) + 1/2G(-x,z)\pi^2\\
&\quad + G(-x,0,0,z) - 2G(-x,1,0,z) - 1/3G(-1,x)\pi^2 + 2G(-1,x)G(-1/x,0,z)\\
&\quad + 2G(-1,x)G(-x,0,z) - 2G(-1,x)G(0,0,z) - 2G(-1,x)G(1,0,z)\\
&\quad - G(0,x)G(-1/x,0,z) - G(0,x)G(-x,0,z) + G(0,x)G(1,0,z) - 1/2G(0,z)\pi^2\\
&\quad + 2G(0,-1,x)G(-1/x,z) - 2G(0,-1,x)G(-x,z) - G(0,0,x)G(-1/x,z)\\
&\quad + G(0,0,x)G(-x,z) + G(0,0,z)G(0,x) + 2G(0,0,-1,x) - G(0,0,0,x)\\
&\quad - 2G(0,0,0,z) + 3G(0,1,0,z) - 1/6G(1,z)\pi^2 + G(1,1,0,z)\,.
\end{aligned}
$$

7-denominator integrals

Finally, there are two independent topologies with 7 denominators. One has 3 MIs:

$$
\mathcal{I}^{(A)}_{247,1} = \left(\frac{S_\epsilon}{16\pi^2}\right)^2 \frac{x^2\,(m^2)^{-2\epsilon-3}}{z(1+x)^4} \sum_{n=-4}^{-1} \epsilon^n\, f^{(247,1)}_n(x,z) + \mathcal{O}(\epsilon^0)\,, \tag{B.10}
$$

with

$$
\begin{aligned}
f_{-4}^{(247,1)}(x,z) &= \frac{1}{4}\,,\\
f_{-3}^{(247,1)}(x,z) &= 1/2G(0,x) - G(-1,x) - G(0,z)\,,\\
f_{-2}^{(247,1)}(x,z) &= 7/12\pi^2 + 4G(-1,x)G(0,z) + 4G(-1,-1,x) - 2G(-1,0,x) - 2G(0,x)G(0,z)\\
&\quad - 2G(0,-1,x) + G(0,0,x) + 4G(0,0,z) - 2G(1,0,z)\,,\\
f_{-1}^{(247,1)}(x,z) &= -2\zeta_3 + 1/3G(-1/x,z)\pi^2 + 2G(-1/x,0,0,z) - 4G(-1/x,1,0,z) + G(-x,z)\pi^2\\
&\quad + 2G(-x,0,0,z) - 4G(-x,1,0,z) - 7/3G(-1,x)\pi^2 + 4G(-1,x)G(-1/x,0,z)\\
&\quad + 4G(-1,x)G(-x,0,z) - 16G(-1,x)G(0,0,z) - 16G(-1,-1,x)G(0,z)\\
&\quad - 16G(-1,-1,-1,x) + 8G(-1,-1,0,x) + 8G(-1,0,x)G(0,z) + 8G(-1,0,-1,x)\\
&\quad - 4G(-1,0,0,x) + 7/6G(0,x)\pi^2 - 2G(0,x)G(-1/x,0,z) - 2G(0,x)G(-x,0,z)\\
&\quad - 7/3G(0,z)\pi^2 + 4G(0,-1,x)G(-1/x,z) - 4G(0,-1,x)G(-x,z)\\
&\quad + 8G(0,-1,x)G(0,z) + 8G(0,-1,-1,x) - 4G(0,-1,0,x) - 2G(0,0,x)G(-1/x,z)\\
&\quad + 2G(0,0,x)G(-x,z) - 4G(0,0,x)G(0,z) + 8G(0,0,z)G(0,x) - 4G(0,0,-1,x)\\
&\quad + 2G(0,0,0,x) - 16G(0,0,0,z) + 10G(0,1,0,z) - 2/3G(1,z)\pi^2 + 4G(1,0,0,z)\\
&\quad + 4G(1,1,0,z)\,.
\end{aligned}
$$

$$
\mathcal{I}_{247,2}^{(A)} = \left(\frac{S_\epsilon}{16\pi^2}\right)^2 \frac{x^2\,(m^2)^{-2\epsilon-2}}{(1-x)(1+x)^3} \sum_{n=-2}^{-1} \epsilon^n\, f_n^{(247,2)}(x,z) + \mathcal{O}(\epsilon^0)\,, \tag{B.11}
$$

with

$$
\begin{aligned}
f_{-2}^{(247,2)}(x,z) &= -\frac{\pi^2}{3} + 4G(0,-1,x) - 2G(0,0,x)\,,\\
f_{-1}^{(247,2)}(x,z) &= -6\zeta_3 - 1/3G(-1/x,z)\pi^2 - 2G(-1/x,0,0,z) + 4G(-1/x,1,0,z) + G(-x,z)\pi^2\\
&\quad + 2G(-x,0,0,z) - 4G(-x,1,0,z) - 4G(-1,x)G(-1/x,0,z) + 4G(-1,x)G(-x,0,z)\\
&\quad + G(0,x)\pi^2 + 2G(0,x)G(-1/x,0,z) - 2G(0,x)G(-x,0,z) - 4G(0,-1,x)G(-1/x,z)\\
&\quad - 4G(0,-1,x)G(-x,z) - 24G(0,-1,-1,x) + 12G(0,-1,0,x) - 2G(1,x)\pi^2\\
&\quad + 2G(0,0,x)G(-1/x,z) + 2G(0,0,x)G(-x,z) + 24G(1,0,-1,x) - 12G(1,0,0,x)\,.
\end{aligned}
$$

$$
\mathcal{I}_{247,3}^{(A)} = \left(\frac{S_\epsilon}{16\pi^2}\right)^2 \frac{x^2\,(m^2)^{-2\epsilon-2}}{(1+x)^4} \left[\sum_{n=-4}^{-1} \epsilon^n\, f_n^{(247,3)}(x,z) + \frac{1}{z}\sum_{n=-2}^{-1} \epsilon^n\, g_n^{(247,3)}(x,z)\right] + \mathcal{O}(\epsilon^0)\,,
$$

with

$$
\begin{aligned}
f_{-4}^{(247,3)}(x,z) &= -\frac{1}{4}\,,\\
f_{-3}^{(247,3)}(x,z) &= -1/2G(0,x) + G(-1,x) + G(0,z)\,,\\
f_{-2}^{(247,3)}(x,z) &= -7/12\pi^2 - 4G(-1,x)G(0,z) - 4G(-1,-1,x) + 2G(-1,0,x) + 2G(0,x)G(0,z)\\
&\quad + 2G(0,-1,x) - G(0,0,x) - 4G(0,0,z) + 3G(1,0,z)\,,\\
f_{-1}^{(247,3)}(x,z) &= 2\zeta_3 - 1/3G(-1/x,z)\pi^2 - 2G(-1/x,0,0,z) + 4G(-1/x,1,0,z) - G(-x,z)\pi^2\\
&\quad - 2G(-x,0,0,z) + 4G(-x,1,0,z) + 7/3G(-1,x)\pi^2 - 4G(-1,x)G(-1/x,0,z)\\
&\quad - 4G(-1,x)G(-x,0,z) + 16G(-1,x)G(0,0,z) - 4G(-1,x)G(1,0,z)
\end{aligned}
$$

$$
\begin{aligned}
&+ 16G(-1,-1,x)G(0,z) + 16G(-1,-1,-1,x) - 8G(-1,-1,0,x)\\
&- 8G(-1,0,x)G(0,z) - 8G(-1,0,-1,x) + 4G(-1,0,0,x) - 7/6G(0,x)\pi^2\\
&+ 2G(0,x)G(-1/x,0,z) + 2G(0,x)G(-x,0,z) + 2G(0,x)G(1,0,z) + 7/3G(0,z)\pi^2\\
&- 4G(0,-1,x)G(-1/x,z) + 4G(0,-1,x)G(-x,z) - 8G(0,-1,x)G(0,z)\\
&- 8G(0,-1,-1,x) + 4G(0,-1,0,x) + 2G(0,0,x)G(-1/x,z) - 2G(0,0,x)G(-x,z)\\
&+ 4G(0,0,x)G(0,z) - 8G(0,0,z)G(0,x) + 4G(0,0,-1,x) - 2G(0,0,0,x)\\
&+ 16G(0,0,0,z) - 14G(0,1,0,z) - 1/6G(1,z)\pi^2 - 8G(1,0,0,z) + G(1,1,0,z)\,.
\end{aligned}
$$

and

$$
\begin{aligned}
g^{(247,3)}_{-2}(x,z) &= -G(1,0,z)\,,\\
g^{(247,3)}_{-1}(x,z) &= 4G(-1,x)G(1,0,z) - 2G(0,x)G(1,0,z) + 4G(0,1,0,z) + 5/6G(1,z)\pi^2\\
&\quad + 4G(1,0,0,z) - 5G(1,1,0,z)\,.
\end{aligned}
$$

The other has 2 MIs:

$$
\mathcal{I}^{(A)}_{446,1} = \left(\frac{S_\epsilon}{16\pi^2}\right)^2 \frac{x\,(m^2)^{-2\epsilon-3}}{z^2(1+x)^2} \sum_{n=-4}^{-1} \epsilon^n\, f^{(446,1)}_n(x,z) + \mathcal{O}(\epsilon^0)\,, \tag{B.12}
$$

with

$$
\begin{aligned}
f^{(446,1)}_{-4}(x,z) &= \frac{1}{4}\,,\\
f^{(446,1)}_{-3}(x,z) &= 1/2G(0,x) - G(-1,x) - G(0,z)\,,\\
f^{(446,1)}_{-2}(x,z) &= \frac{\pi^2}{3} + 4G(-1,x)G(0,z) + 4G(-1,-1,x) - 2G(-1,0,x) - 2G(0,x)G(0,z)\\
&\quad - 2G(0,-1,x) + G(0,0,x) + 4G(0,0,z) - 2G(1,0,z)\,,\\
f^{(446,1)}_{-1}(x,z) &= \frac{\zeta_3}{2} - 4/3G(-1,x)\pi^2 - 16G(-1,x)G(0,0,z) + 8G(-1,x)G(1,0,z)\\
&\quad - 16G(-1,-1,x)G(0,z) - 16G(-1,-1,-1,x) + 8G(-1,-1,0,x)\\
&\quad + 8G(-1,0,x)G(0,z) + 8G(-1,0,-1,x) - 4G(-1,0,0,x) + 2/3G(0,x)\pi^2\\
&\quad - 4G(0,x)G(1,0,z) - 4/3G(0,z)\pi^2 + 8G(0,-1,x)G(0,z) + 8G(0,-1,-1,x)\\
&\quad - 4G(0,-1,0,x) - 4G(0,0,x)G(0,z) + 8G(0,0,z)G(0,x) - 4G(0,0,-1,x)\\
&\quad + 2G(0,0,0,x) - 16G(0,0,0,z) + 8G(0,1,0,z) + 2/3G(1,z)\pi^2 + 14G(1,0,0,z)\\
&\quad - 4G(1,1,0,z)\,.
\end{aligned}
$$

$$
\mathcal{I}^{(A)}_{446,2} = \left(\frac{S_\epsilon}{16\pi^2}\right)^2 \frac{(m^2)^{-2\epsilon-2}}{(1-z)} \left[\frac{1}{z}\sum_{n=-3}^{0} \epsilon^n\, f^{(446,2)}_n(x,z)\right. \tag{B.13}
$$

$$
\left. - \frac{(1+x)^2}{(x+z(1+x+x^2))} \sum_{n=-1}^{-1} \epsilon^n\, f^{(430)}_n(x,z)\right] + \mathcal{O}(\epsilon^0)\,, \tag{B.14}
$$

with

$$
\begin{aligned}
f^{(446,2)}_{-3}(x,z) &= -1/2G(0,z)\,,\\
f^{(446,2)}_{-2}(x,z) &= \frac{\pi^2}{4} + 2G(-1,x)G(0,z) - G(0,x)G(0,z) + 7/2G(0,0,z) - 3/2G(1,0,z)\,,\\
f^{(446,2)}_{-1}(x,z) &= -\zeta_3 + 1/3G(-1/x,z)\pi^2 + 2G(-1/x,0,0,z) - 4G(-1/x,1,0,z) + G(-x,z)\pi^2
\end{aligned}
$$

$$
\begin{aligned}
&+ 2G(-x,0,0,z) - 4G(-x,1,0,z) - 4/3G(-1,x)\pi^2 + 4G(-1,x)G(-1/x,0,z) \\
&+ 4G(-1,x)G(-x,0,z) - 14G(-1,x)G(0,0,z) - 8G(-1,-1,x)G(0,z) \\
&+ 4G(-1,0,x)G(0,z) + 2/3G(0,x)\pi^2 - 2G(0,x)G(-1/x,0,z) - 2G(0,x)G(-x,0,z) \\
&- 23/12G(0,z)\pi^2 + 4G(0,-1,x)G(-1/x,z) - 4G(0,-1,x)G(-x,z) \\
&+ 4G(0,-1,x)G(0,z) - 2G(0,0,x)G(-1/x,z) + 2G(0,0,x)G(-x,z) \\
&- 2G(0,0,x)G(0,z) + 7G(0,0,z)G(0,x) - 37/2G(0,0,0,z) + 23/2G(0,1,0,z) \\
&- 1/12G(1,z)\pi^2 + 21/2G(1,0,0,z) + 1/2G(1,1,0,z)\,.
\end{aligned}
$$

B.2 Master Integrals: Topo B

In this appendix we provide the analytic expressions for the relevant two-loop boxes that appear in the reduction of **Topo B**, classified with respect to the number of denominators. We give the explicit results up to weight three for all MIs except $\mathcal{I}^{(B)}_{213,1}$, for which the expansion starts only at weight four. As already extensively discussed throughout the paper, the computation of this integral required a special treatment and we include here the full expression in order to show what the result looks like. The full results for all MIs up to weight four, including the already known triangle topologies, can be found attached to the arXiv submission of [62] in Mathematica and FORM format. As for the first topology the common normalisation factor of all master integrals is

$$
S_\epsilon = \left[(4\pi)^\epsilon \, \frac{\Gamma(1+\epsilon)\,\Gamma^2(1-\epsilon)}{\Gamma(1-2\epsilon)}\right]. \tag{B.15}
$$

5-denominator integrals

We start listing the two topologies with one single master integral:

$$
\mathcal{I}^{(B)}_{174} = \left(\frac{S_\epsilon}{16\pi^2}\right)^2 \frac{(m^2)^{-2\epsilon-1}}{(1-z)} \sum_{n=-2}^{0} \epsilon^n \, f^{(174)}_n(y,z) + \mathcal{O}(\epsilon)\,, \tag{B.16}
$$

with

$$
\begin{aligned}
f^{(174)}_{-2}(y,z) &= G(0,z)\,, \\
f^{(174)}_{-1}(y,z) &= -\frac{\pi^2}{6} - G(1/z,0,y) + 2G(0,z) - G(0,z)G(1/z,y) - G(0,0,z) \\
&\quad + G(1,0,z) + G(1,0,y)\,, \\
f^{(174)}_{0}(y,z) &= -\frac{11}{4}\zeta_3 - \frac{\pi^2}{3} - \frac{\pi^2}{2}\ln 2 - G(2-z,1/z,0,y) - 1/2G(2-z,y)\pi^2 + 2G(2-z,1,0,y) \\
&\quad + 2G(1/z,1/z,0,y) + 2/3G(1/z,y)\pi^2 - 2G(1/z,0,y) + 2G(1/z,0,0,y) \\
&\quad - 3G(1/z,1,0,y) + 4G(0,z) - 1/6G(0,z)\pi^2 - G(0,z)G(2-z,1/z,y) \\
&\quad + 2G(0,z)G(1/z,1/z,y) - 2G(0,z)G(1/z,y) - 2G(0,0,z) + G(0,0,z)G(1/z,y) \\
&\quad + G(0,0,0,z) + G(0,1,0,z) - 1/6G(1,z)\pi^2 + 2G(1,0,z) + 2G(1,0,z)G(2-z,y) \\
&\quad - 3G(1,0,z)G(1/z,y) + 2G(1,0,y) - G(1,0,0,z) - 2G(1,0,0,y) \\
&\quad + G(1,1,0,z) - 1/2G(2,z)\pi^2 + 2G(2,1,0,z)\,.
\end{aligned}
$$

$$
\mathcal{I}^{(B)}_{182} = \left(\frac{S_\epsilon}{16\pi^2}\right)^2 \frac{(m^2)^{-2\epsilon-1}}{(y+z-2)} \sum_{n=-2}^{-1} \epsilon^n \, f^{(182)}_n(y,z) + \mathcal{O}(\epsilon^0)\,, \tag{B.17}
$$

with

$$
\begin{aligned}
f_{-2}^{(182)}(y,z) &= -1/2\pi^2 - G(1/z,0,y) - G(0,z)G(1/z,y) + 2G(1,0,z) + 2G(1,0,y)\,,\\
f_{-1}^{(182)}(y,z) &= -\frac{7}{2}\zeta_3 - \pi^2\ln 2 - 2G(2-z,1/z,0,y) - G(2-z,y)\pi^2 + 4G(2-z,1,0,y)\\
&\quad + 2G(1/z,1/z,0,y) + G(1/z,y)\pi^2 + 2G(1/z,0,0,y) - 4G(1/z,1,0,y)\\
&\quad - 2G(0,z)G(2-z,1/z,y) + 2G(0,z)G(1/z,1/z,y) + 2G(0,0,z)G(1/z,y)\\
&\quad + 4G(1,0,z)G(2-z,y) - 4G(1,0,z)G(1/z,y) - 4G(1,0,0,z) - 4G(1,0,0,y)\\
&\quad - G(2,z)\pi^2 + 4G(2,1,0,z)\,.
\end{aligned}
$$

Sector 213 contains 4 MIs which read:

$$
\mathcal{I}_{213,1}^{(B)} = \left(\frac{S_\epsilon}{16\pi^2}\right)^2 (m^2)^{-2\epsilon-1}\,\frac{\xi}{(1-\xi^2)}\,\Big[f_0^{(213,1)}(\xi,\zeta) + i\,\pi\, g_0^{(213,1)}(\xi,\zeta)\Big] + \mathcal{O}(\epsilon^1)\,, \tag{B.18}
$$

with

$$
\begin{aligned}
f_0^{(213,1)}(\xi,\zeta) &= \frac{1}{6}\Big\{G(1/\xi,\zeta) - G(\xi,\zeta)\Big\}\Big[- 12\zeta_3 + 12G(-i,-c,-i,\xi) + 12G(-i,-c,i,\xi)\\
&\quad - 12G(-i,-c,0,\xi) + 12G(-i,-\bar{c},-i,\xi) + 12G(-i,-\bar{c},i,\xi) - 12G(-i,-\bar{c},0,\xi)\\
&\quad + 21G(-i,\xi)\pi^2 - 12G(-i,0,-i,\xi) - 12G(-I,0,i,\xi) + 12G(-i,0,0,\xi)\\
&\quad - 12G(-c,-c,-i,\xi) - 12G(-c,-c,i,\xi) + 12G(-c,-c,0,\xi) - 12G(-c,-\bar{c},-i,\xi)\\
&\quad - 12G(-c,-\bar{c},i,\xi) + 12G(-c,-\bar{c},0,\xi) - 44G(-c,\xi)\pi^2 + 12G(-c,0,-i,\xi)\\
&\quad + 12G(-c,0,i,\xi) - 12G(-c,0,0,\xi) - 12G(-\bar{c},-c,-i,\xi) - 12G(-\bar{c},-c,i,\xi)\\
&\quad + 12G(-\bar{c},-c,0,\xi) - 12G(-\bar{c},-\bar{c},-i,\xi) - 12G(-\bar{c},-\bar{c},i,\xi) + 12G(-\bar{c},-\bar{c},0,\xi)\\
&\quad - 44G(-\bar{c},\xi)\pi^2 + 12G(-\bar{c},0,-i,\xi) + 12G(-\bar{c},0,i,\xi) - 12G(-\bar{c},0,0,\xi)\\
&\quad + 12G(i,-c,-i,\xi) + 12G(i,-c,i,\xi) - 12G(i,-c,0,\xi) + 12G(i,-\bar{c},-i,\xi)\\
&\quad + 12G(i,-\bar{c},i,\xi) - 12G(i,-\bar{c},0,\xi) + 21G(i,\xi)\pi^2 - 12G(i,0,-i,\xi) - 12G(i,0,i,\xi)\\
&\quad + 12G(i,0,0,\xi) + 23G(0,\xi)\pi^2\Big] + \frac{1}{2}\Big\{G(1/\xi,1/J_\xi,\zeta) - G(\xi,1/J_\xi,\zeta)\Big\}\Big[7\pi^2\\
&\quad + 4G(-c,-i,\xi) + 4G(-c,i,\xi) - 4G(-c,0,\xi) + 4G(-\bar{c},-i,\xi) + 4G(-\bar{c},i,\xi)\\
&\quad - 4G(-\bar{c},0,\xi) - 4G(0,-i,\xi) - 4G(0,i,\xi) + 4G(0,0,\xi)\Big] + \frac{2}{3}\Big\{ - G(1/\xi,1/I_\xi,\zeta)\\
&\quad + G(1/\xi,-1,\zeta) + G(\xi,1/I_\xi,\zeta) - G(\xi,-1,\zeta)\Big\}\Big[11\pi^2 + 3G(-c,-i,\xi) + 3G(-c,i,\xi)\\
&\quad - 3G(-c,0,\xi) + 3G(-\bar{c},-i,\xi) + 3G(-\bar{c},i,\xi) - 3G(-\bar{c},0,\xi) - 3G(0,-i,\xi)\\
&\quad - 3G(0,i,\xi) + 3G(0,0,\xi)\Big]\\
&\quad - \frac{1}{72}\Big[65\pi^4 + 576G(0,-i,-c,-i,\xi) + 576G(0,-i,-c,i,\xi)\\
&\quad - 576G(0,-i,-c,0,\xi) + 576G(0,-i,-\bar{c},-i,\xi) + 576G(0,-i,-\bar{c},i,\xi)\\
&\quad - 576G(0,-i,-\bar{c},0,\xi) + 1008G(0,-i,\xi)\pi^2 - 576G(0,-i,0,-i,\xi)\\
&\quad - 576G(0,-i,0,i,\xi) + 576G(0,-i,0,0,\xi) - 432G(0,-c,-c,-i,\xi)\\
&\quad - 432G(0,-c,-c,i,\xi) + 432G(0,-c,-c,0,\xi) - 432G(0,-c,-\bar{c},-i,\xi)\\
&\quad - 432G(0,-c,-\bar{c},i,\xi) + 432G(0,-c,-\bar{c},0,\xi) - 1584G(0,-c,\xi)\pi^2\\
&\quad + 432G(0,-c,0,-i,\xi) + 432G(0,-c,0,i,\xi) - 432G(0,-c,0,0,\xi)\\
&\quad - 432G(0,-\bar{c},-c,-i,\xi) - 432G(0,-\bar{c},-c,i,\xi) + 432G(0,-\bar{c},-c,0,\xi)\\
&\quad - 432G(0,-\bar{c},-\bar{c},-i,\xi) - 432G(0,-\bar{c},-\bar{c},i,\xi) + 432G(0,-\bar{c},-\bar{c},0,\xi)\\
&\quad - 1584G(0,-\bar{c},\xi)\pi^2 + 432G(0,-\bar{c},0,-i,\xi) + 432G(0,-\bar{c},0,i,\xi)
\end{aligned}
$$

$$
\begin{aligned}
&- 432G(0,-\bar{c},0,0,\xi) + 576G(0,i,-c,-i,\xi) + 576G(0,i,-c,i,\xi) \\
&- 576G(0,i,-c,0,\xi) + 576G(0,i,-\bar{c},-i,\xi) + 576G(0,i,-\bar{c},i,\xi) \\
&- 576G(0,i,-\bar{c},0,\xi) + 1008G(0,i,\xi)\pi^2 - 576G(0,i,0,-i,\xi) \\
&- 576G(0,i,0,i,\xi) + 576G(0,i,0,0,\xi) + 576G(0,-1,-c,-i,\xi) \\
&+ 576G(0,-1,-c,i,\xi) - 576G(0,-1,-c,0,\xi) + 576G(0,-1,-\bar{c},-i,\xi) \\
&+ 576G(0,-1,-\bar{c},i,\xi) - 576G(0,-1,-\bar{c},0,\xi) + 912G(0,-1,\xi)\pi^2 \\
&- 576G(0,-1,0,-i,x) - 576G(0,-1,0,i,\xi) + 576G(0,-1,0,0,\xi) \\
&- 432G(0,0,-c,-i,\xi) - 432G(0,0,-c,i,\xi) + 432G(0,0,-c,0,\xi) \\
&- 432G(0,0,-\bar{c},-i,\xi) - 432G(0,0,-\bar{c},i,\xi) + 432G(0,0,-\bar{c},0,\xi) \\
&+ 120G(0,0,\xi)\pi^2 + 432G(0,0,0,-i,\xi) + 432G(0,0,0,i,\xi) - 432G(0,0,0,0,\xi)\Big] \\
&+ \Big[G(0,\xi) - G(-i,\xi) - G(i,\xi)\Big]\Big\{2G(1/\xi,1/I_\xi,1/I_\xi,\zeta) - 2G(1/\xi,1/I_\xi,1/\xi,\zeta) \\
&- 2G(1/\xi,1/I_\xi,\xi,\zeta) + G(1/\xi,1/J_\xi,1/\xi,\zeta) - 2G(1/\xi,1/J_\xi,1/I_\xi,\zeta) \\
&+ G(1/\xi,1/J_\xi,\xi,\zeta) + 2G(1/\xi,-1,1/\xi,\zeta) - 2G(1/\xi,-1,1/I_\xi,\zeta) + 2G(1/\xi,-1,\xi,\zeta) \\
&- G(1/\xi,0,1/\xi,\zeta) - G(1/\xi,0,\xi,\zeta) + 2G(\xi,1/I_\xi,1/\xi,\zeta) - 2G(\xi,1/I_\xi,1/I_\xi,\zeta) \\
&+ 2G(\xi,1/I_\xi,\xi,\zeta) - G(\xi,1/J_\xi,1/\xi,\zeta) + 2G(\xi,1/J_\xi,1/I_\xi,\zeta) - G(\xi,1/J_\xi,\xi,\zeta) \\
&- 2G(\xi,-1,1/\xi,\zeta) + 2G(\xi,-1,1/I_\xi,\zeta) - 2G(\xi,-1,\xi,\zeta) + G(\xi,0,1/\xi,\zeta) \\
&+ G(\xi,0,\xi,\zeta)\Big\} + 2G(1/\xi,1/I_\xi,1/\xi,1/J_\xi,\zeta) + 2G(1/\xi,1/I_\xi,1/\xi,0,\zeta) \\
&- 2G(1/\xi,1/I_\xi,1/I_\xi,1/J_\xi,\zeta) + 2G(1/\xi,1/I_\xi,\xi,1/J_\xi,\zeta) + 2G(1/\xi,1/I_\xi,\xi,0,\zeta) \\
&- 2G(1/\xi,1/I_\xi,-1,0,\zeta) - G(1/\xi,1/J_\xi,1/\xi,1/J_\xi,\zeta) - G(1/\xi,1/J_\xi,1/\xi,0,\zeta) \\
&+ 2G(1/\xi,1/J_\xi,1/I_\xi,1/J_\xi,\zeta) - G(1/\xi,1/J_\xi,\xi,1/J_\xi,\zeta) - G(1/\xi,1/J_\xi,\xi,0,\zeta) \\
&- 2G(1/\xi,-1,1/\xi,1/J_\xi,\zeta) - 2G(1/\xi,-1,1/\xi,0,\zeta) + 2G(1/\xi,-1,1/I_\xi,1/J_\xi,\zeta) \\
&- 2G(1/\xi,-1,\xi,1/J_\xi,\zeta) - 2G(1/\xi,-1,\xi,0,\zeta) + 2G(1/\xi,-1,-1,0,\zeta) \\
&+ G(1/\xi,0,1/\xi,1/J_\xi,\zeta) + G(1/\xi,0,1/\xi,0,\zeta) + G(1/\xi,0,\xi,1/J_\xi,\zeta) \\
&+ G(1/\xi,0,\xi,0,\zeta) - 23/6G(1/\xi,0,\zeta)\pi^2 - 2G(1/\xi,0,-1,0,\zeta) - 2G(\xi,1/I_\xi,1/\xi,1/J_\xi,\zeta) \\
&- 2G(\xi,1/I_\xi,1/\xi,0,\zeta) + 2G(\xi,1/I_\xi,1/I_\xi,1/J_\xi,\zeta) - 2G(\xi,1/I_\xi,\xi,1/J_\xi,\zeta) \\
&- 2G(\xi,1/I_\xi,\xi,0,\zeta) + 2G(\xi,1/I_\xi,-1,0,\zeta) + G(\xi,1/J_\xi,1/\xi,1/J_\xi,\zeta) \\
&+ G(\xi,1/J_\xi,1/\xi,0,\zeta) - 2G(\xi,1/J_\xi,1/I_\xi,1/J_\xi,\zeta) + G(\xi,1/J_\xi,\xi,1/J_\xi,\zeta) \\
&+ G(\xi,1/J_\xi,\xi,0,\zeta) + 2G(\xi,-1,1/\xi,1/J_\xi,\zeta) + 2G(\xi,-1,1/\xi,0,\zeta) \\
&- 2G(\xi,-1,1/I_\xi,1/J_\xi,\zeta) + 2G(\xi,-1,\xi,1/J_\xi,\zeta) + 2G(\xi,-1,\xi,0,\zeta) \\
&- 2G(\xi,-1,-1,0,\zeta) - G(\xi,0,1/\xi,1/J_\xi,\zeta) - G(\xi,0,1/\xi,0,\zeta) - G(\xi,0,\xi,1/J_\xi,\zeta) \\
&- G(\xi,0,\xi,0,\zeta) + 23/6G(\xi,0,\zeta)\pi^2 + 2G(\xi,0,-1,0,\zeta)\,,
\end{aligned}
$$

and

$$
\begin{aligned}
g_0^{(213,1)}(\xi,\zeta) = &\frac{1}{3}\Big\{G(1/\xi,\zeta) - G(\xi,\zeta)\Big\}\Big[\pi^2 + 6G(-i,-c,\xi) + 6G(-i,-\bar{c},\xi) - 6G(-i,0,\xi) \\
&- 6G(-c,-c,\xi) - 6G(-c,-\bar{c},\xi) + 6G(-c,0,\xi) - 6G(-\bar{c},-c,\xi) - 6G(-\bar{c},-\bar{c},\xi) \\
&+ 6G(-\bar{c},0,\xi) + 6G(i,-c,\xi) + 6G(i,-\bar{c},\xi) - 6G(i,0,\xi)\Big] \\
&+ \Big[G(0,\xi) - G(-c,\xi) - G(-\bar{c},\xi)\Big]\Big\{2G(1/\xi,1/I_\xi,\zeta) - 2G(1/\xi,1/J_\xi,\zeta) \\
&- 2G(1/\xi,-1,\zeta) - 2G(\xi,1/I_\xi,\zeta) + 2G(\xi,1/J_\xi,\zeta) + 2G(\xi,-1,\zeta)\Big\} \\
&- \frac{1}{3}\Big[24G(0,-i,-c,\xi) + 24G(0,-i,-\bar{c},\xi) - 24G(0,-i,0,\xi) - 18G(0,-c,-c,\xi) \\
&- 18G(0,-c,-\bar{c},\xi) + 18G(0,-c,0,\xi) - 18G(0,-\bar{c},-c,\xi) - 18G(0,-\bar{c},-\bar{c},\xi)
\end{aligned}
$$

$$
\begin{aligned}
&+ 18G(0,-\bar{c},0,\xi) + G(0,\xi)\pi^2 + 24G(0,i,-c,\xi) + 24G(0,i,-\bar{c},\xi) - 24G(0,i,0,\xi) \\
&+ 24G(0,-1,-c,\xi) + 24G(0,-1,-\bar{c},\xi) - 24G(0,-1,0,\xi) - 18G(0,0,-c,\xi) \\
&- 18G(0,0,-\bar{c},\xi) + 18G(0,0,0,\xi)\Big] + 4G(1/\xi,1/I_\xi,1/\xi,\zeta) - 2G(1/\xi,1/I_\xi,1/I_\xi,\zeta) \\
&+ 4G(1/\xi,1/I_\xi,\xi,\zeta) - 2G(1/\xi,1/I_\xi,-1,\zeta) - 2G(1/\xi,1/J_\xi,1/\xi,\zeta) \\
&+ 2G(1/\xi,1/J_\xi,1/I_\xi,\zeta) - 2G(1/\xi,1/J_\xi,\xi,\zeta) - 4G(1/\xi,-1,1/\xi,\zeta) \\
&+ 2G(1/\xi,-1,1/I_\xi,\zeta) - 4G(1/\xi,-1,\xi,\zeta) + 2G(1/\xi,-1,-1,\zeta) + 2G(1/\xi,0,1/\xi,\zeta) \\
&+ 2G(1/\xi,0,\xi,\zeta) - 2G(1/\xi,0,-1,\zeta) - 4G(\xi,1/I_\xi,1/\xi,\zeta) + 2G(\xi,1/I_\xi,1/I_\xi,\zeta) \\
&- 4G(\xi,1/I_\xi,\xi,\zeta) + 2G(\xi,1/I_\xi,-1,\zeta) + 2G(\xi,1/J_\xi,1/\xi,\zeta) - 2G(\xi,1/J_\xi,1/I_\xi,\zeta) \\
&+ 2G(\xi,1/J_\xi,\xi,\zeta) + 4G(\xi,-1,1/\xi,\zeta) - 2G(\xi,-1,1/I_\xi,\zeta) + 4G(\xi,-1,\xi,\zeta) \\
&- 2G(\xi,-1,-1,\zeta) - 2G(\xi,0,1/\xi,\zeta) - 2G(\xi,0,\xi,\zeta) + 2G(\xi,0,-1,\zeta)\,.
\end{aligned}
$$

$$
\mathcal{I}^{(B)}_{213,2} = \left(\frac{S_\epsilon}{16\pi^2}\right)^2 \frac{(m^2)^{-2\epsilon-2}}{(1-yz)} \sum_{n=-2}^{0} \epsilon^n\, f^{(213,2)}_n(y,z) + \mathcal{O}(\epsilon)\,, \tag{B.19}
$$

with

$$
\begin{aligned}
f^{(213,2)}_{-2}(y,z) &= G(0,z) + G(0,y)\,, \\
f^{(213,2)}_{-1}(y,z) &= -\frac{5}{6}\pi^2 - 3G(1/z,0,y) - 3G(0,z)G(1/z,y) - 2G(0,0,z) - 2G(0,0,y) \\
&\quad + 4G(1,0,z) + 4G(1,0,y)\,, \\
f^{(213,2)}_{0}(y,z) &= -6\zeta_3 - 2\pi^2\ln 2 - 4G(2-z,1/z,0,y) - 2G(2-z,y)\pi^2 + 8G(2-z,1,0,y) \\
&\quad + 9G(1/z,1/z,0,y) + 5/2G(1/z,y)\pi^2 + 6G(1/z,0,0,y) - 12G(1/z,1,0,y) \\
&\quad - G(0,1/z,0,y) - 1/6G(0,z)\pi^2 - 4G(0,z)G(2-z,1/z,y) + 9G(0,z)G(1/z,1/z,y) \\
&\quad - G(0,z)G(0,1/z,y) - 2G(0,z)G(1,1/z,y) - 1/6G(0,y)\pi^2 + 6G(0,0,z)G(1/z,y) \\
&\quad + 4G(0,0,0,z) + 4G(0,0,0,y) + 2G(0,1,0,z) + 2G(0,1,0,y) - 2G(1,1/z,0,y) \\
&\quad + 1/3G(1,z)\pi^2 + 1/3G(1,y)\pi^2 + 8G(1,0,z)G(2-z,y) - 12G(1,0,z)G(1/z,y) \\
&\quad + 2G(1,0,z)G(1,y) - 8G(1,0,0,z) - 8G(1,0,0,y) - 2G(1,1,0,z) - 2G(1,1,0,y) \\
&\quad - 2G(2,z)\pi^2 + 8G(2,1,0,z)\,.
\end{aligned}
$$

$$
\mathcal{I}^{(B)}_{213,3} = \left(\frac{S_\epsilon}{16\pi^2}\right)^2 \frac{(m^2)^{-2\epsilon-2}}{(1-z)} \sum_{n=-2}^{0} \epsilon^n\, f^{(213,3)}_n(y,z) + \mathcal{O}(\epsilon)\,, \tag{B.20}
$$

with

$$
\begin{aligned}
f^{(213,3)}_{-2}(y,z) &= 1/2G(0,z)\,, \\
f^{(213,3)}_{-1}(y,z) &= \frac{\pi^2}{6} + 1/2G(1/z,0,y) + 1/2G(0,z)G(1/z,y) - G(0,0,z) - G(1,0,z) - 1/2G(1,0,y) \\
f^{(213,3)}_{0}(y,z) &= \frac{11}{4}\zeta_3 + \frac{\pi^2}{2}\ln 2 + G(2-z,1/z,0,y) + 1/2G(2-z,y)\pi^2 - 2G(2-z,1,0,y) \\
&\quad - 3/2G(1/z,1/z,0,y) - 5/12G(1/z,y)\pi^2 - G(1/z,0,0,y) + 2G(1/z,1,0,y) \\
&\quad + 1/6G(0,z)\pi^2 + G(0,z)G(2-z,1/z,y) - 3/2G(0,z)G(1/z,1/z,y) \\
&\quad + G(0,z)G(1,1/z,y) - G(0,0,z)G(1/z,y) + 2G(0,0,0,z) - 2G(0,1,0,z) \\
&\quad + G(1,1/z,0,y) - 1/3G(1,z)\pi^2 + 1/12G(1,y)\pi^2 - 2G(1,0,z)G(2-z,y) \\
&\quad + 2G(1,0,z)G(1/z,y) - G(1,0,z)G(1,y) + 2G(1,0,0,z) + G(1,0,0,y) \\
&\quad + 2G(1,1,0,z) - 1/2G(1,1,0,y) + 1/2G(2,z)\pi^2 - 2G(2,1,0,z)\,.
\end{aligned}
$$

Finally the last master is equal to the previous one under the exchange $y \leftrightarrow z$:

$$\mathcal{I}^{(B)}_{213,4} = \left(\frac{S_\epsilon}{16\pi^2}\right)^2 \frac{(m^2)^{-2\epsilon-2}}{(1-y)} \sum_{n=-2}^{0} \epsilon^n f_n^{(213,3)}(z,y) + \mathcal{O}(\epsilon)\,. \tag{B.21}$$

6-denominator Integrals

The only irreducible topology with 6 denominators has one MI which reads:

$$\mathcal{I}^{(B)}_{215} = \left(\frac{S_\epsilon}{16\pi^2}\right)^2 \frac{(m^2)^{-2\epsilon-2}}{y(1-z)} \sum_{n=-2}^{-1} \epsilon^n f_n^{(215)}(y,z) + \mathcal{O}(\epsilon^0)\,, \tag{B.22}$$

with

$$\begin{aligned}
f^{(215)}_{-2}(y,z) &= 1/2G(1/z,0,y) + 1/2G(0,z)G(1/z,y) - 1/2G(1,0,y)\,,\\
f^{(215)}_{-1}(y,z) &= -1/2G(1/z,1/z,0,y) - 1/4G(1/z,y)\pi^2 + G(1/z,1,0,y) - G(0,1/z,0,y)\\
&\quad - 1/2G(0,z)G(1/z,1/z,y) - G(0,z)G(0,1/z,y) + 2G(0,z)G(1,1/z,y)\\
&\quad - G(0,0,z)G(1/z,y) + G(0,1,0,y) + 2G(1,1/z,0,y) + 5/12G(1,y)\pi^2\\
&\quad + G(1,0,z)G(1/z,y) - 2G(1,0,z)G(1,y) - 5/2G(1,1,0,y)\,.
\end{aligned}$$

7-denominator Integrals

There is one irreducible topology with 7 denominators with two MIs which read:

$$\mathcal{I}^{(B)}_{247,1} = \left(\frac{S_\epsilon}{16\pi^2}\right)^2 \frac{(m^2)^{-2\epsilon-3}}{y(1-yz)} \sum_{n=-2}^{-1} \epsilon^n f_n^{(247,1)}(y,z) + \mathcal{O}(\epsilon^0)\,, \tag{B.23}$$

with

$$\begin{aligned}
f^{(247,1)}_{-2}(y,z) &= \frac{\pi^2}{3} - 2G(1/z,0,y) - 2G(0,z)G(1/z,y)\,,\\
f^{(247,1)}_{-1}(y,z) &= -7\zeta_3 + 7G(1/z,1/z,0,y) + 3/2G(1/z,y)\pi^2 + 4G(1/z,0,0,y) - 8G(1/z,1,0,y)\\
&\quad + 2G(0,1/z,0,y) + 7G(0,z)G(1/z,1/z,y) + 2G(0,z)G(0,1/z,y)\\
&\quad - 6G(0,z)G(1,1/z,y) - 2/3G(0,y)\pi^2 + 4G(0,0,z)G(1/z,y) + 2G(0,1,0,y)\\
&\quad - 6G(1,1/z,0,y) - 2/3G(1,y)\pi^2 - 8G(1,0,z)G(1/z,y) + 6G(1,0,z)G(1,y)\\
&\quad - 6G(1,0,0,y) + 4G(1,1,0,y)\,.
\end{aligned}$$

$$\begin{aligned}
\mathcal{I}^{(B)}_{247,2} = \left(\frac{S_\epsilon}{16\pi^2}\right)^2 (m^2)^{-2\epsilon-2} \Bigg[&\frac{(1-z)}{(1-y)(1-yz)} \sum_{n=-2}^{-1} \epsilon^n f_n^{(247,2)}(y,z)\\
&+ \frac{1}{y(1-y)} \sum_{n=-2}^{-1} \epsilon^n g_n^{(247,2)}(y,z)\Bigg] + \mathcal{O}(\epsilon^0)\,,
\end{aligned}$$

with

$$f^{(247,2)}_{-2}(y,z) = \frac{\pi^2}{2} + 3/2G(0,0,y) - 3/2G(1,0,z) - 3/2G(1,0,y)\,,$$

$$
\begin{aligned}
f_{-1}^{(247,2)}(y,z) = \frac{15}{4}\zeta_3 + \frac{3}{2}\pi^2 \ln 2 + 3G(2-z,1/z,0,y) + 3/2G(2-z,y)\pi^2 - 6G(2-z,1,0,y) \\
- G(1/z,y)\pi^2 - 3G(1/z,0,0,y) + 3G(1/z,1,0,y) + 3G(0,z)G(2-z,1/z,y) \\
- 3G(0,z)G(1,1/z,y) - 1/4G(0,y)\pi^2 - 9/2G(0,0,0,y) + 3/2G(0,1,0,y) \\
- 3G(1,1/z,0,y) + 1/4G(1,z)\pi^2 - 1/4G(1,y)\pi^2 - 6G(1,0,z)G(2-z,y) \\
+ 3G(1,0,z)G(1/z,y) + 3G(1,0,z)G(1,y) + 3G(1,0,0,z) + 15/2G(1,0,0,y) \\
- 3/2G(1,1,0,z) + 3/2G(1,1,0,y) + 3/2G(2,z)\pi^2 - 6G(2,1,0,z)\,,
\end{aligned}
$$

and

$$
g_{-2}^{(247,2)}(y,z) = -\frac{\pi^2}{4} + 3/2G(1/z,0,y) + 3/2G(0,z)G(1/z,y)\,,
$$

$$
\begin{aligned}
g_{-1}^{(247,2)}(y,z) = \frac{9}{2}\zeta_3 - 9/2G(1/z,1/z,0,y) - 11/12G(1/z,y)\pi^2 - 2G(1/z,0,0,y) + 5G(1/z,1,0,y) \\
- G(0,1/z,0,y) - 9/2G(0,z)G(1/z,1/z,y) - G(0,z)G(0,1/z,y) + 4G(0,z)G(1,1/z,y) \\
+ 1/2G(0,y)\pi^2 - 3G(0,0,z)G(1/z,y) - 2G(0,1,0,y) + 4G(1,1/z,0,y) + 1/2G(1,y)\pi^2 \\
+ 5G(1,0,z)G(1/z,y) - 4G(1,0,z)G(1,y) + 2G(1,0,0,y) - 3G(1,1,0,y)\,.
\end{aligned}
$$

C

Mathematica Packages for Computations with Multiple Polylogarithms

In this appendix the Mathematica (sub-)packages are described which implement the algorithms presented in chapter 3 and used in chapters 4 and 5. The package `MPLTools.m` contains different notations of multiple polylogarithms, tools for their conversion and some basic manipulations and an implementation of the shuffle algebra. It is discussed in section C.1. The package `MPLEval.m` builds upon the previous package and contains the routines for numerical evaluation of MPLs and is described in section C.2. The package `PSLQfast.m` contains an implementation of the PLSQ algorithm and is independent of the previous two. It is described briefly in section C.3 along with a usage example. The symbol calculus and coproduct formalism is contained in `CSimplify.m` which requires all three previous packages. Its most important functions are described in section C.4, whereas appendix D is dedicated to three examples of its usage.

C.1 MPL manipulation - the package MPLTools.m

The package `MPLTools.m` contains definitions for multiple polylogarithms in various notations as well as the rules to convert them into each other. Furthermore, it contains tools for basic index manipulation, such as extraction of divergences or the replacement of products of MPLs by the sum over the MPLs with shuffled indices. At last, it contains helper function to return information on the alphabet, i.e. the indices of the MPLs present in an expression.

C.1.1 Installation

If the file `MPLTools.m` is found at a location contained in the Mathematica environment variable $**Path**, it can be installed using

```
In[1]:= << MPLTools`;
```

C.1.2 Description of the functions contained in the package

A list with all the functions and variables defined in the package can be produced with the command

```
In[2]:= ?"MPTools`*"
```

General definitions and conversion tools

G[ai__,x_]

is the multiple polylogarithm with indices ai and argument x defined in equation (3.1).

G[x_,**L**[ai__]]

is the same in a different notation.

J[a0_, ai__, x_]

is the multiple polylogarithm $I(a_0; a_1, \ldots a_n; x)$ with lower integration bound a0 of weight **Length**[ai] and argument x defined in equation (3.70).

SimpleReplacements

Replacement list to write the **G**[___] that can be written in simple **Log**[_] and **PolyLog**[_,_] functions that way.

SimpletoG

Replacement list to write **Log**[_] and **PolyLog**[_,_] as **G**[__] functions.

G2toPolyLogs

Replacement list to write the **G**[a,b,x] of weight two in function of **PolyLog**[_,_]s.

GtoJ
JtoG

Replacement list to convert **G**[__] to **J**[__] and backwards in an expression.

JShiftLowerIntegrationBound

Replacement list to shift **J**[a0,__] to **J**[0,__] in an expression. Works up to weight four.

JG[**expr**_]

writes expression in terms of **J**[__] properly in terms of functions of **G**[__], e.g. without creating any spurious divergences.

JZeroes

is a replacement list that sets to zero all **J**[a_,___,a_].

GtoOldConvention
GtoNewConvention

Replacement list to change from the **G**[a__,x] to the **G**[x,**L**[a]] notation.

Weight[**expr**_]

computes the transcendental weight of an expression. The result is given as **W**[x]. It also recognizes **PolyLog**[_,_], **Zeta**[_] and powers of π.

W

The wrapper for giving the weight.

GroupByWeight[**expr**_]

returns a list of the expressions split up by weight. It also respects the transcendentality of π and **Zeta**[n].

Shuffle product, manipulation of indices

SP[a_**L**,b_**L**]

is an implementation of the shuffle product (3.7), where

L[a_i]

is a helper function. It is sort of the index of a MPL.

EliminateLeft[**index**_]
EliminateRight[**index**_]

are replacement lists that extract in **G**[__,x_] or **J**[a0_,___,x_] the left/right index **index** and writes the expression involving shuffles and powers of **G**[**index**,x] / **J**[a0,**index**,x]. Attention, the order of the indices is different for both function notations, therefore it has a different effect in both cases!

EliminateDivs

is a replacement list that writes all divergences in expressions of **J**[__,x_] as logarithms of **J**[0,0,x] and **J**[0,x,x].

EliminateShuffles

is a replacement list that eliminates products of **G**[__] functions with the same argument by replacing them with their shuffle product.

ES[**expr**_]

repeatedly applies **EliminateShuffles** and **ExpandAll** to eliminate products of G functions.

ES2[**expr**_]

takes any expression in terms of **J**[ ],**G**[ ], eliminates the shuffles and returns the result in **G**[ ] functions.

Information about the alphabet of an expression, miscellaneous

GInfo[**expr**_]

returns a list of arguments of the G functions in expr together with their indices.

GuessRelations[inputlist_**List**,**Evalf**_,prec_**Integer**:10^9]

guesses relations between the elements of inputlist using the PSLQ algorithm. It does so iteratively until no more relations are found because the norm of the coefficient vector becomes larger than prec. This is usually the case when there is no more relation and the precision of the input has been exhausted. It attempts to find relations expressing the elements at the end of the list as a function of the ones more closer to the beginning. **Evalf**[__] is a function that when applied onto inputlist evaluates this list to numerical values (with high precision). Example:

```
In[1]:= GuessRelations[{Log[2 + Sqrt[3]], Log[2], Log[1 + Sqrt[3]]}, N[#, 200] &]

Out[1]= {Log[1 + Sqrt[3]] -> 1/2 (Log[2] + Log[2 + Sqrt[3]])}
```

C.2 Numerical evaluation of multiple polylogarithms - the package MPLEval.m

The numerical evaluation of multiple polylogarithms is based on their series representation. We introduce yet another notation:

$$\mathrm{Li}_{m_1,\ldots,m_k}(x_1,\ldots,x_k) = (-1)^k G_{m_1,\ldots,m_k}\left(\frac{1}{x_1},\frac{1}{x_1x_2},\ldots,\frac{1}{x_1\ldots x_k};1\right) , \tag{C.1}$$

where

$$G_{m_1,\ldots,m_k}(z_1,\ldots,z_k;y) = G(\underbrace{0,\ldots,0}_{m_1-1},z_1,\ldots,z_{k-1},\underbrace{0,\ldots,0}_{m_k-1},z_k;y) . \tag{C.2}$$

The series representation is then given by

$$\mathrm{Li}_{m_1,\ldots,m_k}(x_1,\ldots,x_k) = \sum_{i_1>i_2>\ldots>i_k>0} \frac{x_1^{i_1}}{i_1^{m_1}}\cdots\frac{x_k^{i_k}}{i_1^{m_k}} . \tag{C.3}$$

The general idea of the numerical evaluation is to use transformations to analytically continue the function into the region where above series representation converges, that is $|y| < |z_i|$ in equation (C.2). This method was described in [225], where additional transformations to speed up convergence are documented as well. The implementation of these algorithms in the GiNaC library by the same authors was made available for use in Mathematica via the MathLink interface.

C.2.1 Installation

`MPLEval` requires an installation of the GiNaC library which can be obtained from `http://www.ginac.de`. The MathLink executable has to be compiled before being usable. The user can do so after setting the locations of the GiNaC and MathLink libraries in the `Makefile` with the terminal command `make`. An optional step is to copy the executable and the package files in the Mathematica application directory with the command `make install`. The installation is very similar to the package PSLQfast which can be found in appendix C.3.3.

C.2.2 Usage

Once the package has been installed to a location which is included in the $**Path** environment variable of Mathematica, it can be loaded using the command

```
In[1]:= Needs["MPLEval`"];
```

A clickable list that displays the information about the functions defined in the package can be produced using

```
In[2]:= ?"MPLEval`*"
```

To evaluate the MPLs an expression, the first step is to set the desired precision (the default value is 100):

```
In[3]:= $MPLPrecision = 100;
```

It is useful to define replacement lists for the values and the signs of infinitesimal imaginary parts of the variables.

```
In[4]:= values = {x -> .5}; signs = {Sgn[x] -> 1};
```

Then, the G[__] functions in an expression can be evaluated using **MPLEval** as a replacement list like

```
In[6]:= G[.1, 4, 3, x] /. MPLEval[values, signs]

Out[6]= 0.00864089501592179827316351143006747592592746747213375239268 3\
          57353139305865814813294225439878877894882 2 -
        0.00134630608232867857697573599019160943673921714084125402837176956 10\
          81275975631352237104740510028274943 I
```

C.2.3 Description of functions contained in the package

All functions and variables defined in the package can be viewed with the command:

```
In[2]:= ?"MPLEval`*"
```

Only the most important ones are given here.

MPLEvalInstall[]

installs the MathLink for such that **MPLEval**[__] can be used. Call in case the MathLink crashes.

expr/.**MPLEval**[**values**_,**signs**_:{}]

evaluates the multiple polylogarithms **G**[a1 , ... , an , arg] in **expr** in precision $MPLPrecision. The variables on which the arguments of the **G**[__] depend should be given as replacement lists in **values** and where needed the signs of their imaginary parts in **signs**. The results are cached.

$MPLPrecision

Determines the precision with which **MPLEval**[**values**,**signs**] computes the MPLs. Default value: 100.

ClearGCache[]

clears the cache from saved results of **MPLEval**[__]. Returns the amount of memory freed.

Sgn[_]

Function used to define the signs of the infinitesimal imaginary part of a variable, e.g. **signs**={**Sgn**[x]->-1}.

Chop2[**expr**_]

works just like **Chop2**[x_]:=**Chop**[x,10^(-$MPLPrecision+10)], i.e. it sets to zero numerical values smaller than $10^{(-\$\mathrm{MPLPrecision}+10)}$.

SetPrec[**expr**_]

sets the precision of the argument **expr** to $MPLPrecision.

MPLEvalRaw[**values**_,**signs**_]

does everything **MPLEval**[__] does, except that it does not send the evaluation to the MathLink in the end. Useful for checking whether the preparation for the numerical evaluation works correctly.

MPLEvalComplex[indexRe_**List**,indexIm_**List**,
indexInfIm_**List**,arg_?**NumericQ**,Prec_**Integer**:17]

evaluates the MPL directly using MathLink where the real and imaginary parts have to be given separately. The argument has to be a positive real number.

DIV[**expr_String**]

denotes a divergence encountered in the evaluation using **MPLEval**.

C.3 The PSLQ algorithm - the package PSLQfast.m

The PSLQ algorithm [222] is a numerical algorithm to determine whether there exists an integer relation between the rational numbers x_i, e.g. whether there exist integers a_i such that equation

$$a_1 x_1 + a_2 x_2 + \ldots + a_n x_n = 0 \tag{C.4}$$

is fulfilled or to give an bounds on the minimal size of these coefficients. In the context of the present problems it can be used to determine the parts mapped to zero by the symbol map or to find new relations between polylogarithms at fixed values.

C.3.1 Description

To determine whether there exists an integer relation between two rational numbers x_1 and x_2, one can compute the continued fraction of their ratio x_1/x_2. If this relation exists, the continued fraction eventually terminates. This algorithm is in principle related to the Euclidean algorithm.

Very loosely speaking, the PSLQ algorithm is a generalization of the Euclidean algorithm to n rational numbers.

C.3.2 Implementation

An existing implementation of the PSLQ algorithm contained in the arbitrary precision arithmetics c++/fortran library `ARPREC` [264] was used and connected to Mathematica using the MathLink interface.

C.3.3 Installation

The `PSLQfast` package is given as c++ source code which has to be compiled and linked with both the MathLink and `ARPREC` libraries. While the former are already installed with Mathematica, the latter have to be obtained and installed from `http://crd-legacy.lbl.gov/~dhbailey/mpdist/`.

Before compilation of the code, the user has to point the compiler to the correct libraries by setting the variables `MLINKDIR`, `ARPRECINCDIR` and `ARPRECLIBDIR` in the `Makefile`. Depending on the architecture of the system, some of the parameters in the part "Mathlink settings" need to be modified. More information about this can be found in the Mathematica help system under `tutorial/MathLinkDeveloperGuide-UnixOverview` in the section named "Building MathLink Programs - Using a Makefile".

If everything is set correctly the command `make` should produce a MathLink executable `PSLQfast` which can conveniently be copied into a directory which is automatically searched by Mathematica together with the package file `PSLQfast.m` because it is contained in the $**Path** environment variable of Mathematica, e.g. `~/.Mathematica/Applications/`. This can be done with the command `make install`.

C.3.4 Usage

After successful installation, the program can be loaded into a Mathematica session using the command

```
In[1]:= Needs[``PSLQfast`'']
```

The functions defined in the package can be displayed using

```
In[2]:= ?"PSLQfast`*"
```

The usage of the function is quite simple:

```
In[3]:= PSLQfast[numbers,precision]
```

Required arguments are

- **numbers**, the list of real numbers (x_i in C.4), either already numeric values with high precision or in a way that **N**[] evaluates it to a numeric value. Imaginary parts smaller than $10^{-\texttt{precision}+10}$ are ignored.
- **precision**, an integer, the precision with which to perform the computation. As a rule of thumb, it should be about 20 digits per number in **numbers**.

The function returns, if evaluation was successful, a list of integers a_i which satisfy equation C.4. If it fails to find a relation it returns the string `ERR_NO_RELATION`.

C.3.5 Examples

As an example, let us show how one can use it to express the values of GPLs at for constant arguments in terms of transcendental numbers. In order to express the MPLs $G(\vec{m}, x)$ with indices $m_i \in \{0, 1, 2\}$ at $x = 1$ it is found that at transcendental weight four the basis

$$\vec{n} = \left(\frac{\log^4(2)}{24} + \mathrm{Li}_4\left(\frac{1}{2}\right), \frac{\pi^4}{360}, \frac{\log^4(2)}{24}, \log(2)\zeta(3), \log^2(2)\frac{\pi^2}{6}\right) \tag{C.5}$$

is sufficient.

The value of $G(2, 1, 0, 2, 1)$ evaluates to

$$\begin{aligned} G(2,1,0,2,1) = -0.&24102207530030056391352609470264 3 \\ &09503305928498999045988057519400365933361 0 \\ &33610259185981671560504391 . \end{aligned} \tag{C.6}$$

Plugging this into the function yields

```
In[142]:= PSLQfast[{-0.24102207530030056391352609470264 3\
          09503305928498999045988057519400365933361 0\
          18598167156050439163778057069307621 22,
          Log[2]^4/24 + PolyLog[4, 1/2], Pi^4/360,
          Log[2]^4/24, Log[2] Zeta[3], Log[2]^2 Zeta[2]},
          100]

Out[142]= {-4, 16, -66, 0, 13, -3}
```

Which gives the result

$$G(2,1,0,2,1) = \frac{11\pi^4}{240} - \frac{\pi^2}{8}\log(2) + \frac{1}{6}\log^4(2) + 4\mathrm{Li}_4\left(\frac{1}{2}\right) + \frac{13}{4}\log(2)\zeta(3)\ . \tag{C.7}$$

Note that in the symbol of this constant vanishes.

Furthermore, the algorithm can also be used to derive relations between logarithms, a feature that is implemented in the function **GuessRelations**[_] of the `MPLTools` package (see section C.1).

C.3.6 Description of the functions in the package

PSLQfast[Alpha_**List** , PREC_**Integer**]

runs the PSLQ algorithm on the number list Alpha, which has to consist of real numeric values of at least precision PREC. PREC is the precision with which the algorithm is run. If it is exhausted without finding a relation the String `ERR_NO_RELATION` is returned. As a rule of thumb about 20 digits precision per number are needed.

ReloadPSLQ[]

In the event that PSLQ crashes, reload the MathLink with ReloadPSLQ[].

C.4 The symbol and coproduct formalism - the package CSimplify.m

The package `CSimplify` contains all the main routines for computation and integration of both the pure symbol calculus as described in section 3.2.4 and the coproduct in section 3.3. Its use is described in examples in Appendix D. In this section we give an overview over the most important functions contained in the package.

The automatic simplification routines that reduce the appearing tensor product factors to a minimal set should work "out of the box" in many cases. If the index structure of the GPLs involved is very complicated, though, some functions need to be modified by the user or extra identities have to be provided separately.

Generally speaking this package contains both algorithms independently of each other, and therefore the symbol in two different notations. They can, however, be converted into each other with ease. For each of the two ways of arriving at a rewritten expression, different settings have to to be chosen, as will be described in the following and can also be seen in the examples in appendix D.

C.4.1 Installation

Once the package file `CSimplify.m` has been copied to a location which is included in the $**Path** environment variable of Mathematica, it can be loaded using the command

In[1]:= <<**CSimplify**‘;

It requires the packages `MPLTools` for general manipulations, `MPLEval` for the numerical evaluation and `PSLQfast` for guessing of the parts lost in the symbol map or primitive elements of the coproduct.

In[2]:= ?”CSimplify‘∗”

produces a list of all public objects defined in the package.

$IntegrationMethod = **UseMPLs**

Option to choose whether to integrate a symbol using projectors (= **UseProjectors**) or to integrate the symbol directly into MPLs (=**UseMPLs**) during the use of **CSimplify**[_].

C.4.2 Functions for numerical evaluation to be modified by the user

During the application of the algorithms, there are several crucial steps where, depending on the problem at hand, the automatic treatment can fail. For this reason the function used for numerical evaluation throughout the package can be modified by the user.

Evalf[**expr**_]:= **expr**/. **MPLEval**[$**values**,$**signs**]//. $**values**

If this standard definition is taken, then the followin two lists have to be defined as well:

$**values** = {}

A replacement list containing numerical values for each variable in the problem with precision $MPLPrecision. Used by **Evalf**[_].

Example:

$**values**={x → 0.418124937089656145694505084975389763712882995605468 75‘100.,
y → 0.095553784044104639328054418001556769013404846191406 25‘100.,
z → 0.486321278866239214977440497023053467273712158203125‘99.976};

$**signs** = {}

A replacement list detailing the infinitesimal imaginary parts of the necessary variables in the problem.

Example:

$**signs**={**Sgn**[x]−>1,**Sgn**[y]−>−1};

C.4.3 Computation of the coproduct

While not always necessary, it is useful to set the following options, also to make the simplification of the symbol possible and ensure proper treatment of cuts:

$limit = {}

When computing transformations on MPLs, often cuts are crossed. $limit is a replacement list that has to contain this transformation in order to ensure that the analytical continuation is performed properly.

$cutTreatmentList = {}

is a list that contains the prescription of how to deal with the cuts encountered in the computation. It has to be of the form and can be generated from the output of **CSimplify**[_,1] automatically.

$cutTreatmentList={**Log**[a]−>**Log**[b]+i π, ...};

t[a_,b__]

implements the tensor product in the space where the coproduct lives with its multilinearity. Multiplication is defined as **t**[a_,b_]**t**[c_,d_] :> **t**[a c,b d].

expr/.Δ

applies the coproduct to any **PolyLog**[_], **Log**[_], **G**[_], **J**[_] and **Zeta**[_], π functions and returns the result in terms of **t**[**J**[_], **J**[_]] tensors. The result is already regularized.

Δ11[**expr**_]

Δ111[**expr**_]
Δ12[**expr**_]
Δ21[**expr**_]

Δ1111[**expr**_]

Δ211[**expr**_]
Δ121[**expr**_]
Δ112[**expr**_]

Δ31[**expr**_]
Δ22[**expr**_]
Δ13[**expr**_]

compute the corresponding quantities $\Delta_{i_1,\ldots,i_k}$ of [**expr**].

CprSF[**expr**_]:= **Collect**[**ExpandAll**[#1,**log**[_]],**t**[__]]& [
expr //. $cutTreatmentList//. $limit/. **Log**−>**log**
//. **log**[x_]:>**logSF**[x,$integrationvars] //. $extraIds]]

is the function used to bring the logarithms in the symbol in the **t**[__] representation into a standard form. It can be modified by the user. The default version first applies $cutTreatmentList, then takes the limit in the rest of the expressions and then performs transformations using **logSF**[_] to bring the cut blind logarithms **log**[_] into a form which can be integrated directly. If this fails the user can add additional identities using $extraIds.

log[x_]

is designed to be a cut-blind logarithm, i.e. log[x]=log[-x], etc. It also does prime factor decomposition for integers and decomposes logarithms of products into sums of logarithms. A symbol that has been brought into its "standardized form" in the **t**[ ] notation is written using these functions.

logSF[**expr**_]

attempts to bring the **log**[x_] terms into a standard form, i.e. a form where the MPL terms can be read off. The terms are manipulated in a way that they have the form **log**[1−x1/f[x2]] or **log**[1−x2/c] or **log**[c] where x1, x2 are the integration variables $integrationvars and c are constants.

$extraIds = {}

Replacement list used by the default version of **CprSF**[_] to transform **log**[_] terms that have not been brought to a form which can be integrated directly 'manually'. It should be of the form {**log**[x]−>**log**[y]+**log**[z],...}.

C.4.4 Computation of the symbol

T[__]

The tensor product of the space the symbol lives in. Its computation rules are described in section 3.2.2.

S[**expr**_]:= CollectT[**S0**[**expr** /. SimpletoG /. **GtoOldConvention** /. {π−>0,**Zeta**[_]:>0}]
//. T[x__]:>T@@(NormalizeTens[#1]&)/@{x}]

is the function that is used internally in the routines **SIntegrate**[ ], **SIntegrateInit**[ ] and **SymSimplify**[ ] to compute the symbol of an expression and writes it in terms of T[__] tensors. It can and has to be modified by the user. It should produce a 'fully expanded' and unambiguous symbol.

The functions that compute the symbol according to the definition in terms of polygons as given in [67] is

S0[**expr**_]

The iterative definition of the symbol is given by

SIterative[**expr**_**G**]

which computes the symbol of **expr**, which has to be a MPL in the 'old' notation using the iterative definition.

S0[**expr**_]

computes the symbol of **expr** using the polygon definition. It performs some simplifications on the arguments.

NormalizeTens[**expr**_]

factors the terms in the tensor such that the variable in there has a prefactor equal to unity and numbers are factored by their absolute value times a number of norm one.

C.4.5 Tests on the symbol, conversion between the two notations

IntegrabilityTest[**symbol**_]

gives zero if **symbol** (in T[__] notation) fulfills the integrability condition. There should be no redundancy in the variables.

δ[**symbol**_]

performs the symmetry operation equation 3.31 on the weight four symbol **symbol**. If the result vanishes the symbol can be integrated in terms of logarithms and polylogarithms.

ttoT[**expr**_]
Ttot[**expr**_]

converts a symbol in terms of **t**[__] tensors to a symbol in terms of T[ ] Tensors and the other way around.

CollectTens[**expr**_]

collects for T[__], **t**[__] tensors in **expr**.

Tensargs[**expr**_]

returns a list of the tensor product factors (both **t**[__] and T[__]) present in expr.

C.4.6 Symbol integration using Projectors

Projectors

expr/.T−>Π

applies the projector Π onto the symbol **expr**.

$projectors

contains the 'tensored' projectors defined in equation (3.37) used to project the symbol onto the different subspaces generated by shuffles of MPLs up to weight four.

The order is

```
{ {1 },
  {2, 1 ⊗ 1 },
  {3, 2 ⊗ 1, 1 ⊗ 1 ⊗ 1},
  {4, 3 ⊗ 1, 2 ⊗ 1 ⊗ 1, 1 ⊗ 1 ⊗ 1 ⊗ 1}}.
```

Basis computation

FindBasis[inputfunctions,inputsymbols]

computes the independent functions of **inputfunctions**. **inputsymbols** have to be the symbols already projected for the desired subspace of $H_1 \otimes \ldots \otimes H_n$.

Example:

```
baseFunctions=Table[FindBasis[baseInput[[i]],(baseInput[[i]]//S)/.$projectors[[i ,1]]],{ i ,1,4}];
```

GenerateBasis[basisfunctions_**List**]

Given a list of lists of independent functions, it returns a complete basis up to weight four to be used with **SIntegrateInit**[ ].

SIntegrateInit[func_**List**,w_**Integer**]

initializes the symbol integration for weight w. func has to be a list containing as sub-lists the basis functions for each step of the integration. **GenerateBasis**[_] generates these lists.

Example:

```
base=GenerateBasis[baseFunctions];

SIntegrateInit[base[[#]],#]&/@Range[1,4];
```

KernelPartGuessInit[funcs_**List**,PSLQPrecision_**Integer**]

initializes the variables needed for guessing the kernel part. See D.1 for example usage.

SIntegrateStateSave[filename_**String**,Description_**String**]

saves the state of the package needed for symbol integration to a text file. Useful when the basis derivation and initialization takes a long time. The definitions can be loaded using the **Get**[_] command (or '<<').

```
$splitfunc
$funcsym
```

After **SIntegrateInit**[_] has been called, $splitfunc[[i , j]] contains for weight i the basis functions used for reconstructing the projection of $projectors[[i , j]] and $funcsym[[i,j]] contains for weight i the symbol of the basis functions used for reconstructing the projection of $projectors[[i , j]] .

```
$SymbolKernelConstants = {{},{π^2/6},{π^2/6 Log[2],Zeta[3]},
                          {1/24 Log[2] +PolyLog[4,\frac{1}{2}],π^4/360} }
```

contains the constants of the kernel part. Can be changed by the user.

$SymbolKernelFunctions

contains the functions that make up the kernel part of the symbol and is written by **KernelPartGuessInit**[].

Symbol integration

SIntegrate[**symbol_**,w_**Integer**]

integrates the symbol **symbol** of weight w using projectors and basis functions.

SymSimplify[**expr_**,**weight_Integer**,**values_List**,**signs_List**]

Computes the symbol of **expr** using **S**[_] and integrates it in terms of basis functions. It then guesses the kernel part using PSLQ.

expr: the expression to simplify
weight: its weight
values: list of rules to use for plugging in values
signs: the signs of the infinitesimal imaginary parts of the values

KernelPartGuess[**expr_**, **weight_Integer**, **values_List**, **signs_List**]

Guesses **expr** in terms of $SymbolKernelConstants and $SymbolKernelFunctions using the **values** and **signs** for numerical evaluation.

C.4.7 Symbol integration in terms of MPLs

CIntegrate[**symbol_**,**weight_Integer**]

integrates the symbol given in **t**[__] notation to an expression in terms of MPLs with arguments $integrationvars.

Cop[**expr_**, **weight_Integer**]

takes an expression, computes the fully decomposed coproduct $\Delta_{1,\ldots,1}$, i.e. the symbol, of the form **t**[__] and integrates it. For this it uses $cutTreatmentList, $limit and $integrationvars. In the end a check is performed (if $SymbolIntegrationCheck is set to **True**) that indeed the fully decomposed coproduct of the integrated expression is equal to that of the input expression.

$cutMonitor is used save possible cuts of the coproduct after an evaluation that have to be reduced to 'integrable form' with $cutTreatmentList. $coproductMonitor is used to write out the terms that show up in the coproduct after everything has been applied and everything should in a form that can be readily 'integrated'. This list can be checked to see that this is indeed the case.

C.4.8 Simplification using the coproduct formalism

CopHi[**expr_**,**Function**]

applies **Function** (usually a coproduct like $\Delta 211$ but not the 'total decompositions' $\Delta 11$, $\Delta 111$, etc.) on **expr** and then uses $lowerweightids to simplify the expression as much as possible and then 'integrates' according to **Function**.

CSimplify[**expr_**,**weight_Integer**]

rewrites an expression in terms of MPLs of $integrationvars. The variables that have to be set are $integrationvars and $limit and evaluation using **Evalf**[_] has to produce numerical values of sufficient precision.

for weights greater than one, $cutTreatmentList has to be set.

for weights greater than two, $lowerweightids have to be set.

$lowerweightids

List that contains all identities needed to reduce all MPLs encountered in the computations of $\Delta 21$, $\Delta 211$ and $\Delta 31$ to the basic set, i.e. the set of MPLs defined by the choice of arguments $integrationvars.

$useSimplelowerweightids = **False**

If set to **True**: enforce cancellations by giving only the parts that will likely remain in the required lower weight identities for that factor. In that case $lowerweightidsFactor1 for the identities of the first tensor product factor and $lowerweightidsFactorn for the other tensor product factors have to be set accordingly. See also the example in section D.2 and the discussion in section 3.3.3.

$lowerweightidsFactor1

should be a replacement list of the lower weight identities for the first factor of the tensor products in simplified form, that means only the constant zeta factors.

$lowerweightidsFactorn

should be a replacement list of the lower weight identities for the second to last factor of the tensor products in simplified form, that means only the parts free of primitive values of the coproduct.

ConstGuess[**expr**_, **weight_Integer**]

guesses the primitive values that make up **expr** which can either be a numerical value or something that evaluates with **Evalf**[ ]

```
$ConstantVector = {{}, {π^2/6}, {Zeta[3]}, {π^4/360, -(π^2 Log[2]^2)/24 +
                          Log[2]^4/24 + PolyLog[4, 1/2] + (7 Log[2] Zeta[3])/8}};

$ConstantVectorIm = {{}, {}, {π^3}, {π Zeta[3]}};
```

contain for each weight the primitive values of the real and imaginary part. $ConstantVector also contains θ_4 which is a constant vanishing under $\Delta_{3,1}$ and nonzero under $\Delta_{1,3}$. Both are used by **ConstGuess**[__] and can be modified by the user.

C.4.9 Miscellaneous

w1SimpleLogGuess[**expr_G**, extraIds_**List**]

This function can be used to express **G**[a_,b_] in **G**[__,$integrationvars [[1]]]
and **G**[__,$integrationvars [[2]]] . However, it only does this up to real parts. It does not compute cuts. Intended for use with in $lowerweightids to automatically derive needed limits for weight one.

ExpressionExport[fileName_**String**,symbols_**List**,Description_**String**]

writes a text file of the definitions of the symbols (in the Mathematica sense!) that can be read into Mathematica using the << operator. Compared to Mathematica's internal functions for exporting expressions it only writes the explicit definitions and nothing else. The list of symbols has to be

given as a list of symbol names as strings, e.g. symbols = {"symbol1", "symbol2"}. Description is a string that contains information which is printed when the file is loaded. The names of the symbols, which are contained in the file are printed as well.

D

Example Applications of the Algebraic Tools for Feynman Integrals

The intention of this appendix is to present concrete use cases for the developed Mathematica code which will also serve as example for the algorithms presented previously. Another goal is to elaborate on the rationale behind the routines.

The installation of the packages and the containing functions are described in appendix C.

The three examples in this appendix illustrate the potential of the proposed methods. In section D.1 it is shown how the packages can be used to shorten a known expression. In section D.2 nontrivial transformations among MPLs which are needed for the solution of the differential equation (5.80) which was described in section 5.4.3. The last example in section D.3 illustrates how the coproduct and symbol formalism in combination with the PSLQ algorithm can be used to solve an integral and rewrite the solution in terms of simple functions with little additional manual input.

D.1 Simplification - shortening a result

In this section it is demonstrated how the symbol formalism can be used to express a complicated result in terms of simple functions with complicated arguments. For this, the symbol integration algorithm as described in section 3.2.4 is suitable. A basis of functions has to be derived first (c.f. equation (3.33)), before the simplification can be performed. The package can be loaded using the command

```
In[1]:= CSimplify`;
```

Generating the basis and initialization

Let us suppose that from previous considerations we know that the symbol of the expression we would like to simplify and express in Polylogarithms contains only terms of the form of equation (3.32), that is

$$x_i,\ 1-x_i \qquad \text{for } \ x_i = x, y, z\ ,$$

Therefore we attempt to write the result in logarithms and polylogarithms of the argument set of table 3.2.3 which we have stored in `args`. Since we suspect that there is, at least at low weights, some redundancy, we create for each weight a list of possible functions.

```
In[2] := baseInput = {Log[#] & /@ args, PolyLog[2, #] & /@ args,
                      PolyLog[3, #] & /@ args, PolyLog[4, #] & /@ args};
```

For each weight, we now select the independent ones, that is, independent up to products of lower weight functions.

```
In[3] := baseFunctions = FindBasis[ baseInput[[#]],
                          (baseInput[[#]] /. x -> 1 - y - z // S) /. $projectors[[#, 1]]]
                         & /@ Range[1, 4];
```

`FindBasis` takes as second argument the symbol of the function (computed using `S`) which has already been projected using the appropriate projector from equation (3.34) and returns the independent functions. x has been replaced by its definition in terms of y and z to remove all redundancy in the variables.

The next step consists of generating all the parts of the basis that consist of products of lower weight of basis functions (see equation (3.33)).

```
In[4] := base = GenerateBasis[baseFunctions];
```

The symbol integration routines can be initialized for weights one to four using

```
In[5] := SIntegrateInit[base[[#]], #] & /@ Range[1, 4];
```

Finally, the kernel part guessing routines are initialized by generating again a list of functions that are can possibly appear in that part.

```
In[6] := KernelVec = {{}, {}, π^2/6 base[[1, 1]],
                      Join[Zeta[3] base[[1,  1]],  π^2/6 Flatten[base[[2]]]]};

In[7] := KernelPartGuessInit[KernelVec, $MPLPrecision - 20];
```

The second argument of `KernelPartGuessInit` is the precision with which the PSLQ algorithm is run. It is in this case 20 digits less than what is used for the evaluation of MPLs. The precision should be about as high as 20 times the number of "kernel elements" (see also appendix C.3). In principle, most of the parts of the original expression lost by the symbol map could also be restored using the coproduct. However, in this context this has the downside that more identities have to be derived. The "guessing" using PSLQ works reasonably well for moderate numbers of basis elements $b_i^{(1,2)}$, which is the case here. At weight four, the PSLQ algorithm has only to be run on 36 different numbers which is reasonably efficient.

We are now ready to perform the simplifications. At this point it is useful to save the state of the initialization to be able to load it more quickly later since some steps of the initialization can be lengthy.

```
In[8] := $Description ="The_basis_of_up_to_weight_four_PolyLogs_of_combinations_of_x,y,z.";

In[9] := SIntegrateStateSave["PolyLogSimplicationBase_xyz.txt"];
```

This file can be loaded and the state of the package restored with the command

```
<<"PolyLogSimplicationBase_xyz.txt";
```

Performing a simplification

At this point we need to choose a valid parameter point for the kernel guessing. The following lines prepare the necessary parameters.

```
In[10]:= xval = SetPrecision[Random[],$MPLPrecision];
         yval = SetPrecision[RandomReal[{0, 1 - xval}],$MLPPrecision];
         $values = {x -> xval, y -> yval, z -> 1 - yval - xval};
         $signs = {};
```

`$values` contains the values that are needed to evaluate all appearing expressions to high precision and `$signs` their infinitesimal signs.

Let the expression to be simplified be

```
In[11]:= expr= G[1 - z, y] G[0, 1, z] - G[0, y] (G[1, 0, z] + 2 G[1, 1, z]) +
    G[-z, y] (G[0, 1, z] + G[1, 0, z] + 2 G[1, 1, z]) +
    G[0, z] (-G[0, 1 - z, y] + G[1, 0, y] - G[1 - z, 0, y] + G[-z, 1 - z, y]) +
    G[1, z] (-2 G[0, 0, y] - 2 G[0, 1 - z, y] + G[0, -z, y] +
    G[1, 0, y] - 2 G[1 - z, 0, y] + G[1 - z, -z, y] + G[-z, 0, y] +
    2 G[-z, 1 - z, y]) + 2 G[0, 0, 1, z] - 2 G[0, 0, 1 - z, y] +
    G[0, 1, 0, y] + G[0, 1, 0, z] + 2 G[0, 1, 1, z] - 2 G[0, 1 - z, 0, y] -
    2 G[0, 1 - z, 1 - z, y] + G[0, -z, 1 - z, y] + 2 G[1, 0, 0, y] +
    G[1, 0, 1, z] + G[1, 0, 1 - z, y] + G[1, 1 - z, 0, y] -
    2 G[1 - z, 0, 0, y] - 2 G[1 - z, 0, 1 - z, y] + G[1 - z, 1, 0, y] -
    2 G[1 - z, 1 - z, 0, y] + G[1 - z, -z, 1 - z, y] +
    G[-z, 0, 1 - z, y] + G[-z, 1 - z, 0, y] + 2 G[-z, 1 - z, 1 - z, y];
```

We can now perform the simplification by using

```
In[12]:= result = SymSimplify[expr, 3, $values, $signs] // Simplify

Out[12]= -(1/ 6) (Log[x] + Log[y] + Log[z]) ( π^2 - 6 Log[1 - x] Log[x] +
   6 Log[x] Log[y] - 6 Log[1 - y] Log[y] - 6 PolyLog[2, x] - 6 PolyLog[2, y])
```

The result is considerably shorter, contains only simple (poly-)logarithms and the symmetry under the exchange of y and x is now manifest.

Up to weight three all combinations of MPLs with above index set can be written using the basis we just used. At weight four, this is not always the case any more. However, we can perform the check whether Goncharov's condition on the symbol is fulfilled (see equation (3.31)). For this, the function δ has been defined, which vanishes if the symbol can be integrated in terms of logarithms and polylogarithms only.

D.2 Deriving nontrivial transformations among MPLs

In chapter 3 it was discussed that often transformations among MPLs are desired where the length of the resulting expressions is of no interest but one would express the result of MPLs of certain simple arguments. In order to do this in this framework, an alternative symbol integration algorithm was presented in section 3.2.7. This framework can be used to take limits of MPLs, perform their analytical continuations or variable transformations.

As an illustration, the transformation of the differential equation required for the integration of the two-loop integral $\mathcal{I}^{(B)}_{213,1}$, equation (5.73), described in section 5.4.3, will be used. In order to do this the following re-writing of MPLs was needed:

$$G\left(a_i; y \to \tfrac{(1+x)^2}{x} - 2 - z\right) \quad \text{with } a_i \in \{0, -1, -2-z, \tfrac{1}{z}\} \tag{D.1}$$

up to weight four, and the result should be expressed in MPLs

$$G(a_i(x); z) \quad \text{and} \quad G(b_i; x) \text{ with } b_i \in \mathcal{C}\ . \tag{D.2}$$

The package can be used to derive these equations with ease. Let us see how this is done.

Initialization

After loading of the package in Mathematica,

```
In[1]:= Needs["CSimplify`"];
```

we set the limit we want to take and how we want to re-express it:

```
In[2]:= $limit = {y -> -(2 - (1 + x)^2/x + z)} // FullSimplify;

In[3]:= $integrationvars = {z, x};
```

The last line sets the order according to equation (D.2).

We then need to initialize the numerical evaluation by setting the precision and choosing random values in the proper region.

```
In[4]:= $MPLPrecision = 100;

In[5]:= xval = SetPrecision[RandomReal[{0, 1}], $MPLPrecision];

In[6]:= zval = SetPrecision[RandomReal[{xval, 1}], $MPLPrecision];

In[7]:= $values = {x -> xval, z -> zval,
                   y -> (y /. $limit /. {x -> xval, z -> zval})};

In[8]:= $signs = {Sgn[x] -> 0, Sgn[y] -> 1, Sgn[z] -> 1};
```

The signs of the infinitesimal imaginary parts of the variables have been chosen according to equation (5.16).

The next step consists of generating the functions to transform:

```
In[9]:= indexSet = {0, -1, -2 - z, 1/z};

In[10]:= inputFunctions = G @@@ # & /@ Table[Append[#, y] & /@
                                              Tuples[indexSet, i], {i, 1, 4}];
```

Now, `inputFunctions` is a list of four lists containing the functions of a specific weight with all possible combinations of indices from `indexSet`.

Derivation of the Identities

Starting from weight one we can now derive the identities. By setting

```
In[11]:= $verbose = 1;
```

or any other value between 0 and 3 we can control how much information is printed during by the functions.

For weight one, where all functions are logarithms, these are derived automatically by performing the transformation disregarding the cuts and then guessing the correct factors of $i\pi$ by numerical evaluation.

```
In[12]:= MPLsOfyInxz1 = # -> CSimplify[#, 1] & /@ inputFunctions[[1]]

Out[12]= {G[0, y] -> -G[0, x] + G[-I, x] + G[I, x] + G[(1 + x^2)/x, z],
          G[-1, y] -> -G[0, x] + G[-(1/2) - (I Sqrt[3])/2, x] +
          G[-(1/2) + (I Sqrt[3])/2, x] + G[(1 + x + x^2)/x, z],
          G[-2 - z, y] -> -G[-2, z] + 2 G[-1, x] - G[0, x] - Log[2],
          G[1/z, y] -> G[1/x, z] + G[x, z]}
```

Before computing the identities for weight two, the prescription for dealing with the cuts have to be set (even though, as in this case, no cuts are crossed). The input from the previous computation can be used for this.

```
In[13]:= $cutTreatmentList = MPLsOfyInxz1 /. SimpleReplacements;
```

`SimpleReplacements` just replaces all G functions by logarithms. The weight two identities can then be computed via

```
In[14]:= MPLsOfyInxz2 = # -> CSimplify[#, 2] & /@ inputFunctions[[2]];
```

For the computation at weight two, the code just computes the symbol of the input, applies the cut prescriptions, integrates it using the algorithm from section 3.2.7 and guesses the remaining factor of π^2 by evaluating both sides numerically.

At weight three the input from lower weights is needed. It is set by

```
In[15]:= $lowerweightids = Join[MPLsOfyInxz2, MPLsOfyInxz2,
                        {G[a_, b_] :> w1SimpleLogGuess[G[a, b], {}]}] // Dispatch;
```

These identities are used during the simplification of

$$\Delta_{2,1}(F - F_{1,1,1}) = \sum_{i_1,i_2} c_{i_1,i_2} \left(f^{(2)}_{i_1} \otimes f^{(1)}_{i_1} \right) , \tag{D.3}$$

where F denotes the function to be transformed and $F_{1,1,1}$ denotes its integrated symbol of F. The identities of lower weight `MPLsOfyInxz1,2` are used to reduce the first factors $f^{(2)}_{i_1}$ of weight 2 to the standard set. What is left unreduced in the second factor (the "limits" discussed in section 3.3.3.) are simplified automatically using the function `w1SimpleLogGuess[_,_]`. The use of `Dispatch` speeds up replacement considerably [1]. After these steps, everything that should be left are tensors of the form

$$\sum_{i_1,i_2} c_{\pi^2,i_2} \left(\pi^2 \otimes f^{(1)}_{i_1} \right) \tag{D.4}$$

which can be 'integrated' by replacing the tensor product $\otimes$ by ordinary multiplication. Finally, the multiples of ζ_3 are determined by evaluating both sides numerically and using PSLQ. All this is done automatically using

```
In[16]:= MPLsOfyInxz3 = # -> CSimplify[#, 3] & /@ inputFunctions[[3]];
```

For weight four all steps are now known and it is in principle sufficient to proceed analogously to weight three, adding the `MPLsOfyInxz3` to `$lowerweightids`. To speed up computations, however, let us add use a trick. As it could be seen from equation (D.3) to (D.4), huge cancellations are taking place in the first factor of the tensor products after the application of `$lowerweightids`, since only the π^2 terms survive. This will be the same during simplification of the result of $\Delta_{2,1,1}$ and $\Delta_{3,1}$ at weight four. We can anticipate these cancellations by only keeping the constant terms in the identities of lower weight.

```
In[17]:= $useSimplelowerweightids = True;

In[18]:= $lowerweightidsFactor1 = #[[1]] ->
          (Coefficient[#[[2]], Zeta[3]] Zeta[3] +
           Coefficient[#[[2]], π, 2] π^2 +
           Coefficient[#[[2]], π] π +
           Coefficient[#[[2]], π, 3] π^3 /. G[__] -> 0) & /@
     Join[MPLsOfyInxz3, MPLsOfyInxz2, MPLsOfyInxz1] // Dispatch;

In[19]:= $lowerweightidsFactorn :=
                    {G[a_, b_] :> w1SimpleLogGuess[G[a, b], $extraIds]};
```

1. Probably Mathematica's best kept secret.

To save even more time we can also switch off the check that the symbol has been properly integrated, as it will likely give an error message elsewhere if it fails (and has been working up to now):

```
In[20]:= $SymbolIntegrationCheck = False;
```

Again, we do

```
In[21]:= MPLsOfyInxz4 = # -> CSimplify[#, 4] & /@ inputFunctions[[4]];
```

to compute the last set of identities.

Exporting the identities

The derived identities can be exported using

```
In[22]:= Description = "<␣some␣descriptive␣Text␣stored␣with␣the␣identites␣>";

In[23]:= ExpressionExport[ "MPLsOfyInxz.txt",
           {"MPLsOfyInxz1", "MPLsOfyInxz2", "MPLsOfyInxz3", "MPLsOfyInxz4"},
             Description ];
```

The definitions are then loaded with the command

```
In[24]:= << "MPLsOfyInxz.txt";
```

which also prints the `Description` along with the symbol names defined in the file.

D.3 Integration

In this section it is demonstrated how the symbol formalism and the packages can be used for an integration. As an example let us take

$$I = \int_0^1 \mathrm{d}x \frac{x \arctan\left(\frac{2\rho x}{1+x^2}\right)}{4\rho^2 x^2 + (1+x^2)^2} \,, \tag{D.5}$$

where ρ is a parameter between 0 and 1. Remembering that

$$\begin{aligned} \arctan(\alpha) &= \frac{1}{2i}(\log(1+i\alpha) - \log(1-i\alpha)) = \\ &= \frac{1}{2i}(G(0;1+i\alpha) - G(0;1-i\alpha)) \,, \end{aligned} \tag{D.6}$$

we realize that the above integral can easily be done in terms of MPLs if we

1. rewrite the MPLs in terms of other MPLs with only x in the argument and
2. use partial fractioning and partial integration that the prefactor of each MPL takes the form $\frac{1}{x-c}$, with c independent of x.

Initialization

Again, as in the previous example, we load the packages, initialize numerical evaluation and set the integration variable.

```
In[1]:= Needs["CSimplify`"];

In[2]:= $values = {x -> SetPrecision[Random[],$MPLPrecision],
                   ρ -> SetPrecision[Random[], $MPLPrecision]};
```

```
In[3]:= $signs = {};

In[4]:= $integrationvars = {x};
```

Integration

The integrand becomes after partial fractioning (for details, see the example Mathematica notebook)

$$\frac{i}{16\rho\sqrt{1+\rho^2}}\left(\frac{1}{i(\rho-\sqrt{1+\rho^2})+x}+\frac{1}{i(\rho-\sqrt{1+\rho^2})-x}+\right.$$
$$\left.+\frac{1}{i(\rho+\sqrt{1+\rho^2})+x}+\frac{1}{i(\rho+\sqrt{1+\rho^2})-x}\right)\times \tag{D.7}$$
$$\times\left(G\left(0;1-\frac{2i\rho x}{1+x^2}\right)-G\left(0;1+\frac{2i\rho x}{1+x^2}\right)\right)$$

The identities rewriting for rewriting the MPLs such that they are of the form $G(c;x)$ can be derived with

```
In[5]:= identities = # -> CSimplify[#, 1] & /@
              {G[0, 1 - (2 I ρ x)/(1 + x^2)], G[0, 1 + (2 I ρ x)/(1 + x^2)]}
                  // Simplify[#, 0 < ρ < 1] &

Out[5]= {G[0, 1 - (2 I ρ x)/(1 + x^2)] -> -G[-I, x] - G[I, x] +
            G[-I (-ρ + Sqrt[1 + ρ^2]), x] + G[I (ρ + Sqrt[1 + ρ^2]), x],
          G[0, 1 + (2 I ρ x)/(1 + x^2)] -> -G[-I, x] - G[I, x] +
            G[I (-ρ + Sqrt[1 + ρ^2]), x] + G[-I (ρ + Sqrt[1 + ρ^2]), x]}
```

These identities can then be used on the partial-fractioned integrand, which is then expanded out and each term is integrated in x using the definition of MPLs equation (3.1):

```
In[6]:= (integrandPartialFractioned /. identities // Expand) /.
            G[a_, x]/(x + b__) :> G[-Plus[b], a, x] // Simplify[#, 0 < ρ < 1] &

Out[6]= (1/(16 ρ Sqrt[1 + ρ^2]))I
          (G[-I (-ρ + Sqrt[1 + ρ^2]), -I (-ρ + Sqrt[1 + ρ^2]), x] + ...)
```

The primitive now contains 16 MPLs of weight two in x with the indices $i(\pm\rho\pm\sqrt{1+\rho^2})$. They have to be evaluated at $x=1$ (at the lower integration boundary all the MPLs in this expression vanish since their rightmost index is different from zero).

Simplification

Let us see whether this result can be further simplified using the available machinery. Computing the symbol, we find that not all tensor product factors have been reduced to the minimal set automatically. In fact, we find that the terms are still not independent of each other.

```
In[7]:= integral = primitive /. x -> 1;

In[8]:= $integrationvars = {ρ};

In[9]:= symbol = integral // Δ11 // Nce // Cprsf // Simplify;
```

```
In[10]:= logFactors = symbol // tCases

Out[10]= {log[1 - I ρ], log[1 + I ρ],
          log[-ρ + Sqrt[1 + ρ^2]], log[-I - ρ + Sqrt[1 + ρ^2]],
          log[I - ρ + Sqrt[1 + ρ^2]], log[ρ + Sqrt[1 + ρ^2]],
          log[-I + ρ + Sqrt[1 + ρ^2]], log[I + ρ + Sqrt[1 + ρ^2]]}
```

Instead of attempting to attempting to compute relations between them "by hand", there is a way to guess these using the PSLQ algorithm. The function `GuessRelations` takes a list of functions, for example logarithms, evaluates them to high precision and then attempts to find a relation between these numbers, therefore finding a relation between the logarithms, provided the functions were evaluated for reasonably "random" variables (see also appendix C.3). This relation is then used to write a replacement list to express the rightmost function in the list in terms of the others. This function is then removed from the list and the PSLQ algorithm run again. When no more relation between the left over functions can be found, the algorithm stops. In the present case three relations are obtained.

```
In[11]:= Logidentities = GuessRelations[
                  Prepend[logFactors /. log -> Log, I π, Evalf] /.Log -> log

Out[11]= {log[I + ρ + Sqrt[1 + ρ^2]] -> I π +
           log[-I - ρ + Sqrt[1 + ρ^2]] - log[I - ρ + Sqrt[1 + ρ^2]]
           + log[-I + ρ + Sqrt[1 + ρ^2]], ...}
```

These identities can be used to simplify the symbol. We find

```
In[12]:= simplifiedsymbol = symbol //. Logidentities //
                  ExpandAll[#, log[__]] & // Simplify

Out[12]= (t[π, log[1 - I ρ]] + t[π, log[1 + I ρ]])
                  /(16 ρ Sqrt[1 + ρ^2])
```

which can be trivially integrated.

The final result is

```
In[13]:= CIntegrate[simplifiedsymbol, 2] /. SimpleReplacements // Simplify;

In[14]:= result = % /. Log[a_] + Log[b_] :> Log[a b] // Simplify
```

$$\int_0^1 \mathrm{d}x \frac{x \arctan\left(\frac{2\rho x}{1+x^2}\right)}{4\rho^2 x^2 + (1+x^2)^2} = \frac{\pi \log(1+\rho^2)}{16\rho\sqrt{1+\rho^2}}\,, \tag{D.8}$$

which can of course be checked numerically:

```
In[15]:= NIntegrate[integrand /. x -> X /. $values, {X, 0, 1}]

Out[15]= 0.0920881

In[16]:= result /. $values

Out[16]= 0.092088066133595606853592874350175145 27.....
```

We remark that during the computation little to none manual manipulation of the integrand was required and that in principle much more complicated integrals could be solved this way, a fact that was exploited in [69] and previous works.

Bibliography

[1] M. PESKIN and D. SCHROEDER, *An Introduction To Quantum Field Theory*. Advanced book classics. Addison-Wesley Publishing Company, 1995.

[2] G. Ecker, *Quantum chromodynamics*, hep-ph/0604165.

[3] A. Denner, *Techniques for calculation of electroweak radiative corrections at the one loop level and results for W physics at LEP-200*, *Fortsch.Phys.* **41** (1993) 307–420, [arXiv:0709.1075].

[4] S. Pokorski, *Gauge Field Theories*. Cambridge Monographs on Mathematical Physics. Cambridge University Press, 2000.

[5] S. Glashow, *Partial Symmetries of Weak Interactions*, *Nucl.Phys.* **22** (1961) 579–588.

[6] P. W. Anderson, *Plasmons, Gauge Invariance, and Mass*, *Phys.Rev.* **130** (1963) 439–442.

[7] F. Englert and R. Brout, *Broken Symmetry and the Mass of Gauge Vector Mesons*, *Phys.Rev.Lett.* **13** (1964) 321–323.

[8] P. W. Higgs, *Broken Symmetries and the Masses of Gauge Bosons*, *Phys.Rev.Lett.* **13** (1964) 508–509.

[9] G. Guralnik, C. Hagen, and T. Kibble, *Global Conservation Laws and Massless Particles*, *Phys.Rev.Lett.* **13** (1964) 585–587.

[10] S. Weinberg, *A Model of Leptons*, *Phys.Rev.Lett.* **19** (1967) 1264–1266.

[11] M. S. Neubauer, *Diboson production at colliders*, *Ann.Rev.Nucl.Part.Sci.* **61** (2011) 223–250.

[12] U. Baur and D. L. Rainwater, *Probing neutral gauge boson selfinteractions in ZZ production at hadron colliders*, *Phys.Rev.* **D62** (2000) 113011, [hep-ph/0008063].

[13] A. Bierweiler, T. Kasprzik, and J. H. Kühn, *Vector-boson pair production at the LHC to $\mathcal{O}(\alpha^3)$ accuracy*, arXiv:1305.5402.

[14] **CMS** Collaboration, S. Chatrchyan et al., *Measurement of the W+W- cross section in pp collisions at sqrt(s) = 7 TeV and limits on anomalous WW gamma and WWZ couplings*, arXiv:1306.1126.

[15] **ATLAS** Collaboration, G. Aad et al., *Measurement of the WW cross section in $\sqrt{s} = 7$ TeV pp collisions with the ATLAS detector and limits on anomalous gauge couplings*, *Phys.Lett.* **B712** (2012) 289–308, [arXiv:1203.6232].

[16] **ATLAS** Collaboration, G. Aad et al., *Measurement of W^+W^- production in pp collisions at $\sqrt{s} = 7$ TeV with the ATLAS detector and limits on anomalous WWZ and $WW\gamma$ couplings*, *Phys.Rev.* **D87** (2013) 112001, [arXiv:1210.2979].

[17] **ATLAS** Collaboration, G. Aad et al., *Measurement of WZ production in proton-proton collisions at $\sqrt{s} = 7$ TeV with the ATLAS detector*, *Eur.Phys.J.* **C72** (2012) 2173, [arXiv:1208.1390].

[18] D. L. Evans, *Diboson production*, in *European Physical Journal Web of Conferences*, vol. 49 of *European Physical Journal Web of Conferences*, p. 8002, May, 2013.

[19] **ATLAS** Collaboration, G. Aad et al., *Measurement of ZZ production in pp collisions at $\sqrt{s} = 7$ TeV and limits on anomalous ZZZ and $ZZ\gamma$ couplings with the ATLAS detector*, *JHEP* **1303** (2013) 128 CERN-PH-EP-2012-318, [arXiv:1211.6096].

[20] **CMS** Collaboration, S. Chatrchyan et al., *Measurement of the ZZ production cross section and search for anomalous couplings in 2 l2l ' final states in pp collisions at* $\sqrt{s} = 7$ *TeV*, *JHEP* **1301** (2013) 063 CMS-SMP-12-007, CERN-PH-EP-2012-336, [arXiv:1211.4890].

[21] M. Gell-Mann, *A Schematic Model of Baryons and Mesons*, *Phys.Lett.* **8** (1964) 214–215.

[22] G. Zweig, *An* su_3 *model for strong interaction symmetry and its breaking; part i*, .

[23] O. Greenberg, *Spin and Unitary Spin Independence in a Paraquark Model of Baryons and Mesons*, *Phys.Rev.Lett.* **13** (1964) 598–602.

[24] M. Han and Y. Nambu, *Three Triplet Model with Double SU(3) Symmetry*, *Phys.Rev.* **139** (1965) B1006–B1010.

[25] D. J. Gross and F. Wilczek, *Ultraviolet behavior of non-abelian gauge theories*, *Phys. Rev. Lett.* **30** (Jun, 1973) 1343–1346.

[26] H. D. Politzer, *Reliable perturbative results for strong interactions?*, *Phys. Rev. Lett.* **30** (Jun, 1973) 1346–1349.

[27] M. Kobayashi and T. Maskawa, *CP-Violation in the Renormalizable Theory of Weak Interaction*, *Progress of Theoretical Physics* **49** (Feb., 1973) 652–657.

[28] A. Bierweiler, T. Kasprzik, H. Kuhn, and S. Uccirati, *Electroweak corrections to W-boson pair production at the LHC*, *JHEP* **1211** (2012) 093, [arXiv:1208.3147].

[29] A. Bierweiler, T. Kasprzik, and J. H. Kuhn, *Electroweak accuracy in V-pair production at the LHC*, arXiv:1208.3404.

[30] E. Accomando, A. Denner, and S. Pozzorini, *Electroweak correction effects in gauge boson pair production at the CERN LHC*, *Phys.Rev.* **D65** (2002) 073003, [hep-ph/0110114].

[31] E. Accomando, A. Denner, and A. Kaiser, *Logarithmic electroweak corrections to gauge-boson pair production at the LHC*, *Nucl.Phys.* **B706** (2005) 325–371, [hep-ph/0409247].

[32] E. Accomando, A. Denner, and C. Meier, *Electroweak corrections to* $W\gamma$ *and* $Z\gamma$ *production at the LHC*, *Eur.Phys.J.* **C47** (2006) 125–146, [hep-ph/0509234].

[33] J. Kuhn, F. Metzler, A. Penin, and S. Uccirati, *Next-to-Next-to-Leading Electroweak Logarithms for W-Pair Production at LHC*, *JHEP* **1106** (2011) 143, [arXiv:1101.2563].

[34] J. Ohnemus, *An Order* $\alpha^- s$ *calculation of hadronic* $W^{\pm}Z$ *production*, *Phys.Rev.* **D44** (1991) 3477–3489.

[35] S. Frixione, *A Next-to-leading order calculation of the cross-section for the production of W+ W- pairs in hadronic collisions*, *Nucl.Phys.* **B410** (1993) 280–324.

[36] J. Ohnemus, *Hadronic* $Z\gamma$ *production with QCD corrections and leptonic decays*, *Phys.Rev.* **D51** (1995) 1068–1076, [hep-ph/9407370].

[37] J. Ohnemus, *Hadronic ZZ,* W^-W^+*, and* $W^{\pm}Z$ *production with QCD corrections and leptonic decays*, *Phys.Rev.* **D50** (1994) 1931–1945, [hep-ph/9403331].

[38] L. J. Dixon, Z. Kunszt, and A. Signer, *Helicity amplitudes for O(alpha*$_s$*) production of* W^+W^-*,* $W^{\pm}Z$*, ZZ,* $W^{\pm}\gamma$*, or* $Z\gamma$ *pairs at hadron colliders*, *Nucl.Phys.* **B531** (1998) 3–23, [hep-ph/9803250].

[39] L. J. Dixon, Z. Kunszt, and A. Signer, *Vector boson pair production in hadronic collisions at order* α_s *: Lepton correlations and anomalous couplings*, *Phys.Rev.* **D60** (1999) 114037, [hep-ph/9907305].

[40] D. De Florian and A. Signer, *W gamma and Z gamma production at hadron colliders*, *Eur.Phys.J.* **C16** (2000) 105–114, [hep-ph/0002138].

[41] J. M. Campbell and R. K. Ellis, *An Update on vector boson pair production at hadron colliders*, *Phys.Rev.* **D60** (1999) 113006, [hep-ph/9905386].

[42] E. N. Glover and J. van der Bij, *Z Boson Pair Production Via Gluon Fusion*, *Nucl.Phys.* **B321** (1989) 561.

[43] C. Kao and D. A. Dicus, *Production of W+ W- from gluon fusion*, *Phys.Rev.* **D43** (1991) 1555–1559.

[44] M. Duhrssen, K. Jakobs, J. van der Bij, and P. Marquard, *The Process $gg \to WW$ as a background to the Higgs signal at the LHC*, *JHEP* **0505** (2005) 064, [hep-ph/0504006].

[45] T. Binoth, M. Ciccolini, N. Kauer, and M. Kramer, *Gluon-induced W-boson pair production at the LHC*, *JHEP* **0612** (2006) 046, [hep-ph/0611170].

[46] J. M. Campbell, R. K. Ellis, and C. Williams, *Gluon-Gluon Contributions to W+ W- Production and Higgs Interference Effects*, *JHEP* **1110** (2011) 005, [arXiv:1107.5569].

[47] V. Del Duca, F. Maltoni, Z. Nagy, and Z. Trocsanyi, *QCD radiative corrections to prompt diphoton production in association with a jet at hadron colliders*, *JHEP* **0304** (2003) 059, [hep-ph/0303012].

[48] F. Campanario, C. Englert, M. Spannowsky, and D. Zeppenfeld, *NLO-QCD corrections to $W\,\gamma\,j$ production*, *Europhys.Lett.* **88** (2009) 11001, [arXiv:0908.1638].

[49] F. Campanario, C. Englert, and M. Spannowsky, *Precise predictions for (non-standard) $W\gamma$ + jet production*, *Phys.Rev.* **D83** (2011) 074009, [arXiv:1010.1291].

[50] S. Dittmaier, S. Kallweit, and P. Uwer, *NLO QCD corrections to WW+jet production at hadron colliders*, *Phys.Rev.Lett.* **100** (2008) 062003, [arXiv:0710.1577].

[51] J. M. Campbell, R. K. Ellis, and G. Zanderighi, *Next-to-leading order predictions for $WW + 1$ jet distributions at the LHC*, *JHEP* **0712** (2007) 056, [arXiv:0710.1832].

[52] T. Binoth, T. Gleisberg, S. Karg, N. Kauer, and G. Sanguinetti, *NLO QCD corrections to ZZ+ jet production at hadron colliders*, *Phys.Lett.* **B683** (2010) 154–159, [arXiv:0911.3181].

[53] F. Campanario, C. Englert, S. Kallweit, M. Spannowsky, and D. Zeppenfeld, *NLO QCD corrections to WZ+jet production with leptonic decays*, *JHEP* **1007** (2010) 076, [arXiv:1006.0390].

[54] V. D. Barger, T. Han, J. Ohnemus, and D. Zeppenfeld, *PAIR PRODUCTION OF $W^{\pm}$, γ AND Z IN ASSOCIATION WITH JETS*, *Phys.Rev.* **D41** (1990) 2782.

[55] C. Anastasiou, E. N. Glover, and M. Tejeda-Yeomans, *Two loop QED and QCD corrections to massless fermion boson scattering*, *Nucl.Phys.* **B629** (2002) 255–289, [hep-ph/0201274].

[56] Z. Bern, A. De Freitas, and L. J. Dixon, *Two loop amplitudes for gluon fusion into two photons*, *JHEP* **0109** (2001) 037, [hep-ph/0109078].

[57] S. Catani, L. Cieri, D. de Florian, G. Ferrera, and M. Grazzini, *Diphoton production at hadron colliders: a fully-differential QCD calculation at NNLO*, *Phys.Rev.Lett.* **108** (2012) 072001, [arXiv:1110.2375].

[58] T. Gehrmann and L. Tancredi, *Two-loop QCD helicity amplitudes for $q\bar{q} \to W^{\pm}\gamma$ and $q\bar{q} \to Z^0\gamma$*, *JHEP* **1202** (2012) 004, [arXiv:1112.1531].

[59] T. Gehrmann and E. Remiddi, *Two loop master integrals for $\gamma^* \to$ 3 jets: The Planar topologies*, *Nucl.Phys.* **B601** (2001) 248–286, [hep-ph/0008287].

[60] T. Gehrmann and E. Remiddi, *Two loop master integrals for $\gamma^* \to$ 3 jets: The Nonplanar topologies*, *Nucl.Phys.* **B601** (2001) 287–317, [hep-ph/0101124].

[61] T. Gehrmann, L. Tancredi, and E. Weihs, *Two-loop QCD helicity amplitudes for $g\,g \to Z\,g$ and $g\,g \to Z\,\gamma$*, *JHEP* **1304** (2013) 101, [arXiv:1302.2630].

[62] T. Gehrmann, L. Tancredi, and E. Weihs, *Two-Loop Master Integrals for $q\bar{q} \to VV$: the Planar Topologies*, arXiv:1306.6344.

[63] D. Zagier, *Polylogarithms, Dedekind zeta functions and the algebraic K-theory of fields*, in *Arithmetic Algebraic Geometry* (J. G.v.d.Geer, F.Oort, ed.), vol. Prog. Math. 89, pp. 391–430., Birkhäuser, 1991.

[64] A. B. Goncharov, M. Spradlin, C. Vergu, and A. Volovich, *Classical Polylogarithms for Amplitudes and Wilson Loops*, *Phys.Rev.Lett.* **105** (2010) 151605, [arXiv:1006.5703].

[65] A. B. Goncharov, *Geometry of configurations, polylogarithms, and motivic cohomology*, *Adv. Math.* **114** (1995), no. 2 197–318.

[66] A. Goncharov, *Multiple polylogarithms and mixed Tate motives*, `math/0103059`.

[67] C. Duhr, H. Gangl, and J. R. Rhodes, *From polygons and symbols to polylogarithmic functions*, *JHEP* **1210** (2012) 075, [`arXiv:1110.0458`].

[68] C. Duhr, *Hopf algebras, coproducts and symbols: an application to Higgs boson amplitudes*, *JHEP* **1208** (2012) 043, [`arXiv:1203.0454`].

[69] C. Anastasiou, C. Duhr, F. Dulat, and B. Mistlberger, *Soft triple-real radiation for Higgs production at N^3LO*, `arXiv:1302.4379`.

[70] L. J. Dixon, J. M. Drummond, and J. M. Henn, *Bootstrapping the three-loop hexagon*, *JHEP* **1111** (2011) 023, [`arXiv:1108.4461`].

[71] E. Weihs and J. Zurita, *Dark Higgs Models at the 7 TeV LHC*, *JHEP* **1202** (2012) 041, [`arXiv:1110.5909`].

[72] P. Langacker, *The Physics of Heavy Z' Gauge Bosons*, *Rev.Mod.Phys.* **81** (2009) 1199–1228, [`arXiv:0801.1345`].

[73] T. Appelquist, B. A. Dobrescu, and A. R. Hopper, *Nonexotic neutral gauge bosons*, *Phys.Rev.* **D68** (2003) 035012, [`hep-ph/0212073`].

[74] T. G. Rizzo, *Z' phenomenology and the LHC*, `hep-ph/0610104`.

[75] K. R. Dienes, C. F. Kolda, and J. March-Russell, *Kinetic mixing and the supersymmetric gauge hierarchy*, *Nucl.Phys.* **B492** (1997) 104–118, [`hep-ph/9610479`].

[76] A. Leike, *The Phenomenology of extra neutral gauge bosons*, *Phys.Rept.* **317** (1999) 143–250, [`hep-ph/9805494`].

[77] J. L. Hewett and T. G. Rizzo, *Low-Energy Phenomenology of Superstring Inspired E(6) Models*, *Phys.Rept.* **183** (1989) 193.

[78] J. Erler, P. Langacker, S. Munir, and E. Rojas, *Z' Bosons from E(6): Collider and Electroweak Constraints*, `arXiv:1108.0685`.

[79] P. J. Fox, J. Liu, D. Tucker-Smith, and N. Weiner, *An Effective Z'*, *Phys.Rev.* **D84** (2011) 115006, [`arXiv:1104.4127`].

[80] F. del Aguila, J. de Blas, and M. Perez-Victoria, *Electroweak Limits on General New Vector Bosons*, *JHEP* **1009** (2010) 033, [`arXiv:1005.3998`].

[81] M. Williams, C. Burgess, A. Maharana, and F. Quevedo, *New Constraints (and Motivations) for Abelian Gauge Bosons in the MeV-TeV Mass Range*, *JHEP* **1108** (2011) 106, [`arXiv:1103.4556`].

[82] K. Babu, C. F. Kolda, and J. March-Russell, *Implications of generalized Z - Z-prime mixing*, *Phys.Rev.* **D57** (1998) 6788–6792, [`hep-ph/9710441`].

[83] R. Foot, H. Lew, and R. Volkas, *A Model with fundamental improper space-time symmetries*, *Phys.Lett.* **B272** (1991) 67–70.

[84] B. Holdom, *Two U(1)'s and Epsilon Charge Shifts*, *Phys.Lett.* **B166** (1986) 196.

[85] R. Schabinger and J. D. Wells, *A Minimal spontaneously broken hidden sector and its impact on Higgs boson physics at the large hadron collider*, *Phys.Rev.* **D72** (2005) 093007, [`hep-ph/0509209`].

[86] B. Patt and F. Wilczek, *Higgs-field portal into hidden sectors*, `hep-ph/0605188`.

[87] J. D. Wells, *How to Find a Hidden World at the Large Hadron Collider*, `arXiv:0803.1243`.

[88] S. Chang, R. Dermisek, J. F. Gunion, and N. Weiner, *Nonstandard Higgs Boson Decays*, *Ann.Rev.Nucl.Part.Sci.* **58** (2008) 75–98, [`arXiv:0801.4554`].

[89] R. Barbieri, T. Gregoire, and L. J. Hall, *Mirror world at the large hadron collider*, `hep-ph/0509242`.

[90] J. Espinosa and M. Quiros, *The Electroweak phase transition with a singlet*, *Phys.Lett.* **B305** (1993) 98–105, [`hep-ph/9301285`].

[91] J. R. Espinosa and M. Quiros, *Novel Effects in Electroweak Breaking from a Hidden Sector*, *Phys.Rev.* **D76** (2007) 076004, [hep-ph/0701145].

[92] J. Choi and R. Volkas, *Real Higgs singlet and the electroweak phase transition in the Standard Model*, *Phys.Lett.* **B317** (1993) 385–391, [hep-ph/9308234].

[93] V. Silveira and A. Zee, *SCALAR PHANTOMS*, *Phys.Lett.* **B161** (1985) 136.

[94] J. McDonald, *Gauge singlet scalars as cold dark matter*, *Phys.Rev.* **D50** (1994) 3637–3649, [hep-ph/0702143].

[95] H. Davoudiasl, R. Kitano, T. Li, and H. Murayama, *The New minimal standard model*, *Phys.Lett.* **B609** (2005) 117–123, [hep-ph/0405097].

[96] V. Barger, M. McCaskey, and G. Shaughnessy, *Complex Scalar Dark Matter vis-à-vis CoGeNT, DAMA/LIBRA and XENON100*, *Phys.Rev.* **D82** (2010) 035019, [arXiv:1005.3328].

[97] C. Burgess, M. Pospelov, and T. ter Veldhuis, *The Minimal model of nonbaryonic dark matter: A Singlet scalar*, *Nucl.Phys.* **B619** (2001) 709–728, [hep-ph/0011335].

[98] Y. Mambrini, *Higgs searches and singlet scalar dark matter: Combined constraints from XENON 100 and the LHC*, *Phys.Rev.* **D84** (2011) 115017, [arXiv:1108.0671].

[99] S. Gopalakrishna, S. J. Lee, and J. D. Wells, *Dark matter and Higgs boson collider implications of fermions in an abelian-gauged hidden sector*, *Phys.Lett.* **B680** (2009) 88–93, [arXiv:0904.2007].

[100] Y. Cai, X.-G. He, and B. Ren, *Low Mass Dark Matter and Invisible Higgs Width In Darkon Models*, *Phys.Rev.* **D83** (2011) 083524, [arXiv:1102.1522].

[101] C. Boehm and P. Fayet, *Scalar dark matter candidates*, *Nucl.Phys.* **B683** (2004) 219–263, [hep-ph/0305261].

[102] R. Barbieri, L. J. Hall, and V. S. Rychkov, *Improved naturalness with a heavy Higgs: An Alternative road to LHC physics*, *Phys.Rev.* **D74** (2006) 015007, [hep-ph/0603188].

[103] W.-F. Chang, J. N. Ng, and J. M. Wu, *Shadow Higgs from a scale-invariant hidden U(1)(s) model*, *Phys.Rev.* **D75** (2007) 115016, [hep-ph/0701254].

[104] D. Feldman, Z. Liu, and P. Nath, *The Stueckelberg Z-prime Extension with Kinetic Mixing and Milli-Charged Dark Matter From the Hidden Sector*, *Phys.Rev.* **D75** (2007) 115001, [hep-ph/0702123].

[105] M. Pospelov, *Secluded U(1) below the weak scale*, *Phys.Rev.* **D80** (2009) 095002, [arXiv:0811.1030].

[106] M. Pospelov, A. Ritz, and M. B. Voloshin, *Secluded WIMP Dark Matter*, *Phys.Lett.* **B662** (2008) 53–61, [arXiv:0711.4866].

[107] Z. Liu, *Hidden Sector Models and Signatures*, *Nucl.Phys.Proc.Suppl.* **200-202** (2010) 133–142, [arXiv:0910.0061].

[108] E. J. Chun, J.-C. Park, and S. Scopel, *Dark matter and a new gauge boson through kinetic mixing*, *JHEP* **1102** (2011) 100, [arXiv:1011.3300].

[109] S. Andreas, T. Hambye, and M. H. Tytgat, *WIMP dark matter, Higgs exchange and DAMA*, *JCAP* **0810** (2008) 034, [arXiv:0808.0255].

[110] M. H. Tytgat, *A light scalar WIMP through the Higgs portal?*, *PoS* **IDM2010** (2011) 126, [arXiv:1012.0576].

[111] C. Arina and M. H. Tytgat, *Constraints on Light WIMP candidates from the Isotropic Diffuse Gamma-Ray Emission*, *JCAP* **1101** (2011) 011, [arXiv:1007.2765].

[112] V. Barger, Y. Gao, M. McCaskey, and G. Shaughnessy, *Light Higgs Boson, Light Dark Matter and Gamma Rays*, *Phys.Rev.* **D82** (2010) 095011, [arXiv:1008.1796].

[113] B. Batell, *Dark Discrete Gauge Symmetries*, *Phys.Rev.* **D83** (2011) 035006, [arXiv:1007.0045].

[114] N. Arkani-Hamed, D. P. Finkbeiner, T. R. Slatyer, and N. Weiner, *A Theory of Dark Matter*, *Phys.Rev.* **D79** (2009) 015014, [arXiv:0810.0713].

[115] M. Pospelov and A. Ritz, *Astrophysical Signatures of Secluded Dark Matter*, *Phys.Lett.* **B671** (2009) 391–397, [arXiv:0810.1502].

[116] **PAMELA Collaboration** Collaboration, O. Adriani et al., *An anomalous positron abundance in cosmic rays with energies 1.5-100 GeV*, *Nature* **458** (2009) 607–609, [arXiv:0810.4995].

[117] J. Kopp, *Constraints on dark matter annihilation from AMS-02 results*, arXiv:1304.1184.

[118] **BABAR Collaboration** Collaboration, B. Aubert et al., *Search for a Narrow Resonance in e+e- to Four Lepton Final States*, arXiv:0908.2821.

[119] J. L. Feng, M. Kaplinghat, and H.-B. Yu, *Halo Shape and Relic Density Exclusions of Sommerfeld-Enhanced Dark Matter Explanations of Cosmic Ray Excesses*, *Phys.Rev.Lett.* **104** (2010) 151301, [arXiv:0911.0422].

[120] K. N. Abazajian, P. Agrawal, Z. Chacko, and C. Kilic, *Conservative Constraints on Dark Matter from the Fermi-LAT Isotropic Diffuse Gamma-Ray Background Spectrum*, *JCAP* **1011** (2010) 041, [arXiv:1002.3820].

[121] A. Hook, E. Izaguirre, and J. G. Wacker, *Model Independent Bounds on Kinetic Mixing*, *Adv.High Energy Phys.* **2011** (2011) 859762, [arXiv:1006.0973].

[122] Y. Mambrini, *The ZZ' kinetic mixing in the light of the recent direct and indirect dark matter searches*, *JCAP* **1107** (2011) 009, [arXiv:1104.4799].

[123] C. Englert, T. Plehn, D. Zerwas, and P. M. Zerwas, *Exploring the Higgs portal*, *Phys.Lett.* **B703** (2011) 298–305, [arXiv:1106.3097].

[124] V. Barger, P. Langacker, M. McCaskey, M. J. Ramsey-Musolf, and G. Shaughnessy, *LHC Phenomenology of an Extended Standard Model with a Real Scalar Singlet*, *Phys.Rev.* **D77** (2008) 035005, [arXiv:0706.4311].

[125] V. Barger, P. Langacker, M. McCaskey, M. Ramsey-Musolf, and G. Shaughnessy, *Complex Singlet Extension of the Standard Model*, *Phys.Rev.* **D79** (2009) 015018, [arXiv:0811.0393].

[126] M. Bowen, Y. Cui, and J. D. Wells, *Narrow trans-TeV Higgs bosons and $H \to hh$ decays: Two LHC search paths for a hidden sector Higgs boson*, *JHEP* **0703** (2007) 036, [hep-ph/0701035].

[127] D. Cerdeno, A. Dedes, and T. Underwood, *The Minimal Phantom Sector of the Standard Model: Higgs Phenomenology and Dirac Leptogenesis*, *JHEP* **0609** (2006) 067, [hep-ph/0607157].

[128] D. O'Connell, M. J. Ramsey-Musolf, and M. B. Wise, *Minimal Extension of the Standard Model Scalar Sector*, *Phys.Rev.* **D75** (2007) 037701, [hep-ph/0611014].

[129] O. Bahat-Treidel, Y. Grossman, and Y. Rozen, *Hiding the Higgs at the LHC*, *JHEP* **0705** (2007) 022, [hep-ph/0611162].

[130] S. Gopalakrishna, S. Jung, and J. D. Wells, *Higgs boson decays to four fermions through an abelian hidden sector*, *Phys.Rev.* **D78** (2008) 055002, [arXiv:0801.3456].

[131] S. Bock, R. Lafaye, T. Plehn, M. Rauch, D. Zerwas, et al., *Measuring Hidden Higgs and Strongly-Interacting Higgs Scenarios*, *Phys.Lett.* **B694** (2010) 44–53, [arXiv:1007.2645].

[132] M. Carena, P. Draper, T. Liu, and C. Wagner, *The 7 TeV LHC Reach for MSSM Higgs Bosons*, *Phys.Rev.* **D84** (2011) 095010, [arXiv:1107.4354].

[133] J. Kumar and J. D. Wells, *CERN LHC and ILC probes of hidden-sector gauge bosons*, *Phys.Rev.* **D74** (2006) 115017, [hep-ph/0606183].

[134] B. Grossmann, B. McElrath, S. Nandi, and S. K. Rai, *Hidden Extra U(1) at the Electroweak/TeV Scale*, *Phys.Rev.* **D82** (2010) 055021, [arXiv:1006.5019].

[135] W.-F. Chang, J. N. Ng, and J. M. Wu, *A Very Narrow Shadow Extra Z-boson at Colliders*, *Phys.Rev.* **D74** (2006) 095005, [hep-ph/0608068].

[136] P. Gondolo, P. Ko, and Y. Omura, *Light dark matter in leptophobic Z' models*, *Phys.Rev.* **D85** (2012) 035022, [arXiv:1106.0885].

[137] C. Cheung, J. T. Ruderman, L.-T. Wang, and I. Yavin, *Kinetic Mixing as the Origin of Light Dark Scales*, *Phys.Rev.* **D80** (2009) 035008, [arXiv:0902.3246].

[138] M. Ahlers, J. Jaeckel, J. Redondo, and A. Ringwald, *Probing Hidden Sector Photons through the Higgs Window*, *Phys.Rev.* **D78** (2008) 075005, [arXiv:0807.4143].

[139] Z. Kang, T. Li, T. Liu, C. Tong, and J. M. Yang, *Light Dark Matter from the $U(1)_X$ Sector in the NMSSM with Gauge Mediation*, *JCAP* **1101** (2011) 028, [arXiv:1008.5243].

[140] B. Bellazzini, C. Csaki, A. Falkowski, and A. Weiler, *Buried Higgs*, *Phys.Rev.* **D80** (2009) 075008, [arXiv:0906.3026].

[141] T. Hahn, *CUBA: A Library for multidimensional numerical integration*, *Comput.Phys.Commun.* **168** (2005) 78–95, [hep-ph/0404043].

[142] S. Profumo, M. J. Ramsey-Musolf, and G. Shaughnessy, *Singlet Higgs phenomenology and the electroweak phase transition*, *JHEP* **0708** (2007) 010, [arXiv:0705.2425].

[143] P. Bechtle, O. Brein, S. Heinemeyer, G. Weiglein, and K. E. Williams, *HiggsBounds: Confronting Arbitrary Higgs Sectors with Exclusion Bounds from LEP and the Tevatron*, *Comput.Phys.Commun.* **181** (2010) 138–167, [arXiv:0811.4169].

[144] P. Bechtle, O. Brein, S. Heinemeyer, G. Weiglein, and K. E. Williams, *HiggsBounds 2.0.0: Confronting Neutral and Charged Higgs Sector Predictions with Exclusion Bounds from LEP and the Tevatron*, *Comput.Phys.Commun.* **182** (2011) 2605–2631, [arXiv:1102.1898].

[145] **LEP Working Group for Higgs boson searches, ALEPH Collaboration, DELPHI Collaboration, L3 Collaboration, OPAL Collaboration** Collaboration, R. Barate et al., *Search for the standard model Higgs boson at LEP*, *Phys.Lett.* **B565** (2003) 61–75, [hep-ex/0306033].

[146] **OPAL Collaboration** Collaboration, G. Abbiendi et al., *Decay mode independent searches for new scalar bosons with the OPAL detector at LEP*, *Eur.Phys.J.* **C27** (2003) 311–329, [hep-ex/0206022].

[147] **ALEPH Collaboration, DELPHI Collaboration, L3 Collaboration, OPAL Collaboration, LEP Working Group for Higgs Boson Searches** Collaboration, S. Schael et al., *Search for neutral MSSM Higgs bosons at LEP*, *Eur.Phys.J.* **C47** (2006) 547–587, [hep-ex/0602042].

[148] **LEP Higgs Working for Higgs boson searches, ALEPH Collaboration, DELPHI Collaboration, CERN-L3 Collaboration, OPAL Collaboration** Collaboration, *Searches for invisible Higgs bosons: Preliminary combined results using LEP data collected at energies up to 209-GeV*, hep-ex/0107032.

[149] **L3 Collaboration** Collaboration, P. Achard et al., *Search for an invisibly-decaying Higgs boson at LEP*, *Phys.Lett.* **B609** (2005) 35–48, [hep-ex/0501033].

[150] **OPAL Collaboration** Collaboration, G. Abbiendi et al., *Search for invisibly decaying Higgs bosons in e+ e- → Z0 h0 production at s**(1/2) = 183-GeV - 209-GeV*, *Phys.Lett.* **B682** (2010) 381–390, [arXiv:0707.0373].

[151] **CDF Collaboration, D0 Collaboration** Collaboration, T. T. Group, *Combined CDF and D0 Upper Limits on Standard Model Higgs-Boson Production with up to 6.7 fb^{-1} of Data*, arXiv:1007.4587.

[152] **CDF Collaboration, D0 Collaboration** Collaboration, T. Aaltonen et al., *Combined Tevatron upper limit on $gg \to H \to W^+W^-$ and constraints on the Higgs boson mass in fourth-generation fermion models*, *Phys.Rev.* **D82** (2010) 011102, [arXiv:1005.3216].

[153] M. S. Chanowitz, *A Z' Boson and the Higgs Boson Mass*, arXiv:0806.0890.

[154] M. E. Peskin and J. D. Wells, *How can a heavy Higgs boson be consistent with the precision electroweak measurements?*, *Phys.Rev.* **D64** (2001) 093003, [hep-ph/0101342].

[155] M. E. Peskin and T. Takeuchi, *A New constraint on a strongly interacting Higgs sector*, *Phys.Rev.Lett.* **65** (1990) 964–967.

[156] T. Hahn, *FormCalc 6*, *PoS* **ACAT08** (2008) 121, [arXiv:0901.1528].

[157] B. Holdom, *Oblique electroweak corrections and an extra gauge boson*, *Phys.Lett.* **B259** (1991) 329–334.

[158] H. Flacher, M. Goebel, J. Haller, A. Hocker, K. Monig, et al., *Revisiting the Global Electroweak Fit of the Standard Model and Beyond with Gfitter*, *Eur.Phys.J.* **C60** (2009) 543–583, [arXiv:0811.0009].

[159] T. G. Group, *Gfitter - a generic fitter project for hep model testing*, June, 2009.

[160] D. Y. Bardin, P. Christova, M. Jack, L. Kalinovskaya, A. Olchevski, et al., *ZFITTER v.6.21: A Semianalytical program for fermion pair production in e+ e- annihilation*, *Comput.Phys.Commun.* **133** (2001) 229–395, [hep-ph/9908433].

[161] A. Arbuzov, M. Awramik, M. Czakon, A. Freitas, M. Grunewald, et al., *ZFITTER: A Semi-analytical program for fermion pair production in e+ e- annihilation, from version 6.21 to version 6.42*, *Comput.Phys.Commun.* **174** (2006) 728–758, [hep-ph/0507146].

[162] **ATLAS** Collaboration, *Search for the Standard Model Higgs boson in the $H \to WW \to ll\nu\nu$ decay mode using 1.7 fb-1 of data collected with the ATLAS detector at sqrt(s)=7 TeV*, ATLAS-CONF-2011-134, ATLAS-COM-CONF-2011-161.

[163] **ATLAS** Collaboration, G. Aad et al., *Search for the Higgs boson in the $H \to WW \to lvjj$ decay channel in pp collisions at sqrts = 7 TeV with the ATLAS detector*, *Phys.Rev.Lett.* **107** (2011) 231801, [arXiv:1109.3615].

[164] **CMS** Collaboration, *Search for the Higgs Boson in the Fully Leptonic W^+W^- Final State*, CMS-PAS-HIG-11-014.

[165] **ATLAS** Collaboration, G. Aad et al., *Search for the Standard Model Higgs boson in the decay channel $H \to ZZ(*) \to 4l$ with the ATLAS detector*, *Phys.Lett.* **B705** (2011) 435–451, [arXiv:1109.5945].

[166] **ATLAS** Collaboration, G. Aad et al., *Search for a Standard Model Higgs boson in the $H \to ZZ \to l^+l^-\nu\nu^-$ decay channel with the ATLAS detector*, *Phys.Rev.Lett.* **107** (2011) 221802, [arXiv:1109.3357].

[167] **ATLAS** Collaboration, G. Aad et al., *Search for a heavy Standard Model Higgs boson in the channel $H \to ZZ \to llqq$ using the ATLAS detector*, *Phys.Lett.* **B707** (2012) 27–45, [arXiv:1108.5064].

[168] **CMS** Collaboration, *Search for a Standard Model Higgs boson produced in the decay channel 4l*, CMS-PAS-HIG-11-015.

[169] **CMS** Collaboration, *H to ZZ to 2l2nu*, CMS-PAS-HIG-11-016.

[170] **CMS** Collaboration, *Search for the standard model Higgs Boson in the decay channel H to ZZ to llqq at CMS*, CMS-PAS-HIG-11-017.

[171] **CMS** Collaboration, *Study of the Higgs $\to$ ZZ $\to$ 2l + 2 tau final state with CMS detector.*, CMS-PAS-HIG-11-013.

[172] **ATLAS** Collaboration, G. Aad et al., *Search for the Standard Model Higgs boson in the two photon decay channel with the ATLAS detector at the LHC*, *Phys.Lett.* **B705** (2011) 452–470, [arXiv:1108.5895].

[173] **CMS** Collaboration, *Search for a Higgs boson decaying into two photons in the CMS detector*, CMS-PAS-HIG-11-021.

[174] **ATLAS** Collaboration, *Search for neutral MSSM Higgs bosons decaying to tau+tau- pairs in proton-proton collisions at sqrt(s) = 7 TeV with the ATLAS detector*, ATLAS-CONF-2011-132, ATLAS-COM-CONF-2011-155.

[175] **CMS** Collaboration, *Search for Neutral Higgs Bosons Decaying to Tau Pairs in pp Collisions at sqrts=7 TeV*, CMS-PAS-HIG-11-020.

[176] **CMS** Collaboration, *Search for Higgs Boson in VH Production with H to bb*, CMS-PAS-HIG-11-012.

[177] *ATLAS Sensitivity Prospects for 1 Higgs Boson Production at the LHC Running at 7, 8 or 9 TeV*, ATL-PHYS-PUB-2010-015, ATL-COM-PHYS-2010-726.

[178] **LHC Higgs Cross Section Working Group** Collaboration, S. Dittmaier et al., *Handbook of LHC Higgs Cross Sections: 1. Inclusive Observables*, arXiv:1101.0593.

[179] **ATLAS** Collaboration, *Search for the Standard Model Higgs boson produced in association with a vector boson and decaying to a b-quark pair with the ATLAS detector at the LHC*, ATLAS-CONF-2011-103, ATLAS-COM-CONF-2011-121.

[180] J. M. Butterworth, A. R. Davison, M. Rubin, and G. P. Salam, *Jet substructure as a new Higgs search channel at the LHC*, *Phys.Rev.Lett.* **100** (2008) 242001, [arXiv:0802.2470].

[181] P. Draper, T. Liu, and C. E. Wagner, *Prospects for MSSM Higgs Searches at the Tevatron*, *Phys.Rev.* **D80** (2009) 035025, [arXiv:0905.4721].

[182] P. Draper, T. Liu, and C. E. Wagner, *Prospects for Higgs Searches at the Tevatron and LHC in the MSSM with Explicit CP-violation*, *Phys.Rev.* **D81** (2010) 015014, [arXiv:0911.0034].

[183] **ATLAS** Collaboration, *Combined Standard Model Higgs boson searches with up to 2.3 fb-1 of pp collisions at sqrts=7 TeV at the LHC*, ATLAS-CONF-2011-157, ATLAS-COM-CONF-2011-181.

[184] **CMS** Collaboration, *Combined Standard Model Higgs boson searches with up to 2.3 inverse femtobarns of pp collision data at sqrt(s)=7 TeV at the LHC*, CMS-PAS-HIG-11-023.

[185] F. Boudjema and G. Drieu La Rochelle, *SUSY Higgs searches : beyond the MSSM*, *Phys.Rev.* **D85** (2012) 035011, [arXiv:1112.1434].

[186] C.-R. Chen, M. M. Nojiri, and W. Sreethawong, *Search for the Elusive Higgs Boson Using Jet Structure at LHC*, *JHEP* **1011** (2010) 012, [arXiv:1006.1151].

[187] A. Falkowski, D. Krohn, L.-T. Wang, J. Shelton, and A. Thalapillil, *Unburied Higgs boson: Jet substructure techniques for searching for Higgs' decay into gluons*, *Phys.Rev.* **D84** (2011) 074022, [arXiv:1006.1650].

[188] B. Bellazzini, C. Csaki, J. Hubisz, and J. Shao, *Discovering a Higgs boson decaying to four jets in supersymmetric cascade decays*, *Phys.Rev.* **D83** (2011) 095018, [arXiv:1012.1316].

[189] D. E. Kaplan and M. McEvoy, *Associated Production of Non-Standard Higgs Bosons at the LHC*, *Phys.Rev.* **D83** (2011) 115004, [arXiv:1102.0704].

[190] I. Low, P. Schwaller, G. Shaughnessy, and C. E. Wagner, *The dark side of the Higgs boson*, *Phys.Rev.* **D85** (2012) 015009, [arXiv:1110.4405].

[191] **ATLAS** Collaboration, *A particle consistent with the Higgs Boson observed with the ATLAS Detector at the Large Hadron Collider*, *Science* **338** (2012) 1576–1582.

[192] **CMS** Collaboration, *A new boson with a mass of 125-GeV observed with the CMS experiment at the Large Hadron Collider*, *Science* **338** (2012) 1569–1575.

[193] *Measurements of the properties of the higgs-like boson in the two photon decay channel with the atlas detector using 25* fb^{-1} *of proton-proton collision data*, Tech. Rep. ATLAS-CONF-2013-012, CERN, Geneva, Mar, 2013.

[194] *Measurements of the properties of the higgs-like boson in the four lepton decay channel with the atlas detector using 25 fb1 of proton-proton collision data*, Tech. Rep. ATLAS-CONF-2013-013, CERN, Geneva, Mar, 2013.

[195] *Updated atlas results on the signal strength of the higgs-like boson for decays into ww and heavy fermion final states*, Tech. Rep. ATLAS-CONF-2012-162, CERN, Geneva, Nov, 2012.

[196] *Combined coupling measurements of the higgs-like boson with the atlas detector using up to 25* fb^{-1} *of proton-proton collision data*, Tech. Rep. ATLAS-CONF-2013-034, CERN, Geneva, Mar, 2013.

[197] *Coupling properties of the new higgs-like boson observed with the atlas detector at the lhc*, Tech. Rep. ATLAS-CONF-2012-127, CERN, Geneva, Sep, 2012.

[198] *Combined measurements of the mass and signal strength of the higgs-like boson with the atlas detector using up to 25 fb^{-1} of proton-proton collision data*, Tech. Rep. ATLAS-CONF-2013-014, CERN, Geneva, Mar, 2013.

[199] *Combination of standard model higgs boson searches and measurements of the properties of the new boson with a mass near 125 gev*, Tech. Rep. CMS-PAS-HIG-12-045, CERN, Geneva, 2012.

[200] *Properties of the higgs-like boson in the decay h → zz to 4l in pp collisions at sqrt s =7 and 8 tev*, Tech. Rep. CMS-PAS-HIG-13-002, CERN, Geneva, 2013.

[201] *Evidence for a particle decaying to w+w- in the fully leptonic final state in a standard model higgs boson search in pp collisions at the lhc*, Tech. Rep. CMS-PAS-HIG-13-003, CERN, Geneva, 2013.

[202] *Search for the standard-model higgs boson decaying to tau pairs in proton-proton collisions at sqrt(s) = 7 and 8 tev*, Tech. Rep. CMS-PAS-HIG-13-004, CERN, Geneva, 2013.

[203] *Combination of standard model higgs boson searches and measurements of the properties of the new boson with a mass near 125 gev*, Tech. Rep. CMS-PAS-HIG-13-005, CERN, Geneva, 2013.

[204] *Search for invisible decays of a higgs boson produced in association with a z boson in atlas*, Tech. Rep. ATLAS-CONF-2013-011, CERN, Geneva, Mar, 2013.

[205] G. Belanger, B. Dumont, U. Ellwanger, J. Gunion, and S. Kraml, *Global fit to Higgs signal strengths and couplings and implications for extended Higgs sectors*, `arXiv:1306.2941`.

[206] C. Englert, J. Jaeckel, V. V. Khoze, and M. Spannowsky, *Emergence of the Electroweak Scale through the Higgs Portal*, `arXiv:1301.4224`.

[207] Y. Mambrini, M. H. Tytgat, G. Zaharijas, and B. Zaldivar, *Complementarity of Galactic radio and collider data in constraining WIMP dark matter models*, *JCAP* **1211** (2012) 038, [`arXiv:1206.2352`].

[208] M. T. Frandsen, F. Kahlhoefer, A. Preston, S. Sarkar, and K. Schmidt-Hoberg, *LHC and Tevatron Bounds on the Dark Matter Direct Detection Cross-Section for Vector Mediators*, *JHEP* **1207** (2012) 123, [`arXiv:1204.3839`].

[209] A. Djouadi, O. Lebedev, Y. Mambrini, and J. Quevillon, *Implications of LHC searches for Higgs–portal dark matter*, *Phys.Lett.* **B709** (2012) 65–69, [`arXiv:1112.3299`].

[210] J. M. Cline, K. Kainulainen, P. Scott, and C. Weniger, *Update on scalar singlet dark matter*, `arXiv:1306.4710`.

[211] N. Craig, J. Galloway, and S. Thomas, *Searching for Signs of the Second Higgs Doublet*, `arXiv:1305.2424`.

[212] G. M. Pruna and T. Robens, *The Higgs Singlet extension parameter space in the light of the LHC discovery*, `arXiv:1303.1150`.

[213] E. Remiddi and J. Vermaseren, *Harmonic polylogarithms*, *Int.J.Mod.Phys.* **A15** (2000) 725–754, [`hep-ph/9905237`].

[214] V. Del Duca, C. Duhr, and V. A. Smirnov, *An Analytic Result for the Two-Loop Hexagon Wilson Loop in N = 4 SYM*, *JHEP* **1003** (2010) 099, [`arXiv:0911.5332`].

[215] S. Caron-Huot, *Superconformal symmetry and two-loop amplitudes in planar N=4 super Yang-Mills*, *JHEP* **1112** (2011) 066, [`arXiv:1105.5606`].

[216] L. J. Dixon, J. M. Drummond, and J. M. Henn, *The one-loop six-dimensional hexagon integral and its relation to MHV amplitudes in N=4 SYM*, *JHEP* **1106** (2011) 100, [`arXiv:1104.2787`].

[217] V. Del Duca, C. Duhr, and V. A. Smirnov, *The massless hexagon integral in D = 6 dimensions*, *Phys.Lett.* **B703** (2011) 363–365, [`arXiv:1104.2781`].

[218] V. Del Duca, C. Duhr, and V. A. Smirnov, *The One-Loop One-Mass Hexagon Integral in D=6 Dimensions*, *JHEP* **1107** (2011) 064, [arXiv:1105.1333].

[219] V. Del Duca, L. J. Dixon, J. M. Drummond, C. Duhr, J. M. Henn, et al., *The one-loop six-dimensional hexagon integral with three massive corners*, *Phys.Rev.* **D84** (2011) 045017, [arXiv:1105.2011].

[220] S. Buehler and C. Duhr, *CHAPLIN - Complex Harmonic Polylogarithms in Fortran*, arXiv:1106.5739.

[221] A. von Manteuffel and C. Studerus, *Top quark pairs at two loops and Reduze 2*, *PoS* **LL2012** (2012) 059, [arXiv:1210.1436].

[222] H. R. P. Ferguson and D. H. Bailey, *A polynomial time, numerically stable integer relation algorithm.*, *RNR Techn. Rept.* **RNR-91-032** (1992).

[223] F. C. S. Brown, *Multiple zeta values and periods of moduli spaces $\mathfrak{M}_{0,n}$*, *ArXiv Mathematics e-prints* (June, 2006) [math/0606].

[224] A. B. Goncharov, *Polylogarithms in arithmetic and geometry*, vol. 1,2 of *Proc. of the International Congress of Mathematicians*. Birkhuser, 1995.

[225] J. Vollinga and S. Weinzierl, *Numerical evaluation of multiple polylogarithms*, *Comput.Phys.Commun.* **167** (2005) 177, [hep-ph/0410259].

[226] A. B. Goncharov, *Galois symmetries of fundamental groupoids and noncommutative geometry*, *ArXiv Mathematics e-prints* (Aug., 2002) [math/0208].

[227] F. Brown, *On the decomposition of motivic multiple zeta values*, *ArXiv e-prints* (Feb., 2011) [arXiv:1102.1310].

[228] V. Costantini, G. Pistoni, and B. Tollis, *On the nonlinear effects in quantum electrodynamics: the coalescence of photons in a nuclear coulomb field*, *Il Nuovo Cimento A* **46** (1966), no. 4 684–689.

[229] V. Baier, E. Kurayev, and V. Fadin, *Production of gluon jets in e+ e- collisions*, *Sov. J. Nucl. Phys.* **31** (1980), no. 3 364–368.

[230] M. Laursen, K. Mikaelian, and M. Samuel, *Z0 Decay into three Gluons*, *Phys.Rev.* **D23** (1981) 2795.

[231] J. van der Bij and E. N. Glover, *Photon Z boson pair production via Gluon Fusion*, *Phys.Lett.* **B206** (1988) 701.

[232] J. van der Bij and E. N. Glover, *Z Boson Production and Decay via Gluons*, *Nucl.Phys.* **B313** (1989) 237.

[233] E. N. Glover and J. van der Bij, *Vector Boson Pair Production via Gluon Fusion*, *Phys.Lett.* **B219** (1989) 488.

[234] K. Adamson, D. de Florian, and A. Signer, *Gluon induced contributions to $Z\gamma$ production at hadron colliders*, *Phys.Rev.* **D67** (2003) 034016, [hep-ph/0211295].

[235] T. Binoth, J. Guillet, E. Pilon, and M. Werlen, *A Full next-to-leading order study of direct photon pair production in hadronic collisions*, *Eur.Phys.J.* **C16** (2000) 311–330, [hep-ph/9911340].

[236] Z. Bern, L. J. Dixon, and C. Schmidt, *Isolating a light Higgs boson from the diphoton background at the CERN LHC*, *Phys.Rev.* **D66** (2002) 074018, [hep-ph/0206194].

[237] C. Berger, Z. Bern, L. Dixon, F. Febres Cordero, D. Forde, et al., *An Automated Implementation of On-Shell Methods for One-Loop Amplitudes*, *Phys.Rev.* **D78** (2008) 036003, [arXiv:0803.4180].

[238] R. K. Ellis, Z. Kunszt, K. Melnikov, and G. Zanderighi, *One-loop calculations in quantum field theory: from Feynman diagrams to unitarity cuts*, *Phys.Rept.* **518** (2012) 141–250, [arXiv:1105.4319].

[239] G. Cullen, N. Greiner, G. Heinrich, G. Luisoni, P. Mastrolia, et al., *Automated One-Loop Calculations with GoSam*, *PoS* **RADCOR2011** (2011) 013, [arXiv:1201.2782].

[240] G. Bevilacqua, M. Czakon, M. Garzelli, A. van Hameren, A. Kardos, et al., *HELAC-NLO*, *Comput.Phys.Commun.* **184** (2013) 986–997, [arXiv:1110.1499].

[241] V. Hirschi, R. Frederix, S. Frixione, M. V. Garzelli, F. Maltoni, et al., *Automation of one-loop QCD corrections*, *JHEP* **1105** (2011) 044, [arXiv:1103.0621].

[242] F. Cascioli, P. Maierhofer, and S. Pozzorini, *Scattering Amplitudes with Open Loops*, *Phys.Rev.Lett.* **108** (2012) 111601, [arXiv:1111.5206].

[243] L. Garland, T. Gehrmann, E. N. Glover, A. Koukoutsakis, and E. Remiddi, *Two loop QCD helicity amplitudes for e+ e- → three jets*, *Nucl.Phys.* **B642** (2002) 227–262, [hep-ph/0206067].

[244] T. Gehrmann, M. Jaquier, E. Glover, and A. Koukoutsakis, *Two-Loop QCD Corrections to the Helicity Amplitudes for H → 3 partons*, *JHEP* **1202** (2012) 056, [arXiv:1112.3554].

[245] T. Binoth, E. N. Glover, P. Marquard, and J. van der Bij, *Two loop corrections to light by light scattering in supersymmetric QED*, *JHEP* **0205** (2002) 060, [hep-ph/0202266].

[246] L. J. Dixon, *Calculating scattering amplitudes efficiently*, hep-ph/9601359.

[247] T. Gehrmann and E. Remiddi, *Analytic continuation of massless two loop four point functions*, *Nucl.Phys.* **B640** (2002) 379–411, [hep-ph/0207020].

[248] P. Nogueira, *Automatic Feynman graph generation*, *J.Comput.Phys.* **105** (1993) 279–289.

[249] L. Garland, T. Gehrmann, E. N. Glover, A. Koukoutsakis, and E. Remiddi, *The Two loop QCD matrix element for e+ e- → 3 jets*, *Nucl.Phys.* **B627** (2002) 107–188, [hep-ph/0112081].

[250] J. Vermaseren, *The FORM project*, *Nucl.Phys.Proc.Suppl.* **183** (2008) 19–24, [arXiv:0806.4080].

[251] A. von Manteuffel and C. Studerus, *Reduze 2 - Distributed Feynman Integral Reduction*, arXiv:1201.4330.

[252] F. Tkachov, *A Theorem on Analytical Calculability of Four Loop Renormalization Group Functions*, *Phys.Lett.* **B100** (1981) 65–68.

[253] K. Chetyrkin and F. Tkachov, *Integration by Parts: The Algorithm to Calculate beta Functions in 4 Loops*, *Nucl.Phys.* **B192** (1981) 159–204.

[254] S. Laporta, *High precision calculation of multiloop Feynman integrals by difference equations*, *Int.J.Mod.Phys.* **A15** (2000) 5087–5159, [hep-ph/0102033].

[255] C. Studerus, *Reduze-Feynman Integral Reduction in C++*, *Comput.Phys.Commun.* **181** (2010) 1293–1300, [arXiv:0912.2546].

[256] T. Gehrmann and E. Remiddi, *Differential equations for two loop four point functions*, *Nucl.Phys.* **B580** (2000) 485–518, [hep-ph/9912329].

[257] T. Gehrmann and E. Remiddi, *Numerical evaluation of harmonic polylogarithms*, *Comput.Phys.Commun.* **141** (2001) 296–312, [hep-ph/0107173].

[258] T. Gehrmann and E. Remiddi, *Numerical evaluation of two-dimensional harmonic polylogarithms*, *Comput.Phys.Commun.* **144** (2002) 200–223, [hep-ph/0111255].

[259] D. Maitre, *HPL, a mathematica implementation of the harmonic polylogarithms*, *Comput.Phys.Commun.* **174** (2006) 222–240, [hep-ph/0507152].

[260] D. Maitre, *Extension of HPL to complex arguments*, *Comput.Phys.Commun.* **183** (2012) 846, [hep-ph/0703052].

[261] W. Research, *Mathematica*. Wolfram Reserach, Champaign, Illinois, USA, 9.0 ed., 2013.

[262] S. Catani, *The Singular behavior of QCD amplitudes at two loop order*, *Phys.Lett.* **B427** (1998) 161–171, [hep-ph/9802439].

[263] J. Vollinga, *GiNaC: Symbolic computation with C++*, *Nucl.Instrum.Meth.* **A559** (2006) 282–284, [hep-ph/0510057].

[264] D. H. Bailey, Y. Hida, X. S. Li, and B. Thompson, *Arprec: An arbitrary precision computation package,*, *LBNL* **53651** (2002).

[265] A. Brandhuber, G. Travaglini, and G. Yang, *Analytic two-loop form factors in N=4 SYM*, *JHEP* **1205** (2012) 082, [arXiv:1201.4170].

[266] E. Accomando and A. Kaiser, *Electroweak corrections and anomalous triple gauge-boson couplings in W^+W^- and $W^\pm Z$ production at the LHC*, *Phys.Rev.* **D73** (2006) 093006, [hep-ph/0511088].

[267] J. Ohnemus, *Order α_s calculations of hadronic $W^\pm\gamma$ and $Z\gamma$ production*, *Phys.Rev.* **D47** (1993) 940–955.

[268] U. Baur, T. Han, and J. Ohnemus, *QCD corrections to hadronic $W\gamma$ production with nonstandard $WW\gamma$ couplings*, *Phys.Rev.* **D48** (1993) 5140–5161, [hep-ph/9305314].

[269] U. Baur, T. Han, and J. Ohnemus, *QCD corrections and anomalous couplings in $Z\gamma$ production at hadron colliders*, *Phys.Rev.* **D57** (1998) 2823–2836, [hep-ph/9710416].

[270] T. Gehrmann, N. Greiner, and G. Heinrich, *Photon isolation effects at NLO in gamma gamma + jet final states in hadronic collisions*, *JHEP* **1306** (2013) 058, [arXiv:1303.0824].

[271] S. Dittmaier, S. Kallweit, and P. Uwer, *NLO QCD corrections to $pp/p\bar{p} \to WW + jet + X$ including leptonic W-boson decays*, *Nucl.Phys.* **B826** (2010) 18–70, [arXiv:0908.4124].

[272] G. Chachamis, M. Czakon, and D. Eiras, *W Pair Production at the LHC. I. Two-loop Corrections in the High Energy Limit*, *JHEP* **0812** (2008) 003, [arXiv:0802.4028].

[273] C. Anastasiou and A. Lazopoulos, *Automatic integral reduction for higher order perturbative calculations*, *JHEP* **0407** (2004) 046, [hep-ph/0404258].

[274] A. Smirnov, *Algorithm FIRE – Feynman Integral REduction*, *JHEP* **0810** (2008) 107, [arXiv:0807.3243].

[275] A. Kotikov, *Differential equations method: New technique for massive Feynman diagrams calculation*, *Phys.Lett.* **B254** (1991) 158–164.

[276] E. Remiddi, *Differential equations for Feynman graph amplitudes*, *Nuovo Cim.* **A110** (1997) 1435–1452, [hep-th/9711188].

[277] M. Caffo, H. Czyz, S. Laporta, and E. Remiddi, *The Master differential equations for the two loop sunrise selfmass amplitudes*, *Nuovo Cim.* **A111** (1998) 365–389, [hep-th/9805118].

[278] R. Bonciani, A. Ferroglia, T. Gehrmann, D. Maitre, and C. Studerus, *Two-Loop Fermionic Corrections to Heavy-Quark Pair Production: The Quark-Antiquark Channel*, *JHEP* **0807** (2008) 129, [arXiv:0806.2301].

[279] R. Bonciani, A. Ferroglia, T. Gehrmann, and C. Studerus, *Two-Loop Planar Corrections to Heavy-Quark Pair Production in the Quark-Antiquark Channel*, *JHEP* **0908** (2009) 067, [arXiv:0906.3671].

[280] R. Bonciani, A. Ferroglia, T. Gehrmann, A. Manteuffel, and C. Studerus, *Two-Loop Leading Color Corrections to Heavy-Quark Pair Production in the Gluon Fusion Channel*, *JHEP* **1101** (2011) 102, [arXiv:1011.6661].

[281] A. von Manteuffel and C. Studerus, *Massive planar and non-planar double box integrals for light N_f contributions to $gg \to tt$*, arXiv:1306.3504.

[282] F. Brown, *The Massless higher-loop two-point function*, *Commun.Math.Phys.* **287** (2009) 925–958, [arXiv:0804.1660].

[283] J. Vermaseren, *New features of FORM*, math-ph/0010025.

[284] J. M. Henn, *Multiloop integrals in dimensional regularization made simple*, arXiv:1304.1806.

[285] J. Tausk, *Nonplanar massless two loop Feynman diagrams with four on-shell legs*, *Phys.Lett.* **B469** (1999) 225–234, [hep-ph/9909506].

[286] U. Aglietti and R. Bonciani, *Master integrals with 2 and 3 massive propagators for the 2 loop electroweak form-factor - planar case*, *Nucl.Phys.* **B698** (2004) 277–318, [hep-ph/0401193].

[287] R. Bonciani, P. Mastrolia, and E. Remiddi, *Vertex diagrams for the QED form-factors at the two loop level*, *Nucl.Phys.* **B661** (2003) 289–343, [hep-ph/0301170].

[288] R. Bonciani, A. Ferroglia, P. Mastrolia, E. Remiddi, and J. van der Bij, *Planar box diagram for the $N_F = 1$ two loop QED virtual corrections to Bhabha scattering*, *Nucl.Phys.* **B681** (2004) 261–291, [hep-ph/0310333].

[289] T. Birthwright, E. Glover, and P. Marquard, *Master integrals for massless two-loop vertex diagrams with three offshell legs*, *JHEP* **0409** (2004) 042, [hep-ph/0407343].

[290] F. Chavez and C. Duhr, *Three-mass triangle integrals and single-valued polylogarithms*, *JHEP* **1211** (2012) 114, [arXiv:1209.2722].

[291] A. Smirnov and M. Tentyukov, *Feynman Integral Evaluation by a Sector decomposiTion Approach (FIESTA)*, *Comput.Phys.Commun.* **180** (2009) 735–746, [arXiv:0807.4129].

[292] S. Borowka, J. Carter, and G. Heinrich, *Numerical Evaluation of Multi-Loop Integrals for Arbitrary Kinematics with SecDec 2.0*, *Comput.Phys.Commun.* **184** (2013) 396–408, [arXiv:1204.4152].

[293] S. Borowka and G. Heinrich, *Massive non-planar two-loop four-point integrals with SecDec 2.1*, arXiv:1303.1157.